QiR
" Quality in Research "

Proceeding

THE 10th INTERNATIONAL CONFERENCE ON QUALITY IN RESEARCH (QIR)

"Research For Future Better Life"



Faculty of Engineering

Engineering Center University of Indonesia, Depok

4 - 6 December 2007

Industrial, Manufacturing, Material Engineering, and Management
&
Biomedical Engineering and Biotechnology
&
Nanomaterials and Nanotechnology

Supported by :

LEMTEK FT UI

FOREWORDS
Dean of Faculty of Engineering, University of Indonesia

The Quality in Research (QIR) Conference is the annual event organized by the Faculty of Engineering, University of Indonesia. Since started in 1998, it has become an excellent forum of discussion for all researchers from research institutions and universities all over the nation of Indonesia. The 1st and 6th QIR Conferences had been successfully organized as the high quality national conferences, and starting from the 7th QIR conference, has been organized to invite international research papers.

The 10th Quality in Research International Conference having a theme of "Research for future better life" is to provide an international forum for exchange of the knowledge, information, experience and result as well as the review of progress and discussion on the state of the art and the future trend various issues and the developments in the multi-fields of scientific and technology. The main purposes of this conference are to provide a forum for free discussion of new ideas, development and applications, including techniques and methods to stimulate and inspire pioneering work, to provide opportunities for students and young engineers to meet their experienced peer and to provide a meeting that will enforce progress, stimulate growth and advance the state of knowledge in the multi-fields of science and technology.

We would like to express our heartiest to thank to all authors and participants for their active participations in the 10th on Quality in Research (QIR) International Conference 2007, and also to all the paper reviewers, member of the technical committees, and member of the organizing committees, for their support to the success of this conference. Last but not the least; we would also like to invite all participants to the next on Quality in Research (QIR) Conference.

Faculty of Engineering, University of Indonesia
Dean,

Prof. Ir. Rinaldy Dalimi, Ph.D

FOREWORDS
Chairman of 10th International Conference on QIR 2007

The 10th Quality in Research International Conference will provide an international forum for exchange the knowledge, information, experience and recent researches of various fields. With a strong support and presentations from academic, industry and entrepreneurs, the conference will provide an ideal platform to learn various fields and understand technological trends in the region.

The 10th Quality in Research (QIR) International Conference has a theme of "Research for Better Future Life" being the third time to go internationally, has invited limited papers from other nations such as Korea and Malaysia. The conference is organized in parallel sessions focusing on the 8 (eight) research areas such that many researchers and peer groups may focus their discussion on the relevant topics. All submitted papers had been reviewed by the technical committees and had been arranged into 8 (eight) sub-themes according to the following fields:

- **Energy, Process and Environmental Engineering and Management:** Energy and environmental issues, combustion technology, fluids mechanics and thermal fluid machinery, thermodynamics and heat transfer, geotechnical and environmental engineering, etc.
- **Industrial, Manufacturing, Material Engineering, and Management:** Production Engineering, Supply Chain Management, Innovation System, Maintenance System, Quality Management System, Human Factors Engineering, Organizational System, Fabrication and Industrial Automation, Manufacturing System: Control Management and Information Technology, etc
- **Biomaterial, Biomedical Engineering and Biotechnology:** Biomedical numerical modeling, Biomaterial, Biosensor, Biocompatibility, Biomechanics, Biotechnology, Biomedical Instrumentation, Biomedical Imaging
- **Design and Infrastructure Engineering and Management:** Product design and development, composite: Materials and applications, structural dynamics, mechanics of materials, Construction Management, Public Infrastructures and Services, Structural Engineering, etc
- **Special Session on Electronics Engineering**
- **Information and Computation Technology**
- **Sustainable Architecture**
- **Nanomaterials and Nanotechnology:** Nano structured material, Nanotechnology, Nanocomposite, MEMS, Self Assembled Monolayer, Thin Film, etc

The main purposes of this conference are to provide a forum for free discussion of new ideas, development and applications, including techniques and methods to stimulate and inspire pioneering work, to provide Opportunities for students and young engineers to meet their experienced peer and to provide opportunities for students and young engineers to meet their experienced peer and to provide a meeting that will enforce progress, stimulate growth and advance the state of knowledge in the multi-fields of science and technology.

Depok, 4 December 2007
The Organizing Committee,
Chairman,

Gunawan Wibisono, Ph.D

Steering Committee

1. Prof. Dr-Ing. Axel Hunger, Universitaet, Duisburg-Essen, Germany
2. Prof. Dr. Carlo Morandi, Universida Degli Studi de Parma, Italy
3. Prof. Dr. Iwao Sasase, KEIO University, Japan
4. Prof. Kim Kyoo-ho, Yeungnam University, Korea
5. Prof. Dr. Ir. Irwan Katili, University of Indonesia
6. Prof. Dr. Ir. Bambang Suryawan, MT, University of Indonesia
7. Prof. Dr. Ir. Dadang Gunawan, M.Eng, University of Indonesia
8. Prof. Dr. Ir. Johny W Soedarsono, DEA, University of Indonesia
9. Prof. Ir. Gunawan Tjahjono, M.Arch, Ph.D, University of Indonesia
10. Prof. Dr. Ir. M. Nasikin, University of Indonesia
11. Isti Surjandari, Ph.D, University of Indonesia
12. Prof. Dr. Ir. Budi Susilo Soepandji, University of Indonesia
13. Prof. Dr. Ir. Sutanto Soehodho, University of Indonesia
14. Prof. Dr. Ir. Sulistyoweny Widanarko, Dilp. SE. MPH, University of Indonesia
15. Prof. Dr. Ir. I Made Kartika Dipl. Ing, University of Indonesia
16. Prof. Dr. Ir. Tresna P. Soemardi, University of Indonesia
17. Prof. Dr. Ir. Sardy, M.Eng, M.Sc, University of Indonesia
18. Prof. Dr. Ir. Bagio Budiardjo M.Sc, University of Indonesia
19. Prof. Dr. Ir. Djoko Hartanto, M.Sc, University of Indonesia
20. Prof. Dr. Ir. Eddy Siradj, M.Eng, University of Indonesia
21. Dr. Ir. Kemas Ridwan K, University of Indonesia
22. Prof. Dr. Widodo Wahyu P, DEA, University of Indonesia
23. Ir. Boy Nurtjahyo M.,MSIE, University of Indonesia
24. Dr. Ir. Dedi Prihadi DEA, University of Indonesia
25. Ir. Hendri D.S. Budiono, M.Eng, University of Indonesia
26. Dr. Ir. Sigit Pranowo Hadiwardoyo, DEA, University of Indonesia
27. Dr. Ir. Herr Soeryantono, University of Indonesia
28. Prof. Rinaldy Dalimi, Ph.D, University of Indonesia

Chairman of the Conference

Ir. Gunawan Wibisono, M.Sc, Ph.D

Technical Committee

1. Ir. Gunawan Wibisono, M.Sc, Ph.D
2. Dr. Yosia Irwan
3. Dr. Engkos Kosasih
4. Purnomo Sidi P, Ph.D
5. Abdul Muis, Ph.D
6. Badrul Munir, Ph.D
7. Tania Surya Utami, MT
8. Ir. Beatrianis, M.Si

TABLE OF CONTENTS

Industrial, Manufacturing, Material Engineering, and Management
Design and Infrastructure Engineering and Management
Nanomaterials and Nanotechnology

IMM-18	Failure Analysis of Motor Bike Steering Shaft *by: Winarto, Zulkifli, and Dwi Marta Nurjaya*
IMM-19	Development of Nodular Indefinite Chilled Iron (NICI) by Combination of Controlled Cooling Heat Treatment and Copper Alloying Element *by: Y. Prasetyo, S. K. Lee, E. R. Baek*
IMM-20	Application Response Surface Methodology in Developing Tool Life Prediction Models when End Milling Titanium Alloys Ti-6Al-4V. *by: A.S. Mohruni, S. Sharif, M.Y. Noordin,V.C. Venkatesh*
IMM-21	On The Estimation of Visco-elastic Properties for Nylon and GFRP materials *by: Gatot Prayogo, Danardono A.S.*
IMM-22	Interfacial Shear Strength and Debonding Mode Between The Ramie (Boehmeria Nivea) Fiber Surface and Polymers Matrix. *by: Eko Marsyahyo*
IMM-23	Fabrication of CuO Added-BaTiO3 Ceramics for NTC Thermistor *by: Dani Gustaman Syarif*
IMM-24	Structure and Properties of $Cu(In_{1-x}A1_x)Se_2$ Thin Films Grown by RF Magnetron Sputtering for Solar Cells Applications *by: Badrul Munir, Kyoo Ho Kim*
IMM-25	Amorphous Nature of TiO2-PMMA nanohybrids and Tecniques to Enhance its Nanocrystallinity *by: A. H.Yuwono*
IMM-26	Deposition of SnO2 transparent conducting films and their characterization *by: Dwi Bayuwati and Syuhada*
IMM-27	Development of multi-axis force detector for 5-DOF articulated robot *by: Gandjar K, Aji S*
IMM-28	The development of portable blood carrier by using thermoelectrics and heat pipes *by: Nandy P, Hiban H, and Parlin Adi S*
IMM-29	Object Recognition based on Its Features for Human Robot Dialog *by: Rahmadi Kurnia*
IMM-30	Development of analytic solution of inverse kinematics and motion simulation for 5-DOF milling robot *by: Gandjar K, Hafid B*
IMM-31	Effects of parallel and zigzag blade configuration an dflow passage in casing cover on centrifugal pump performance *by: Harinaldi and Sugeng Sunarto*
IMM-32	Determination of Flow Proporties of Mud Slurry *by: Ridwan, Yanuar, Budiarso, and Raldi AK*
IMM-33	Development of Prototype of Hybrid Vehicle Controller *by : Gandjar Kiswanto, Danardono S., Endiandika TP, Pranadityo*
IMM-34	Role of fibres on the shear strength of peat Case: Tampan-Riau Peat *by: Wiwik Rahayu*
IMM-35	Comparison Analysis of Paddy Dryer Recirculatory Batch Original and Its Modification Through Implementation of CFD *by: Adi Surjosatyo*
IMM-36	Minimize of Ceramic Defects using Six Sigma to Decrease Customer Complain *by: Isannul Kamil, Feri Afrialdi, Yossy Risman*

ISSN: 1411-1284

Interest Relativity Mapping of Stakeholders Perceptions on the Proposed Plan of Integrated Ticketing System Policy in DKI Jakarta's Land Transportation using *DANA* Method

Akhmad Hidayatno[1] and Dita Ade Susanti[2]

Industrial Engineering Department, Faculty of Engineering, University of Indonesia
Tel. [1]0811811115, [2]08158922942 , email : [1]akhmad@eng.ui.ac.id , [2]dita_tiui2003@yahoo.com
University of Indonesia, Kampus UI Depok 16424, Indonesia
Ph. 62-21-78888805, Fax 62-21-78885656

Abstract– **Starting in 2003, Jakarta has initiated a program to re-invent the city mass transportation systems, known as dedicated line bus way, monorail light transports, and subway. One of the key policy aspects is to develop an Integrated Ticketing System. We need a policy analysis to map out possible differences and common grounds for all actors from government and the private sectors.**

DANA[1] is a semi-quantitative method, tools and open source software developed by Delft University of Technology by P.W.G Bots, which could precisely help us to do this. This mapping process targeted the stakeholders who have influence, role, and power in implementing (or obstructing) a policy. The central actors, is the Jakarta Planning Board (Bapeda DKIJ), Others include PT.KAI (Indonesia State Railways), financing institutions(banks), private investors, BLU Trans Jakarta (Bus way Operating Company), Economic Bureau of Government of Jakarta and representatives from public transport (KWK).

We started by identifying the problem, continuing with identification of arena[2] and actors with the Head of Bapeda DKIJ, perception mapping of the actors (using depth interview), obtaining the interest relativity mapping of the stakeholders (using DANA),and developing summary analysis.

The research primary result is that the integrated ticketing system in the views of all actors identified has no goal conflict, low of action conflict and suitable inferred strategy. It also recommended the strategy of each stakeholder to minimize conflicts and which aspects must be accentuate to make the system more attractive to all actors, and increase the acceptance of this policy.

Keywords- DANA, Policy analysis, Relativity mapping

I. INTRODUCTION

Indonesia transportation is a big delay duty which should be solved directly by this country as to construct public service for civilization. Successful parameter for transportation system could be seen in a big city, mainly in Indonesia homeland, Jakarta. Nowadays, DKI governor is constructing macro transportations system that expected could be the solution traffic jams in Jakarta on 2010.

Based on the purpose for renovating transportation system in DKI Jakarta, it would be better, if it could be supported by integrated ticketing system.

Much interest and actor participate in implementation of ticketing system could create some problems. Therefore it is needed for creating a beginning process of interest relativity mapping from all the part who take in group of set of governor's planning to build an institution for managing the integrated ticketing system.

Dynamic Actor Network Analysis is an approach method in interest relativity mapping from many actors. This approaching obeys a comparison analysis form actor's perceptions. DANA is based on the using of causal diagram from each actor, a diagram which establishes could show the factors and instruments which are relevant to the condition.

The output is on the development of a policy which will be created by DKI governor; making a set of recommendation, If the policy could be success or not, and also giving the worst possibility description when the policy is not success.

The purpose of this research is to obtain relativity mapping among stake holder's interests in a case of implementation integrated ticketing system.

II. BASIC THEORY

Multi actor policy

On multi actor condition, public policy could not be explained by one or two actors central, but the generalization among actor's network which all kinds of actors are related in a systematis way or not exactlty (Kenis and Schneider, 1991).

[1] DANA or Dynamic Actor Network Analysis
[2] Arena is an imaginary place in DANA where actors "wrestle"
their perceptions

Actor is "people or groups which have an ability on policy making and act in a coordination way" (Burns et al, 1985, p.x).

DANA (*DYNAMIC ACTOR NETWORK ANALYSIS*)

Base assumption of DANA is actor's perception for a certainty condition who could manage and include on the policy making process. They decide how an actor act properly wins all policy process. Definition of an actor's perception include of all part (opinion, concept) where he thinks about that condition.

Purpose

DANA can contribute in making quality of the policy maker by helping the entire actor understand the condition and communicating about all what they have and the other perception.

III. EXPERIMENTAL RESULTS

4.1 Identify the problem

Talking about the policy, the boundary is so huge. Focusing on one problem will really help in making policy analysis by using DANA.

Based on process of discussion among the experts and writer, focus of this research is in the policy of implementing integrated ticketing system for public transportation in DKI Jakarta.

4.2 Identify the arena

The policy of implementing integrated ticketing system could create many problems; is it should be built an institution for manage this system? How about the price of the ticket? Which type of the trip that will be chosen? etc. Therefore, it's needed for making a specification of this problem.

By process of discussion among the actors and writer, the next focus of this problem is on the isue; if an institution will be established for managing this integrated ticketing system. And this focus is defined as arena for DANA.

4.3 Identify the actors

There are many actors who will take part on the policy of building an institution for managing integrated ticketing system, start form the regulator, operator investor, etc who could influence the process of that policy making.

Identifying the proper actors is an important step in DANA method. Based on brainstorming process among the experts and writer, it could be identified that the actors of this arena are presented on the **table 1** below.

Table 1 Stakeholder's List

NO	Instansi	Nara Sumber	Identifikasi Peran
1	BAPEDA DKI	Kepala BAPEDA dan Sub bid perhubungan	Perencana regulasi
2	Banking	Divisi Marketing BNI 46	Investor
3	BLU Trans Jakarta	Kepala bagian keuangan dan Bid Sarana Prasarana	Calon badan pengelola dan operator
4	PT KAI Div Jabotabek	Kepala operasional	Operator
5	KWK	Kepala Operasional	Operator
6	Investor swasta	Divisi Marketing PETRONAS	Pemasang iklan/marketing
7	Biro PEMDA DKI	Kepala Biro Administrasi Perekonomian	Perencana regulasi

.4 Identify the actors' perceptions

Process of identifying actors' perception is obtained by interview. Interview is a chosen method because by interviewing, exploration of information from the stakeholders could be done easier and more accurately than the other method such as polling and quesioner.

Process of interview to the stakeholders in order to ge some perception of some isues; the stakeholder's interest of this policy; the problems which could appear when this policy is implemented; the causes factor of that problems; the relativity among the causes factor of the problems; and the solution whisch are recomended.

4.5 Obtain the interest relativity mapping of the stakeholder by using DANA

After identifying the stakeholders' perceptions, the other step will be continoued by making a mental models from each actors. The process of making mental models, starting with identify the factors, actions, relation among the factors and actions, and also the goals from each stakeholders.

BAPEDA DKI Jakarta

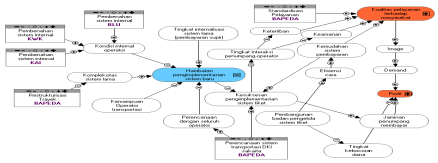

Fig.1. Mental models of BAPEDA DKI Jakarta

From BAPEDA DKI Jakarta's perspective, the implementation of integrated ticketing system will gives a positive impact to improve service quality to civilization and also increasing the profit of Pemda DKI Jakarta it self. The factor which is wanted to be minimized is the barriers of the policy implementation.

Establishing an institution for managing the ticketing system will increase the efficiency of the process that it could making an easy way for payment that it will be the parameter of the implementation integrated ticketing system's succeed.

Banking

From the banking perspective, the interest which will be obtained only in profit sectors for this bank. This profit can be obtained from the infestation and marketing sector. In addition, those two sources are depended by the proposal which is offered.

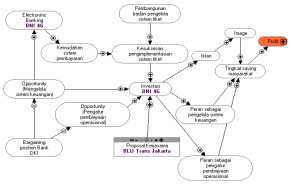

Fig.2. Mental models of banking

On the aspect of establishing an institution for managing ticketing system, banking considers, it could give a positive impact for the successful of implementing this policy.

BLU Trans Jakarta

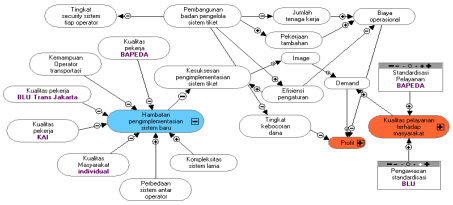

Fig.3. Mental models of BLU Trans Jakarta

BLU Trans Jakarta believes that there will be many problems which appear when this policy implemented. The interest from BLU it self are on two sectors; improvement of service quality and profit for BLU Trans Jakarta.

Plan of establishing an institution for managing the ticketing system will increase the efficiency of control, decrease amount of the workers, and decrease security system of each operator. Event though there are many negative effects, but the improvement of control efficiency will support the successful of the implementation of this policy.

PT KAI Jabotabek Division

PT KAI believes that the establishment of an institution for managing ticketing system will increase the control efficiency and decrease amount of workers.

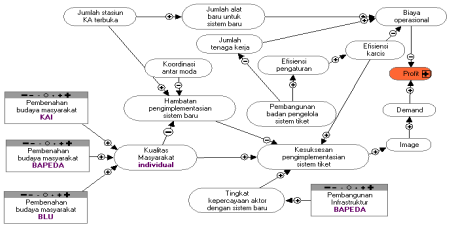

Fig.4. Mental models of PT KAI Jabotabek division

The interest of PT KAI from this policy is on improvement of profit aspect.

Mini Vehicle

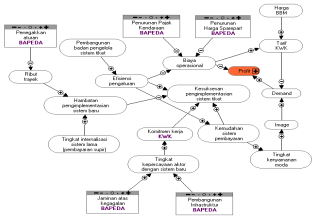

Fig.5. Mental models of mini vehicle

From the mini vehicle's perspective that on the future will be functioned as a feeder of macro transportation profit improvement is the only interest of this implementation of the policy.

Establishment of an institution will increase control efficiency that it could increase the simple process for payment and that factor will be a successful parameter of implementation of the policy.

Private Investor

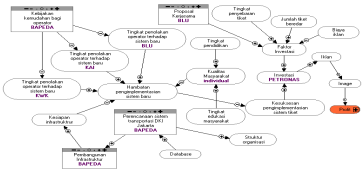

Fig.6. Mental models of private investor

Private investor believes when this policy be implemented, there will be many problems appear when the barriers could not be solved firstly.

Profit improvement is the interest of private investor by this policy. And this profit could be obtained by a good proposal that will be offered.

Administration and Economy Bureau

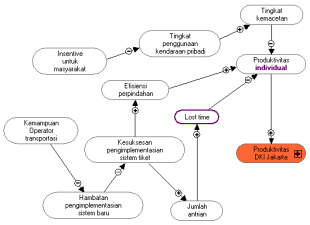

Fig.7. Mental models of administration and economy bureau of DKI Jakarta

Administration and Economy Bureau of DKI Jakarta's perspective shows when this policy appear, the productivity of DKI Jakarta will increase. The productivity could be increased when lost time and traffic jams could be minimized, and the movement efficiency could be increased.

4.6 Analysis from DANA compute result

4.6.1 Analysis of *Percentage of Utility*

Percentage of utility shows utility's score or expected utility by the actor's column to the strategies in actor's row. Although actors giving score or comparing some strategies have a high score, preferred *strategies* will be on it. By *percentage of utility*, we could identify antagonist or protagonist actors form particular instruments. On scoring all the utilities form an instrument in an arena, utility of an instrument for an actor calculate aggregately by summing all goals from actor's group.

DANA results shows utility score among BAPEDA DKI Jakarta and the other actors. From all the score which showed below, not all the score absolute to one score, but there is also in range. This shows us there is no absolute score should be chosen, because the

positive score of an actor defeated by negative score of the other actors.

Negative score on the utility shows that between useful and negative is balance. Therefore the last score only across of i,d,m which has negative base coefficient.

From the DANA Analysis could be identified that antagonist's actor on the boundary with BAPEDA DKI Jakarta is BLU Trans Jakarta, administration and economy bureau, and private investor, because three of this actor have some negative utilities, that means negative side of the factors could balancing utility score For the actors who have possibility to become antagonist are mini vehicle, banking, and PT KAI Jabotabek division. Because the negative side could balance the utility side in particular condition.

For the protagonist's actors on the boundary with BAPEDA DKI Jakarta is only the actor's probability who could be protagonist in particular time. They are mini vehicle, banking and PT KAI Jabotabek division, because the positive side could be bigger than the negative ones.

4.6.2 Analysis of *Percentage of Satisfaction*

Percentage of satisfaction shows the utilities which are expected form actor's column to the strategies of actor's row. Satisfaction means the positive relation between actor A and actor B.

DANA analysis shows satisfaction scores among BAPEDA DKI Jakarta and the other actors. It could be identified that the scores are varied. There is no actor who contributes 100% scores of satisfaction; there is only range 0% to 100%. It means there is a possibility the actors could give satisfaction scores 100% when the particular condition is happened. But the other condition could be happened too, that satisfaction score of 0% that could be given by the actors to BAPEDA DKI Jakarta. These actors are mini vehicle, banking, administration and economy bureau of DKI Jakarta and PT KAI division Jabotabek. The other actors are certainly could not give 100% score of satisfaction, Private sector, only 33% and BLU Trans Jakarta which only 0%.This condition appropriate with the utility scores before, which are negative. To the BLU Trans Jakarta, the %satisfaction 0% appropriate with utility score which only -0.25, that means the negative side is balance with the utility side but the score of i*d*m is little, that couldn't give a big impact to the goal.

4.6.3 Analysis of *Percentage of Shares*

Percentage of shares is a sub system of similarity category. Similarity is counted for the factors and causal relations as the ratio of share/own, whereby 'share' is summing of relation factors which is happened in both actors. And 'own' is summing of relation factors in a perception on the actor who is selected.

Scores on DANA Analysis is asymmetry. It couldn't be showed the inconsistency of DANA. This differentiates only caused by share among actors, but the total of factors form each actor is not same. Scores of share actors could be same if the total of factors among actors are exactly same.

Scores of share factor which are short of 90% show the factors among the actors are different; therefore it could have a possibility to create conflict. And also on the contrast one, scores of share factor above 90% show there are many similarities between two actors, which could create cooperation among the actors.

DANA shows that the score of share factor which less than 20%, in despite of the DANA calculation, it could be seen the differentiate condition and action among actors contribute score of share factor becoming small, it's only 11% to 53%, therefore it could be implied the differentiate of background, function and action will influence significantly to the score of share factor of each actors. The least describes there is a probability creating conflict among actors, caused by a large differentiations.

4.6.4 Analysis of *Goal Conflict*

The actors may have difference perceptions. The conflict results below are calculated based on the first aspect; goals.

Goals aspect describes that there are differentiation between vector of the expected changes, it is scored by the priority (whatever the scores >0 indicates the conflict condition). The simple way, it can be seen when the actor A wants the improvement of service quality to the civilization, in despite of actor B wants the contrast one. If it's happened, it can be concluded that goal conflict is happened between both actors. Overall calculating for the aspect goals are shown in DANA.

Scores on DANA is zero (0), shows there is no conflict on the goal of the actors. No goal conflict doesn't mean all actor supporting each other. All the actors perhaps don't have conflict on the goals, but they may have different view on some issues.

If we flash back to the mental models above, goals of the actors are not contrast each other; most of the actor has a goal to improve their profit, beside the other kinds of goal.

4.6.5 Analysis of *Action Conflict*

Action conflict describes there is a possibility for a conflict among actions which are held by the actors. Conflict in action can be occurred when there is different vector of action between two actors. For instance: between actor PT KAI division Jabotabek and mini vehicle. Mini vehicle push its action to the things which could be done by PEMDA; policy making, declining vehicle tax and spare part's price, constructing infrastructure, guarantee of the failure, and also severing the rule to solve routing problems. PT KAI division Jabotabek depresses its action to the things which are not only PEMDA who can do it, but also the other stakeholders. The differentiation of these things causes action conflict's score between KAI and mini vehicle, 0.39 (scores >0 describes an action conflict).

4.6.6 Analysis of *Inferred Strategies*

The calculated result of inferred strategies describes recommendation of strategies which offered by DANA software. There are some scenarios, will be explained later, adopted to the real situation.

Table 7 shows all actions that possible be done which are got from diagram perspective. DANA analyzes all these solution probabilities that may be done by each of actors and presents the result on three types; positive, negative or zero. If one actor get a positive score, it means the actions are well be done to the positive vector that has a purpose getting interest from that actor. If the other hand occurred, DANA advices actor to do action on the negative vector that has a purpose to protect the interest of that actor. And the zero score of an action shows it would be better for not doing that action at all.

DANA Analysis shows that there are some factors which held an alteration significantly. It can be seen from the differentiation action when in base condition and ideal one. On the ideal condition, the strategies which are recommended by DANA can be used properly .From all of the recommendation, there is no recommendation which is not proper to the actor's expectation.

For instance, PT KAI division Jabotabek is better if it do an action to construct civilization's culture that is held not only PT KAI, but also by the other actors. From the data, it shows more completely. It shows the total of strategies which can be chosen by the actors, for instance PT KAI Jabotabek's division has five strategies; on the other hand, mini vehicle only has one strategy that can be chosen.

IV. CONCLUSIONS

From the research by using DANA in interest relativity mapping of stakeholder in implementation integrated ticketing system of policy in Transportation DKI Jakarta, it can be concluded:

1. Awareness of single transportation mode is still low (from the effect and impact). It can be seen from the interview's result.
2. The thing above occurred because there are still many concept of single transportation mode on each of actors (there is no fix concept from DKI Jakarta's governor).
3. Awareness of all actors can be improved by doing a socialization and making a congregate plan among all operators and actors that has purpose to create a first awareness.
4. From all the actors; BAPEDA DKI Jakarta, banking, BLU Trans Jakarta, PT KAI Divisi Jabotabek, Administration dan economy bureu, private investor, and mini vehicle, it shows there is no *goal conflict*, suitable *inferred strategy* and low of a*ction conflict.*
5. From the analysis, it could be implied, all the actors have a cooperation relation with BAPEDA DKI Jakarta.
6. BAPEDA DKI Jakarta can make this policy when all the actors obtain their profit properly to their expectation and that profit can be obtained when PEMDA DKI Jakarta has done its action (look **Table 7)**
7. Most of all actors on this research recomend to create a congregate plan among all the operators and the other actors; therefore the plan will could improve the service quality of transportation for DKI Jakarta's society, and also the policy will give a profict which suitable with the actors' expectation.
8. The other consideration of the actors is on the quality of DKI Jakarta civilization it self. Socialization and education are needed to be done by all stakeholder.
9. There are some steps that be a particular consideration on DANA method; identifying arena, stakeholders, and perceptions of stakeholders.

REFERENCES

[1] Bale, Michael. *Managing with Systems Thinking.* McGraw Hill, UK. 1994.

[2] Bots, Pieter W.G Pieter. *Journal of Dynamic Actor Network Analysis :Introduction and Overview.* 2000

[3] Bots, Pieter W.G. , Mark J.W. van Twist, and Ron van Duin. *Journal of Designing a Power Tool for Policy Analysts: Dynamic Actor Network Analysis.* 1999.

[4] Bots, Pieter W.G, Mark J.W. van Twist, and J.H. Ron van Duin. *Journal of Automatic Pattern Detection in Stakeholder Networks* 2000.

[5] *Journal of DANA Appendices :no.6. Africa's Sustainable Development Council (ASUDEC)*

[6] L.M. Hermans. *Journal of Dynamic actor network analysis for diffuse pollution in the province of North-Holland.* 2004.

[7] Proefschrift. *Journal of Actor Analysis for Water Resources Management,* hlm: 9 – 53. 2005.

[8] Soekardi, S. *Journal of Ten Actors Blowing Their Triumphs*, hlm 3-8. 2005.

ISSN: 1411-1284

Supplier Performance Evaluation Based on Efficiency Rate Using AHP and DEA Methods at PT.X

Erlinda Muslim[1],Fauzia Dianawati[2], Dola Vani[3]
Industrial Engineering Department University of Indonesia
Faculty of Engineering University of Indonesia,
Kampus Baru UI, Depok – 16424, Indonesia, Telp 62-21-78888805, 78884805
E-mail: [1]Erlinda@eng.ui.ac.id, [2]fauzia@ie.ui.ac.id, [3]dola_ti03@yahoo.com

***Abstract* —** Supplier selection in supply chain management becomes more important due to the competition between supply chains rather than companies. Today's consumers demand cheaper, high quality products, on-time delivery and excellent after-sale services. Achieving this starts with supplier selection and evaluation of supplier performance. Selection and evaluation of supplier performance include quantitative and qualitative criteria that must be considered in evaluation. So, the author uses combination of AHP (*Analytical Hirarchial Process)* and DEA (*Data Envelopment Analysis*) method in this research. AHP is a method of hierarchy contains a number of criteria evaluation. The result of AHP is a priority/weight from each criterion. DEA is a mathematical programming procedure for evaluating the relative efficiencies of multiple DMU (*Decision Making Unit*) that involve multiple inputs and multiple outputs. DEA measures the relative efficiency of each DMU in comparison to other DMUs. An efficiency score of a DMU is generally defined as the weighted sum of outputs divided by the weighted sum of inputs. In this research, quality is criteria that have the biggest priority in supplier selection and evaluation. Supplier got 100% will became efficient one. While, supplier not got 100% will became inefficient supplier.

***Keywords* —** *Supplier Performance, AHP, DEA*

1. Introduction

To compete effectively in global market, a company must have competent supply chain. In supply chain management, relationship between buyer and supplier support the success of company's strategic goal. So, doing business together is important aspect that cannot be separated in company's supply chain. Supplier is a part that determines total quality of company's final product. Because, total quality is cannot be obtained without qualified input

PT. BMS is a service company that core of its business is supplying Indonesian Labor to work abroad. So, dependence rate of the company to its supplier is very high to meet customer requirements and customer expectations. Hence, today the company is in condition where it tries to prevent the problems relating to supplier.

That condition obliges PT.X to evaluate supplier performance. The company has to find intersection point between company expectation and output that received by company. Without evaluation, the company cannot improve supplier performance. And finally, the improvement of supplier performance will give effect to company's performance.

One of the techniques to evaluate supplier is *benchmarking*. In this case, one supplier is compared relatively to others supplier. During the time, the method that most used is *Analytical Hierarchical Process* (AHP). In this method, the company makes hierarchy that contain criterion that expected by the company to its supplier. Evaluation by this method is usually subjective. Because, the data used is qualitative.

Beside AHP method, performance evaluation and productivity can be done by *Data Envelopment Analysis* (DEA). This method has used widely for helping decision making process and very useful in evaluating the system that have multiple criterion. The method also gives target of improvement in the system. Evaluation by this method is objective. Because, the data used is quantitative.

Because the supplier selection and evaluation include qualitative and quantitative criterion, so in this research both of methods is combined. The purpose is to get result that objective and subjective. The objective of the research is to evaluate supplier performance based on efficiency rate by AHP and DEA methods.

2. Methodology

First step is collecting criterion and sub criterion that will be offered to respondents in questionnaire 1. Criterion and sub criterion is obtained from multiple references that shown in Table 1.[1] Criterion and sub criterion that will be

offered is stimulus to respondent in determining which criterion and sub criterion to evaluate supplier performance.

Table 1. Criterion and sub criterion supplier performance evaluation from refrences [1]

Criterion	Dickson (1966)	Weber et al (1991)
	Rank	Rank
Net price	6	1
Quality	1	3
Delivery	2	2
Production Facilities and Capacity	5	4
Technical Capability	7	6
Financial Position	8	9
Geographical Location	20	5
Management and Organization	13	7
Performance History	3	9
Operating Controls	14	13
Communication System	10	15
Reputation and Position in Industry	11	8
Repair Service	15	9
Packaging Ability	18	13
Training Aids	22	15
Procedural Compliance	9	15
Labor Relations Record	19	15

Furthermore, respondents choose criterion and sub criterion to evaluate supplier performance in questionnaire 1. Selecting criterion and sub criterion is all at once. The purpose is to get whole figure of hierarchy model by respondent. Questionnaire 1 is a half opened. In this questionnaire respondent asked to give score to criterion and sub criterion that offered in Likert scale (1-5). Beside, respondent also give new addition criterion and sub criterion and give the score to it by Likert scale (1-5). Likert scale used in questionnaire is extremely agreeing (5) to extremely disagree (1). igunakan adalah skala sangat setuju (5) sampai skala sangat tidak setuju (1). Table 2 present Likert scale used in questionnaire 1. To give priority, the author gives the questionnaire to 3 respondents (expert) from PT.X.

Table 2. Likert scale

Likert Scale	Definition
5	Extremely agree the criterion and sub criterion used to evaluate supplier performance of Indonesian Labor.
4	Agree the criterion and sub criterion used to evaluate supplier performance of Indonesian Labor.
3	Hesitant/ neutral that the criterion and sub criterion used to evaluate supplier performance of Indonesian Labor.
2	Disagree the criterion and sub criterion used to evaluate supplier performance of Indonesian Labor.
1	Extremely disagree that the criterion and sub criterion used to evaluate supplier performance of Indonesian Labor.

After that, weighting the criterion and sub criterion is done by respondent. In this step, collecting data done using closed questionaire. Respondents asked to give weight to criterion and subcriterion supplier performance evaluation by filling pairwaise comparison (qustionaire 2). Respondent asked to compare the weigth of one criteria to others pairwisely.

The result of weight in AHP used furthermore to DEA. By this manner, the subjective criterion can be quantitatived and calculate by DEA (Data Envelopment Analysis) [2]. *Data Envelopment Analysis* (Charnes et al 1978) is mathematical program to estimate production frontiers and evaluate relative efficiency of organisation unit named *Decision Making Units* (DMUs). *Data Envelopment Analysis* focuses on certain ratio gave to each DMUs. Efficient DMUs got full score. And inefficient DMU got lower score than efficient DMUs.

DEA calculates technical efficiency for whole unit. Efficiency score for each unit is relative depends on efficiency rate other unit in sample. Each unit considered have positive efficiency rate that 0-1. Units have value 1 used to make envelope for efficiency frontier. Other unit, that is out of envelope show inefficiency rate (Figure 1).

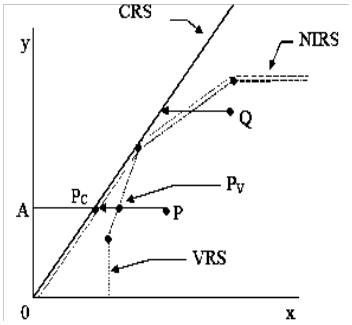

Figure 1. CRS and VRS DEA [3]

Basic model of DEA is CCR (Charnes Choper Rhodes) model. CCR model include : input oriented dan output oriented model. In this reserach, model used is output oriented model This model is defined as primal program linier model as shown in function (1).

Maximize $$\frac{\sum_i u_i y_{iq}}{\sum_j v_j x_{jq}}$$

$$\text{Constraint to} \quad \begin{array}{ll} \frac{\sum_i u_i y_{ik}}{\sum_j v_j x_{jk}} \le 1 & k = 1,2,...,n \\ u_i \ge \in & i = 1,2,..s \\ v_j \le \in & j = 1,2,....m \end{array} \qquad (1)$$

While dual model shown in function (2).

$$\text{Maximize} \quad g = \phi + \in (e^T s^+ + e^T s^-)$$
$$Y\lambda - s^+ = \theta Y_q$$
$$\text{Constraint to} \quad X\lambda + s^- = X_q \qquad (2)$$
$$\lambda, s^+, s^- \ge 0$$

The model can be interpreted: unit DMU_q is efficient one by using CCR model, if goal function in function (1) is 1 and value of g^*=1. If the value of this function bigger than 1, then that unit is inefficient. Variable ϕ indicates that unit has to increase the output to reach efficiency.

Function (1) and (2) assume *Return to Scale*. However, in doing analysis Variable Return to Scale (VRS) model also must be considered. In this case, the function (2) has to rewrite in convex condition $e^T\lambda$=1 as shown on function (3)

$$\text{Maximize} \quad : h_0 = \sum_{i=1}^{s} u_r y_{i0} + C_0$$
$$\text{Constraint to} \quad : \quad \sum_{i=1}^{m} v_i x_{r0} = 1 \qquad (3)$$
$$\sum_{i=1}^{s} u_r y_{i0} - \sum_{i=1}^{m} v_i x_{r0} - C \le 0$$
$$u_r, v_i \ge \varepsilon$$

Beside, basic model of DEA (CCR and BCC), there are some modification made. One of them is SBM model made by Tonen (2001) [4]. The Model is basic definition for super efficiency. In this model, efficiency score measured by slack variable.

Beside Tonen, there is also research done by Anderson and Peterson (A&P) [5]. They see DEA score for inefficient units in ranking. In ranking efficient unit, they suggest to give score bigger than one unit efficient unit by deleting constraint envelope score of unit that evaluating (*k*). the model named by primal model. The model primal for super efficiency model is:

$$\text{Maximize} \quad h'_{kk} = Max \sum_{r=1}^{k} u_{rk} y_{rk}$$

$$\text{Constraint to} \quad \begin{array}{l} \sum_{r=1}^{s} u_{rk} y_{rk} - \sum_{i=1}^{m} v_{ik} x_{ik} \le 0 \quad untukj=1,....,n \\ \sum_{i=1}^{m} v_{ik} x_{ik} = 1 \\ u_r \ge \in \quad untuk\ r = 1,.....,s \\ v_r \ge \in \quad untuk\ r = 1,.....,m \end{array} \qquad (4)$$

Where
x_{ij} : *input* i from unit j, where there is m input and n unit.
y_{rj} : *output* r from unit j where there is s *output*;
u_{rk} : ideal weight for *output* r from unit k,
v_{ik} : ideal weight for *input* i from unit k.
ε > 0: value of non-Archimedian infinitesimal
h_{kk}: A&P score for unit k

The dual model is formulated:

$$Min\, E_k - \varepsilon[\sum_{i=1}^{m} s_i^- + \sum_{r=1}^{s} s_r^+$$
$$E_k x_k = \sum_{j=1}^{n} \lambda_j x_{ij} + s_i^- \qquad i = 1,.....m$$
$$\text{Constraint to} \quad y_k = \sum_{j=1}^{n} \lambda_j y_{rj} + s_i^+ \qquad r = 1,.....s \qquad (5)$$
$$\lambda_j, s_i^+, s_i^- \ge 0$$

Initial idea for super efficiency model is to compare unit evaluating (*k*) by linier combining of all units. By this method, unit will be excluded from initial frontier, and h_{kk} will calculate the radial distance from new frontier.

3. Result and Discussion

Based on questionnaire 1, the criterion used to evaluate supplier performance at PT.X is group in to criterion and sub criterion as shown in Table 3.

Table 3. Chosen criterion and sub criterion supplier performance according to respondent

No	Criterion and Sub Criterion Performance Evaluation for Supplier of Indonesian Labor
1	**Quality**
1.1	Indonesian labor condition
1.2	Completion of document
1.3	Supplier internal quality program
1.4	Quality guarantee
2	**Price/Cost**
2.2	Payment method
2.3	Price/cost policy
3	**Delivery**

3.1	Location of supplier
3.2	Speed of deliveries
4	**Service**
4.1	After sale service
4.3	Respond to demand (communication system)
5	**Flexibility**
5.1	Flexibility of quantity
5.2	Flexibility of time
6	**Attitude**

Furthermore, respondents asked to give weight to each criterion and sub criterion. The result is shown in Figure 2.

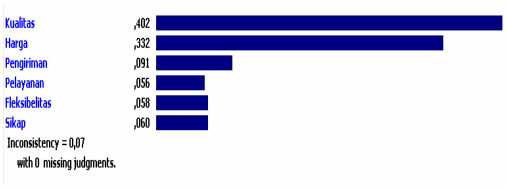

Figure 2. The result of weighting criterion

While, weight calculation for each supplier presented in Figure 3.

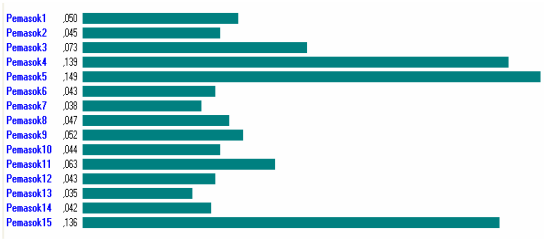

Figure 3 The result of weighting supplier

Then, the next step is identifying input and output variable. From discussion with PT.X, variable categorize as variable input is price/cost. While variable output is amount of Indonesian Labor delivered, frequency of delivered, result of AHP and quality. Value of each variable input and output, then transform in ratio as presented in Table 4

Table 4. Ratio input and output variable

DMU	Price	Frequency of delivery	Result of AHP	Delivery quantity	Quality
f1	0,79	0,47	0,05	0,73	0,88
f2	0,78	0,28	0,05	0,74	0,82
f3	0,88	0,53	0,07	0,87	0,91
f4	0,82	0,78	0,14	0,79	0,87
f5	1,15	1,00	0,15	0,99	0,88
f6	0,85	0,78	0,04	0,67	0,87
f7	0,85	0,34	0,04	0,67	0,87
f8	0,71	0,38	0,05	0,73	0,86
f9	0,81	0,38	0,05	0,67	0,91
f10	0,89	0,66	0,04	0,72	0,90
f11	0,98	0,78	0,06	0,87	0,85
f12	0,83	0,94	0,04	0,67	0,90
f13	0,83	0,91	0,04	0,67	0,76
f14	0,78	0,31	0,04	0,72	0,78
f15	0,94	0,25	0,14	1,00	0,77

After that, the calculation of DEA scores done by EMS software version 1.3. The calculation done in two ways: CRS and VRS. The comparison of it is shown in Table 5.

Table 5 Comparison CRS and VRS score

Supplier	CRS Score	VRS Score	Inefficiency scale
1	107,01%	101,17%	5,84%
2	108,79%	107,01%	1,78%
3	101,82%	100%	1,82%
4	100%	100%	0,00%
5	110,81%	100%	10,81%
6	108,48%	103,57%	4,91%
7	118,17%	104,41%	13,76%
8	100%	100%	0,00%
9	107,91%	100%	7,91%
10	112,58%	100,55%	12,03%
11	109,36%	103,39%	5,97%
12	100%	100%	0,00%
13	102,11%	102,11%	0,00%
14	111,01%	110,01%	1,00%
15	100%	100%	0,00%

From Table above, we can see that efficient supplier in both methods is supplier 4,8,12 and 15. Beside, obtain score for each supplier, the calculation of primal model also result weight value, benchmark and intensity of benchmark for each supplier.

Weight is value that shows strength of supplier. While, benchmark is compare inefficient supplier to efficient supplier. Intensity of benchmark describe how big the effect of efficient supplier to in efficient supplier. By knowing who the benchmark is, the inefficient supplier can be efficient supplier by increasing its ability as much as intensity of its benchmark. The value of weight and benchmark presented in Table 6.

Table 5 Value of weight each supplier

Supplier	Price		Frequency of delivery		Result of AHP		Delivery quantity		Quality	
	VRS	CRS	VRS	CRS	VRS	CRS	VRS	CRS	VRS	CRS
1	1	1	0,02	0,14	0	0	0,06	0,29	0,57	0,93
2	1	1	0	0	0	0	0,66	0,91	0,09	0,34
3	1	1	0	0,09	0	0	0,41	0,91	0	0,59
4	1	1	0,3	0,1	0,7	0,44	0	0	0,46	0
5	1	1	0,54	0,46	0,06	0	0,39	0,54	0	0
6	1	1	0,03	0,21	0	0	0	0,26	0,53	0,97
7	1	1	0	0	0	0	0	0	1	1
8	1	1	0,02	0	0,91	0	0,06	0,48	0,52	0
9	1	1	0	0	0	0,08	0	0	0,92	1
10	1	1	0,03	0,18	0	0	0	0,27	0,55	0,97
11	1	1	0,13	0,12	0	0	0,74	0,88	0	0,13
12	1	1	0,51	0,54	0	0	0	0	0,46	0,49
13	1	1	0,59	0,53	0	0	0,42	0,47	0	0
14	1	1	0	0	0	0	0,67	0,91	0,09	0,33
15	1	1	0	0	0,09	0,08	0,91	0,92	0	0

Table 6. Benchmark and intensity of benchmark

Supplier	Intensity and Benchmark CRS	Intensity adn Benchmark VRS
1	4 (0,0423) 8 (0,9071) 12 (0,1360)	3 (0,2447) 8 (0,3609) 9 (0,2873) 12 (0,1071)
2	8 (0,8951) 15 (0,1521)	3 (0,3420) 8 (0,6099) 15 (0,0480)
3	4 (0,2199) 8 (0,9838)	7
4	8	2
5	4 (1,3340) 12 (0,0706)	1
6	4 (0,0028) 8 (0,2678) 12 (0,7927)	3 (0,3197) 12 (0,6803)
7	8 (1,1913)	3 (0,5479) 9 (0,4521)
8	9	4
9	4 (0,0327) 8 (1,0973)	2
10	4 (0,0006) 8 (0,6139) 12 (0,5414)	3 (0,6840) 12 (0,3160)
11	4 (0,9721) 8 (0,2530)	3 (0,1960) 4 (0,3464) 5 (0,4246) 15 (0,0330)
12	5	4
13	4 (0,0821) 12 (0,9179)	4 (0,0818) 8 (0,0002) 12 (0,9181)
14	8 (0,8258) 15 (0,2001)	3 (0,1884) 8 (0,6693) 15 (0,1423)
15	2	3

Table 7 Value of slack

Supplier	Price		Frquency of delivery		Result of AHP		Delivery quantity		Quality	
	CRS	VRS	CRS	VRS	CRS	VRS	CRS	VRS	CRS	VRS
1	0	0	0	0	0,0009	0,004	0	0	0	0
2	0	0	0,068	0,12	0,0138	0,012	0	0	0	0
3	0		0		0,0025		0		0,113	
4										
5	0		0		0,0234		0		0,254	
6	0	0,01	0	0	0,0004	0,008	0	0,039	0	0
7	0	0	0,04	0,1	0,0111	0,024	0,07	0,079	0	0
8										
9	0		0,032		0		0,096		0	
10	0	0,02	0	0	0,0027	0,019	0	0,085	0	0
11	0	0	0	0	0,0781	0,065	0	0	0,137	0
12										
13	0	0	0	0	0,0151	0,015	0	0	0,122	0,12
14	0	0	0,012	0,04	0,0194	0,018	0	0	0	0
15										

After doing calculation by CRS-DEA and VRS –DEA model, we will get 4 efficient suppliers. To know who is the super efficient supplier from 4 suppliers, we can do super efficiency calculation. By this manner, the efficient supplier will be compared to other efficient suppliers. The result of super efficiency calculation is shown in Table 8. From the Table, we can see that supplier 8 is super efficient supplier compared to other efficient supplier.

Table 8 Super efficiency score

DMU	Score CRS	Score VRS
f1	107,01%	101,17%
f2	108,79%	107,01%
f3	101,82%	95,14%
f4	75,59%	56,86%
f5	110,81%	79,60%
f6	108,48%	103,57%
f7	118,17%	104,41%
f8	90,93%	big
f9	107,91%	98,55%
f10	112,58%	100,55%
f11	109,36%	103,39%
f12	91,09%	90,65%
f13	102,11%	102,11%
f14	111,01%	110,01%
f15	92,45%	87,76%

4. Conclusion

Based on result of calculation by AHP and DEA methods for supplier at PT. BMS we conclude that:

- Criterion used to evaluate supplier performance at PT.X is quality, price, delivery, attitude, flexibility, and service.
- Criteria has the biggest priority is quality.
- Supplier group into efficient supplier based on CRS-DEA are supplier 4,8,12 and 15. While supplier group into efficient supplier based on VRS-DEA are supplier 4,5,8,9,12 and 15. And supplier group into efficient supplier based on both methods are supplier 4,8,12,15.
- From 4 supplier group as efficient supplier, supplier 8 is super efficient suppler.

REFERENCES

[1] Bross, Megan E. & Guangbin Zhao, *Supplier Selection Process in Emerging Market*, Master Thesis, Göteborg University, p. 25, Göteborg University, Göteborg, 2004.

[2] Tsuyoshi, Ogawa, *Analysis Support System Based On Subjective Judgment Based On* DEA, School of Information Science and Technology, Jepang, 1998, p 1.

[3] J, Coelli T, *A Guide of DEAP version 2.1: DEA Program*, University of New England, New England, 1996, p.20.

[4] Vincová , Ing. Kristína: Using DEA Models To Measure Efficiency, Kosice, 2004, p. 2.

[5] Y. Hadad et al, DEA *Super Efficiency Multistage Ranking*, Computer Modeling & New Technologies, Volume 7, 2003, p. 37-46.

ISSN: 1411-1284

Measurement and Comparison of Subcontractor's Performance Using Data Envelopment Analysis (DEA) in PT. X

Fauzia Dianawati[1], Erlinda Muslim[2], Lina Rosliana[3]
Industrial Engineering Department University of Indonesia
Faculty of Engineering University of Indonesia,
Kampus Baru UI, Depok – 16424, Indonesia, Telp 62-21-78888805, 78884805
E-mail: [1]fauzia@ie.ui.ac.id, [2]erlinda@eng.ui.ac.id, [3]linarosliana_ti2003@yahoo.com

Abstract **—** Company's performance evaluation is a part of operational improvement program. This thesis describes a conceptual approach to measure and compare the productivity of resources utility which is given by the contactor, using a set of quantitative method known as Data Envelopment Analysis (DEA). This evaluation is adapted for various specific work of the subcontractor by comparing input and output variable that fill the evaluation's criteria. DEA is managed to maximize subcontractor's expected output, which has material cost, work hour, and labor as input variables, and net revenue and job volume as output variables. The interaction between input and output forms a linear programming model that gains efficiency score from each Decision Making Unit (DMU). Efficiency score is hoped that it will help the company in decision making process to optimize subcontractor's performance and as a benchmarking program for the inefficient. This performance evaluation obtained fours cluster which classify subcontractors based on their performance and the efficiency score. The cluster could be used to get know closer to subcontractor characteristic so that the company could gain some information to motivate subcontractors' performance into the optimum one.

Keywords **—** *Construction productivity, construction efficiency, data envelopment analysis, subcontractor's performance evaluation.*

1. Introduction

Nowadays, the rush demand of land space development especially in construction service is one of those that indicates the coming-back of property business in Indonesia. The tight competition to get the entering market tender will push developers to show their best at, so that one can distinct it from others. Newly developed construction management system starts to form the construction approaching the supply-chain management system which assumes the project as a part of production system's activity. In manufacturing field, this supply-chain management application has cut millions dollars of project's budget while improving its customer service quality [1].

PT. X is a general contractor in construction which is having contracts with some subcontractors to complete specific project activities which may vary. These relationships affect directly to general contractor's productivity which is depend on subcontractor's productivity. The difference between subcontractors causes difficultness when it comes to assess subcontractor's performance objectively, due to controlling and coordinating function of the company. Internally, establishing performance measurement would help the company to identify its strength and weakness which indirectly could increase the productivity and organization's capability, and also optimize the use of project resources [2].

This research uses Data Envelopment Analysis (DEA) method, one of modern performance measurements which could define a simple measurement based on an organization's efficiency level by the measurement of various input [3] and output [4] factors. DEA method is used because it has the qualification that close enough to this assessment characteristic as stated before. In spite of that, this method also had been used in the same kind of research done by El-Mashaleh (2005). Its purpose is to obtain subcontractor's performance evaluation in the same field job in order to facilitate the availability of information needed in decision making process by using DEA method.

2. Methodology

DEA is non-parametrical method to estimate production efficiency of the company/organization. DEA then forms a frontier in the ratio of its input and output by using the linear programming technique. These procedures aren't based on the explicit model of a frontier, or the relation of observation to the frontier, but on its fact of observation that shown in the frontier.

DEA have some advantages and disadvantages. It advantage are DEA could handle many inputs and outputs once at a time of measurement, and it don't need functional relation assumption between input and output variables, it means that input and output could have different unit of measurement. It disadvantages are it's sample specific, DEA could only measure relative efficiency, not the absolute efficiency, and also statistic hypothesis test of DEA result is difficult to be done. Formula 1 is the basic

model of DEA which adapted from the basic efficiency principle, output/input.

Maximize: ……..**(1)**

$$h_o = \frac{\sum_{r=1}^{s} u_r y_{r0}}{\sum_{i=1}^{m} v_i x_{i0}}$$

$$\frac{\sum_{r=1}^{s} u_r y_{rj}}{\sum_{i=1}^{m} v_i x_{ij}} \leq 1; j = 1, 2, ..., n$$

subject to:

$$\frac{u_r}{\sum_{i=1}^{m} v_i x_{i0}} > \varepsilon; r = 1, ..., s$$

$$\frac{v_i}{\sum_{i=1}^{m} v_i x_{i0}} > \varepsilon; i = 1, ..., m$$

$$\varepsilon > 0$$

DEA has some assumption which are positivity (1), DEA requires both, the input and output variables, in positive value, isotonicity (2), it means every unit of increase in input variable will result minimal a unit of increase in output variable and there isn't output variable that decrease, number of Decision Making Unit (3) is a body that evaluated, minimal number which evaluated is three DMUs in each output and input variable to gain its degrees of freedom. The fourth is windows analysis to ensure the stability of DMUs' efficiency value. Value determination (5) has to be as simple as possible for each of relative unit to the other unit in a set of data. Practically, the project management is the one who sets the value. Last assumption is homogeneity (6) that all of evaluated DMUs have the same kind of variable.

DEA could estimate efficiency in the constant returns-to-scale (CRS) and variable returns-to-scale (VRS) assumption. DEA model that used is Charnes, Cooper, and Rhodes (CCR) version which was developed in 1978. It evaluate DMUs' relative productivity, in this case, DMU is an entity which is functioned to change input become output. The CRS assumption is only appropriate when all DMUs are operating at an optimal scale. Imperfect competition, constraints on finance, etc. may cause a DMU to be not operating at optimal scale. Banker, Charnes, and Cooper in 1984 suggested an extension of the CRS DEA model to calculate for variable returns-to-scale (VRS) situations.

This method is based on technical efficiency principle which forms a frontier where there are efficient DMUs and inefficient DMUs combined in linear programming to produce as much output with available input, or to optimize input to obtain the targeted output. This efficiency frontier is build by sample data which forms a linear line connecting a set of input and output combination from the company, which also shows a set of efficiency level from each company.

DEA model uses two types of assumption; those are input orientated and output orientated. One point that should be stressed is that the output and input orientated models will estimate exactly the same frontier and therefore, by definition, identify the same set of DMU's as being efficient. It is only the efficiency measures associated with the inefficient DMU's that may differ between the methods.

In early stage of this research, it is begun by identifying subcontractor that will become the main object of the research (DMU), and then determining the evaluation criteria which will be defined as output and input variables and afterwards formulating DEA model and assumption which will be used according to the period of subcontractor's data set.

Once the DEA model's obtained, data gathering will be started to dig from subcontractor's weekly project evaluation summary. This data then classified into input and output variable and calculated by Efficiency Measurement System software version of 1.3. The result will be analyzed in order to gain benchmarking implication for the subcontractors which are inefficient and other suggestions for project management that would improve company's productivity.

3. Result and Discussion

PT. X is doing 200 hectares Bukit Golf Mediterania project in a strategic beach reclamation area which is designed to be located between the ocean and the lake, Pantai Indah Kapuk. PT. X is having contracts with many different contractors to help its town house and exclusive home office project.

After exploring about the problem exist through discuss session with field management side, so it's decided that three subcontractors which is doing stone finishing job would be assessed of their performance based on efficiency score comparison. Those subcontractors are RN, MN and TN. There are nine activities which would be evaluated, those are celcon brick setting, celcon parapet brick setting, begisting and casting, plastering and smoothing, profile making, finishing, expose making, scaffolding making, and the last is SAP-PVC making.

Chosen input variables are work hours and number of workers which describes subcontractors' performance, and operational cost that describes general contractor's investment performance for this project. Meanwhile, chosen

output variables are subcontractors' income to describe their given values from their general contractor, and volume job resulted which describes technical productivity from each subcontractors.

DEA models that used are CRS and VRS by output orientated assumption. Output orientated is used because in the construction company, input has been standardized, the subcontractor will be given the target, and also the measured amount of material resources used. Table 1 to table 3 are data summaries from each subcontractor's job which is gained from one period project activities from September 21, 2006 until December 21, 2006.

Table 1
Job Summary of RN Subcontractor

No	Keterangan	Volume	Satuan	Pendapatan (Rp)	Jumlah Pekerja (orang)	Biaya (Rp)	Jam Kerja (jam)
1	*Celcon*	63.7	m2	415,238.33	19	4,883,233.33	14.29
2	*Celcon Parapet*	34.5	m2	315,024.00	8	3,008,116.00	10.51
3	*Begisting* dan cor	67.4	m2	313,260.87	4	8,559,526.09	12.16
4	Plester dan aci	69.6	m2	820,401.55	20	2,292,287.50	17.66
5	Pembuatan profil	21.3	m2	661,302.08	9	979,939.58	5.81
6	*Finishing*	8.0	unit	409,224.14	5	418,025.78	4.17
7	*Ekpos*	24.3	unit	735,000.00	3	2,402,444.93	39.96
8	*Scaffolding*	4.3	unit	257,500.00	5	727,500.00	12.64
9	*SAP PVC*	6.0	unit	510,000.00	6	750,000.00	15.00

Table 2
Job Summary of TN Subcontractor

No	Keterangan	Volume	Satuan	Pendapatan (Rp)	Jumlah Pekerja (orang)	Biaya (Rp)	Jam Kerja (jam)
1	*Celcon*	93.2857	m2	624,621.43	20	9,295,921.43	17.84
2	*Celcon Parapet*	31.35	m2	261,230.50	8	3,366,990.00	8.39
3	*Begisting* dan cor	45.45	m2	221,250.00	4	5,574,448.75	13.43
4	Plester dan aci	57.8571	m2	469,343.75	20	1,204,171.43	14.96
5	Pembuatan profil	20.5	m2	709,375.00	8	416,312.50	5.44
6	*Finishing*	14	unit	325,000.00	5	570,500.00	8.05
7	*Ekpos*	3.35	unit	272,500.00	3	350,674.65	7.06
8	*Scaffolding*	1	unit	50,000.00	5	150,000.00	5.00
9	*SAP PVC*	7	unit	595,000.00	6	875,000.00	21.00

Table 3
Job Summary of MN Subcontractor

No	Keterangan	Volume	Satuan	Pendapatan (Rp)	Jumlah Pekerja (orang)	Biaya (Rp)	Jam Kerja (jam)
1	*Celcon*	129.628	m2	914,380.62	19	10,662,675.56	29.91
2	*Celcon Parapet*	55.9884	m2	452,325.70	8	4,306,843.94	14.23
3	*Begisting* dan cor	86.517	m2	377,403.85	5	9,754,389.75	12.78
4	Plester dan aci	163.587	m2	1,159,106.15	20	4,762,153.53	21.25
5	Pembuatan profil	43.9521	m2	736,293.78	8	793,075.77	11.05
6	*Finishing*	10.1573	unit	911,971.83	5	959,414.73	4.29
7	*Ekpos*	4.54	unit	256,000.00	3	505,739.63	10.49
8	*Scaffolding*	8.5	unit	585,000.00	5	1,211,250.00	30.88
9	*SAP PVC*	8.25	unit	701,250.00	6	1,046,718.75	16.50

To simplified forms of input and output from DMUs' model, quantitative ratio then made. The ratio is obtained from comparison between variable values that calculated with the maximal of same variable value, i.e. to get volume ratio then:

$$\text{Volume} = \frac{\text{variable value of volume}}{\text{max.variable value of volume between subcontractors}}$$

Those ratios are added on DEA measurement by Efficiency Measurement System software version of 1.3, as input or output variables. Table 4 is an example of quantitative ratio calculation of celcon brick setting.

Table 4
Celcon Brick Setting Ratio

Subkontraktor	Volume	Pendapatan	Jumlah Pekerja	Biaya	Jam Kerja
RN	0.491	0.454	0.95	0.458	0.478
TN	0.720	0.683	1	0.872	0.596
MN	1	1	0.95	1	1

According company's policy, it's decided that the weight of those two subcontractor's output variables are the same, volume compared to income equal to 1: 1, by basic model of DEA is,

Maximized: $$\eta_k = \frac{\sum_{r=1}^{s} u_r y_{rk}}{\sum_{i=1}^{m} v_i x_{ik}} \qquad \text{.....(2)}$$

subject to: $$\frac{\sum_{r=1}^{s} u_r y_{rj}}{\sum_{i=1}^{m} v_i x_{ij}} \le 1 \; ; \; j = 1, 2, ..., n$$

that is mean there are k DMUs that use i amount of inputs and is hoped to produce r amount of output. From formula 2 above, then a linear programming could be made from optimal form of subcontractor's productivity, according to table 4, this is the linear programming to celcon brick setting:

$Z = 0.491\omega_v + 0.454\omega_p$

d.k. $0.95\omega_l + 0.458\omega_c + 0.478\omega_h = 1$

$0.491\omega_v + 0.454\omega_p - (0.95\omega_l + 0.458\omega_c + 0.478\omega_h) \le 0$

$0.720\omega_v + 0.683\omega_p - (\omega_l + 0.872\omega_c + 0.596\omega_h) \le 0$

$\omega_v + \omega_p - (0.95\omega_l + \omega_c + \omega_h) \le 0$

$\omega_v - \omega_p \ge 0$

$\omega_v, \omega_p, \omega_l, \omega_c, \omega_h \ge 0$

Information:

ω_v : output variable of volume

ω_p : output variable of income

ω_l : input variable of workers

ω_c : input variable of operational cost

ω_h : input variable of work hours

This thesis uses added assumption of data calculation because of minimal number of evaluated DMU, three DMUs. The added assumption is super-efficiency in VRS model. It's used to rank the DMU which are all efficient

from previous calculation using non-super efficiency assumption. If there were different scores obtained from the first non-super efficiency calculation, so that the first score would be taken as evaluation result, but if there were the same scores at first calculation, then super-efficiency score is used as evaluation result. Table 5 describes calculation results using both assumptions.

Table 5
Celcon's Efficiency Score Classification

DMU	Efisiensi		Super Efisiensi		Skala Inefisiensi	Identifikasi
	CRS	VRS	CRS	VRS		
RN	100.00%	100.00%	93.25%	big	-	HE
TN	100.00%	100.00%	84.41%	84.30%	0.11%	HE
MN	100.00%	100.00%	64.90%	45.41%	19.49%	HE

There are four values obtained from DEA calculation, which are:

1. Efficiency score for each subcontractor in nine kinds of project activities, there are percent form score that describes efficiency level form each subcontractor as shown in table 5. 'Big' value in table 5 at super efficiency score of RN refers that any increase at RN's input will also increase its output proportionally so that its efficiency level remains the same even by changing period. This value shows that this DMU's reached its optimal level in operating process. The efficient is DMU with 100% of efficiency score, and the inefficient is DMU with non 100% of efficiency score. In table 6 below is shown the efficient DMU for each subcontractor's specific activities

Table 6 Ranked Efficient DMU

No.	Activities	Efficient DMU
1	Celcon brick setting	**MN**, TN
2	Celcon Parapet brick setting	**MN**, RN
3	Begisting and casting	**MN**, RN, TN
4	Plastering dan smoothing	**MN**, TN, RN
5	Profile making	**TN**, MN
6	Finishing	**RN**, MN, TN
7	Expose making	**TN**, RN
8	Scaffolding making	**MN**, RN
9	SAP-PVC making	**RN**, MN, TN

2. Weights value of input and output criteria, which could be used to determine subcontractor's strength in specific criteria, for example in table 7 at operational cost variable is shown that TN's weight is the biggest among all subcontractors in CRS and VRS model. It describes the TN's strength at operational cost management.

Table 7 Input-output Weight Values of Profile Making

CRS						
DMU	Score	Workers {I}{V}	O. Cost {I}{V}	Work Hours {I}{V}	Volume {O}{V}	Income {O}{V}
RN	104.11%	0	0	1.04	0.91	0.09
TN	52.86%	0	0.29	0.24	0	1
MN	46.64%	0.47	0	0	1	0
VRS						
DMU	Score	Workers {I}{V}	O. Cost {I}{V}	Work Hours {I}{V}	Volume {O}{V}	Income {O}{V}
RN	103.77%	0	0	1.14	1	0
TN	big	3.79	1.00E+10	6.50E+09	0.58	0.42
MN	46.64%	0.57	0	0	1	0

3. Intensity value and benchmark for the inefficient subcontractors resulted from DEA calculation. It also needs to be harmonized with management's evaluation results during the same period. Practically, if one DMU has more than one benchmark, the company may be tending to benchmark the inefficient one to the DMU which has a better efficiency score.
4. Slack value for the inefficient one describes the amount of output that need to be increased by the inefficient. Slack value is resulted from intensity value in order to benchmark it to the efficient. Benchmarking is a new step that company could do to specify those three subcontractors job. The most efficient in a specific activity could be specialized only to complete that one kind of activity. This effort may optimize the use of existing project resources

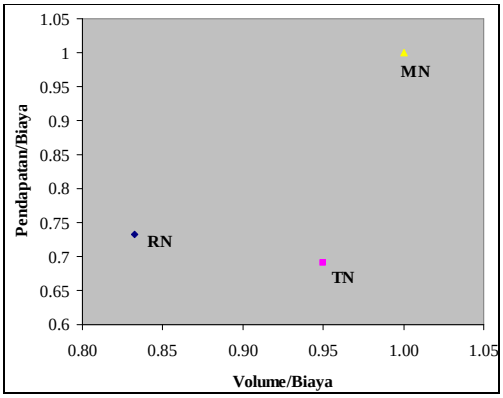

Figure 1 Example of interaction analysis between input and output

From the output point of view, volume that obtained by RN and MN shows a fine productivity level, but not with one showed by TN. It could happen in construction field due to the subcontractor's failure so that they have to repeat their job while their income still count according to the visible

volume resulted in field, whereas the total volume done might be double or more because of previous failure. Beside that, there're also uncontrolled factors such as change in customer or owner preferences of building structures or ornaments, because this construction job is a make-to-order type. Those matters also could affect to operational cost, project schedule and resources needed whish might change anytime according to the needs.

This performance evaluation results four cluster that classify subcontractors according to combination of DEA score and management's evaluation decision, there are High performers and efficient (HE), Low performers and efficient (LE), High performers and inefficient (HI), Low performers and inefficient (LI).

4. Conclusion

Based on subcontractors' evaluation result, we can conclude that:

1. This performance evaluation uses operational cost, number of workers, and work hours as input variables, and income and subcontractors' volume resulted as output variables.
2. Efficiency score is obtained from comparison of two kinds of efficiency score using non-super efficiency and super efficiency assumption to rank the set of efficient DMUs. This assessment shows all of the subcontractors are able to work efficiently in four kinds of project activities; there are begisting and casting, plastering and smoothing, finishing, and the last is SAP-PVC making. Meanwhile in the rest of activities; celcon brick setting, celcon parapet brick setting, profile making, expose making, scaffolding making, there are averagely two subcontractors that work efficiently.
3. This performance evaluation obtained fours cluster which classify subcontractors based on their performance and the efficiency score. The cluster could be used to get know closer to subcontractor characteristic so that the company could gain some information to motivate subcontractors' performance into the optimum one.

REFERENCES

[1] Arntzen, et. al, quoted by O'Brien, William. 1998. Construction Supply-Chain Management: A Vision for Advanced Coordination, Costing, and Control.

[2] John Hailey & Mia Sorgenfrei. 2005. Measuring Success, Issues in Performance Measurement.

[3] Tim J. Coelli & George E. Battese. An Introduction to Efficiency & Productivity Analysis. *CEPA Working Paper*, 1998, pg.3

[4] El-Mashaleh et al., 2005. Envelopment Methodology to Measure and Compare Subcontractor productivity at the Firm Level.

ISSN: 1411-1284

Analyzing Investment Effectiveness of LQ 45 Stocks Using Factorial Designs

Isti Surjandari[1] and Clara Rosalia Rangga Mone [2]
Industrial Engineering Department, Faculty of Engineering, University of Indonesia
Kampus UI, Depok, 16424, Indonesia
E-mail:[1] surjandari.2@osu.edu; [2]clara_ti03@yahoo.com

Abstract — **Investment in capital market grows rapidly which is indicated by many companies listing in Jakarta Stock Exchange. In this case, an analysis of the effectiveness of investment in Jakarta Stock Exchange is needed, so the investors know exactly the advantages and risks of investments. The effectiveness of investments can be seen by the combination of controlled factors which are related to stock investment at capital market. The factors are risk level of investments, industrial sector, and the company within industrial sector. Factorial and Nested designs are used to analyze the combination of factors that may influence stock investments in capital market. The objective of this study is to analyze factors which have significant effect on investments of LQ 45 Stocks. Using LQ 45's stock data period of 2004-2006, this study shown that risk and company within industrial sector have significant influence on stock price. This study also shown that investment on Infrastructure, Utility and Transportation sector gives the highest profit. The result of this study can be used to support investor activity in capital market.**

Keywords— investment, LQ 45 stocks, factorial design, nested design

I. INTRODUCTION

Capital markets in Indonesia keeps growing in the middle of economic and political changes which happen in this era. This phenomenon can be shown in figure 1. From figure 1, we can see that investment in Indonesian capital market has extremely grown up. Investment of capital market use some instruments which is usually called portfolio. One part of the portfolio is called stock. Stock prices may vary. If selling price of stock is higher than buying price, the investor can get capital gain. On the other hand, if selling price of stock is lower than buying price, then the investor can get capital loss. There are several classifications of stocks in Jakarta Stocks Exchange; one of them is LQ 45 stocks. The fixation effectiveness of stock investment in capital market can be seen by the factor configuration, and this configuration may support the price formation that becomes profit indicator. The fixation of factor configuration can be analyzed using nested design.

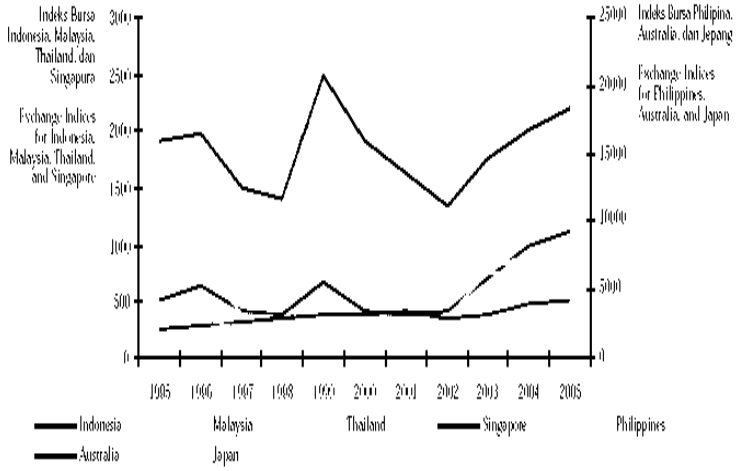

Figure 1: Development of Capital Market of the world

This study will use data of LQ 45 socks from year 2004 to 2006. The objective of this study is to analyze whether risk (shown by stock index), type of the industrial sector, and the company within industrial sector who listing in Jakarta Stocks Exchange influence stocks prices as profit indicator for investor when they buy stocks from year 2004 to 2006. This study also analyze whether there is any interaction among those factors which may give maximum profit.

II. RESEARCH METHODS

LQ 45 stocks consist of 45 stocks that are chosen after pass trough several criteria, which are: (1) get in top of 60 from total stocks transaction in regular market (average transaction value in last 12 months); (2) get in rank of 45 based on value of capitalization market (average capitalization market in the last 12 months); (3) listed in Jakarta Stocks Exchange for 3 months minimum; (4) the company must have good financial condition, development prospect, and frequency and transaction in regular market. In other words, this index will consist of stocks that have high liquidity and also market capitalization from the stocks. These stocks are chosen by investor because they may give maximum profit for the investor. Factorial and Nested design can be used to analyze the stock effectiveness of LQ 45. Factorial design is a statistical method that uses combination of several control factors to find the most dominant factor, and choose the optimum combination from those factors to get the optimum result [1]. This method is believed as one of the most effective method to get an optimum result for a process performance, and process variability [2]. *Nested design* is a statistical method which can be used if one factor has a branch but different for each main factor.

Design of Experiments is the statistical method which is an effective technique to do an experiment, so that the right data can be collected and analyzed with statistical method and at the end we can make valid conclusion of our experiments [3]. Factorial and nested design is part of Design of Experiments so that the method used in this study will be the same with that of the Design of Experiments.

Design of Experiment has seven steps, which are: (1) recognition of and statement of the problem; (2) selection of the response variable; (3) choice of factors, factors, level, and ranges; (4) choice of experimental design; (5) performing the experiment; (6) statistical analysis of the data; (7) conclusion and recommendations.

In this study, three factors are chosen, which are: risk, industrial factor, and the companies within industrial sector. The first factor, risk, has tree levels which are: 150-200, 200-250, and 250-300. These choices are based on data from year 2004 to 2006. The second factor has nine levels, which are: Agriculture, Mining; Basic industry & Chemistry; Various industry; Industry of Consumer Good; Property & Real Estate; Infrastructure, Utility & Transportation; Money; Trade, Services & Investment sectors. Those factors are based on Jakarta Stocks Exchange agreement. The third factor which is a nested factor is the companies within industrial sector. For every sector, two companies are randomly chosen to be the level of factor. The companies are Astra Agro Lestari, Tbk and Bakrie Sumatra Plantations Tbk in Agriculture sector; Aneka Tambang (persero) Tbk and Timah Tbk in Mining sector; Indocement Tunggal Prakasa Tbk and Holcim Indonesia Tbk in Basic Industry & Chemistry sector; Astra International Tbk and Gajah Tunggal Tbk in Various Industry; Indofood Sukses Makmur Tbk and Unilever Indonesia Tbk in Industry of Consumer Good sector; Jakarta International Hotel & Dev. Tbk and Kawasan Industri Jababeka Tbk in Property & Real Estate; Indosat Tbk and Telekomunikasi Indonesia Tbk in Infrastructure, Utility & Transportation sector; Bank Central Asia Tbk and Bank Danamon Tbk Money sector; Ramayana Lestari Sentosa Tbk and United Tractors Tbk in Trade, Services & Investment sector.

A Full factorial Design was used in this study. For the Response variable, stock price is chosen as profit indicator for investors who are investing on stocks. Minitab 14 is used for computation and analyzing the data.

Designs of Experiments require normally distributed data. After plotting the residual data, stock prices are not normally distributed, as can be shown in figure 2.

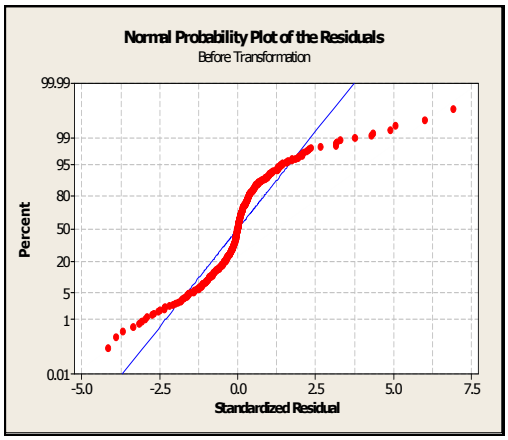

Figure 2 Residual Data before Transformation

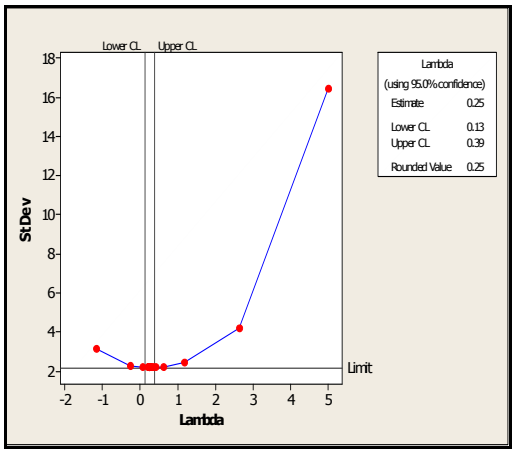

Figure 3: Box-Cox Transformations

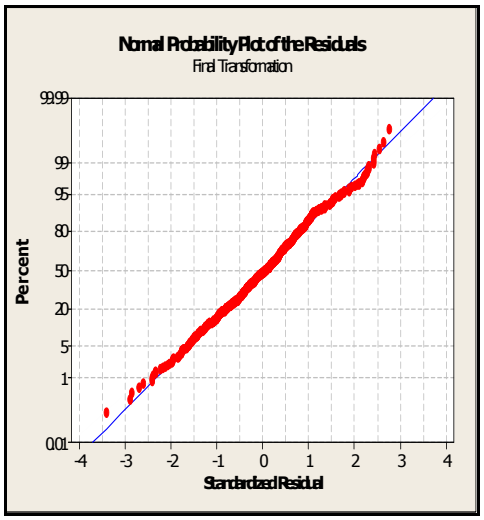

Figure 4 Residual Data after Transformation

For the purpose of this study, data transformation using Box-Cox transformation is used to get the residual data normally distributed. The Box-Cox transformation can be seen in figure 3. After conducting Box-Cox transformation, data residual are normally distributed as can be seen in figure 4. In addition, figure 5 shown that the data are randomly distributed without having a special pattern and outlier values.

The model for this study can be formulized as [4]:

$$y_{ijkl} = \mu + \tau_i + \beta_j + \gamma_{k(j)} + (\tau\beta)_{ij} + (\tau\gamma)_{ik(j)} + \varepsilon_{ijkl}$$

where μ is average for all response variable, τ_i is the effect of risk factor with level i, β_j is the effect of industrial sector factor with level j, $\gamma_{k\,(j)}$ is the effect of company within industrial sector factor with level k(j), $(\tau\beta)_{ij}$ is the effect of interaction between risk and industrial sector factors, $(\tau\gamma)_{ik(j)}$ is the effect of interaction between risk and company within industrial sector factor. The output of ANOVA table can be seen in table 1.

Table 1 The ANOVA Table

Source	DF	SS	MS	F	P
Index	2	1.9581	0.9791	3.74	0.044
Sektor	8	41.6848	5.2106	1.35	0.330
Perusahaan (Sektor)	9	34.7231	3.8581	14.73	0.000
Index*Sektor	16	1.34	0.0838	0.32	0.987
Index*Perusahaan(Sektor)	18	4.7154	0.262	108.66	0.000
Error	594	1.4321	0.0024		
Total	647	85.8535			

S = 0.0491006
R-Sq = 98.33%
R-Sq(adj) = 98.18%

III. RESULTS AND DISCUSSIONS

Using 95% confidence level or α 5%, we can see from table 1 that risk and companies within industrial sector factors significantly influence stock prices. The influence of risk on stock prices is understandable with the real economic situation where the higher the risk, the higher the profit can be attained.

Industrial sector does not significantly influence stock prices for LQ 45. It might due to the behavior of investors that considering more on the internal factor of a company than the sector of industry in buying stocks. This situation indicates that the management of a company may significantly influence investors on deciding which company they want to invest.

The results of this study also show that there is no significant interaction between risk and industrial sector. On the other hand, there is significant interaction between risk and company within industrial sector that influence stock prices.

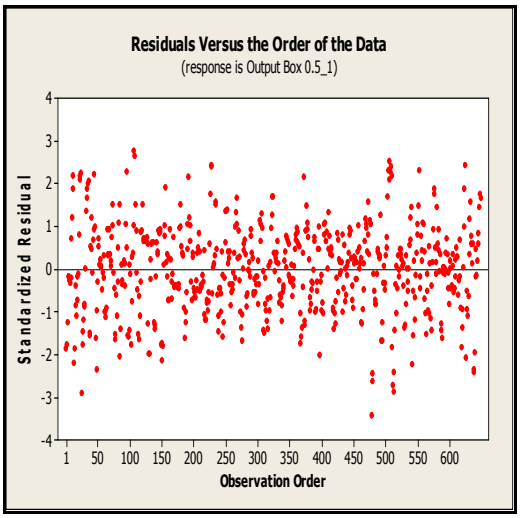

Figure 5: Scatter diagram of Residual Data Vs Run Order

From the R-Square value, it can be seen that the 98.33% of the variation in stock prices can be explained by those three factors, and only 1.67% of the variation is influenced by other factors.

The results of this study show factor combination which gives maximum stock prices as an indicator of profit for investor. Figure 6 shows the main effect plot of risk, industrial sector, and company within industrial sector factors. It shows that investment in high risk, (i.e., in Indosat Tbk within Infrastructure, utility & transportation sector), will give maximum profit of investment from year 2004 to 2006.

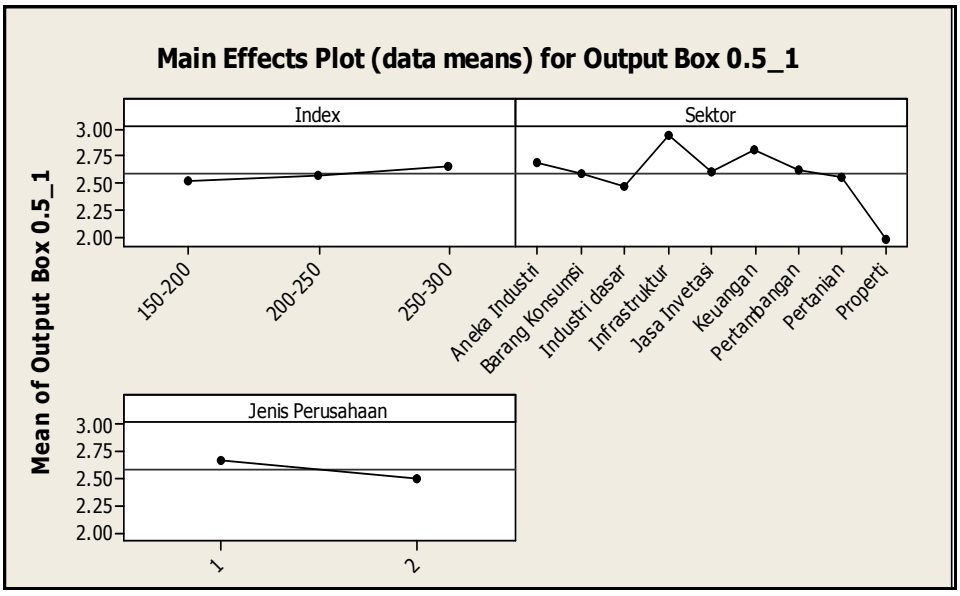

Figure 6: Main Effect Plot of Risk, Industrial Sector, and Company within Industrial Sector Factors

IV. RESULTS AND DISCUSSIONS

Stock prices are profit indicator for investor in buying stocks in Jakarta Stocks Exchange. Using Factorial and Nested design, this study shows that risk and company within industrial sector factors have significantly influence stock prices especially for LQ 45. In addition, there is an interaction between risk and company within industrial sector factors which significantly influence stock prices especially for LQ 45 stocks.

For new investors that want to invest especially in LQ 45 stocks and want to get a maximum profit, an investment should be made on high risk and in Indosat Tbk within Infrastructure, Utility & Transportation sector.

REFERENCES

Journals:

[1] Marit Risberg Ellekjaer, "The Use of Experimental Design in the Development in New Products", International Journal of Quality Science, Vol. 3, No. 3, 1998, hal. 254.

[2] Jiju Antony, "Improving the manufacturing process quality using design of experiments: a case study", *International Journal of Operation & Production Management*, Vol. 21, No. 5/6, 2001, hal. 812.

[3] Jiju Antony, Steve Warwood, Kiran Fernandez, dan Hefin Rowlands, "Process optimisation using Taguchi Method of experimental design ", *Work Study*, Vol. 50, No. 2, 2001, hal. 51.

Book:

[4] Douglas C. Montgomery, *Design and Analysis of Experiments*, Fourth Edition, John Wiley & Sons, New York, 1997, hal. 519.

ISSN: 1411-1284

Six Sigma Application To Improve The Quality Of Cam Chain On Assembly Process In PT. FSCM

T. Yuri M. Zagloel[1], Indra Kurniawan[2].

Industrial Engineering Department, Engineering Faculty, University of Indonesia,
Kampus UI Depok 16424, Indonesia

E-mail: [1]yuriza@indosat.net.id ,[2]indra_ui2003@yahoo.com

Abstract

The Indonesian market of motorcycle industry is a significant growing sector. For this reason, many manufacturing companies outside Indonesia are joining competition. This high competition has grown the need of many companies to improve their quality of products. The motorcycle manufacturing such as PT. FSCM must sustain their customer loyalty, otherwise the company will lose market share.

Quality improvement will be conducted by define-measure-analyze-improve-control (DMAIC) from Six Sigma approach. The Six Sigma approach will measure the current problem with sigma capability, also to improve its capability as known as problem solving. This Six Sigma applies in assembly process at PT. FSCM has a result of 2,79 sigma value. This statement means the process is still far from the ideal target of 6 sigma value. The solution starts with generating capability improvement. It has been conducted by Failure identifications using Cause-Failure-Modes-Effect (CFME) diagram and Failure Mode and Effect Analysis (FMEA).

Finally, the Six Sigma approach will generate the solution by prioritizing. the highest Risk of failure modes, planning the solution and controlling the process.

Keywords : Quality Improvement, Six Sigma Quality, Cause Failure Modes Effect (CFME) and Failure Mode and Effect Analysis (FMEA)

1. Introduction

PT. FSCM Manufacturing Indonesia is local venture company producing motorcycle's spare parts such as chain components. Their main products are cam chain, drive chain, and silent chain. The challence of this company is to assure their customer loyalty concequenthy PT. FSCM should increase and preserve the quality of the products.

Six Sigma way is the one of the commonly quality improvements method which has been introduced by Motorola Company in 1986. There are lot successful company implementing Six Sigma such as General Electric and Xerox, Six Sigma methodology goes beyond statistics, also total management commitment and philosophy of excellence, customer focus, process improvement, and the rule of measurement [1].

Six Sigma way can be certain to increase the quality of product with continuous improvement tools. It has loop model that is "define measure analyze improve control" (DMAIC) and the measurement reaching out for the result. Since PT. FSCM should have a clear commitment to preserve their quality of product by reducing dramatically customer claim problems.

2. Methods

Linderman et. al. [2] emphasized the need for a common definition of Six Sigma and proposed: "Six Sigma is an organized and systematic method for strategic process improvement, new product and service development that relies on statistical methods and the scientific method to make dramatic reductions in customer defined defect rates". Meanwhile Peter S. Pande [3] developed a

definition that captures the breadth and flexibility of Six Sigma as a way to boost performance.

The sigma symbol (σ) is the one of Greek letter that be used in statistical calculation measuring the deviation of standard or variability in process. If the business process has reach Six Sigma capability is meant the output of process has twelve standards deviation (σ) where located between statistical control such as upper-control-limit and lower-control-limit. The occurrence of this variation was controlled to 3,4 defects from 1 million opportunity in out of specification. If the sigma value was 6, it means the ideal target is reached.

Six Sigma methodology had been adopted the well known approach that is plan-do-check-action (PDCA) with addition on strategy to acquire the breakthrough. This approach has one function showing clearly the right way to quality project. The all of element from Six Sigma also called DMAIC model, this model contains:

1. Define
2. Measure
3. Analyze
4. Improve
5. Control

There are many tools in the element or step in DMAIC model of Six Sigma and similarly with the other tools in quality improvement such as PDCA. However, in Six Sigma, it is more interesting in application that tools in the systematically way to get result in quality improvement until to implement in manufacturing and services industry. The next process is the selection of quality tools that will be used in the Six Sigma implementation on assembly process at PT. FSCM are follows :

1. Pareto Analysis, Moment of Truth, Critical to Quality (CTQ) Tree, and Supplier-input-process-output-customer (SIPOC) diagram
2. Pareto Diagram, Control Chart (especially U Chart), Process Capability and Yield Value
3. Fishbone Diagram, Cause Failure Modes Effect (CFME) Diagram, and table of Failure Modes and Effect Analysis (FMEA)
4. Table of Action Planning for Failure Modes
5. Control Chart especially U Chart

3. Data Formulation and Analysis

Firstly, the Quality Assurance Department is being observed considering customer perspectives. Then the facts were founded through report of customer claims. The data was conversed to pareto analysis as the first step of Define. Phase the result shows the product of cam chain has the highest number of customer claims as shown in figure 1.

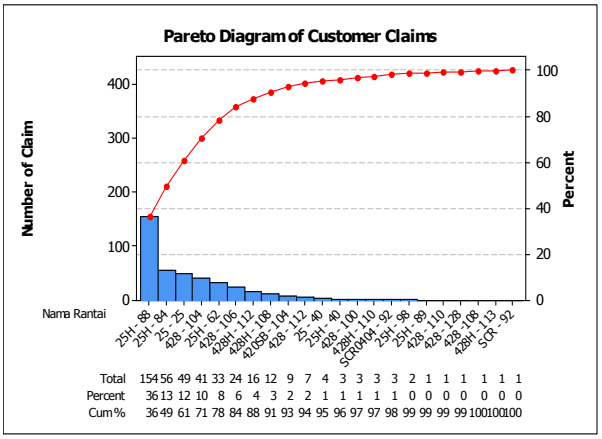

Figure 1 Customer claims conversed in the pareto diagram

The pre-requirement of product output can be defined more specific by using the moment of Truth tool. The meaning is every raw materials before process must fulfill the requirements' in the Moment of Truth as shown in figure 2.

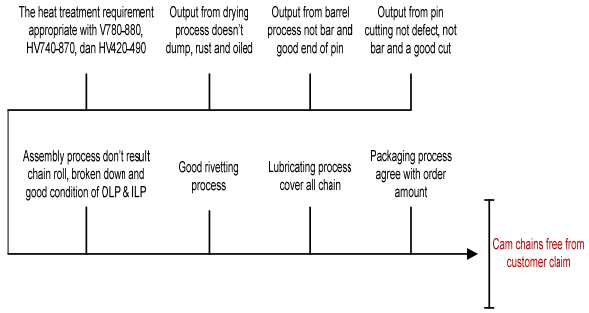

Figure 2 Moment of truth

The quality must be identified known as Characteristic Critical-to-Quality (CTQ) to assure how specification of the cam chain product will meet the customer expectations. These quality characteristics are divided in two critical aspects which are manufacturing quality and assembly quality as shown in the figure 3.

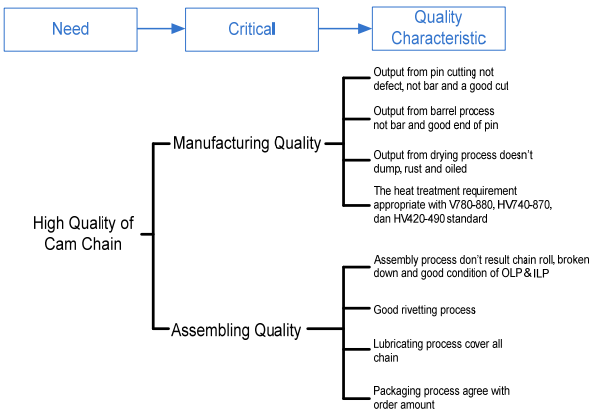

Figure 3 Critical to Quality tree

After identifying quality problems it is necessary to define the types of quality problems that had been claimed by the customers. This result can be used postulate the problem statement. As shown as a Pareto Diagram in the figure 4.

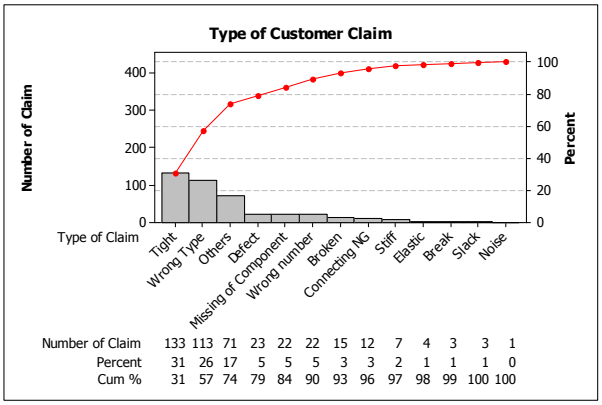

Figure 4 Types of customer claim converted to Pareto Diagram

In the Measure Phase the process capability study is conducted to get the sigma value. The result of this Phase can be seen in the following steps.

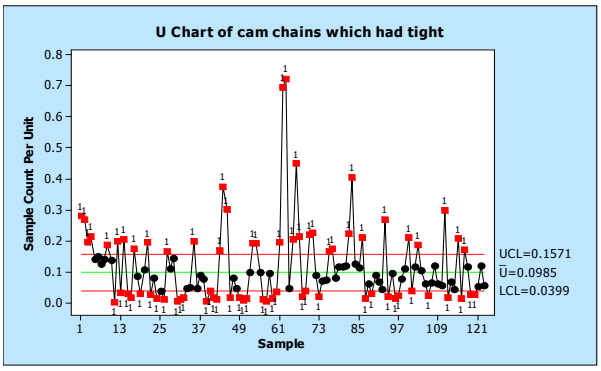

Figure 5 U chart of assembly process

In the figure 5, the U chart shows the assembly process of the cam chain is uncontrollable. The spread of data dominanly are outside the upper-control-limit (UCL) and the lower control limit (LCL). This result indicated these are special causes beside the commonly causes.
The Table 1 below shows the table of Sigma value calculating

Table 1 The means of sigma value calculation

Sample Size	322048	unit
Defect (D)	31717	unit
Opportunity (Opp)	1	
Total Opportunity (Topp)	Topp = U x Opp	322048
Defect per Unit (DPU)	DPU = D / U	0.09848532
Defect per Total Opportunity	DPO = D / Topp	0.09848532
Defect per Million Opportunity	DPMO = DPO x 1000000	98485.3190
The means of sigma value		**2,79**

The process capability has done with the Motorola Six Sigma (shitted 1.5 sigma). By coverting defeet per million opportunity (DPMO) value to 2,79 sigma.

Toward the Analyze Phase, the focus of this step is to look for potential solutions using data had been obtained. In figure 7, the fishbone diagram identifies the potential causes for the cam chain product.

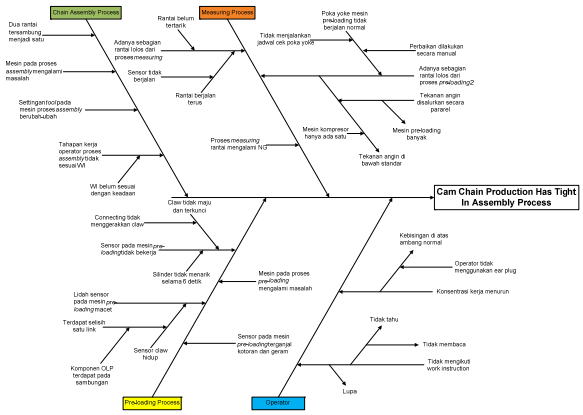

Figure 7 Fishbone diagram

Identifying the relationship between "the cause" and "the effect" should be done with qualitative method called Cause Failure Modes Effect (CFME) diagram. This diagram shows "event" between the cause and effect, which is failure modes. The failure modes was assumed as an incident or failure of quality starting from "the cause" and finally ending by "the effect".

The figure 9 the CFME diagram identifying the failure modes from potential causes.

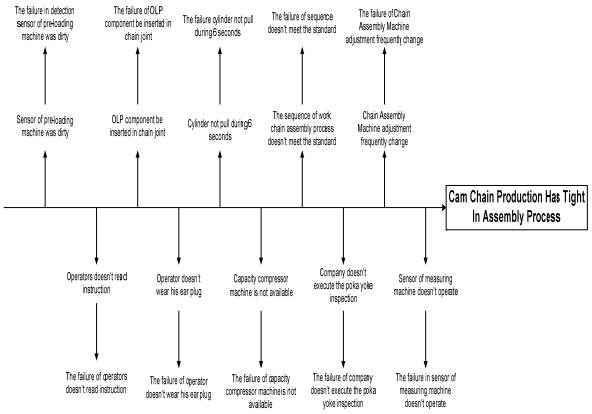

Figure 9 CFME diagram

The next steph in this Analyze please is classifying failure modes that had been obtained from CFME diagram to the table of Failure Modes and Effect Analysis (FMEA). FMEA table is used to a solution in order to anticipate the potential causes that generating the effects. Risk Priority Number (RPN) is obtained from seventy x occurance x detection values (1-10).

Concensus helps to determine the value of each elements.

Table 3 FMEA

Function or item	Failure Modes	Severity	Occurance	Detection	RPN
Chain Assembly Process	The failure of Chain assembly machine adjustment frequently change	8	7	5	280
	The failure of sequence doesn't meet the standard	8	9	6	432
Pre-loading Process	The failure cylinder not pull during 6 seconds	8	8	2	128
	The failure of OLP component be inserted in chain joint	8	5	8	320
	The failure in detection sensor of pre-loading machine was dirty	8	8	7	448
Measuring Process	The failure in sensor of measuring machine doesn't operate	8	6	4	192
	The failure of company doesn't execute the poka yoke inspection	8	9	8	576
	The failure of capacity compressor machine is not available	8	7	6	336
Operator	The failure of operator doesn't wear his ear plug	8	8	7	448
	The failure of operators doesn't read instruction	8	8	7	448

The next phase is Improve which aims to generate improvements also validate the improvements. The proposal considers FMEA table, counsisting of improvements planning for failure modes. Can be seen in table 4.

Table 4 Action planning for failure mode

Failure Mode	Potential Causes	Potential Solution	Responsibility
The failure of routine inspection	There's no effective Poka Yoke inspection	Poka Yoke inspection is based on current situation	Maintenance Department
	The current atmosphere is not ideal for poka yoke mechanism	Develop a new atmosphere that move suitable to Poka Yoke	Research & Development Department
	The lack of operators disciplines to protect company assets	The strict discipline for all operator to maintenance the poka yoke system	Production Department
	poor Poka Yoke knowledge	Training program for operators and technicians	Human Resource Department
	There's no invertment of new Poka Yoke system	Invest new Poka Yoke system which have better performance than the current Poka Yoke system	Financial Department

From the proposal of solution & implementation, the company can monitor the new capability of the assembly process and the compare it with the current capability. In Control phase the control chart tool can be used, especially U chart to monitor the customer claim in the cam chain products.

4. Conclusion

First in the Define phase, it is identified the cam chain products is the highest number of customer claim. The most frequently occurred is too tight of the cam chain. In the Measure phase, the sigma value is 2,79 sigma which means this process is still far from the ideal target of 6 sigma. In Analyze phase, through FMEA the RPN highest number is identified. In the Improvement phase the proposal solving failure modes is generated. Finally, the last phase is Control step, monitoring, those improvements using U chart tools.

References

[1] Pande, Peter and Holp, Larry, 2002, What Is Six Sigma?, McGraw-Hill, p.3
[2] Linderman, K., Schroeder, R., Zaheer, S., Choo, A., 2003, "Six Sigma: A Goal-Theoretic Perspective", Journal of Operations Management, vol. 21, n. 2, Mar., p.195
[3] Pande S. Peter et, al., 2000, The Six Sigma Way, McGraw-Hill, p.preface xi
[4] Stamatis, H. Dean, 2004, Six Sigma Fundamentals: A Complete Guide to the System, Methods and Tools, Productivity Press

ISSN: 1411-1284

RESPONSE PLANNING ANALYSIS IN PROJECT RISK MANAGEMENT OF TELECOMMUNICATION TOWER CONSTRUCTION

M. Dachyar[1] and Maryono NB[2]
Industrial Engineering Department, Faculty of Engineering, University of Indonesia,
Kampus UI Depok 16425, Indonesia.
E-mail: [1]mdachyar@yahoo.com, [2]maryono_ti03@yahoo.com

Abstract

In every project activity we will find number of risks, each with different probabilities and severity levels prior to the achievement of the project's goal. Project team is expected to be able to identify carefully and thoroughly every project activity. One of the methods applicable in identifying project risk is by identifying and grouping project risks using *Work Breakdown Structure* (WBS).

Based on the WBS that comprises of 103 activities, there are 32 high level risks, 37 medium level risks, and 20 low level risks. The identified risks then ranked based on treatment priority list from the probability – impact matrix so that then be obtained a list of risk priority. This list comprises of 32 high level risks and 7 medium level risks. In general, every activity in a project lines in a sequence. This interrelationship might allow a risk treatment activity to deal with the treatment of more than one existing risks in the project. In contrast, a single risk might be treated by several risk action activities. In order to find the most effective treatment activities to apply to the project risks, the source of the risks along with the risks' interrelationship will need to be defined by using risk interrelationship analysis.

Finally we can get a total weight of every treatment activity alternatives from the analysis of the project's critical path combined with *House of Quality* (HOQ). Based on the project critical path analysis and the HOQ approach, this research came to the finding of 11 major treatment activities sorted by the priority to be chosen and taken.

Keywords: Risk management, Work Breakdown Structure, House of Quality, Project risk, Telecommunication

1. Introduction

Nowadays, information and communication technology rapidly grow. It had been motivating companies to perform their competitive advantage by offering the best service for their customer. Network range or signal strength has been one major factor for customer satisfaction that needs to be fulfilled by operators.

This issue drives operators in telecommunication industry to broaden their communication network range of service. This can be achieved by building communication towers in places from population centers to rural areas. Nevertheless, the need of a significantly large amount of time and cost has led telecommunication business operators to apply an effective and efficiency based business decision; that is to outsource the building of communication towers. This shift in industry has caused the emergence of new communication tower building companies.

Along with the advancement of communication technology, there has been a significant increase in the demand of telecommunication tower building from operators. This increase of demand may not only offers company with increased revenues but also face the company to the quality issue, that is as a company that puts customer satisfaction as one primary concern, could company keep its product and service quality steady or even improve it. Customer satisfaction can be achieved if the company applies well managed project and risk management in the planning phase and the implementation phase of their projects. This is the reason that bases the need of risk management implementation by company's management to support the company's telecommunication tower building projects.

In other words project may never be separated from its risk. Because of this a well managed risk management is a must in a project management. Elkington and Smallman found that there is a strong link between the amount of risk management and the level of project

success; more successful projects use more risk management [1].

Company need to be able to identify, analyze, and measure every probable risk and design several effective risk treatment strategies prior to the relevant risks. This may be done to allow company to improve its profits through the increase in positive impact events probability and the decrease in negative impact events probability in every project. The ability to identify potential risks and to take steps to avoid them are two of the most important aspects of good project management [2].

2. Research Method

Generally, this research consists of five steps – risk identification, qualitative risk analysis, quantitative risk analysis, risk response planning and risk monitoring and control. There are 3 methods using in data collecting. They are interviewing project team to identify risks in each project activity; propagate questioner to determine risk level; and brainstorming with the project team to determine the best risk response planning that should be taken.

The first step of this research is identifying risk to find out risks that possibly occur in each project activity. Risk identification was conducted by interviewing and document reviewing. Identified risk would be categorized by using *Work Breakdown Structure* (WBS) method. Risk is categorized based on the project activities where they occur. The primary outputs from this step are risks event, source of risks and risks impact.

Outputs from the risk identification will be used as input on qualitative risk analysis. Qualitative risk analysis assesses the priority of identified risks using their probability of occurring, the corresponding impact on project objective if they occur. Risk level is determined by multiplying level of probability and risk impact. We have propagated questioners for *director of tower*, *general manager* from each division, and *manager* form each department to find level of probability and impact of identified risk.

Level of probability and impact are determined according to responder's opinion on those questioners. Level of probability consist of five levels those are "almost certain", "likely", "possible", "unlikely", and "rare". Numerical scales assign values to these probabilities. These values are 5, 4, 3, 2, and 1 [3]. The impact scale reflects the significant of impact on each project objective if a risk occurs. Relative scale for impact consists of "extreme", "critical", "major", "minor", and "insignificant" that represent numeric scale values of 16, 8, 4, 2, and 1 [4]. Risks are prioritized according to their potential implications for meeting the project's objective. The typical approach to prioritizing risks is to use a probability and impact matrix below.

Probability and impact matrix categorizes risks into high risk (dark gray area), medium risk (medium gray area) and low risk (light gray area). The risk categorization helps guide risk responses. For example, risk that is in the high risk (dark gray) zone of the matrix may require priority action and aggressive response strategies. There are 39 major risks in telecommunication tower construction project based on result of questioner.

Risk Level			Impact				
			Insignificant	Minor	Major	Critical	Extreme
			1	2	4	8	16
Probability	Almost certain	5	5	10	20	40	80
	Likely	4	4	8	16	32	64
	Possible	3	3	6	12	24	48
	Unlikely	2	2	4	8	16	32
	Rare	1	1	2	4	8	16

Figure 1. Probability and impact matrix

Table 1. Major risk in telecommunication tower construction project

Risk ID	Risk Level	
SA7a	56.00	High
SA6a	53.33	High
SA7b	53.33	High
CR4a	48.00	High
CR4b	48.00	High
CR1c	34.67	High
CR3a	34.67	High
PM1f	34.67	High
PM2a	34.67	High
PM1c	32.00	High
PM2b	32.00	High
CR3b	30.67	High
SA1a	30.67	High
PM3.1a	29.33	High
PM1i	28.00	High
SA10a	26.67	High
PM3.1b	26.67	High
CR1a	25.33	High
L2c	25.33	High
L1b	24.00	High
PM1h	24.00	High
L1d	22.67	High
PM3.3b	22.67	High
SA1d	21.33	High
L3b	21.33	High
SA8a	20.00	High
SA10b	18.67	High
L1c	18.67	High
PM1d	18.67	High
ED2.1a	17.33	High
PM1a	17.33	High
PM4.2a	17.33	High
SA4b	16.00	Medium
SA8b	16.00	Medium
SA1b	14.67	Medium
SA6b	14.67	Medium
L1a	14.67	Medium
PM1g	14.67	Medium
PM3.4b	14.67	Medium

3. Result and Analysis

Every activity in a project lines in a sequence. This sequence places every activity in a relation with another activity. The condition of interrelated activities in the project leads the research to the possibility of the interrelating risks within different activities. This interrelationship might allow a risk treatment activity to deal with the treatment of more than one existing risks in the project. In contrast, a single risk might be treated by several risk action activities. In order to find the most effective treatment activities to apply to the project risks, the source of the risks along with the risks' interrelationship will need to be defined by using risk interrelationship analysis or risks – risk treatment activity alternatives interrelationship diagram.

Table 2. Risk response planning alternatives

ID Action	Description
1	Contractor capacity analysis
2	Assessing continuous contractor performance
3	Making the work standard (information) of what to be done and reported by site acquisition contractors
4	Defining standard contractor work time and quality along with agreement for penalties
5	Increasing amount of interdepartmental communication and coordination
6	Increasing communication and coordination with operators and contractors
7	Workload and job analysis
8	Training and knowledge transfer
9	Redesigning and adjusting information standards (work specification) needed in purchase orders
10	Creating and maintaining good relationship with local government
11	Redesign standard for BAPS procedure
12	Redesigning project's standard cost with respect to cost tolerance for the works that more less into funding standard of the upcoming tower construction projects
13	Increasing public socialization through mass media

Next step of this research is to choose the best risk response planning. Risk response planning is the process of developing options, and determining actions to enhance opportunities and reduce threats to the project's objectives [5]. The risk response planning is a major phase in the project risk management process [6]. For cost-effective management it is desirable to distinguish not only between size of impact and probability of impact occurring, but also other factors such as the nature of feasible responses, and the time available for responses [7]. Therefore, we have to analyze the priority of action planning to obtain effective risk action.

From risk interrelationship analysis and risk response planning alternatives above, we will obtain an interrelationship between risk response and the risk. Black circle represent a strong interrelationship, white circle represent medium interrelationship, and triangle for a low interrelationship. Critical path risk on the matrix diagram (Risk ID written in bold and italic letters) represents that the risk is involved on project's critical path. Risks that are the members of this critical path are better to be prioritized in term of treatment to prevent delays or lateness in the achievement of project's finishing time. According to table 3, ID CR4a didn't involve on project's critical path and it is responded only by a single action that is ID action 11. Therefore, we shouldn't take this action to increase the effectiveness of risk response cost. We can assign ID action 6 to response this risk.

We can find something in common with risk L1a. This risk also may be handled only by redesigning project's standard cost with respect to cost tolerance for the works that more less into funding standard of the upcoming tower construction projects. (ID action 12). In addition, it can also decrease the probability of over budget that is caused by other risks. Therefore, it may be included in risk response planning.

Table 3. Risk diagram matrix

Risk ID	Risk Level	ID Action																									
		1		2		3		4		5		6		7		8		9		10		11		12		13	
		P	I	P	I	P	I	P	I	P	I	P	I	P	I	P	I	P	I	P	I	P	I	P	I	P	I
SA7a	56					●										●										●	
PM3.3b	22.667																				○						
SA6a	53.333																				△						
CR3b	30.667																										
CR4b	48															●											
SA6b	14.667																										
SA7b	53.333																										
SA10a	26.667																										
CR4a	48												○									●					
CR1c	34.667		●												●												
CR3a	34.667	●								●				●				○									
SA8b	16																										
PM1f	34.667			●		●			●																		
PM3.4b	14.667																										
PM2a	34.667	●		●		●		●		●		●		●		●		●		●						●	
PM3.1a	29.333																										
SA1a	30.667		○											●			○										
PM1c	32																										
PM2b	32	●		●		●		●		●		●		●		●		●		●						●	
PM3.1b	26.667																										
PM1i	28																								●		
CR1a	25.333											●						●									
L3b	21.333																										
L2c	25.333	●																									
L1c	18.667																										
L1b	24	●																									
PM1h	24	●																									
L1d	22.667			●					●																		
SA1d	21.333																										
SA8a	20			●																							
SA10b	18.667																			●							
PM1d	18.667													●			●										
PM4.2a	17.333																										
ED2.1a	17.333									●				○													
SA1b	14.667																										
PM1a	17.333							○		●																	
SA4b	16					●										●											
L1a	14.667																							●			
PM1g	14.667											●															

Table 4. Weighted scoring of risk response planning

ID Action	Weigthed Score	Priority
8	4028	1
1	2744	2
7	2712	3
3	2544	4
2	2076	5
4	1948	6
5	1860	7
13	1812	8
6	1800	9
9	1628	10
10	1325.333333	11
11	432	12
12	384	13

Based on matrix diagram above, we can determine total weight of every treatment activity alternatives from the analysis of the project's critical path combined with *House of Quality* (HOQ) approach where the risk represents customer's needs and risk treatment activities represents technical response. Strong relationships are converted into the value of 9 while medium strength relationships converted into 3 and weak relationships converted into 1 [8]. Technical characteristic in HOQ is represented by risk treatment actions, customer needs are represented by risks, and the weights of customer needs are represented by risk levels. By quantifying these relationships we can get the weight of importance out of every risk treatment actions. This result may provide considerations in choosing action alternatives.

Based on total weight analysis, we can conclude that ID action 11 and ID action 12 are two of risks response plans with the lowest total weight. This finding shows that in actual time project team is better not to be applying other risk treatment actions other than the risks with higher total weights.

Final step of this research is monitoring and controlling risks to obtain a risk trend and effectiveness of risk response planning.

4. Conclusion

The result of critical path analysis and total weight analysis with HOQ approach the research has came up to the finding of 11 treatment actions that is prioritized in the following list:

1. Training and knowledge transfer
2. Contractor capacity analysis
3. Workload and job analysis
4. Making the work standard (information) of what to be done and reported by site acquisition contractors
5. Assessing continuous contractor performance
6. Defining standard contractor work time and quality along with agreement for penalties
7. Increasing amount of interdepartmental communication and coordination
8. Increasing public socialization through mass media
9. Increasing communication and coordination with operators and contractors
10. Redesigning and adjusting information standards (work specification) needed in purchase orders
11. Creating and maintaining good relationship with local government

Reference

[1] P. Elkington and C. Smallman, "Managing Project Risk: A Case Study from the Utilities Sector", in *International Journal of Project Management*, Cambridge University Press, United Kingdom, 2002, p.53.

[2] R.W Stewart and J. Fortune, "Application of Systems Thinking to the Identification, Avoidance and Prevention of Risk", in *International Journal of Project Management*, Elsevier Science Ltd, Vol.13, No.5, 1995, p.279

[3] F.D Patterson and Neailey, "A Risk Register Database System to Aid the Management of Project Risk" in *International Journal of Project Management*, vol.20, Elsevier Science Ltd, Great Britain, 2002, p.369

[4] Office of Project Management Process Improvement, "Project Risk Management Handbook" First Edition, Sacramento, 2003, p.2

[5] Project Management Institute, "A Guide to the Project Management Body of Knowledge (PMBOK) Third Edition", Project Management Institute Inc, Pennsylvania, 2004, p. 260

[6] B. David and T. Raz, "An Integrated Approach for Response Development in Project Planning", Vol.52, No.1, Operational Research Society Ltd, 2001, p.14

[7] S C Ward, "Assessing and Managing Important Risks" in *International Journal of Project Management*, vol.17, no.6, Elsevier Science Ltd, Great Britain, 1999, p.331

[8] A. Rao et al, *Total Quality Management: A Cross Functional Perspective*, John Wiley & Sons Inc, 1996, Canada, p.397

ISSN: 1411-1284

Developing A Performance Measurement System in Maintenance Department With Balanced Scorecard Method

M. Dachyar[1], Muhammad Darliansa Hilmy[2]
Industrial Engineering Department, Faculty of Engineering, University of Indonesia,
Kampus UI Baru, Depok, 16424, Indonesia
Mail: [1]mdachyar@yahoo.com, [2]darliansa@gmail.com

Abstract

Research on maintenance performance has been done in many ways and well advanced in many domains. Traditional measures such as productivity, efficiency, and effectiveness have many limitations that make them less applicable in today's complex industrial environment; whereas they do not provide a balanced viewpoint of maintenance system performance as a whole.

BSC performance measurement method is very comprehensive whereas the measurement is reviewed on four perspectives, which are consumer perspective, financial perspective, internal process perspective, and learning & growth perspective. BSC also balances financial and non-financial aspects, long term and short term aspects, and internal and external aspects.

This research shows that from six strategic objectives it has, Maintenance Department has not yet achieved any of them perfectly, because it has just got 4 KPIs from total 14 KPIs. In spite of that, overall we can say that their performance is quite well since it had fulfilled their monthly targets and currently in progress in achieving their yearly targets. This research also formulates 20 strategic initiatives which it can use to improve their performance.

Keywords: System, Balanced Scorecard, Performance, Measurement, Maintenance, Management.

1. Introduction

Performance measurement is one of the main elements of management, and the selection of performance measurement system is necessary for a company to achieve its goals. It is also become very important for the managers knowing whether it has achieved their goals or not, and help it in making strategic decisions. Until today, many experts around the world have developed lots of maintenance methods to increase maintenance capability by concerning in performance measurement system [1].

Balanced Scorecard (BSC) is one of popular methods which have been used in many companies. Introduced in 1992 by Kaplan and Norton, this method has been altered so that it can gives other advantages, such as measuring company's performance and helping them to achieve their goals. Performance will be measured in four different perspectives, which are finance perspective, consumer perspective, internal business perspective, and learning & growth perspective. It also translates the company's missions and strategies into strategic objectives along with its measurements that useful for communicating business strategies to all employees at every level of organization. By implementing BSC, company would increase maintenance productivity and enabling them to achieve their strategic objectives.

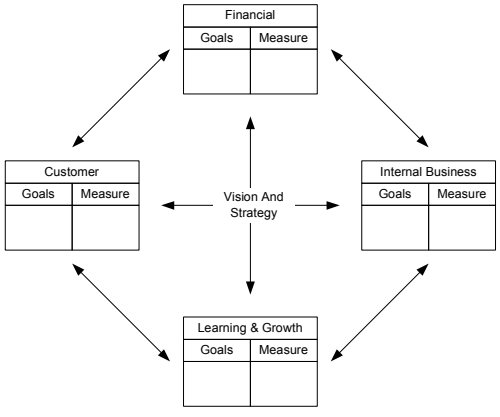

Figure 1. Balanced Scorecard Method

Furthermore, a research about maintenance performance measurement had been conducted in industry to improve their maintenance performance measurement system.

The main objective of this research paper is to obtain a BSC model which is fit for Maintenance Department of

company. Other objective is to formulate strategic initiatives which can improve their performance. In formulating the initiatives, performance measurement is also conducted with the BSC model which had been developed before.

2. Methodology

In developing a BSC model, methodology that writer used is as follows [2]:

1. Analyzing internal and external condition of Maintenance Department.
2. Analyzing the existing performance measurement system.
3. Identifying missions, strategies, and key success factors of Department.
4. Formulating strategic objectives for each BSC perspectives.
5. Giving weight to every strategic objective in each perspective with Analytic Hierarchy Process (AHP) method.
6. Assigning key performance indicators (KPI) and its targets for each strategic objective.
7. Conducting performance measurement with BSC model.
8. Formulating strategic initiatives which suitable for Department Maintenance.

This methodology will be used in this research.

3. Maintenance Department

One of telecommunication tower leasing companies which established since 2000. It has become a market leader in Indonesia since then. In 2004 this company deployed a policy to concern on customer satisfaction. Then it assigned new Division and Department handling consumer's needs which are Operation & Maintenance Division and Maintenance Department. Their organization structure describes in figure 2.

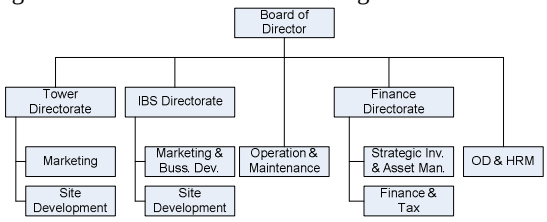

Figure 2. Organization structure

Maintenance Department has identified strategic planning where there are mission and key success factors (KSF) need to be fulfilled. This strategic planning concerned in achieving long range company's goal, includes strategies which can improve their quality. Maintenance Department mission is as follows:

"To prioritize quality of service with focus on quality, cost, delivery, safety and morale."

And also there are some KSFs which it has to obtain, which are:

a. *Excellent Service Maintenance.* This KSF makes it has to give only the best services for their consumers.
b. *Cost Efficiency*. This KSF is a policy from the company to suppress maintenance cost. So then it has to eliminate all non-value added activities.

To achieve those mission and KSFs, it needs accurate strategies. In formulating what strategies are needed, internal factors (strengths and weaknesses) and external factors (opportunities and threats) become important. This strategy formulating method is called SWOT (Strength – Weakness – Opportunity – Threat) Analysis. Currently, this method is very popular and has been used in many companies to formulate correct strategies [3]. SWOT factors of Maintenance Department are as follows:

– Strengths
  a. Skilled maintenance personnel.
  b. 24 hours help desk service.
  c. Have many sites.
  d. Widely coverage area.
  e. Have management information system.
  f. Clustering system which really helpful.
  g. Maintenance personnel are deployed all over Indonesia.
– Weaknesses
  a. A maintenance capacity increment is not proportional with sites increment.
  b. There some procedures that have not been applied yet.
– Opportunities
  a. There are many telecommunication operators in Indonesia.
  b. Telecommunication industry is growth significantly.
  c. Technology is advancing in many ways that can support this industry.
– Threats
  a. Many new entrants competitor in the last few years.
  b. Indonesia consists of many islands.
  c. Their sites are located all over Indonesia.
  d. Consumers become much more aware of quality.

Based on this research, proper strategies for Maintenance Department are as follows:

1. Maintaining first tier consumers by increasing the satisfaction level.
2. Doing investment in maintenance capacity.
3. Increasing the service quality by reducing duration in solving problems.
4. Building a new branch office to support coordination.
5. Increasing maintenance efficiency by applying all operation procedures.
6. Adding training time for personnel.

4. Developing Balanced Scorecard

In an early stage of developing BSC model, a team consists of experts and managers from every field in the

company should be established. This team will be guided by consulting groups who are expert in BSC method. But, in this research, managers' team from the company did not established, so hopefully this model could be a base BSC model which can be implemented by Maintenance Department later, or as an example for other companies.

In deciding what perspectives used for mission, KSFs, and strategies translation, we concern on the balance between financial aspect and non financial aspect; past and future aspects; external and internal aspects. According Kaplan and Norton (1996) in BSC method, there are four perspectives, which are:

1. Finance perspective.
2. Consumer perspective.
3. Internal business perspective.
4. Learning & growth perspective.

Those four perspectives is considered proper for Maintenance Department, but we only change the name of the third perspective into internal process perspective, appropriate with this research scope – Department level.

The next process of developing BSC is evaluating the mission, KSFs, and strategies, then map them into four perspectives of BSC. In this research, mission and KSFs did not need to be changed because it's already fit to company's long range goals. So it can be directly mapped into four perspectives of BSC. The mapping process can be seen in table 1.

Table 1. Mission, KSF, and Strategies Mapping into BSC

Perspective	Mission	Key Success Factors	Strategy
Finance	...focus on cost...	Cost Efficiency	-
Consumers	To prioritize quality of service...	Excellent Service Maintenance	Maintaining first tier consumers by increasing the satisfaction level
Internal Process	...focus on delivery and safety...	Excellent Service Maintenance	- Doing investment in maintenance capacity. - Increasing the service quality by reducing duration in solving problems. - Building a new branch office to support coordination. - Increasing maintenance efficiency by applying all operation procedures.
Learning & Growth	...focus on morale.	-	- Adding training time for personnel.

From master plan of Maintenance Department, discussions with managers, and result of mapping process, then the next step of developing BSC, formulating strategic objectives in each perspective, can be done. Final result of formulating strategic objectives of Maintenance Department is as follows:

a. Consumer perspective:
   - Increasing customer satisfaction index.
b. Finance Perspective:
   - Reducing maintenance cost.
c. Internal Process Perspective:
   - Increasing maintenance capacity.
   - Increasing maintenance service quality.
d. Learning & growth perspective:
   - Increasing maintenance personnel's skill.
   - Increasing work commitment of every personnel.

These strategic objectives basically are mapped from mission, KSFs, and strategies of Maintenance Department. At this point, evaluation must be conducted to make sure interrelation between mission, KSFs, and strategies with each perspective and its strategic objectives. To get more accurate performance measurement in BSC's perspectives, Maintenance Department should determine priorities between those strategic objectives by giving weight to each objective. The priority assignment can be done by giving weight to each perspective as criteria, and each objective as sub criteria. In this research, we use Analytic Hierarchy Process (AHP) method with *Expert Choice 2000* software. The weighting result of strategic objectives can be seen in table 2.

Table 2. Strategic objectives priorities

Strategic Objectives	Weight	Priority
Increasing customer satisfaction index	0,519	1
Reducing maintenance cost	0,221	2
Increasing maintenance capacity	0,086	3
Increasing maintenance service quality	0,086	3
Increasing work commitment of every personnel	0.052	4
Increasing maintenance personnel's skill	0.05	5

To explain each strategic objective into key performance indicators (KPI), we analyze the maintenance business process so that critical factors which influence objectives achievement can be identified. In this research, we use discussion and literature study, and also using KPIs that had been used

before. Totally, there are 14 KPIs for all objectives as a result of this research. Each KPI must have SMART principles, which are specific, measurable, achievable, realistic, and time bound. And also must have cause effect relation between one and another.

After all KPIs had been decided, then the next step is setting target for each KPIs. Methods which can be used for setting target are looking on historical data or setting the target based on discussion along with managers. In this research there are some KPIs that haven't been set targets yet, because those are new KPIs so managers cannot set the appropriate target for sure. For more explanation, all KPIs and its relation to one another can be seen in strategic map, in figure 3.

The comprehensive BSC model with the strategic objectives and KPIs, can be used for measuring the maintenance performance. Table 3 shows the final result of maintenance performance measurement at company. There are some KPIs haven't been measured yet because those are new KPIs and the data was not available on that time. But, overall, their performance is quite well since it had fulfilled the monthly targets and on progress in achieving yearly targets. This research is conducted in early 2007, but their performances on that time nearly achieve yearly targets. And the last step of this research is formulating strategic initiatives for Maintenance Department. These initiatives is formulated by observation all opportunities during the research.

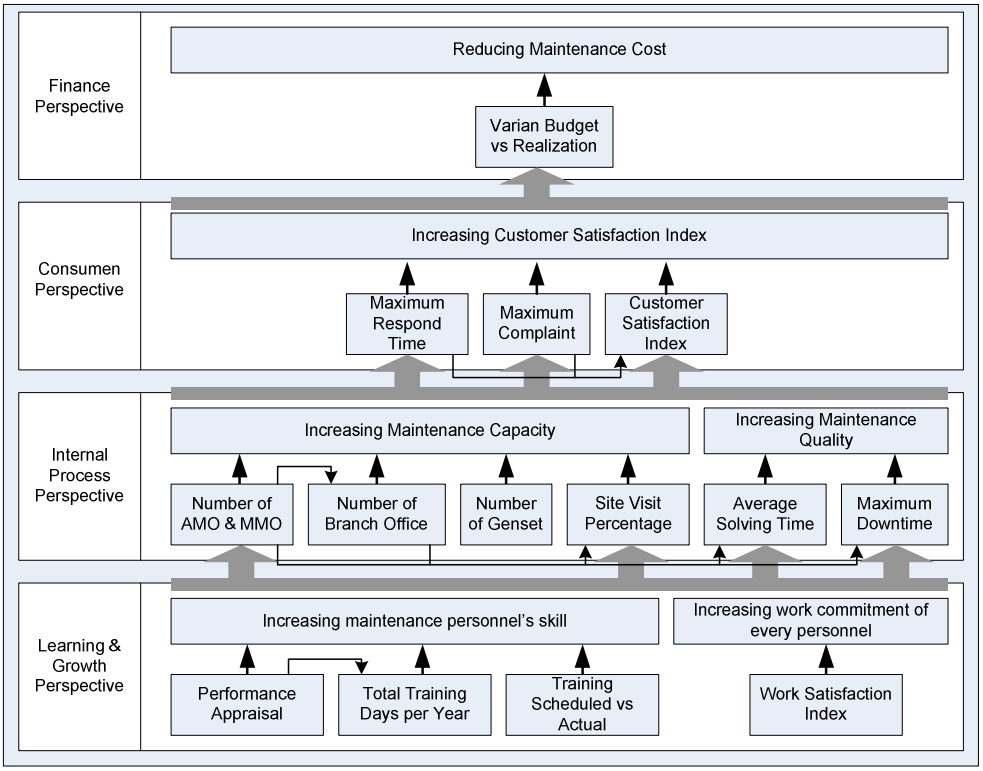

Figure 3. Strategic map of BSC

These are strategic initiatives for each perspective of BSC.

a. Consumer Perspective
   - Applying competitive pricing strategy for gaining more consumers.
   - Making new promotioln programs to appreciate consumers.
   - Increasing efforts to maintain good relationship with old consumers.
   - Maintaining the response time dan solving time.
   - Doing market research to know how hard their competitors are.

b. Finance Perspective
   - Replacing budgeting system with a better one.
   - Monitoring effectiveness of expenditures in Maintenance Department.
   - Maximizing efficiency in operational activities to avoid high maintenance cost.
   - Doing risk analysis of maintenance business process.

Table 3. BSC Model of Maintenance Department with Its Measurements

Perspectives	Strategic Objectives	KPIs	Units	Target	Results
Consumer	- Increasing customer satisfaction index.	- maximum respond time	- Hours per case	- 2 Hours	- Achieved
		- maximum complaints	- % per month	- 2%	- Achieved
		- Customer satisfaction index	- % per 6 months	- 80%	- Not Achieved
Finance	- Reducing maintenance cost.	- Variance budget vs. realization	- % per bulan	- 5%	- Achieved
Internal Process	- Increasing maintenance capacity.	- Number of AMO & MMO	- Value per year	- 10 AMO; 125 MMO	- Not Achieved
		- Number of Genset	- Value per year	- 300 Units	- Not Achieved
		- Number of branch offices	- Value per year	- 4 Office	- Not Achieved
		- Site visit percentage	- % per site per month	- 80%	- N/A
	- Increasing maintenance service quality.	- Average solving time	- Hours per case	- N/A	- N/Ai
		- Maximum downtime	- Hours per case	- 2 Hours	- Achieved
Learning & Growth	- Increasing maintenance personnel's skill.	- Performance Appraisal	- % per 6 months	- 80%	- Not Achieved
		- Total Training Days per Year	- Days per month	- N/A	- N/A
		- Training scheduled vs. actual	- % per year	- 100%	- N/A
	- Increasing work commitment of every personnel.	- Work satisfaction index	- % per 6 months	- N/A	- N/A

c. Internal Process Perspective
   - Recruiting new maintenance personnel for high density area.
   - Maximizing the usage of technology to support the maintenance activities.
   - Outsourcing the supporting activities so that it can focus on the main business.
   - Applying all procedures to every personnel as it is written down.
   - Evaluating the maintenance capacity by evaluating the equipment usage.
   - Doing generators need analysis every 6 months.
   - Making standards for maintenance personnel's work load.

d. Learning And Growth Perspective
   - Creating good and harmonic coordination between personnel and managers.
   - Increasing the number of training days to improve personnel's skills.
   - Involving all personnel in improving Department so it would feel is needed by the company.
   - Making a gathering program to make a better relation between personnel and managers.

5. Conclusion

Based on the research that had been conducted, then we can make a conclusion as follows:

- Developing performance measurement system in Maintenance Department of company with BSC method has given results six strategic objectives for all perspectives and totally 14 KPIs are used.
- The highest priority of strategic objectives is increasing consumer satisfaction index, while the lowest priority is increasing maintenance personnel's skill.
- Ideally we cannot decided whether it has good performance or not, because some measurement could not be conducted. But overall we can say their performance is quite well since it had fulfilled the monthly targets and on progress in achieving yearly targets.
- From this research there are 20 initiatives are formulated, each five initiatives for consumer perspective, four initiatives for finance perspective, seven initiatives for internal process perspective, and four initiatives for learning & growth perspectives.

6. References

[1] Ahmed, Syamsuddin, "Performance Measurement and Evaluation in an Innovative Modern Manufacturing System", *Journal of Applied Sciences*, 1995, pg. 385.

[2] Kaplan, Robert S and David P. Norton, 1996, *Balanced Scorecard: Translating Strategy Into Action*, Havard Business School Press: Boston, pg. 37.

[3] David, Fred R, 2005, *Strategic Management: Concept and Cases*, 10th Edition, Prentice Hall: New Jersey, pg. 75.

ISSN: 1411-1284

A New Paradigm : From Logistics To Supply Chain Management

Dadang Surjasa

Industrial Engineering Trisakti University
Jl. Kiai Tapa No 1 Grogol Jakarta Barat
d_surjasa@yahoo.com, dadang@trisakti.ac.id

Abstract- **According to Council of Logistics Management, logistics is a branch of knowledge which defined as a part of supply chain management. Generally it is about how to procure something, how to storage something and how to deliver something. The problem of this paper is what is something to be procured, stored and delivered. This is the first fact and the focus of this paper.**

Secondly this paper will see chronologically what is the meaning of logistics management. How did the expert from practice or academics define this concept. And how can it be transformed to supply chain management. Then by exploring it with epistemology approach it would be defined new paradigm of logistics management as a part of supply chain management.

With this paradigm, logisticians and supply chain managers will cover the new entity or something new that have to be handled which will make a business environment effectively and efficiently.

Keywords : Logistics Management, Supply Chain Management, New Paradigm

I. INTRODUCTION

Logistics Management in the first idea or in society generally is known as a bundle-handling of 4 flows, namely flows of goods, services, information and money. Logistics Management also has a unique utility that we call it with time and place utilities. Time utility is the value created by making something available at the right time while place utility is the value created or added to a product by making it available for purchase or consumption in the right place. (Stock, 2001). With time utility, value of time will improve because of logistics activities. An example, at night we can improve more our time utilities because there is a flow of information such as internet or tv-cable to our room than before this flow exist. The same as time utility is place utility. With this another one, value of place will also improve because of logistics activities. Example, at one place, without logistics activity like distribution, there is nothing at that place. But with distribution activities, that place would become better in utilization.

This illustration was depicted at figure 1 (Coyle, J.J., 2003)

Figure 1. Utilities in Logistics Management

II. GROWTH OF LOGISTICS AND SUPPLY CHAIN MANAGEMENT

2.1. Logistics Management

Logistics which we recognize in this time, practically had been exploited by military that must insist on state regional of its neighbor. As noted in the year 700 SM, military of Assiria have owned a lot of made armament from iron. They also own a lot of clothes and also carts. They manage it better and they have to provide it in various battle field as in mountain and desert. (www.rickard.karoo.net)

According to La Londe (1994), history expressed that term of "logistique" have been recognized at Napoleon era. A term which is passed to heroic team divisor and to worker whom searching and collecting food for the other livestock animal and horse

Furthermore La Londe (1994), said that in the year of 1920, term of how to manage goods flow which can decrease expense and to increase the

service, its term of that moment is called as physical distribution. In the year 1948, The American Marketing Association define physical distribution management as "the movement and handling of goods from point of production to point of consumption or use"

Approach to logistics management, started from first approach that is physical distribution. This approach focus on how to move finished goods from a firm to out of a firm. Second approach is called as material management that more focus at purchasing, receiving, material handling, production and inventory control. Third approach is called as business logistics, this approach include two previous approach that is merger between material management and physical distribution (La Londe, 1994).

Simply, this illustration depicted at figure 2 below (Rutner, 2007)

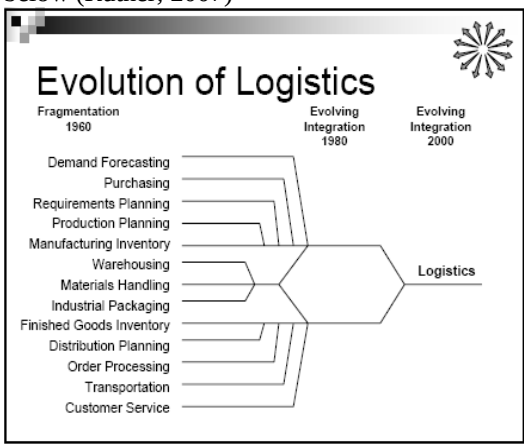

Figure 2. Evolution of Logistics

Approach totally of logistics was given by La Londe (1994) with term "logistics business" and define it as total approach to the management of all activities involved in physical acquiring, moving and storing raw material, in-process inventory and finished goods inventory from point of origin to the point of use or consumption.

Rutner give integrity picture between material management and physical distribution in more totally reflecting logistics business. Simply, it can be seen at figure 3

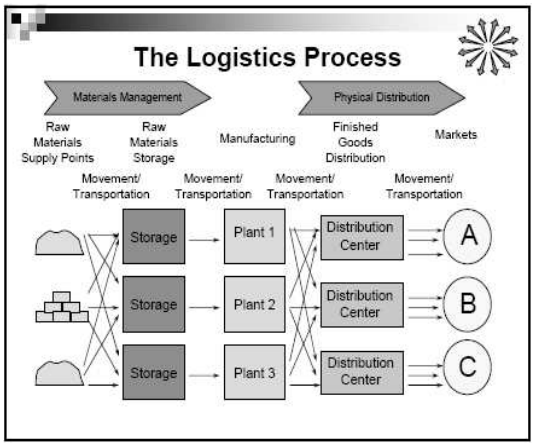

Figure 3. Business Logistics

Meanwhile Johnson (1996) itemizing related things with transfer of goods from all suppliers referred as inbound logistics, movement of goods in one company referred as material management, evacuation of finished goods from a company to customers referred as physical distribution. While logistics itself defined by entire process of materials and products moving into, through and out of a firm.

National Council of Physical Distribution Management (NCPDM) which has changed to Council of Logistic Management (CLM) (Blanchard, 1998), define logistics as the process of planning, implementing, controlling the efficient, cost-effective flow and storage of raw materials, in-process inventory, finished goods, and related information from point of origin to the point of use or consumption for the purpose of conforming to customer requirements.

According to Council of Logistic Management (CLM) which has changed to Council of Supply Chain Management Professional (CSCMP), they define that logistics management is a part of supply chain management that plans, implements, and controls the efficient, effective forward and reverse flow and storage of goods, services and related information between the point of origin and the point of consumption in order to meet customers' requirements. (http://cscmp.org)

Here, important definition about logistics comes from Prof. Yossi Sheffi from MIT. He define it with managing the flow of items, information, cash and ideas through the coordination of supply chain processes and through the strategic addition of place, period and pattern values (Caplice, 2007).

Development of logistics definition comes from (http://en.wikipedia.org) that define logistics as the art and science of managing and controlling the flow of goods, energy, information and other resources like products, services, and people, from the source of production to the marketplace.

2.2. Supply Chain Management (SCM)

Supply chain management is a concept that will become secondly focus of attention at this paper after logistics management. Broadness of SCM scope totally in fact is very large. According to Damrongwongsiri (2003) related to this fact that there will be no one model which can cover all aspects of all SCM activities.

A lot of party gives definition about SCM. Like Global Supply Chain Forum in Croxton (2001) define that SCM is an integration from various process of business key, start from supplier up to final consumer by preparing goods, service and information which can assign value added for customer and other stockholders.

A model for SCM that given by Croxton (2001) depicted at figure 4

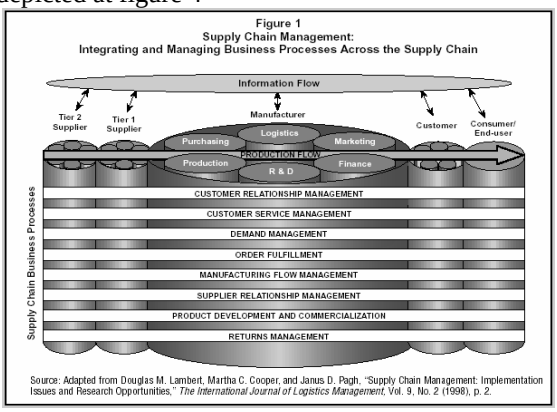

Figure 4. SCM Model

In this model, SCM covers eight processes, namely : Customer Relationship Management, Customer Service Management, Demand Management, Order Fulfillment, Manufacturing Flow Management, Supplier Relationship Management, Product Development and Commercialization and Return Management.

Bolststof (2003) interpreting that SCM is an integrated process from an institution activity started from phase plan, source, make, deliver and return to handle goods, service and also information from supplier early untill to final hand customer.

Meanwhile Levy (2003) interpreting that SCM is a set of approach which efficiently integrate supplier, manufacturer and warehousing so that the product yielded can be distributed with appropriate amount to right place so that minimization of total cost can be reached whereas customer service level remain to be kept. According to Christofer (2005), SCM is an upstream and downstream relationship management with all suppliers and consumers to deliver superior customer value with low expense to entire chain.

Here is an illustration of SCM depicted by Russel (2006) at figure 5.

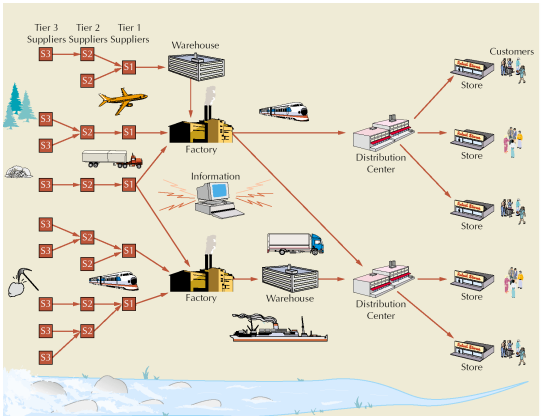

Figure 5. An Illustration of SCM

A new idea of SCM given by Rutner (2007) like depicted at figure 6 that SCM cover three functions of management like what Coyle presented at figure 1. According to Rutner here that SCM cover logistics, production and marketing function, so we can say that SCM also cover all utility : time, place, form and possession utility.

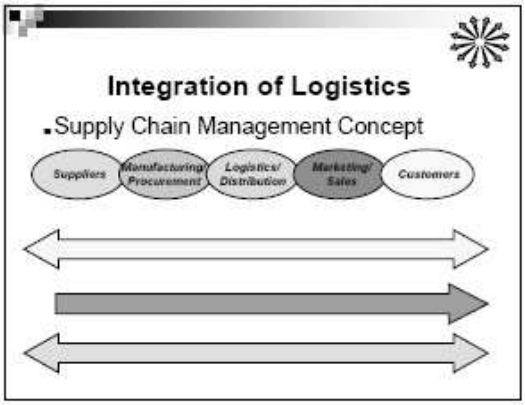

Figure 6. Rutner`s Concept of SCM

III. DISCUSSION AND RESULT

From those various definitions, we can see that logistics management basically is science, but there is also enhancing of it as art. So we can say that logistics management is not only act as science but also act as an art which plan, handle and control of various flows. Started only from flow of goods, flows of goods and money, flows of goods and service, flows of goods and information, flows of goods, service and information and then flows of goods, information, money and idea. Finally, flows that handled in logistics management are flows of goods, service, information, people and energy.

Here, it will be proposed a new definition of logistics management. New definition of logistics

management is science and also art which plan, apply and control 10 flows by reversible through procurement, storage and distribution from supplier up to customer as a mean to decrease logistics costs and also give satisfaction to customer and supported by its supporter activity. The ten flows are flows of goods, service, information, money, idea, people, energy, place and time and also trust. While supporter activity for procurement is : demand forecasting, purchasing, receiving, order processing, reverse logistics and also information system. Storage activity supported by warehousing, material handling, production planning and inventory control, information system , reverse logistics and packaging. While distribution activity supported by traffic and transportation, information system, customer service and also reverse logistics

This new definition can be easily seen at conceptual model like figure 6 below.

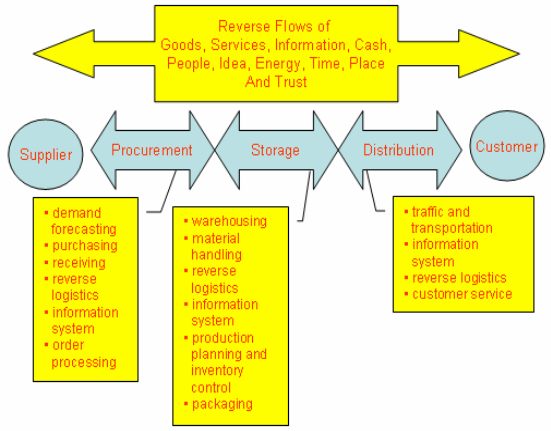

Figure 6. A Model of New Logistics Definition

Firstly based on Council of Supply Chain Management Professional (CSCMP) definition that logistics management is a part of supply chain management. Secondly based on mathematical logical thinking that A subset B if and only if for any x which is element at A is element at B. So we can say that SCM in a new paradigm is also management of ten flows like all of flows in logistics management. And a new paradigm in SCM covers not only logistics and production function but also marketing function. This model depicted at figure 7.

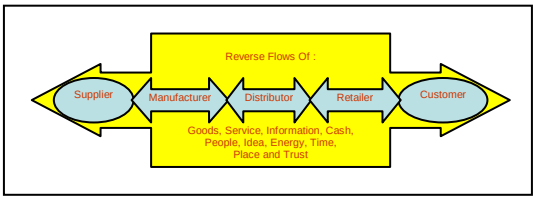

Figure 7. A Model of New SCM

IV. CONCLUSION

New definition of logistics and new paradigm os SCM have the character of reversible for every flows and in each supporter activity. With this one for example for energy flow, logisticians and supply chain manager will give big attention at how many energy, specially at energy which do not newly (oil fuel, electrics, gas, inclusive also the nuclear) which must be kept. As a result at one particular process manufacturing for example, related input of energy will be calculated carefully with capacities produce and the product goals which must be yielded.

With existence flow of time, all logisticians and supply chain manager will claim tightly, how to get product goals with time constraint which is available.

For the purpose of flow of place, here logisticians and supply chain manager in each phase will design all of place with efficiently and effectively which can give highest satisfaction to all customer both internal customer and also external customer.

Last flow is trust flow. With this flow, logisticians and supply chain manager (specially at transportation and distribution) will concern with trusty between and among member of supply chain. They will keep this trusty with their partner that always make good relationship. Oftentimes one company have special trusty to one shipping company to deliver his/ her goods although more expense than other company. At this case, trust more valuable than cost

V. REFERENCES

1. (http://cscmp.org) CSCMP Definition of Logistics Management. http://cscmp.org/AboutCSCMP/Definitions/Definitions.asp**,** 27/09/2007, 14.30 pm

2. (http://www.rickard.karoo.net) Military Logistics:A Brief History. http://www.rickard.karoo.net/articles/concepts_logistics.html, 27/09/2007, 14:00 pm
3. Blanchard, Benjamin S. Logistics Engineering and Management. 1998
4. Bolststof, Peter. 2003. Supply Chain Excelence. New York: AMACOM
5. Caplice Chris, Supply Chain Management Overview I, MIT Center for Transportation & Logistics. 2007
6. Christopher, Martin. 2005. Logistics And Supply Chain Management: Creating Value-Adding Networks. London: Prentice-Hall, Inc

7. Coyle, J.J., Bardi, E.J., Langley, C.J. Jr (2003), The Management of Business Logistics, 7th ed., South-Western, Mason, OH, .
8. Croxton, Keely L., Sebastián J. García-Dastugue And Douglas M. Lamber. 2001. The Supply Chain Management Processes. The Intern. Journal Of Logistics Management, Vol 12, Number 2
9. Damrongwongsiri, Montri. 2003. Global Modelling Strategic Resource Allocation in Probabilistic of Supply Chain System with Genetic Algorithm. Phd Thesis. The Strait Of Florida, Atlantic University
10. Johnson, James C. Contemporary Logistics. 6th edition. Prentice Hall. 1996
11. La Londe, Bernard. Evolution of the Integrated Logistics Concept. dalam Robeson, James F. The Logistics Handbook. 1994
12. Levi, David S., Philip Kaminsky, and Edith Simchi Levi. 2003. Designing And Managing the Supply Chain: Concepts, Strategies, and Case Studies. Singapore: Irwin Mcgraw-Hill
13. Logistics Origins_and_definition Origins, http://en.wikipedia.org/wiki/Logistics#Origins_and_definition Origins and definition, 27/09/2007,14.45pm
14. Russell, Roberta & Bernard W. Taylor.2006. Operations Management - 5th Edition: Supply Chain Management, Jhon Wiley and Sons.
15. Stock, James R., Douglash Lambert. 201. Strategic Logistics Management. Mc Graw-Hill, Irwin

ISSN: 1411-1284

Design Of Vendor Performance Rating Model Using The Analytic Network Process

M. Dachyar[1], Ade Amalia Lubis[2]
Industrial Engineering Department, Faculty of Engineering, University of Indonesia
Depok, 16424, Indonesia
E-mail: [1] mdachyar@yahoo.com ; [2] ade_tiui03@yahoo.com

Abstract

Site Acquisition (Sitac) is one of the most important process which may determine the success of Base Transceiver Station (BTS) tower construction project. Company which run a business in providing BTS tower construction and rental, trusting their vendor for most of activities in site acquisition process. Therefore, to support the success of tower construction project, it needs to evaluate the performance of site acquisition's vendor which can also accommodate vendor selection for next project. Company should also identify factors which influence the success of contractor or vendor performance in site acquisition, both qualitative and quantitative. Beside that, it needs a model to evaluate vendor performance based on those factors.

In this research, it will be created a rating model for site acquisition vendor performance using the Analytic Network Process (ANP), a decision making method that makes it possible for us to deal systematically with all kinds of dependence and feedback. All supported data which used to generate this rating model is derived from subjective decision by several experts in company who experienced in tower construction project, including its shareholder.

Rating model construction is started from selecting criteria and sub criteria which influence the success of site acquisition contractor performance, identifying relationship between sub criteria and criteria, and then weighting those criteria and criteria. This research also generates rating sample and a form which can be implemented in evaluating site acquisition contractor performance.

Keywords: Decesion, Contractor Selection, Site Acquisition, Rating, Analytic Network Process.

1. Introduction

Materials and services are the main requirement to run a business. Also in a Base Transceiver Station (BTS) tower construction project, materials and services are needed in constructing a tower, start from site acquisition process which will be located for the tower until the construction process is well done. Site acquisition is one of the most important and difficult process in a tower construction project, regard that there are many people who related in getting permissions to build the tower in that site.

Company which run a business in providing tower construction and rental to the telecommunication providers (operators). In order to accomplish the site acquisition process, company usually hire a vendor who provides site acquisition service. Together along with the growth of cellular phone's users in Indonesia, Company immediately uses this opportunity by increasing their target number of tower construction projects. But, the increase of project's target number also needs the increasing of optimum performance by everyone who related in tower construction, including their vendor performance. Company needs to be more selective in choosing their site acquisition vendors. Vendor selection can be accommodated by result of vendors rating whose past performance have been known . Vendor rating decisions are complicated by the fact that various criteria must be considered in decision making process [9]. Vendor rating is one of the decision making process which consider various criteria either qualitative or quantitative. In this problem, those criteria are considered as the important factors which influence the success of site acquisition contractor performance, based on the need of company. This kind of vendor rating problem is also recognized as a decision making problem which has interdependencies and feedbacks among criteria,

so that it needs the Analytic Network Process to be implemented in solving this problem.
The Analytic Hierarchy Process serves as a starting point for the ANP [4,5,8,10], which is proposed earlier by Thomas L. Saaty in 1980. Nevertheless, AHP is used only for problem solving which has linier structure. ANP, the general case of AHP, makes possible the representation of any decision problem without assumption about the linier structure. So, it can be used for problem solving which have complex relationship (interdependencies and feedbacks) among criteria.

2. Methods

This research was started from determining its topic, goal, and problem's scope. And then the next step would be done by collecting and processing the data which used for creating rating model for site acquisition's contractors. There were 5 main step in designing this rating model, that was choosing the criteria and sub criteria for Sitac's contractors rating, identifying relationship between sub criteria, weighting the criteria and sub criteria, determining and weighting the intensity scale of rating model and making rating model's form.
This rating model could be used for ranking a number of Sitac's contractors who had joined the tower construction project, based on their past performance. In the first step, that was choosing the criteria and sub criteria, several experts would be asked to fill a questionnaire to determine criteria and sub criteria which considered as the important factors that influence the success of Sitac's contractor performance. Respondents were also allowed adding criteria and sub criteria which had not been written in the questionnaire yet.
The second step, that was identifying relationship among sub criteria, was also done by spreading questionnaire to same respondents as the previous questionnaire. This questionnaire was used to identify various relationships among sub criteria which happened in this rating model. After all the relationship among sub criteria had been identified, the network of rating model could be constructed by using Super Decisions which is used for ANP problem solving.
The next step would be done by weighting the criteria and sub criteria by using pair-wise comparisons. Pair-wise comparisons were done according to relationship among sub criteria which had been identified. Collecting data was also supported by questionnaire, where the respondents would be asked to do all the pair-wise comparisons among nodes (sub criteria) with respect to a parent node (node comparison) and also pair-wise comparisons among criteria with respect to a parent criterion (*cluster comparison*) [7,3]. Pair-wise comparison is performed by using a nine point scale of judgement in ANP. The consistency of each comparison must be checked to ensure validity of resulted decision [2]. After averaging the total score from all respondents, priority vectors can be obtained from each pair-wise comparison. Then, enter in the appropriate position the priority vectors derived from node comparisons as parts of the corresponding column of a supermatrix called the unweighted supermatrix [7,3]. Meanwhile, priority vectors derived from cluster comparisons are entered as parts of the corresponding column of a matrix called cluster matrix [7,3]. And then, each column in unweighted supermatrix must be normalized by the corresponding cluster priorities to ensure the columns sums to unity [3,10]. This matrix is called the weighted supermatrix. After that, it will be resulted the limit matrix by raising the weighted supermatrix to k (large power) in order to have the stable values [3,10]. Priority vectors which belong to limit matrix is the final priority vectors of all node or sub criteria in this rating model.
In this model, when one rate the alternatives, they must be independent one another. Therefore, this kind of ranking of alternatives is called absolute measurement or rating [6]. In order to rate alternatives with respect to an a criterion or sub criterion, we need to create intensity scale of variation of quality of this criterion or sub criterion (such as very good, good, not good enough, and poor) The fourth step of design of rating model, that was determining and weighting the intensity scale of rating model, also done by spreading questionnaire. In this questionnaire, respondents were asked to do the pair-wise comparisons of intensity scale's level for each sub criteria. Intensity scales were indicated the variation of quality of each sub criteria which consist of few levels. From the pair-wise comparison, idealized priorities for each sub criteria could be obtained. Idealized priorities of each sub criteria are derived by dividing its vector priorities by the largest value among them [6]. The consistency of each comparison must also be checked.
The last step of design of rating model is making rating model's form. In this step, a form of rating model had been created in a form of Microsoft Excel file which can be used for Sitac's contractors rating application in company.
The results from data processing were need to be analyzed, that is the analyzing of network of rating model which consist of criteria, sub criteria, and relationships which were happened in this rating model. And then, the final priorities of criteria and sub criteria which considered as the factors in influencing the success of Sitac contractors' performance were also analyzed in

this research. In addition, sensitivity analysis has also been done by using a sample case of rating problem of Sitac's contractors.

3. Result and Discussion

From data processing in step 1, it was resulted a number of criteria and sub criteria which considered as the factors which influence the success of Sitac contractors' performance. There were 5 criteria and 25 total sub criteria in this rating model. From 25 sub criteria, there were 5 sub criteria which considered as quantitative sub criteria, they were frequency of reporting progress, punctuality of work completion, notification of possible delays, speed of negotiation process, and speed of survey process. And then from identifying relationships among sub criteria, there were 3 kinds of relationship in this rating model, they were inner dependence, outer dependence, and feedback dependence. Outer dependence would be happened if there are relationships between among sub criteria within a cluster, outer dependence would be happened if there are influences from elements in a criterion to other elements in other criteria, and feedback dependence would be happened if there are mutual outer dependences of sub criteria in two different criteria [8,1].

Data processing in step 3 resulted priorities of all sub criteria. There are two kinds of priorities, they are limiting priorities and priorities which normalized by cluster.

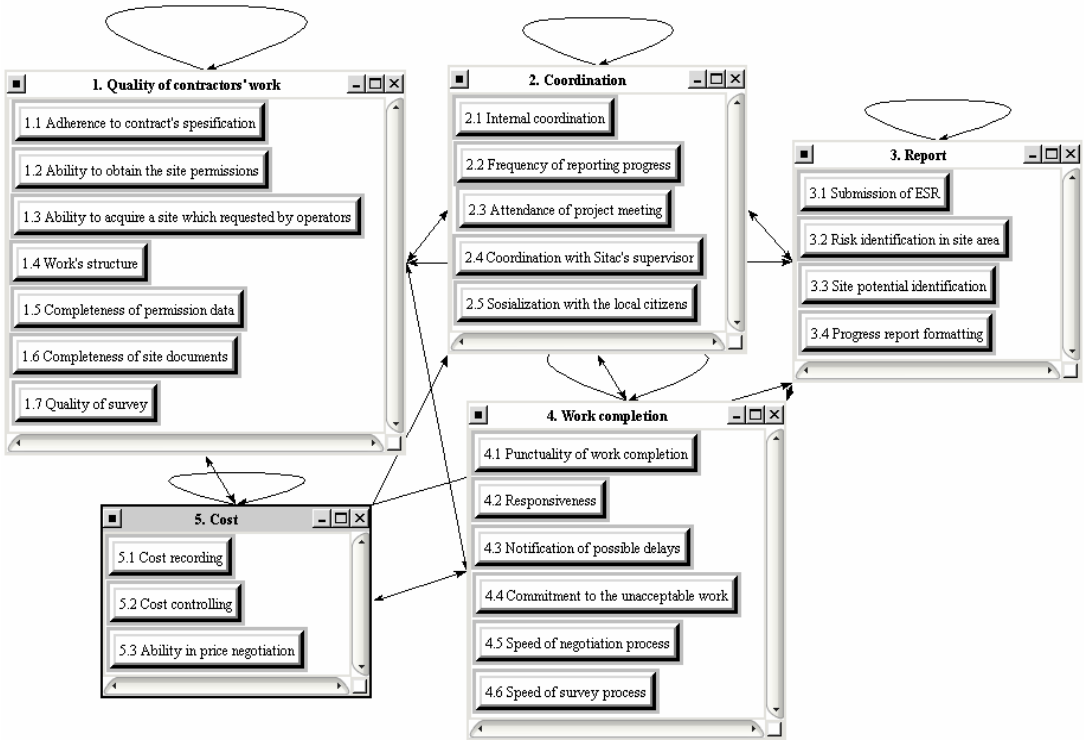

Gambar 1. Rating model for Sitac's contractor

Limiting priorities and priorities normalized by cluster for each sub criteria can be seen in Table 1. It can be summarized that quality of contractor's work (0.4053) is the most important factor which influence the success of Sitac contractor's performance. From the whole rating model, it resulted 5 most important sub criteria, they successively were coordination with Sitac's supervisor (0.116233), completeness of site documents (0.103577), adherence to contract's specification (0.092898), format of progress report (0.089274), and completeness of site permissions (0.082869). Completeness of site documents (0.25557) was the most important factor to evaluate the quality of contractor's work. In coordination, the most important evaluation should be focused on coordination with Sitac's supervisor (0.38421). Format of progress report (0.5617), responsiveness (0.52158), and ability in price negotiation (0.63934) successively were the most important evaluation in report, work completion, and cost.

Table 1. The Priorities of sub criteria

Code	Criteria and Sub Criteria	Limiting Priorities	Normalized by cluster
1	Quality of contractor's work		
1.1	Adherence to contract's specification	0.092898	0.22922
1.2	Ability to obtain site permissions	0.007878	0.01944
1.3	Ability to acquire a site which requested by operator	0.017942	0.04427
1.4	Work's structure	0.043346	0.10695
1.5	Completeness of permission data	0.082869	0.20447
1.6	Completeness of site documents	0.103577	0.25557
1.7	Quality of survey	0.056769	0.14007
2	Coordination		
2.1	Internal coordination	0.042084	0.13911
2.2	Frequency of reporting progress	0.066336	0.21928
2.3	Attendance at project meeting	0.052812	0.17457
2.4	Coordination with Sitac's supervisor	0.116233	0.38421
2.5	Socialization with the local citizens	0.025057	0.08283
3	Report		
3.1	Submission of *Engineering Survey Report* (ESR)	0.05887	0.3704
3.2	Risk identification in site area	0.005491	0.03455
3.3	Site potential identification	0.0053	0.03335
3.4	Progress report formatting	0.089274	0.5617
4	Work completion		
4.1	Punctuality of work completion	0.024005	0.21829
4.2	Responsiveness	0.057358	0.52158
4.3	Notification of possible delays	0.005214	0.04741
4.4	Commitment to the unacceptable work	0.009125	0.08298
4.5	Speed of negotiation process	0.008443	0.07678
4.6	Speed of survey process	0.005824	0.05296
5	Cost		
5.1	Cost recording	0.00047	0.02018
5.2	Cost controlling	0.007932	0.34049
5.3	Ability in price negotiation	0.014894	0.63934

Meanwhile, from the data processing in step 4, it was resulted the intensity scale of each sub criteria in this rating model with each idealized priority. In this research, intensity scale is divided into 4 levels. For the application, intensity scale of quantitative sub criteria were explained by giving an interval for each level of intensity scale in order to give a clearer explanation. Figure 2 showed the intensity scale of each sub criteria in cost and also their idealized priorities.

This research is also provided sensitivity analysis by using a sample case of rating problem of Sitac's contractors.

Sensitivity analysis in ANP method is a what-if type of sensitivity that allows you to select any combination of independent variables [7]. Sensitivity analysis in this research was divided into two steps, they are analysis if the experiments were using variable which has significant influence on the model and analysis if the experiments were using variable which has not significant influence on the model. From the result of experiments were using a variable which has significant influence, alternatives' priorities changed together along with the experiments, especially if the experiments were using multi-variables. Nevertheless, those priorities did not significantly change, only ± 0.001 for each experiment.

Meanwhile, if the experiments using a variable which has significant influence, only one or two alternatives which experienced the priorities changes, but these changes were only happened in one or two experiments. And if the experiments were using multi-variables, all alternatives did not experience the priorities changes at all.

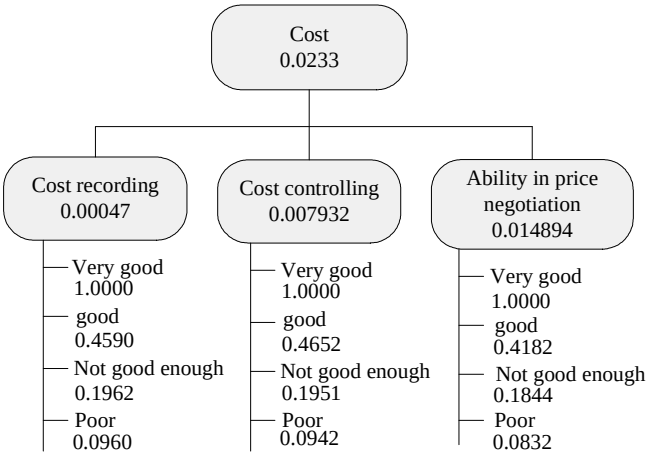

Figure 2. Intensity scale of sub criteria in cost cluster

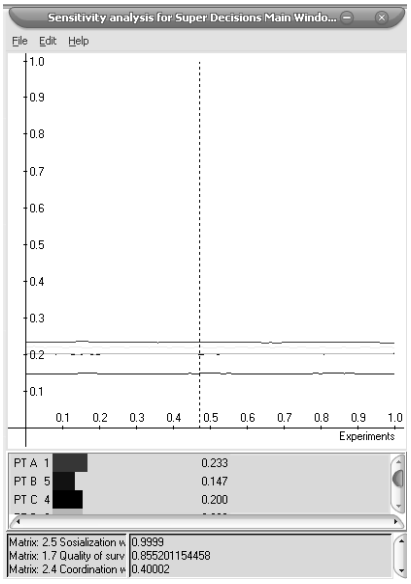

Figure 3. Experiments using the multi-variables with significant influence

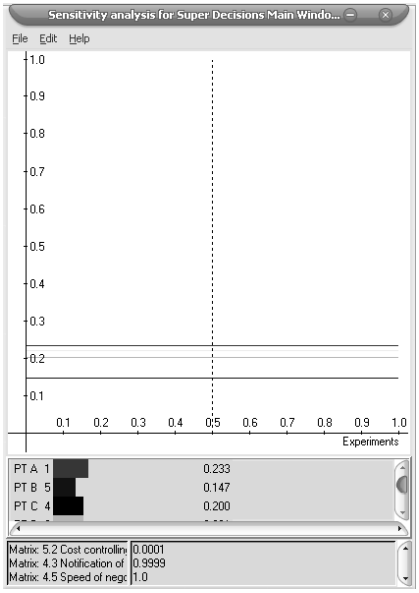

Figure 4. Experiments using the multi-variables without significant influence

It can be concluded that in this rating model which use the Analytic Network Process, the outcome was not sensitive to the parameter changes. It showed that the outcome of the model which with *feedback* are more stabil and robust. If the sensitivity analysis needs to be performed, the experiment should use the multi-variable which Kalaupun analisis sensitivitas tetap ingin dilakukan, sebaiknya eksperimen menggunakan *multi-variabel* which has significant influence on the model.

4. Conclusion

In this research, it has been created a performance rating model for a kind of vendor , which is site acquisition (Sitac) contractor. This rating model consists of 5 main criteria with 25 total number of sub criteria considered as the factors which influence the success of Sitac contractors' performance. There are 3 kinds of relationship which happened within this rating model, they are inner dependence, outer dependence, and feedback dependence. Rating model of Sitac contractors' performance can also be used for ranking a number of contractors and analyzing the important factors which influence the success of Sitac contractors' performance.

Reference

[1] Büyükyazici, Murat dan Meral Sucu,"The Analytic Hierarchy and Analytic Network Processes", Hacettepe Jounal of Mathematics and Statistics", vol.32, 2002, p. 65-73

[2] Gencer, Cevriye dan Didem Gürnipar,"Analytic Network Process in Supplier Selection: A Case Study in an Electronic Firm", Elsevier, 2006, p.1-12.

[3] Piantanakulchai, Mongkut, "Analytic Network Process Model for Highway Corridor Planning", ISAHP, Hawaii, 2005. p.1-10.

[4] Ravi, V. et al.,"Analyzing Alternatives in Reverse Logistics for End-of-Life Computers: ANP and Balanced Scorecard Approach", Elsevier, 2005, vol. 48, p.327-356.

[5] Saaty, T.L, "Fundamentals of The Analytic Network Process", ISAHP, Japan, 1999, p.1-14.

[6] Saaty, L. Thomas,"Rank from Comparisons and from Ratings in the Analytic Hierarchy/Network Processes", Elsevier, 2004, vol. 168, p. 557-550.

[7] Saaty, Rozann. W., *Decision Making in Complex Environment*, Creative Decision Foundation, Pittsburgh, 2003, p.1-114.

[8] Uysal, Kanat et al.,"ANP Application For Evaluating Turkish Mobile Communication Operators", MCDM 2006, Greece, 2006, p.1-10.

[9] Weber, C.A., J.R Current, W.C. Benton,"*Vendor* Selection Criteria and Methods", European Journal of Operational Research, North-Holland, 1991, vol.50, p.2-18.

[10] Yu, Rachung dan Gwo-Hshiung Tzeng,"A Soft Computing Method for Multi-criteria Decision Making with Dependences and Feedback, Elsevier, 2006. p.1-13.

ISSN: 1411-1284

Optimization of Multi-Responses Process using Response Surface Methodology (RSM) Approach

Sachbudi Abbas Ras, Purdianta
Industrial Engineering Department, University of INDONUSA Esa Unggul, Jakarta
Sachbudi.abbas.ras@indonusa.ac.id ; abbasras@yahoo.com, purdianta_ti@yahoo.com

Abstract– **This research was motivated by the problem faced by PT. XYZ in optimizing one of their processes in order to response the Corrective Action Request (CAR) from their biggest customer. The associated process is the bonding process that joining two layer of papers together using specified glue. In bonding process there are two primary responses, that are Bonding Force with the specification of 10±0.3 kgf and Thickness with the specification of 110±0.2 μm. From specific statistical analysis, it was derived that both responses have no relation at all. The process characteristics which have significant influence to the two responses are Machine Temperature in °C and Machine Pressure in Psi.**
This research have developed unique extension of the regular Response Surface Methodology (RSM) from the Design of Experiments (DoE) discipline, in order to accommodate the two important responses. Using the overlaid of the resulted contour plot for both responses, it was derived the optimal process setting are Machine Temperature on 60.82°C and Machine Pressure on 92.28 Psi.

Keywords: Optimization, Bonding, Multi-Responses, Response Surface Methodology, Contour Plot, Overlaid

I. INTRODUCTION

The manufacturing system always have their highest challenge in the form of the requirement in continuously optimization of their processes. This optimization is extremely important not only to reduce the defect rate impacted, but also in surviving on the rapid industrial competition.

The term 'Customer Satisfaction' are frequently used as the goal of any improvements. PT. XYZ had received many field-claims from their biggest customer that complaining about the quality of their supplied products. To stay on the competition, PT. XYZ should be able to give fast and accurate responses to these complaints.

They have found two primary output characteristics, also known as responses, from their bonding process which are Bonding Force and Thickness with specified specification from the customer. They also found that are two process characteristics, also known as factors, which require intense attention in process optimization. They are Machine Temperature and Machine Pressure.

The associated optimization could be facilitated by using Design of Experiments (DoE) Technique to achieved the requested performances by setting the process on their optimal level. Specifically, this could done by the Response Surface Methodology (RSM) Approach which provided surface and contour plot of the associated factors and responses.

Unfortunately, by far the RSM discussed in many literatures have strict limitation that the approach only discussed single response on the experiment. Meanwhile, it is common for the industry to face several responses in the effort to optimize their processes.

II BASIC THEORY

Every engineering system or process is designed with an intended purpose. The purpose frequently entails a desired performance of the operation of the product being manufactured or of the process that manufactures it. In many cases, engineering design activities involve test or experimentation, since the product or process is not well understood, and desired performance can be guaranteed.

Statistical Design of Experiment (DoE) refers to th process of planning th experiment so that appropriate data that can be analyzed by statistical methods will be collected, resulting in valid and objectives conclusions[**1**]. On the other hand, Response Surface Methodology (RSM) could defined as a collection of mathematical and statistical techniques that are useful for modeling and analysis of problem in which a response of interest is influenced by several variabel and the objectives is to optimize this response.

In process optimization and DoE, the input correspond to variabel we can control during an experiment, and we will refer to these as controllable factors. The output of he process correspond to variables we wish to modify by varying the controllable factors and we will refer to them as process responses. The general model of RSM can be write as following.

$$y = f(x_1, x_2) + \varepsilon \qquad (1)$$

Where ε represent the noise or error observed in response *y*. If we denote the expected response by E(y)= $f(x_1,x_2)$ = ή, then the surface represented by ή = $f(x_1,x_2)$.In the most RSM problem, the form of relationship between response and the independent variable is unknow. Thus, th first step in RSM is to find a suitable appromixation for the true functional relationship between *y* and the set of independent variabel. If the response is well modeled by a linear function of the independent variables, the approximating function is the first-order model.

$$y = \beta_0 + \beta_1 x_1 + \beta_2 x_2 + ... + \beta_k x_k + \varepsilon \qquad (2)$$

If there is curvature in the system, then a polynomial of higher degree must be used, such as the second order model.

$$y = \beta_0 + \sum_{i=1}^{k} \beta_i x_i + \sum_{i=1}^{k} \beta_{ii} x_i^2 + \sum\sum_{i<j} \beta_{ij} x_i x_j + \varepsilon \qquad (3)$$

III. MODEL DEVELOPMENT

The objective of this research is developing a unique extension of RSM approach from DoE discipline to provide the solution of the problem faced by PT. XYZ. The model development scheme is shown on the following Figure 1.

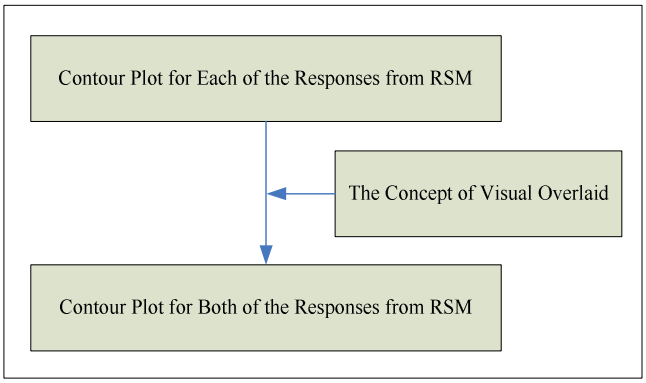

Figure 1. Model Development Scheme

IV. SOLUTION AND ANALYSIS

Screening experiment used to identify influenced factors to output process or response. After screening experiment has done to factors process, so that we obtain information that only two factors whose influence to responses, they are temperature and machine pressure. Meanwhile, consideration responses are bonding force and thickness.

In this research, low and high level for temperature 50 ^{o}C and 80 ^{o}C, respectively. Whereas low and high level for pressure machine 75 Psi and 100 Psi, respectively. Five replication has done for each run. Condition and result experiment for each respon as in table 1.

Tabl. 1 Condition and result of experiment

Run Order	Temp	Press	Bonding Force	Thickness
1	80	100	9.2	109.6
2	50	100	10.5	109.3
3	50	100	10.7	109.2
4	50	75	9.1	110.6
5	50	100	10	110.1
6	50	75	9.5	110.3
7	50	100	10.3	110
8	80	75	10.2	109.7
9	80	75	10.7	111.2
10	80	75	10.6	110.6
11	80	100	9.8	109.4
12	80	75	8.9	110.5
13	80	100	9	109.8
14	50	75	11	110.2
15	80	100	8.9	110.2
16	80	100	9.1	109.8
17	50	75	10.2	110.3
18	50	75	10.5	110.5
19	80	75	9.3	109.7
20	50	100	10.7	110.8

Using MINITAB 15.0 software attained main and interaction effect for temperature and machine pressure to responses as in figure 2 and 3. The result of Analysis of varian (ANOVA) for each responses as in table 2 and 3. After, we have analyzed the responses, we did'nt find interaction between bonding force and thickness. So that the problem can be solved with univariate statistics technique. Throughout RSM approach, specially with contour plot. The factor interaction to responses can be represented in graphically , as in figure 4 and 5.

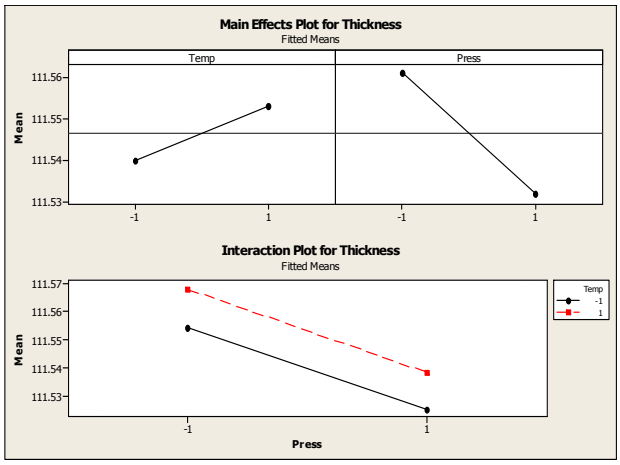

Figure 2. Main and Interaction Effec Plot for Thickness

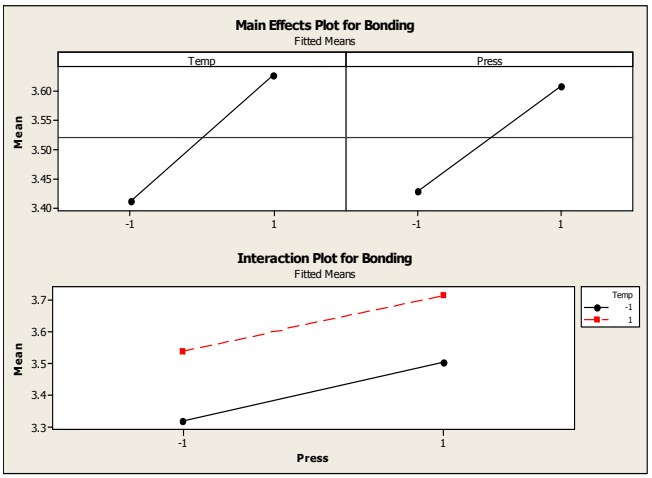

Figure 3. Main and Interaction Effec Plot for bonding

Table 2. Analysis of Varian for Thickness

Source	DF	Seq SS	Adj SS	Adj MS	F	P
Main Effect	2	1.49000	0.86963	0.434814	1.82	0.194
2-Way Interactions	1	0.00800	0.00800	0.008000	0.03	0.857
Residual Erro	16	3.82000	3.82000	0.238750		
Pure Error	16	3.82000	3.82000	0.238750		
Total	19	5.31800				

Table 3. Analysis of Varian for Bonding

Source	DF	Seq SS	Adj SS	Adj MS	F	P
Main Effect	2	2.47400	1.33691	0.668500	1.86	0.188
2-Way Interactions	1	1.56800	1.56800	1.568000	4.36	0.053
Residual Erro	16	5.75600	5.75600	0.359800		
Pure Error	16	5.75600	5.75600	0.359700		
Total	19	9.79800				

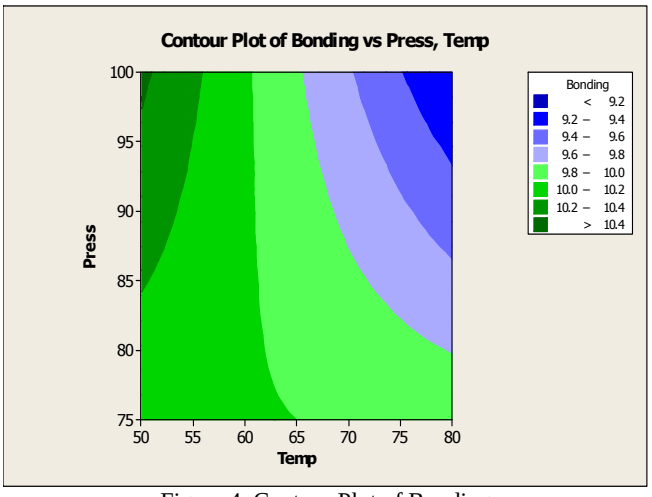

Figure 4. Contour Plot of Bonding

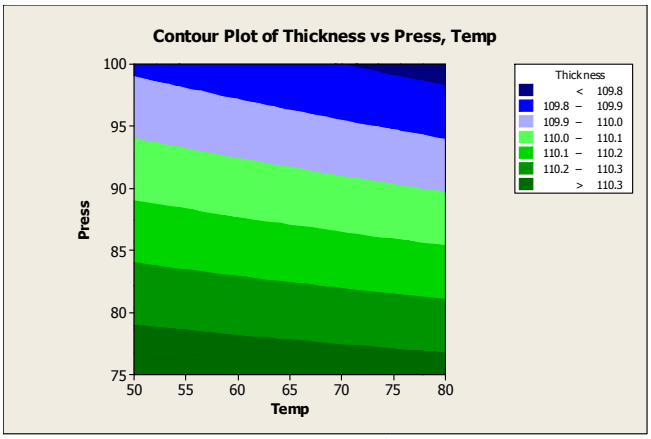

Figure 5. Contour Plot of Thickness

Based on countor plof for bonding force and thickness, it was seen that chosen of level for each factors, precesely. Its things proven by target value of responses in contour plot area as shown above, in which target value of bonding force is 10 Kgf and thickness is 110 µm. Because of bonding force and thickness as result from one process. So that, its impossible to optimize setting of factor process, separately, both bonding and thickness must be optimized concurrently. In which obtained two equations that are bonding y_1 and thickness y_2 as the following.

$$y_1 = 3.52 + 0.108x_1 + 0.08987x_2 - 0.00149x_1x_2 \quad (4)$$

$$y_2 = 111.547 + 0.007x_1 - 0.015x_2 - 1.06667E-04x_1x_2 \quad (5)$$

In this research, overlaid contour plot used to combined two contour plots to get optimal setting in which that setting can give the optimal value for bonding and thickness. Its purpose is to show across of point of response equation, in order to obtained feasible area and optimal solution. Using MINTAB 15.0, we get overlaid contour plot as in figure 6.

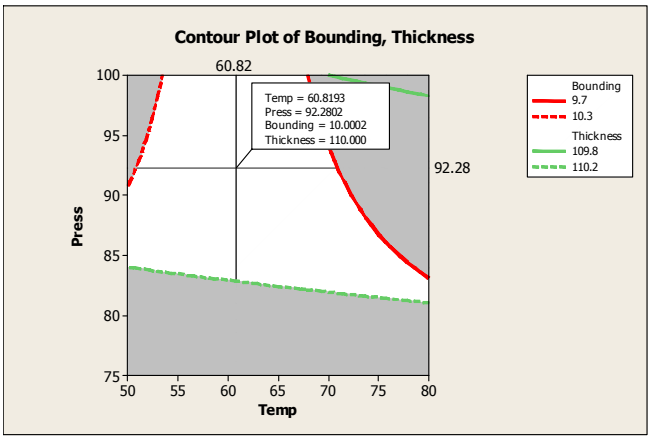

Figure 6. Overlaid Contour Plot of Bonding and Thickness

From figure 6, we know that optimal setting to satisfy specification of bonding force 10±0.3 Kgf and thickness 110±0.2 µm by 92.28 Psi for machine pressure and 60.82

^{o}C for temperature. Based on that point, PT.XYZ can satisfy that specification until 10.0002 Kgf for bonding force and 110.0000 Psi for thickness.

V. CONCLUSIONS

From the examination results based on the data sets, it could be concluded that the developed extension could solve the problem well. This proved that the developed extension would work as expected, but still need further verification for more complex and complicated cases.

Further research that could be developed are the ones that analyzed and discussed various variation on the model characteristics. Such as from the number of responses, the number of factors, the accommodation of multivariate analysis, etc.

REFERENCES

[1]. Montgomery, D.C., "Analysis and Design of Experiments", John Willey & Sons, New York, 2001.

[2].Montgomery, D.C., "Introduction to Statistical Quality Control", 5th Edition, John Willey & Sons, New York, 2005.

[3].Tong, Lee-Ing et al., "Optimization of Multiple Responses using Principal Component Analysis and Technique for Order Preference by Similarity to Ideal Solution", Int J Adv Manuf Technol (2005) 27:407-414.

[4].Tong, Lee-Ing et al., "Optimization of Multi-Response Processes using the VIKOR Method", Int J Adv Manuf Technol (2005).

ISSN: 1411-1284

A Study To Design Of Information Catalog Of Academic Division In Andalas University

Insannul Kamil, Hilma Raimona Zaidry, Dewi Ike Andriyani
[1]Industrial Engineering Department, Andalas University, Padang-Indonesia

sankamil@yahoo.com, dewiike84@yahoo.com

ABSTRACT

Nowadays, the accurated and integrated of information with the best quality output become more important than before for the organizations. The information have a role as element to function the intergrated resources like man, material, machine, method and money, it will be more easier than to take the decisions so given the added value and competitive advantages for the organizations.

Andalas University (Unand) is one of the state university in Indonesia. Where the location is in Padang, West Sumatera. Today, the current of information still used the paper based and stand alone, it is happen especially in Academic division. The information about the student's marks just could be see at computer center, the information about the university tuition just could be see at finance division and the others. Now, every divisions just have the information about their tasks but they don't know about the others in computation. We called that is stand alone. It will be more slowly to find the information that will needed and have consequences to appears the human errors so lossing some data will be happen immediately. The more important in the current of information in Unand is to lossing the miss communication or miss information between divisions in organization. To solving this problems, this researh would build an information system is Information Resource Catalog (IRC).

IRC is design by using a System Development Life Cycle Method (SDLC). The first step in SDLC is survey the system, it is usefull to know what happenning in the system directly. The best choice in survey is interview with the user's system. From that, we can know is what the user's system want, what should they do for the future and what must they learn to do the best for the current of information. The second step is analysis the system, it is depend on the result of interview. From the interview, we can know what is the problem happen and what should do to solve that in academic divion. The last step is software design. This software could help the users to save their time to find the information they need.

The advantages of IRC could provide the informations that used in academic, it's covers are acceptance new student, study, graduation, library and alumnus in web based. The output of Information Resouce Catalog could help the users to look for the information especially in academic, save their time and the all the imformations are valid.

Keyword: Information Resource catalog, System Development Life Cycle,Academic.

1. INTRODUCTION

Background

Nowadays, information flow increase to be prior need for the organization. Easier to find information that we need to be the focus in this paper.

Andalas University (Unand) is one of the state university in Padang. Now, the information flow still on manual. It will need much longer time to find something that will be used for the element. So that, to handle this problem, so the catalog information to be the key for this problem.

Formulation of problem

Based on background, require to do the study which can know how are the informations at academic divisions in real time which can given.

Target of research, is :

To get an information catalog on Academic divion. Includes are Academic, Financial, Human Resources, Logistic and Computer Center.

Boundaries of research

1. Research done specialist on education. It happen in Academic Division.
2. Data collect on even semester and odd semester.

3. Method using based on system information and data flow that been used Academic divisions on Andalas University.

2. THEORITICAL BACKGROUND

System Information Concept

A system have current purposes. It can to get goal and sometimes it can to get objectives. Sistem is an element integrated which have the same purpose to get a goal. A company, it could called as an organization (Mcleod, 2004). Information is a processing data to be a good purpose and has meaning for the people who will use that system Jogiyanto (1995). way

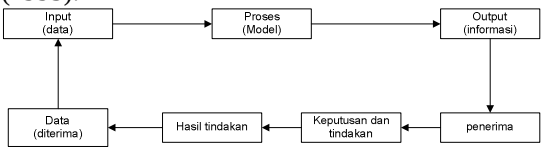

Pic. 1 Information cycle
(Source : Jogiyanto, 1995)

Characteristics of Information System

Based on Tata Sutabri (2004) develop characteristic of information system which used by customers in evaluate information system. According to Tata Sutabri (2004), found eight dimensions of information system:

1. *Components*, a system consist of integrated components to get the one purpose. The components have functions and affects the system.
2. *Boundary*, that is region which bound a system with the others.
3. *Environment*, that is everything in outer system and will affect the systems.
4. *Interface*, which is to connect the components.
5. *Input*, that is element input to the system.
6. *Output*, that is element input to the system.
7. *Proces*, that is to change the input became output.
8. *Objective*, A system have goal and objectives.

Dimension of Information

Output from the system have dimension. This dimension will give the contribute to information's mark. The dimensions are (Mcleod, 2004):

1. *Accurate*, the informations have the accurate data. So, it will give the satisfaction for the user.
2. *Up to date*, the information must up to date. If we need the information about today it must be happen.
3. *Relevance*, the informations have benefit for the user.
4. *Complete*, the information present the complete solver.

Resources of Information System

The resources of information system cocnsists (McLeod, 2004):

1. *Hardware*
2. *Software*
3. *Spesialist*
4. *Users*
5. *Facility*
6. *Database*
7. *Information*

System Develop Life Cycle (SDLC)

System Develop Life Cycle decided the phases, it begins from system in planned until the system used (Jogiyanto, 1999).

The prior phase in System Develop Life Cycle consists, it can be seen in Pic 2.

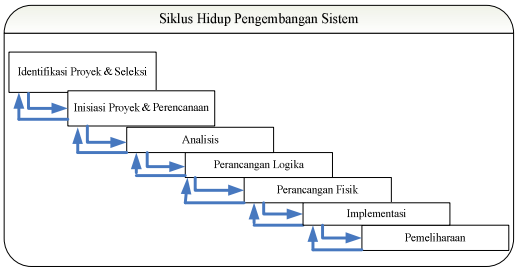

Pic. 2 System Develop Life Cycle
(Source: Nugroho, 2004)

3. RESEARCH METHOD

Research started with antecedent study and antecedent survey. From antecedent study, can know about concepts of system information and catalog. From antecedent survey, can know about problems of the system which could be researched. Then, formulate the problem into the problem statement and determine the purpose of research. Compilation of problem in the academic division. Indicators and statements in questioners adapted with actual condition.

The conditional data from system, it will be a web based. All the data from the academic division, will be a catalog. And the catalog will be in web based. So, everybody can get the information as guick as possble

4. RESULT AND DISCUSSION

Nowadays, the flow data in academic division is manual. Every information that needed, difficult to look for. Sometimes, humans error will be happened. Likelihood, in computer centre. To handle that situations, proposed the web-based for the information. With web-based, it will make easier to find the information that we needed.

5. CONCLUSION

1. Design of catalog information has done, consists of 7 phases that are the acceptance of new students, study, academic, graduation, human resource, financial and logistics. Each phases presents the activities on education sides are 8 activity detil on acceptance of new students, 5 activity detil on study, 12 activity detil on academic, 1 activity detil on graduation, 4 activity detil on human resources, 1 activity detil on financial and logistic.
2. The advantages of catalog information, are:
    1. To prepare the catalog of information about the activities on academic division especially on education side.
    2. More easy and more short time to looking for the informations.

SUGGESTION

To make this catalog more complete and efficient than before, it suggest the activities not only on education side but also on all sides.

6. REFERENCES

Heryanto, Imam, 2006, *Membuat Database dengan Microsoft Access*, Penerbit Informatika, Bandung

Jogiyanto, 1995, Analisis *dan Desain Sistem Informasi*; *Pendekatan Terstruktur*, *Teori dan Praktek Aplikasi Bisnis*, Edisi Kedua, Yogyakarta, Andi Offset.

Leman, 1998, *Metodologi Pengembangan Sistem Informasi*, Elex Media Komputindo, Jakarta.

Mc.Leod. 1995. *Sistem Informasi Manajemen*. Jilid 1. Edisi Bahasa Indonesia. Jakarta. PT. Prenhallindo.

Mc.Leod. 1995. *Sistem Informasi Manajemen*. Jilid 2. Edisi Bahasa Indonesia. Jakarta. PT. Prenhallindo.

Nugroho, Adi, 2004, *Konsep Pengembangan Sistem Basis Data*, Cetakan Pertama, Penerbit Informatika Bandung.

Sarwono, Jonathan, 2006, *Metode Penelitian Kuantitatif dan Kualitatif*, Yogjakarta, Graha Ilmu.

Setiawan, Budi Erwin, dkk, *Information Resource Catalog* (Studi Kasus : STT Telkom).

Universitas Andalas, 2006, *Informasi Salingka Unand*, Padang.

Universitas Andalas, 2006, *Peraturan Akademik Program Sarjana Universitas Andalas*, Padang.

Universitas Andalas, 2006, *Panduan Pendaftaran Mahasiswa Universitas Andalas Strata 1 Tahun Akademik 2006/2007*,Padang.

Wahana Komputer. 2006. *Menguasai Pemograman Web dengan PHP 5*. Semarang. CV. Andi Offset.

Yolanda, Meidy, 2005, *Perancangan Metode Quick Count*, Padang, Universitas Andalas.

ISSN: 1411-1284

A Study To Choose The Domestic Airlines For Padang – Jakarta Route Using Analytic Hierarchy Process

Insannul Kamil, Ahmad Ridha Putra

Industrial Engineering Department at Andalas University

Abstract

The Go Into Effect Of Law No. 15 / 1992 about air transport represent one of bollard of deregulation of air transport business in Indonesia. With this law existence, hence sum up service firm of air transport keen storey. Progressively the keen storey sum up service firm of air transport result emulation usher air transport firm progressively tighten. For that all air transport firm claimed always survive in the centre of the the emulation such as gift of mass promotion price, giving packet of promotion spesial of inclusive of hotel, offering certain air transport clocks addition of extra flight and others.

But in the middle of the emulation, air transport world surprised with many air transport incident that happened in five the last year. From year 2002 until early 2007 noted have been happened 45 case of air transport incident in all the world which because of assorted factor, 19 case among other things be happened in Indonesia region [Wikipedia, 2007] so that influence consumer in firm election to be used. To chosen correct air transport firm to be used, hence be specified criteria in decision making. Research to utilize to know how criterions influence representing fundamental norm to lead decision making in firm election for the domestic air transport of route Padang-Jakarta use approach of Analytic Hierarchi Process.

To know most criterion have an effect on from criterions which have been specified, hence be a processing use approach of Analyitc Hierarchy Process by determining hierarchy of election of alternative of decision making, comparing criterion one with other criterion by giving assesment, determination of matrix of comparison couple (pairwise comparison matrix), wight calculation relative used, calculation of normalized principal eigenvector, calculation of consistency ratio, and election of alternative of air transport firm operating for route Padang-Jakarta. Airlines of air transport Operating for route Padang-Jakarta are Garuda Indonesia Airlines, Adam Air, Sriwijaya Air, Batavia Air, Asian Air, Lion Air and Mandala Airlines.

Pursuant to data processing and inferential analysis that chosen firm alternative in firm election for the domestic air transport route Padang-Jakarta is Garuda Indonesia Airrlines by totalizing score equal to 0,273 and the most criterion having an effect on sociability of employees of air transport firm (ticketing, check in counter, dll) by totalizeing score equal to 0,1170.

Key word: *Criterion, Analytic Hierarchy Process, Consistency Ratio, Choosen Alternative.*

1. INTRODUCTION

Background

Law No. 15 / 1992 about air transport represent one of bollard of deregulation of air transport business in Indonesia. With this law existence, hence sum up service firm of air transport keen storey. Before this law existence, service firm of air transport in Indonesia only be consisted of some company, specially which is merged into International Air Transport Association (IATA). More player in service industries of this air transport for example since air transport industry give the possibility of obtaining advantage which high enough [Sipahelut, 2003].

Progressively the keen storey sum up service firm of air transport result price emulation even also progressively tighten. If we see to return condition of some years ago, commercial implement represent costliest transportation appliance of its price so that the many people use bus, boat and other transportation appliance but now that happened on the contrary. In This Time, a lot of one who use commercial implement since price is not clinged by far from price of other; dissimilar transportation appliance such as bus or boat so that the emulation usher air transport firm even also progressively tighten and they have to struggle to survive in the centre of the the emulation.

To always survive in the centre of the emulation, various effort of promotion and marketing progressively often be conducted by air transport firms. Through gift of mass promotion price, giving packet of promotion spesial inclusive of hotel, offering certain air transport clocks addition of extra flight and others. This matter become challenge for air transport firms in front there so that can compete to get consumer which more amount.

Besides doing promotion and better marketing, all air transport firms which there have been claimed to be able to provide peaceful facility, adequate and balmy to all passenger candidate in doing their journey. But, latterly the the facility is uncared. More incident of air transport commercial implement five year lately cause consumer attitude in conducting firm election for the domestic air transport become very critical and indirectly will influence psychological factor of passenger. From year 2002 until early 2007 noted have been happened by 45 case of air transport incident in all the world which because of assorted factor, 19 case among

other things be happened in Indonesia region [Wikipedia, 2007].

To the number of air transport incidents that happened cause party of penyedia of service of air transport firm have to comprehend is the desired by consumer. consumer of Multifarious itself manner in age, gender, work and appetite, with motivation, perception, process to learn and also attitude and different confidence between one and other. If service of air transport firm able to comprehend variety and consumer behavior, hence will assist in determination of marketing strategy so that the company able to ride out emulation usher humanity competitor which progressively tighten.

Pursuant to the clarification, hence this research study to hit criterions influence representing fundamental norm in leading decision to firm election for the domestic air transport route Padang-Jakarta with approach of Analytic Hierarchy Process.

As for target want to be reached in this research is to yield correct decision in firm election for the domestic air transport route Padang-Jakarta use approach of Analytic Hierarchy Process.

2. THEORITICAL

Analityc Hierarchi Process developed by Dr. Thomas L. Saaty from Wharton School Of Business in the year 1970 for organizing of information and judgement in chosening most taken a fancy to alternative. This method excess his ability if given on to a complex situation that or do not have framework, where data and statistical information from problem faced slimmest. Existing data only have the character of qualitative based for perception, experience and intuition

Principle work AHP is moderation of complex problem which do not the structure , strategic, and dinamik become sharess, and also arrange in hierarchy structure. Later;Then mount importance of each variable given by value numerik in subjektif about important meaning oft he variable relatively be compared to a other variable. From various the consideration later;then be conducted by sintesa to specify varaibel owning high priority and share to influence result the system (Marimin, 2004).

Model of AHP using Assumed human being perception ' ekspert' as input of the core important. Criterion 'ekspert' here non meaning that the people shall jenius, bright, titled of doctor etcetera but rather relate at one who understand conducted problems correctness, feeling effect a problem or have importance to the problem. Things measurement qualitative represent matter which of vital importance remember to more and more its complex problems in world and mount uncertainty which more and more high. Model of AHP approach almost same as with political model attitude, that is represent decision model (individual) by using collective approach from decision-making processes. AHP Developed by Thomas L. Saaty, earn to solve problem complex where aspect or criterion taken quite a lot. Also this complexity because of unclear problem structure, uncertainty of perception of decision taker and also the available uncertainty of accurate statistical or even no at all. Sometimes arise felt by decision problem and perceived the need taken as soon as, but its variation complicated so that its data not possible to earn noted in numeric, only in just qualitative which can be measured, that is pursuant to experience and intuition (Kadarsah,1998).

3. RESEARCH METHODE

Pre Survey

Antecedent study aim to to identify problems and possibility of trouble-shooting which can be conducted. At this phase conducted by a information gathering of early so that be obtained by a problems picture. Study conducted to assorted of service of air transport of route Padang-Jakarta which have operated.

Book Study

Literature study conducted by studying with antecedent study. At this step learned by things related to studied research topic that is hit decision making and theory about Analytic Hierarchy Process.

Identify and Problem Formulation

This phase aim to know cause the happening of problem. Early, identify problem is by given the condition and situation from domestic air transport in this time. This present moment there are seven domestic air transport service route Padang - Jakarta that is Garuda Indonesia Airlines, Adam Air, Sriwijaya Air, Batavia Air, Asian Air, Lion Air and Mandala Airlines. Each of air transport service Operating give service with excess each to prospecting customer or passenger. Passenger candidate given on to various choice which on the market by each of air transport service. Each of air transport service try to provide best service to get attention from prospecting customer or passenger candidate. Pursuant to that matter, hence need be conducted by a analysis to chosen firm of most air transport service precisely.

Especial problems in this research is chosening firm of domestic air transport service route Padang-Jakarta to be used pursuant to criterions matching with the consumer desire.

Determination of criteria And Decision Alternatif of Airlines Route Padang-Jakarta

Target identify criterion is to know criterion having an effect on in firm election for the domestic air transport route Padang-Jakarta. Criterion of Alternative election represent attribute or factors influencing alternative election and function as indicator of alternative assessor. Each alternative assessed pursuant to criterions. Criterion later be depicted into value tree. Value Tree used for forming of structure of decision hierarchy. Hierarchy structure aim to to show relation between criterion and alternative in hierarchy. Pursuant to this research topic hierarchy structure consisted of three level that is target to be reached (field goal), criterion and alternative.

First level is target, that is chosen firm of domestic air transport service of correct route Padang-Jakarta suit fancy consumer. While criterion in alternative election shall be as follows:

1. Competing ticket price.
2. Sociability of employees of air transport firm (ticketing, check in counter, and other).
3. Air transport security.
4. Softbility during air transport.
5. Gift program
6. Facility implement of air transport firm (food, beverage, smooking area, and other).
7. Influence of advertisement and promotion from air transport firm.
8. Service of air transport firm during 24 hours (ticket, information, criticize and suggestion).
9. Good service equivalence.
10. Knowledge of implement condition to be used (type, elegibility flown, and other).
11. Experience / response / other passenger policy.
12. Belief / fanatism to a firm of air transport.

While solution alternative represent alternative of domestic air transport service route Padang-Jakarta to be selected. Alternative in decision election in target attainment becoming third level in hierarchy are Garuda Indonesia Airlines, Adam Air, Sriwijaya Air, Batavia Air, Asian Air, Lion Air and Mandala Airlines.

Data Collecting

This shares comprise datas used in firm election for the domestic air transport route Padang-Jakarta. Required to be datas obtained from result quisioner interview by using question of couple comparison. In data collecting specified criterion of firm election for the domestic air transport route of Padang-Jakarta and firm alternative for the domestic air transport route Padang-Jakarta.

Data collected by value have interest factors having an effect in the case of chosening firm of domestic air transport service route of Padang-Jakarta to 30 responder. The data in the form of question with question type in the form of question of pairwise comparison that is with each other compare each criterion and alternatives. Assess importance of factor or criterion as according to scale of pairwise comparison given by Saaty that is scale 1 until 9.

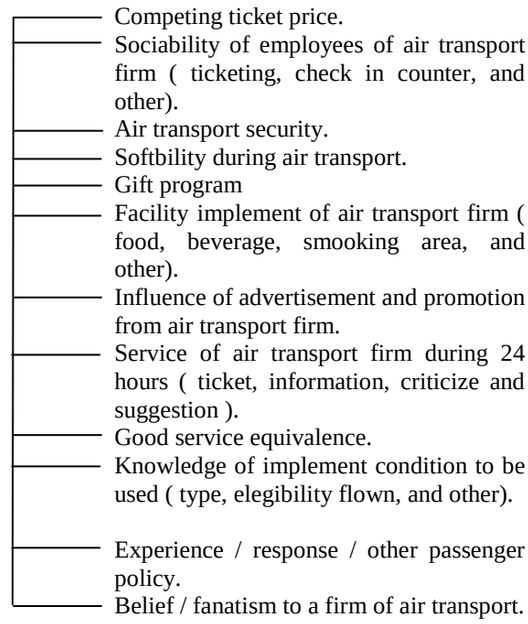

Picture 3.1. *Value Tree* of Choosen of Firm Airlines Domestic Route Padang – Jakarta

Data Processing

After data collected hence hereinafter be conducted by data processing by using concept and appropriate method. Calculation taken the following:

1. Determination of hierarchy of Election Alternative Decision Making
   Hierarchy formed by determining value tree beforehand. Hierarchy structure consisted of three level that is target, criterion and decision alternative. Attribute determination to be used in firm election for the domestic air transport route Padang-Jakarta represent early will conduct of data processing in research hit Analytic Hierarchy Process. This atribut represent criterion in election of decision alternative. The criterion later be depicted into value tree. Value Tree represent hierarchy from problem depicting level differ in tired effort target or finish problem. Value Tree show important aspects assessed in firm election for the domestic air transport route - Jakarta. Value Tree consisted of 12 criterions. Each alternative compared to pursuant to criterions of value tree.

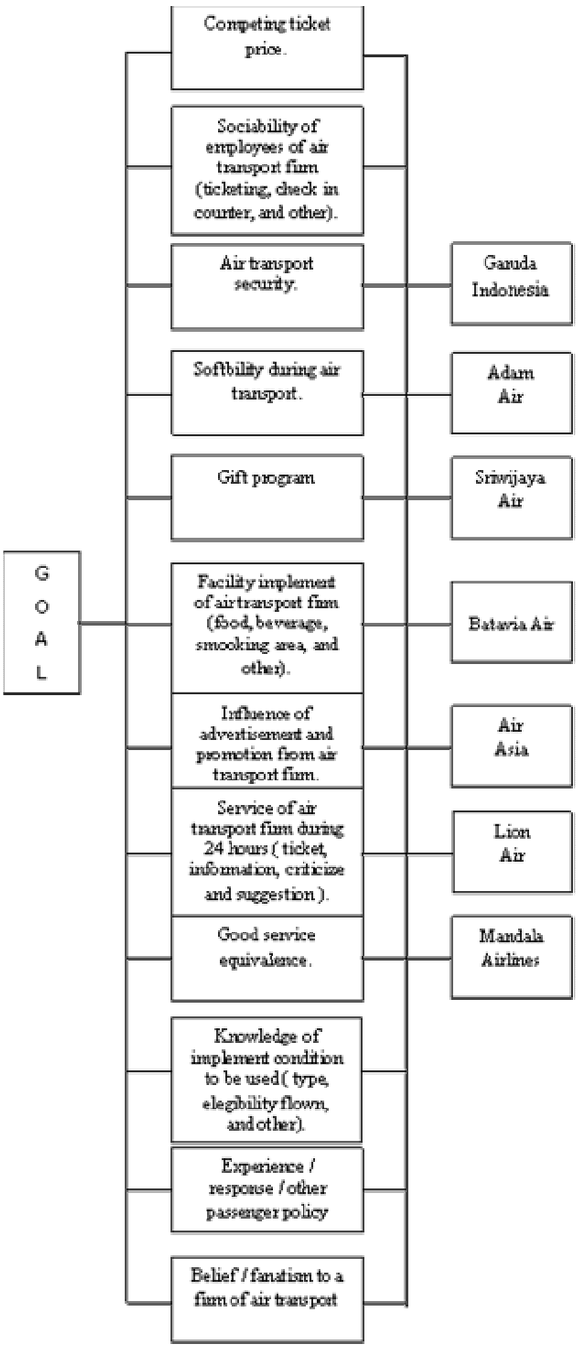

Picture 3.2 *Hierarchy Structure* of Choosen of Firm Airlines Domestic Route Padang – Jakarta

Hereinafter step is making hierarchy structure. Problem to be finished to be elaborated to become elements that is field goal (target), criterion, and the compiled to later alternative become hierarchy structure. Hierarchy in election of firm of domestic air transport service route Padang-Jakarta consisted of three level. First Level [of] target that is chosen firm of domestic air transport service route Padang-Jakarta which suit fancy client, level of second of criterion and third level is decision alternative. As for structure of hierarchy of election of firm of domestic air transport service route Padang-Jakarta and hierarchy structure can be visibled at picture 3.2.

Each criterion compared to one by one be found sequence of criterion priority specified with comparison scale. comparison scale used in pairwise comparison to each criterion and alternative scale according to Saaty. According to Saaty (1983), to various scale problem 1 until 9 is best scale in expressing opinion or perception. Scale Of Saaty can be showed at tables 1.

Nilai	Keterangan
1	A of Equal Important than B
3	A A little more important than B
5	A more important than B
7	A very more important than B
9	A absolute more importan than B
2,4,6,8	Hesitate between two value bunching up.

Table 1. Scale of Saaty (1983)

2. Determination of Pairwise Comparison Matrix
   Conducted by comparing each criterion in berpasangan so that be obtained [by] a score to each criterion determining most criterion have an effect on in alternative election. Step hereinafter, level criterion consisted of twelve criterion and by using matrik. Responden Perceived 30 people, representing service user of domestic air transport route Padang-Jakarta. Proses of assessment of comparison assessment with consistency ratio less than 0,1. Consistency ratio will become indicator that assessment done onsistently. Assess used to consistency ratio relate to decision Saaty, where have to be more minimize or equal to 10%. question amount Raised in filling matrix n(n-1)/2 with n [is] criterion amount. Matrix present which the

inversion each other and its diagonal valuable always one.
3. Calculation of Wight Relative which be Normalized
4. Calculation of Normalized Principal Eigenvector
5. Calculation of Consistency Ratio
6. Assesment and Election Alternative .

4. ANALYSIS OF DATA PROCESSING

As for analysis aken the following step :
1. Analyse criterions representing assessment attribute in firm election for the domestic air transport route Padang-Jakarta
2. Analisis to pairwise comparison matrix as according to score of responden answer perceived
3. Analysis to assessment wight in most criterion determination have an effect in alternative election
4. Analyse calculation of Consistency Ratio

5. CONCLUSION AND SUGGESTION

This shares contain conclusion and suggestion. Conclusion got from data-processing result and the alternative selected pursuant to calculation result and analyse. While suggestion made upon which input for consumer party in taking decision and input for research hereinafter. Pursuant to data processing and inferential conducted analysis that chosen firm alternative by passenger in firm election for the domestic air transport route Padang-Jakarta Garuda Indonesia by totalizeing score equal to 0,273. From calculation of alternative of decision of Garuda Indonesia often get compared to biggest score other alternative and the most criterion have an effect on in firm election for the domestic air transport route Padang-Jakarta sociability of employees of air transport firm (ticketing, check in counter, and other). This matter seen from totalizeing score of alternative second perceived that is equal to 0,1170. Totalizeing the the score come from wight calculation each joined to later responder become one group wight. second criterion Influencing in election of decision alternative storey of security and freshment of dalm implement with score equal to 0,1095. While next criterion influencing election of decision alternative knowledge of implement condition to be used (type, elegibility flown, and other;dissimilar - other;dissimilar by totalizeing score equal to 0,1086.

As for becoming suggestion which can be given from research result taken are:
1. Pursuant to calculation result and analyse hence the alternative which better be selected by consumer Garuda Indonesia
2. determination of Criterion wight better be conducted all expert which is true master the problem
3. Calculation of Analytic Hierarchi Process in this research better be conducted periodically in order to the more accurate reached result.

5. REFERENCE

Fülöp, János. ***Intoduction to Decision Making Methods***. Hungarian Academy of Sciences.

Getuk. 2007. ***Analisa Proses Hirarki***. http://www.getuk.wordpress.com/analisa proses hirarki. 9 April 2007.

Hanafi, Abdillah. 1984. ***Memahami Komunikasi Antar Manusia***. Usaha Nasional: Surabaya.

Latifah, Siti. 2005. ***Prinsip-Prinsip Dasar Analytical Hierarchy Process.*** Fakultas Pertanian Universitas Sumatera Utara: Medan.

Marimin. 2004. ***Teknik dan Aplikasi Pengambilan Keputusan Kriteria Mejemuk***. PT. Grasindo: Jakarta.

Mulyono, Sri. 1996. ***Teori Pengambilan Keputusan***. Lembaga Penerbit Fakultas Ekonomi Universitas Indonesia: Jakarta.

Saaty, Thomas L. 1994. ***Fundamentals of Decision Making And Priority Theory With The Analytic Hierarchy Process Vol. VI***. RWS Publications: United States of America.

Saaty, Thomas L. 1988. ***Multicriteria Decision Making, The Analytical Hierarchy Process: Planning, Priority Setting, Resourse Allocation.*** RWS Publications: United States of America.

Sipahelut, Fitharia Elvisa. 2003. ***Faktor Psikologis yang Mempengaruhi Keputusan Konsumen di Surabaya dalam Pemilihan Maskapai Penerbangan Domestik untuk Rute Surabaya-Jakarta.*** Universitas Kristen Petra.

Suryadi, Kadarsyah, dan Ali Ramdhani. 2000. ***Sistem Pendukung Keputusan: Suatu Wacana Struktural Idealisasi dan Implementasi Konsep Pengambilan Keputusan***. PT. Remaja Rosdakarya: Bandung.

Teknomo, Kardi dkk. 1999. ***Penggunaan Metode Analytic Hierarchy Process Dalam Menganalisa Faktor-Faktor Yang Mempengaruhi Pemilihan Moda Ke Kampus***. No.1, Volume 1, halaman 31.

Wikipedia. 2007. ***Analytical Hierarchy Process,*** http://www.en.wikipedia.org/wiki/ *Analytical Hierarchy Process*. 7 April 2007.

Wikipedia. 2007. ***Insiden-insiden Pesawat Terbang,*** http://www.en.wikipedia.org/ wiki/Daftar Kecelakaan dan Insiden Pesawat Penumpang, 7 April 2007.

ISSN: 1411-1284

Effect of Heat Treatment on the Characteristics of SiO_2 Added-$ZnFe_2O_4$ Ceramics for NTC Thermistors

Wiendartun[1)], Dani Gustaman Syarif[2)], Fitri Anisa[1)]

[1)] Physics Department, UPI, Jl.Dr Setiabudhi 229 Bandung, email: wien@upi.edu
[2)] PTNBR BATAN, Jl.Tamansari 71 Bandung 40132,
email: danigustas@batan-bdg.go.id

ABSTRACT-**A study on the effect of heat treatment on the characteristics of SiO_2 added - $ZnFe_2O_4$ ceramics for NTC thermistor has been carried out. The ceramics were produced by pressing an homogenous mixture of ZnO, Fe_3O_4 and SiO_2 (0,5 weight %) powders in appropriate proportions to produce $ZnFe_2O_4$ based ceramics and sintering the pressed powder at 1200^{o}C for 2 hours with cooling rate of 6^{0}C in air. Some sintered pellets were heat treated by heating them at 1000^{o}C for 10 minutes with cooling rate of 2^{o}C/minutes, 10^{o}C/minutes and quenching. Electrical characterization was done by measuring electrical resistivity of the ceramics at various temperatures. Microstructure and crystal structure analyses were done by using an optical microscope and x-ray diffractometer (XRD). The XRD analyses showed that the $ZnFe_2O_4$ ceramics with and without addition of 0,5 w/o SiO_2 had cubic structure. No peak from second phase was observed from the XRD profiles. From the electrical characteristics data, it was known that the heat treatment could change the electrical characteristics of the $ZnFe_2O_4$ based-thermistor. The resistivity decreased with the cooling rate of 10^{o}C/minutes and quenching, and increased with the cooling rate of 2^{o}C/minutes. All ceramics made had thermistor characteristics that fit the market requirement namely B = 3014-3978K and ρ_{RT} = 12 - 154 kΩcm. It was known that the addition of 0,5 w/o SiO_2 increased the B and ρ_{RT} of the $ZnFe_2O_4$ based-ceramics.**

Key words-Thermistor, NTC, heat treatment, $ZnFe_2O_4$, SiO_2

I. INTRODUCTION

NTC thermistors are widely used in the world due to their potential use for many applications such as temperature measurement, circuit compensation, suppression of in rush-current, flow rate sensor and pressure sensor in many sectors [1]. It is well known that most NTC thermistors are produced from spinel ceramics based on transition metal oxides with general formula of AB_2O_4 where A is metal ion in tetrahedral position and B is metal ions in octahedral position [2-10]. Many studies have been done to improve the characteristics of the spinel based-NTC thermistors [6, 7, 10 and 11]. However, the study on the effect of heat treatment on $ZnFe_2O_4$ spinel ceramics added with 0,5 mole % SiO_2 has not been reported yet. In our previous work, it has been known that the resistance of the $ZnFe_2O_4$ ceramics added with 0,5 mole % SiO_2 was high, although the ceramic can be applied as the NTC thermistor.

The electrical characteristic of the NTC ceramic theoretically can be controlled using several methods. One of the methods is a heat treatment. The heat treatment theoretically can change the electrical characteristics such as electrical resistivity and thermistor constant [12] because the charge carrier of the ceramic is dependent to the surrounding environment. In this research the heat treatment was done by heating the $ZnFe_2O_4$ ceramics added with SiO_2 at 1000^{o}C in air with different cooling rates. The electrical characteristics of the ceramics were studied after the heat treatment.

II. THEORETICAL BACKGROUND

An NTC thermistor has a special characteristic as shown in Fig.1 below:

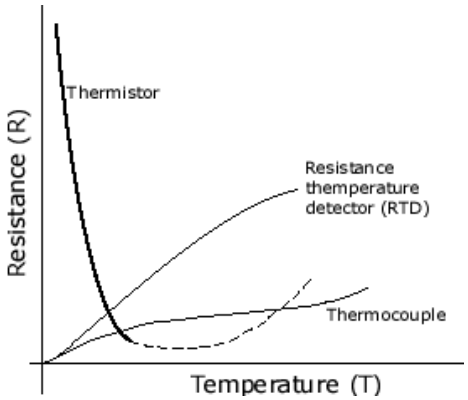

Fig.1. The relation between resistance and temperature for several temperature sensors.

As can be seen from Fig.1, the resistance of a NTC thermistor decreases exponentially with the increase of temperature. The relation between the resistance and temperature can be expressed by equation 1 [1-12] :

$$R = R_0 . Exp.(\frac{B}{T}) \quad (1)$$

where, R is thermistor resistance (Ohm), R_0 is a constant which is the same with the resistance at the infinite temperature (ohm), B is thermistor constant (K) and T is temperature of thermistor (K)

The relation between the thermistor constant and the activation energy can be written as : [10],

$$B = Ea/k \quad (2)$$

where, B is the thermistor constant, Ea is activation energy (eV) and k is the Boltzmann constant (eV/K)

Sensitivity of a thermistor can be calculated using equation 3 below [11,12]:

$$\alpha = - B/T^2 \quad (4)$$

where, α is sensitivity of thermistor, B is the thermistor constant (K) and T is the temperature in Kelvin (K). The larger the value of α and B, the higher the quality of the thermistor.

III. METHODOLOGY

Powders of ZnO, Fe_3O_4 and SiO_2 were weighed in appropriate proportions to fabricate SiO_2 added-$ZnFe_2O_4$ ceramics where the SiO_2 concentration was 0,5 weight %. The homogeneous mixture of powders was calcined at 800°C for 2 hours. After calcination, the powder was crushed and sieved with a siever of < 38 μm. The sieved powder was then pressed with pressure of 4 ton/cm^2 into green pellets. The green pellets were sintered at 1200°C for 2 hours in air with cooling rate of 6°C/minutes. The sintered pellets were subjected to some heat treatments. The heat treatments were heating at 1000°C for 10 minutes with heating and cooling rate of 10°C/minutes (which then written as 1000°C / 10min / 10°C/10°C), 1000°C / 10min/ 10°C / 2°C and 1000°C / 10min / 10°C / quenching.

The crystal structure of the sintered pellets was analyzed with x-ray diffraction (XRD) using Kα radiation at 40KV and 25mA. After grinding, polishing, etching the pellets, the microstructure of the pellets was investigated by an optical microscope. The opposite-side surfaces of the sintered pellets were coated with Ag paste. After the paste was dried at room temperature, the Ag coated-pellets were heated at 750°C for 10 minutes. The resistivity was measured at various temperatures from 25 to 100°C in steps of 5°C.

IV. RESULTS AND DISCUSSION

4.1 Visual appearance and XRD analyses

Fig. 2 shows the appearance of typical SiO_2 Added-$ZnFe_2O_4$ ceramics**.** The ceramics are visually good. Fig. 2, and Fig. 3 show the XRD profiles of $ZnFe_2O_4$ ceramic with and without addition of 0.5 weight % SiO_2, respectively. As shown in the figure 2 and 3, the profiles are similar. The XRD profiles show that the crystal structure of the ceramics is cubic spinel after being compared to the XRD standard profile of $ZnFe_2O_4$ from JCPDS no.22-1012. No peaks from second phases are observed. It may be due to the small concentration of the added SiO_2 which is smaller than the precision limit of the x-ray diffractometer used. From a calculation of lattice parameter, there is no significant effect on the lattice parameter can be observed where the lattice parameter of the $ZnFe_2O_4$ is 8.4354Å and that of the 0.5 weight % SiO_2 added-$ZnFe_2O_4$ is 8.4359Å. The added SiO_2 may be dissolved or not. It cannot be concluded from the XRD profiles in this works. The microstructure and electrical data may be used to evaluate whether the SiO_2 added was dissolved or not.

Fig. 2. Visual appearance of typical SiO_2 Added-CuF_2O_4 ceramics.

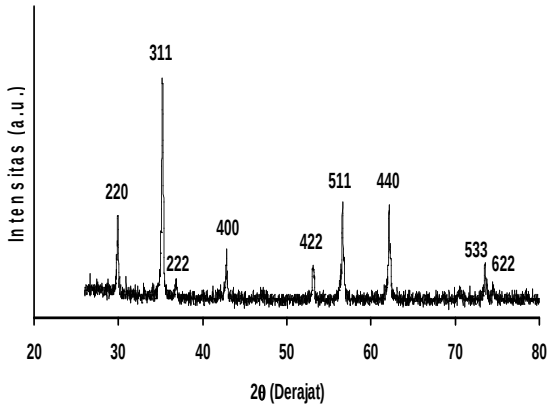

Fig. 3. XRD profile of $ZnFe_2O_4$ without addition of SiO_2 sintered at 1200^0C for 2 hours with heating and cooling rate of 6^0C/minutes, showing a cubic crystal structure.

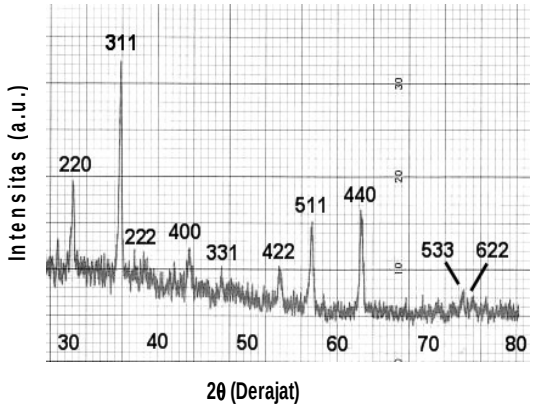

Fig. 4. XRD profile of $ZnFe_2O_4$ added with 0.5 weight % SiO_2 sintered at 1200^0C for 2 hours with heating and cooling rate of 6^0C/minutes, showing a cubic crystal structure.

4.2 Microstructure

Microstructures of the $ZnFe_2O_4$ with and without addition of 0.5 weight % SiO_2 are depicted in Fig. 5 and 6, respectively. From Fig. 5 and 6, it can be seen that the grains of the ceramic added with SiO_2 are smaller than those of the ceramic without SiO_2 addition. This may be due to segregation of the added SiO_2 in grain boundaries which then inhibits the grain growth during sintering. If this is true, it means that the added additive of SiO_2 is not dissolved in the $ZnFe_2O_4$ ceramic.

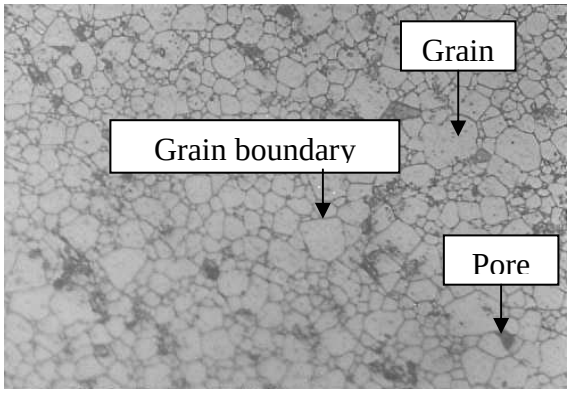

Fig. 5. Microstructure of $ZnFe_2O_4$ ceramic without SiO_2 addition) sintered at 1200^0C for 2 hours in air with heating and cooling rate of 6^0C/minutes.

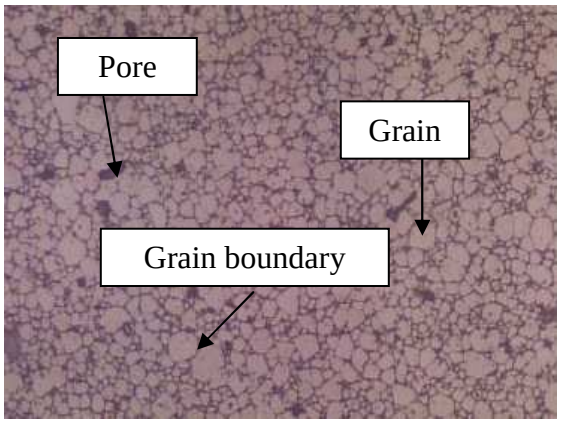

Fig. 6. Microstructure of $ZnFe_2O_4$ ceramic added with 0.5 weight % SiO_2 1200^0C for 2 hours in air with heating and cooling rate of 6^0C/minutes.

From Fig. 5 and 6, it can be seen that the grains of the ceramic added with SiO_2 are smaller than those of the ceramic without SiO_2 addition. This may be due to segregation of the added SiO_2 in grain boundaries which then inhibits the grain growth during sintering. If this is true, it means that the added additive of SiO_2 is not dissolved in the $ZnFe_2O_4$ ceramic.

4.3 Electrical Characterization

Fig. 7. shows the relation between ln resistivity and 1/T of the SiO_2 added-$ZnFe_2O_4$ ceramics and Table 1 shows the electrical characteristics of the ceramics. The linear curves in Fig. 7 show that the resistivity follows the Arhennius equation of equation 1. It is clearly seen that the initial room temperature electrical resistivity of the SiO_2 added-$ZnFe_2O_4$ ceramic is high (98 Kohm). After heat treatment with step of 1000^0C

/10min/10^0C/10^0C and 1000^0C/10min/10^0C/quenching, the electrical resistivity decreases to 38 kohm and 12 kohm respectively and after step of 1000^0C/10min/10^0C/2^0C the electrical resistivity increases to 154 kohm. This fact indicates that the resistivity is cooling rate dependent. As the cooling rate increases, the resistivity decreases. In Fig. 7, the higher position means high resistivity and the lower position means low resistivity. During process, the ceramic which is cooled with high cooling rate has no chance to interact with oxygen, making the ceramic is lack of oxygen and the oxygen vacancies are formed inside the ceramic. These oxygen vacancies are compensated by a formation of electron in conduction band. Therefore, the ceramics that are processed with higher cooling rate have smaller electrical resistivity. The activation energy of the ceramics having many charge carrier is small as shown in Table 1. The values of the thermistor constant (B), sensitivity (α) and room temperatura resistivity (ρ_{RT}) of 0.5 weight % SiO_2 added-$ZnFe_2O_4$ ceramics can be seen in Table 1. As shown in Table 1, the value of the thermistor constant (B), sensitivity (a) and ρ_{RT} fit the market requirement where B is about 2000K, α (alpha) is about 2,2%/K and ρ_{RT} is from 10 ohm.cm to 10^6 ohm.cm.

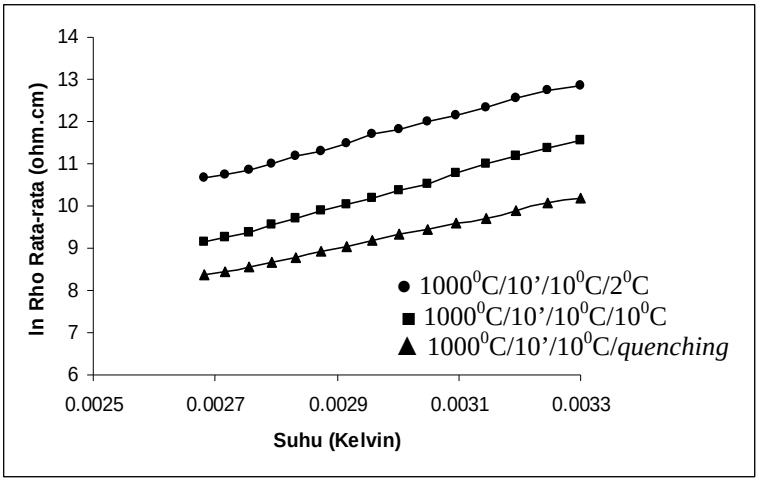

Fig. 7. The relation between ln ρ and 1/T of heat treated SiO_2 added-$ZnFe_2O_4$ ceramics.

Tabel 1. The value of the thermistor constant (B), sensitivity (α) and room temperature resistivity (ρ_{RT}) of 0.5 weight % SiO_2 added-$ZnFe_2O_4$ ceramics.

No.	Heat treatment	B (^{0}K)	Ea (eV)	α (%/ ^{0}K)	ρ_{RT} (kOhm-cm)
1	Sintered at 1200^0C/2hours/6^0C/6^0C) (Initial)	-	-	-	98
2	1000^0C/10min/10^0C/10^0C	3978	0.34	4.42	38
3	1000^0C/10min/10^0C/2^0C	3705	0.32	4.12	154
4	1000^0C/10min/10^0C/*quenching*	3014	0.26	3.35	12

V. CONCLUSION

The grain size of the $ZnFe_2O_4$ ceramics decreases by addition of SiO_2 because the added SiO_2 segregated at grain boundaries and inhibited grain growth during sintering. The heat treatment influences the electrical characteristics of the 0.5 weight % SiO_2 added-$ZnFe_2O_4$ ceramics. The high cooling rate during heat treatment decreases the electrical resistivity of the ceramics while low cooling rate increases the electrical resistivity. The heat treatment can be adopted in thermistor fabrication to control the electrical characteristics of the thermistor. The values of the thermistor constant (B) 3014-3978K and the room temperature resistivity (ρ_{RT}) of 12–154 kΩcm fit the market requirement.

ACKNOWLEDGMENT

The authors wish to acknowledge their deep gratitude to DIKTI, Department of National Education of Indonesian Government for financial support under hibah PEKERTI program with contract No. 014/SPP/PP/DP2M/II/2006.

REFERENCES

[1]. BetaTHERM Sensors [on line]. Available: http://www.betatherm.com.

[2]. Eun Sang Na, Un Gyu paik, Sung Churl Choi, "The effect of a sintered microstructure on the electrical properties of a Mn-Co-Ni-O thermistor", Journal of Ceramic Processing Research, Vol.2, No. 1, pp 31-34, 2001.

[3]. Yoshihiro Matsuo, Takuoki Hata, Takayuki Kuroda, " Oxide thermistor composition, US Patent 4,324,702, April 13, 1982

[4]. Hyung J. Jung, Sang O. Yoon, Ki Y. Hong, Jeon K. Lee, "Metal oxide group thermistor material", US Patent 5,246,628, September 21, 1993.

[5]. Kazuyuki Hamada, Hiroshi Oda, "Thermistor composition", US Patent 6,270,693, August 7, 2001.

[6]. K. Park, "Microstructure and electrical properties of $Ni_{1.0Mn2-x}Zr_xO_4$ ($0 \leq x \leq 1.0$) negative temperature coefficient thermistors", Materials Science and Engineering, B104, pp. 9-14, 2003.

[7]. K. Park, D.Y. Bang, "Electrical properties of Ni-Mn-Co-(Fe) oxide thick film NTC thermistors", Journal of Materials Science: Materials in Electronics, Vol.14, pp. 81-87, 2003.

[8]. Shopie Gulemet Fritsch, Jaouad Salmi, Joseph Sarrias, Abel Rousset, Shopie Schuurman, Andre Lannoo, "Mechanical properties of nickel manganites-based cermics used as negative temperature coefficient thermistors", Materials Research Bulletin, Vol. 39, pp. 1957-1965, 2004.

[9]. R. Schmidt, A. Basu, A.W. Brinkman, , "Production of NTCR thermistor devices based on $NiMn_2O_{4+\delta}$", Journal of The European Ceramic Society, Vol. 24, pp. 1233-1236, 2004.

[10]. K. Park, I.H. Han, "Effect of Al_2O_3 addition on the microstructure and electrical properties of $(Mn_{0,37}Ni_{0,3}Co_{0,33-x}Al_x)O_4$ ($0 \leq x \leq 0.03$) NTC thermistors", Materials Science and Engineering, B119, pp. 55-60, 2005.

[11] Dani Gustaman Syarif, Wiendartun, Mimin S., Synthesis and Characterization of TiO_2 Addition added-$ZnFe_2O_4$ Ceramics for NTC Thermistor, Proceeding of The 9th International Conference on Quality in Research (QIR) 2006, UI, Depok, 6-7 September 2006.

[12]. Dani Gustaman Syarif, *Karakterisasi Keramik Termistor Fe_2O_3: 1mTi Hasil Sinter dan Perlakuan Panas*, JURNAL MESIN Universitas Trisakti Vol. 9, No. 1 (2007).

ISSN: 1411-1284

Failure Analysis of 42” Pipeline Rupture

Deni Ferdian and Winarto

Department of Metallurgy & Materials Engineering, University of Indonesia
Kampus Baru UI Depok – 16424
Email: deni@metal.ui.ac.id

Abstract— **Weld joint of a 42” gas pipeline was reported failed after 23 years in operation. The failed location was considered highly risk area where landslide movement more likely occurred especially during wet season. Visual examination of failed surface showed the failure took place along the fusion line between HAZ and base metal. Other than that, incomplete penetration of the weld was noticed. Metallographic examination of weld cross section found porosity at the middle of the weld and SEM revealed some small porosity distributed at the root weld area. The porosity is more likely due to gas entrapment during weld solidification. Improperly base metal surface preparation before welding may contribute to the creation of gas entrapment at the weldment. Incomplete penetration also indicated poor inspection quality to the welding procedure specification (WPS) considered that the weld joint for gas transmission pipeline is required a 100% radiography examination in every pipe joint.**

Keywords— Pipeline, Incomplete penetration, Gas entrapment

I. INTRODUCTION

A 42’ Gas transmission pipeline were reported failed during operation. From excavation of the leak area, identification of the leaking source was found an open crack at position 07:00 to 03:00 o’clock at welding joint area (Figure 1). Pipeline operator informed that the field condition where the crack found is considered as a high risk area, where landslide movement more likely to be occurred. No information regarding the welding procedure provided. From the material specification standpoint, the pipe should meet the specifications for API 5LS Gr X56. The investigation was conducted on a failed pipe to study the failure mode, to find out the origin of the failure, and to make recommendations for preventive action to this problem

Figure 1. Picture of 42” pipeline rupture in weld join area.

II. METHODOLOGY

The visual and stereoscopic examinations were carried out on the failed surface. The chemical composition of the base material was analyzed by emission optical spectrophotometer. Sectioned pipe then prepared for metallurgical evaluation. The specimens were prepared using standard metallographic sample preparation techniques, and Nital 2% was used as an etchant to reveal the microstructure. Tensile test were used for the pipe base metal. Hardness profile measurements were performed in micro Vickers method. SEM equipped with EDX analysis was used for surface fractography and microanalysis examination of the failed section.

III. RESULTS & DISCUSSION

Chemical Analysis/Identification

The chemical analysis of the failed 42” pipe sample given in Table 1 is shown conformity to the specification of API 5L Gr X56 PSL 1. According to the mill sheet specification, the material should conform to API 5LS X56, therefore, the comparison was made to API specification 5L Standard 2004. No conclusion regarding an inappropriate chemical composition-induced failure can be made in this paper.

Table 1. Chemical Composition Results **[1]**

Material	%C	%Si	%Mn	% P	% S	% Ti
API 5L - X56	0.26 max	-	1.400 max	0.03 max	0.03 max	0.04 max
Sample	0.097	0.343	1.318	0.02	.004	< 0.001

Visual Examination

The visual examination of failed part shown that the failed occurred at the weld joint of the pipe, with most of the fracture took place along the fusion line of HAZ and weld metal. In some area of the joint incomplete fusion is observed, as seen in Figure 2. Most of the fracture surface already covered with corrosion product, but no significant scales or deposit was noted.

Figure 2. The photo of root joint area where incomplete fusion occurred

Metallography Examination

The optical microscopy examination of the base material was shown in Figure 3. Base material microstructure consists of ferrite and pearlite. The grain appeared elongated, these microstructures occurred as a result of manufacturing process, such as rolling. Grain growth observed at the area adjacent to the HAZ to the failed surface, as seen in Figure 4.

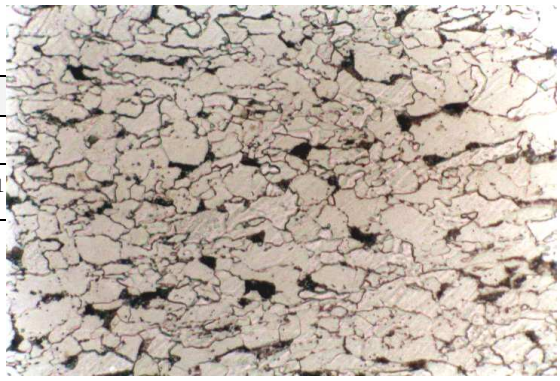

Figure 3. The microstructure of base metal consisting of ferrite (light) and pearlite (dark), 2 % Nital etch, (500X)

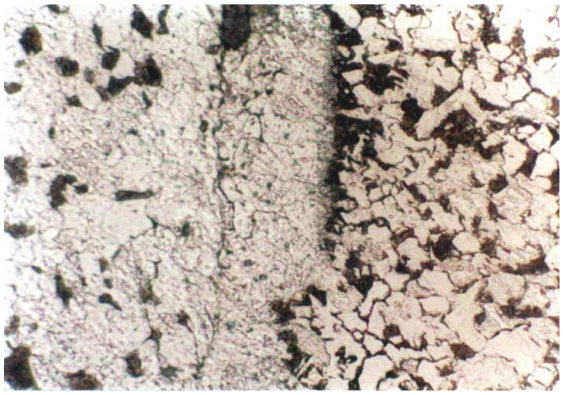

Figure 4. The microstructure of HAZ shows some grain growth was occurred on it, 2 % Nital etch, (500X)

Macro-Fractography Examination

Macro-structures of the pipe cross section were taken at the fracture failed and the good weld joints, under magnification 7X, as seen in Figure 5 and Figure 6.

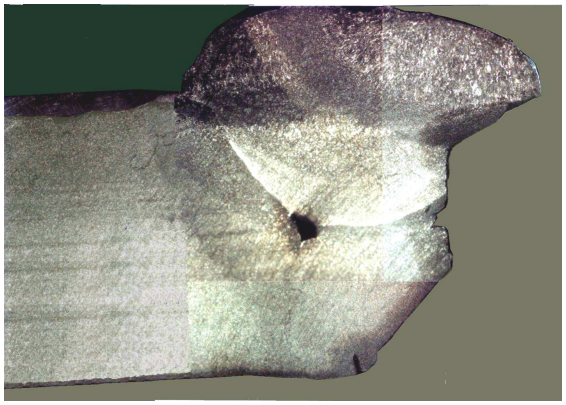

Figure 5. The macrostructure of fractured weld joint shows a big pores in the middle of the joint, 2 % Nital & 7 X

The results of macrostructure in Figure 5 show that there is a big pore at the middle of weld joint

(between weld pass). The macrostructure in Figure 6 is also found some pores at the middle of weld metal and near the root weld area. Small amount of hard phase such bainite and martensite were detected at HAZ of root pass

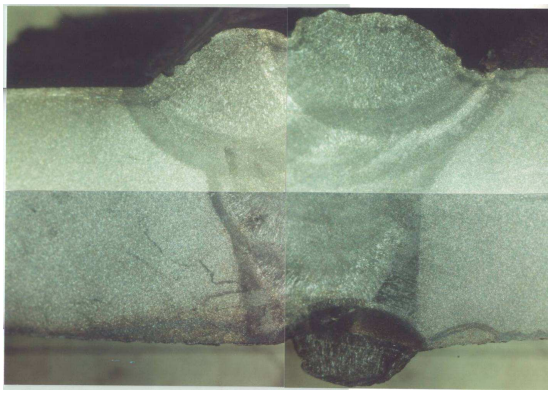

Figure 6. The macrostructure of non-fractured weld joint area shows a hard phase were detected, 2 % Nital etch & 7 X

The surface fracture morphology revealed an incomplete penetration (IP) at the root weld joint. Other than that, most of the fracture took place at the fusion line.

From the fracture mode, it seems that the back weld (root weld) is detached from the joint and shows that the weld fusion is not fully melted into the base metal at the root (incomplete penetration).

Figure 7. Fractography of fracture surface and the incomplete fusion is occurred at the root weld joint magnification of 7 X

Mechanical Testing

Tensile test of the base metal failed pipe conducted referring to ASTM E 8-00.[2] The average result of the tensile testing is 656 MPa for ultimate tensile strength (UTS) and 568 MPa for yield strength (YS) with the elongation of 30%. The ultimate tensile strength and the yield strength result is above the requirement for API 5L X56 PSL 1 which minimum tensile strength is 490 MPa and minimum yield strength required is 386 MPa. According to the result, the pipe base metal can be classified to the API standard 5L grade X80.

The hardness test was carried out on the across section of welded pipe that had been cut and polished in order to remove the cutting effects. The measurements were taken at the weld area, HAZ and base metal of the pipe. The hardness of a cross section pipe joint was carried out in accordance with micro Vickers hardness testing method.

The results are given in Table 1. A slight fluctuation appearing in hardness value might be caused by variation in microstructure. This high hardness at HAZ-3 is caused by high cooling rate when root weld was made at the final pass of multi layer welds and also due to a small size of weld metal fusing into the root weld area.

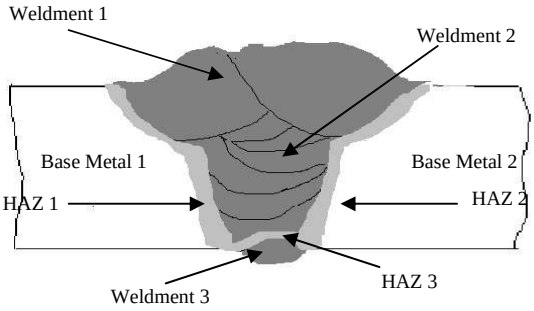

Figure 8. Schematic location of hardness test

Table 1. Hardness value of the weld pipe cross section

No.	Location	Hardness (HV)
1.	Base Metal 1	211
2.	HAZ 1	227
3.	Base Metal 2	207
4.	HAZ 2	222
5.	Weldment 1	229
6.	Weldment 2	224
7.	Weldment 3	221
8.	HAZ 3	382

Micro-Fractography Examination

Investigation by SEM at the pores area found that the pore is caused by gas entrapment, since no indication of slag or non metallic inclusion embedded to the pores, can be seen in Figure 9 and Figure 10.

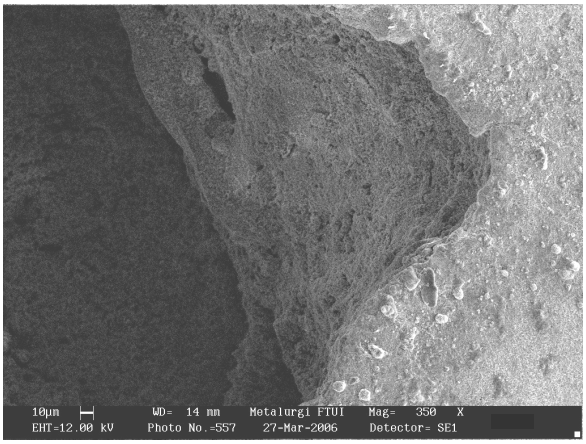

Figure 9. SEM Photographs taken near the root weld showed no inclusion in pores, SE detector and magnification of 350X

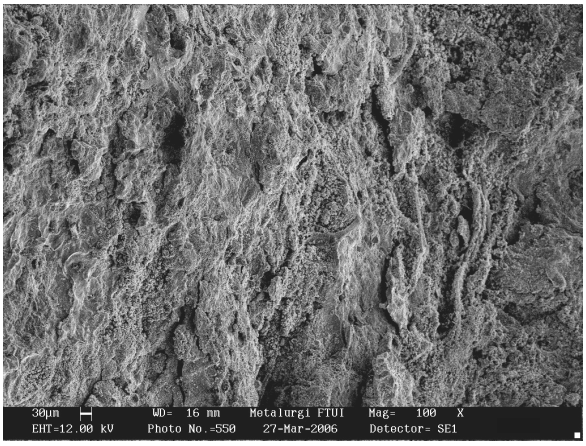

Figure 10. SEM Photographs taken at the surface of failed weld joint pipe consisting of some corrosion products (scale), SE detector 100X

EDX analysis of the failed surface scale consisted of iron oxide and some other element such aluminum, sulfur, calcium and potassium. No significant scale or corrosion products can contribute to the pipe failure.

The rupture of 42' pipeline can be caused by the poor welding quality. The condition of the land topography enhanced the failure to be occurred. Lack of strength due to the poor welding joint has caused the pipe failed as the pipe cannot accommodate the force against the load created by the land slide or movement.

The pipe fracture was initiated from the back weld (root weld) of the pipe, where the high hardness of the HAZ indicated a brittle material structure, which is more susceptible to cracking. [3]

In addition, the welding defects such as weld porosity and incomplete weld fusion penetration play a part to the failure to be occurred. In this case, porosity presents in the weld area, especially at the HAZ between two welding pass. Porosity is the result of gas entrapment in the solidifying metal. Most porosity is not visible and it can cause crack in weld. Several caused that could create porosity are: [4]

1. Improper surface preparation such as contamination by the atmosphere and other materials such as oil, dirt, rust, and paint.
2. Changes in the physical qualities of the filler wire due to excessive current.
3. Entrapment of the gas evolved during weld metal solidification.
4. Improper welding technique, excessive stick out, improper electrodes angle, and too fast moving of electrode and the stopping area at the end of the weld.

The porosity probably caused by improperly base metal surface preparation before welding and this may contribute to the creation of gas entrapment at the weldment.

Incomplete fusion indicated that the welding procedure specification (WPS) and the inspection of weld joint are not followed by the welding contractor, considering that the weld joint for gas transmission pipeline is required a 100% radiography examination in every pipe joint. [5]

VI. CONCLUSION

Based on data from investigation as well as testing results, several conclusions are drawn as follows:

1. The rupture 42" pipeline is mainly initiated by welding defects at the root weld (back weld) due to an inproperly welding process at the root weld. The welding defects was mainly found at the root weld such as porosity, incomplete penetration (IP), the brittle structures of HAZ (bainite and martensite) which is more susceptible to cracking.
2. Lack of strength due to poor welding joint containing weld defects can cause the pipe failed since the pipe cannot accommodate the force against the load created by the land slide or land movement.

VI. RECOMMENDATION

1. The welding procedure specification (WPS) of pipeline joint shall be qualified in conformance with the standard code. Lack of conformance with the parameters outlined in the WPS may result in the deposition of a weld that does not meet the quality requirements imposed by the code

2. The inspection process before, during and after welding process must be carried out in order to avoid the presence of welding defects in the weld of pipeline..

REFERENCES

[1]. API 5L, Specification for Line Pipe, 43rd Edition, **American Pipeline Institute Standard**, 2004

[2]. ASTM E 8M, Standard Test Methods for Tension Testing of Metallic Materials [Metric], **American Standard for Testing Material Book**, 2004

[3]. Colangelo VJ, Heiser FA. Analysis of Metallurgical Failure. **John Wiley and Sons**; 1987.

[4]. Kou, Sindo., Welding Metallurgy, **John Wiley & Son**, 1987.

[5]. API Standard 1104, Welding of Pipelines and Related Facilities, 19th Edition, **American Pipeline Institute Standard,** 2001

ISSN: 1411-1284

Optimization of Surface Roughness when End Milling Ti-6Al4V using TiAlN Coated Tool.

A.S. Mohruni*, S. Sharif**, M.Y. Noordin**, V.C. Venkatesh

*Faculty of Engineering, Sriwijaya University, Jl. Raya Prabumulih Km.32, Indralaya, 30662
Tel. +62-711-410745 email : mohrunias@yahoo.com, mohrunias@unsri.ac.id
**Faculty of Mechanical Engineering, Universiti Teknologi Malaysia, 81310-UTM Skudai, Johor, Malaysia

Abstract– **Investigation on the surface roughness of titanium alloy, Ti-6AL4V during end milling using TiAlN coated solid carbide tools was conducted at various cutting conditions under flood coolant. Surface roughness as one of the component for surface integrity was examined using response surface methodology at various primary cutting parameters such as cutting speed, feed and radial rake angle. Results showed that the second order surface roughness model was the best model and used to ascertain the optimum cutting conditions using response surface methodology. ANOVA was employed to validate the predictive surface roughness models.**

Keywords– surface roughness models, end milling, titanium alloys, responses surface methodology, TiAlN coating

I. INTRODUCTION

Titanium alloys are used extensively in the aerospace industry for structural components and as compressor blades, disc, casing, etc. in the cooler parts of gas turbine engines. They are also found suitable to be used in such diverse areas such as energy and chemical processing industries, offshore and marine applications, automotive industry, medical implants, and sporting equipment. Titanium alloys have excellent strength-to-weight ratio and good elevated temperature properties (up to approximately 550 ^{o}C). Consequently, when operating temperatures exceed 130 ^{o}C, titanium alloys can be used as an alternative to aluminum, or at higher temperatures still, titanium can be used as a lightweight alternative to nickel-based alloys or steel [1] - [6].

Surface integrity which includes surface roughness is very critical to the functionality of a machined component. It influences several functional attributes of a part, such as coefficient of friction, mating characteristics, fatigue, heat transfer etc. Thus surface finish measurement represents one of the most important aspects in the analysis of machining process. As reported by previous researchers [7] - [10] the appropriate range of cutting speed, feed, which provide a satisfactory surface finish and tool life are very limited. According to their findings, the tool geometry effect was not taken into consideration during end milling operation. An effort to include the effect of tool geometry on surface roughness in turning [11] and milling [12] – [14] operations using response surface methodology were carried out by few researchers.

In this investigation, the tool geometry (radial rake angle), cutting speed and feed were evaluated when end milling Ti-6Al4V using solid TiAlN coated carbide tools.

To cover lack of information in tool geometry effect in machining titanium alloy this study was carried out. The objectives of this study were to develop the surface roughness mathematical models and to determine the optimum cutting conditions when end milling titanium alloy Ti-6Al4V using response surface methodology.

II. DESCRIPTION OF THE MATHEMATICAL MODEL

The first step in developing a mathematical model for surface roughness is to propose the postulation of the mathematical models in relations to the machining process. To formulate the postulated mathematical model, the proposed surface roughness model is considered as a function of cutting speed V, feed f_z and radial rake angle γ_o. Other factors such as machine tools, stability, entry and exit condition etc are kept constant.

Thus the proposed surface roughness model when end milling Ti-6Al4V in relation to the independent variables investigated, can be formulated as

$$R_a = C.V^k f_z^l.\gamma_o^m.\varepsilon^{'} \quad (1)$$

where R_a is the experimental (measured) surface roughness (μm), V is the cutting speed (m.min^{-1}), f_z is the feed per tooth (mm.tooth^{-1}), γ_o is the radial rake angle (^{o}), $\varepsilon^{'}$ is the experimental error and C, k, l, m are parameters to be estimated using experimental data.

To determine the constants and exponents of Equation (1), the mathematical model will have to be linearized by performing natural logarithmic

transformation, and Equation (1) can be written as follow:

$$\ln R_a = \ln C + k \ln V + l \ln f_z + m \ln \gamma_o + \ln \varepsilon' \quad (2)$$

which can also be transformed into:

$$y = b_0 x_0 + b_1 x_1 + b_2 x_2 + b_3 x_3 + \varepsilon \quad (3)$$

and rewritten in the following form:

$$\hat{y}_1 = y - \varepsilon = b_0 x_0 + b_1 x_1 + b_2 x_2 + b_3 x_3 \quad (4)$$

where y is the true response of surface roughness on a natural logarithmic scale, $\hat{y}_1$ is the natural logarithmic value of predicted (estimated) surface roughness, $x_0 = 1$ (a dummy variable), x_1, x_2 and x_3 are the natural logarithmic transformation (in coded variables) of V, f_z and γ_o respectively, ε is the natural logarithmic transformation of the experimental error ε' and b_0, b_1 and b_3 are the model parameters to be predicted using the experimental data.

To facilitate the investigation of extended observation region, a second order model is required when the second order and interaction effect of V, f_z, γ_o are significant. The first order model in Equation (4) can be extended to the second order model as:

$$\begin{aligned}\hat{y}_2 &= y - \varepsilon \\ &= b_0 x_0 + b_1 x_1 + b_2 x_2 + b_3 x_3 \\ &\quad + b_{12} x_1 x_2 + b_{13} x_1 x_3 + b_{23} x_2 x_3 \\ &\quad + b_{11} x_1^2 + b_{22} x_2^2 + b_3 x_3^2\end{aligned}$$

where $\hat{y}_2$ is the predicted response based on the experimental measured surface roughness on a natural logarithmic scale and b values are the parameters, which are to be estimated by the least squares method [7][8] [12][13][14].

Validity of the resulted prediction model, which is used for optimizing the machining process has to be tested using ANOVA, while Design Expert 6.0 software [15] was used to analyze the experimental results.

III. EXPERIMENTAL DETAILS

III.1 EXPERIMENTAL DESIGN

In performing the experimentation, the design of experiment has a major effect on the number of experiments to be conducted. It is essential to have a well designed experiment so that the number of experiments required can be minimized [14]. The screening trials were conducted using 2^k-factorial design with replicated center points, which utilized the first 12 tests (Fig. 1), to observe the significant factors [16].

In order to gain more information in the extended range of observation, the central composite design (CCD) was applied, which is 2^k-factorial design augmented with axial stars points as presented in Fig. 1

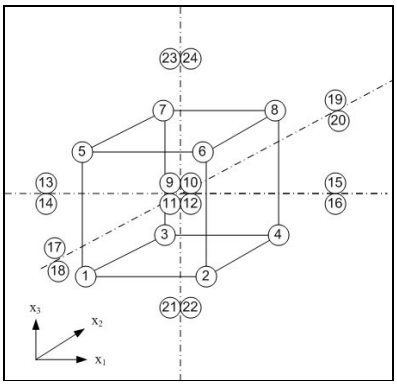

Fig. 1 Design of experiments employed in the development of prediction models.

From previous study [17], the distance between center points and star points, α is 1.4142 for $n_c = 4$ with 3 factors.

III.2 CODING OF INDEPENDENT VARIABLES

Cutting parameters (V, f_z, γ_o) are coded using transformed Equation (6) according to the particular circumstance of limitation of the milling machine.

$$x = \frac{\ln x_n - \ln x_{n0}}{\ln x_{n1} - \ln x_{n0}} \quad (5) \qquad (6)$$

where x is the coded variable of any factor corresponding to its natural x_n, x_{n1} is the natural value at the +1 level and x_{n0} is the natural value of factor corresponding to the base or zero level [7] - [10], [14] and [17]. Another similar coding was reported by [12] and [13]. The level of the independent variables and coding identification are illustrated in Table 1.

Table 1 Coding of independent variables for end milling Ti-6Al4V

Independent Variable	**Level in coded form**				
	-α	-1	0	+1	+α
V (mm.min^{-1}) x_1	124.53	130	144.22	160	167.03
f_z (mm.tooth^{-1}) x_2	0.025	0.03	0.046	0.07	0.083
γ_o (^{o}) x_3	6.2	7.0	9.5	13.0	14.8

III.3 EXPERIMENTAL SET-UP

Surface roughness of the machined surface was measured using a portable Taylor Hobson Surftronic +3 at the initial cut of the new solid carbide end mill, grade K30 with different radial rake angle.

A sequentially end milling trials were conducted on a CNC MAHO 700S machining centre with a

constant axial depth of cut (a_a) 5 mm and radial depth of cut (a_p) 2 mm under wet conditions using 6% of water base coolant.

IV. EXPERIMENTAL RESULTS

The surface roughness of machined surface was measured five times at the end of each cutting trial and the average values were tabulated accordingly in Table 2.

After conducting the analysis of appropriate surface roughness models (2^k-factorial model, 1st order CCD model and 2nd order CCD model), it was found that the 3F1 surface roughness model was the most accurate model among them.

Table 2 Coding of independent variables for end milling Ti-6Al4V

Std. Order	Type	Cutting Speed V (m/min)	Feed per tooth (mm/th)	Radial rake angle (^{o})	Ra (μm
1	Factorial	-1	-1	-1	0.32
2	Factorial	1	-1	-1	0.21
3	Factorial	-1	1	-1	0.45
4	Factorial	1	1	-1	0.42
5	Factorial	-1	-1	1	0.40
6	Factorial	1	-1	1	0.23
7	Factorial	-1	1	1	0.48
8	Factorial	1	1	1	0.46
9	Center	0	0	0	0.368
10	Center	0	0	0	0.360
11	Center	0	0	0	0.324
12	Center	0	0	0	0.304
13	Axial	-1.4142	0	0	0.348
14	Axial	-1.4142	0	0	0.34
15	Axial	1.4142	0	0	0.25
16	Axial	1.4142	0	0	0.24
17	Axial	0	-1.4142	0	0.30
18	Axial	0	-1.4142	0	0.31
19	Axial	0	1.4142	0	0.58
20	Axial	0	1.4142	0	0.65
21	Axial	0	0	-1.4142	0.31
22	Axial	0	0	-1.4142	0.30
23	Axial	0	0	1.4142	0.38
24	Axial	0	0	1.4142	0.39

The following discussion was focused on the 3F1 surface roughness model, its result is written as follows:

$$\hat{y}_1 = -1.0196 - 0.13189x_1 + 0.23772x_2 + 0.057986x_3 + 0.10751x_1x_2 \quad (7)$$

ANOVA was carried out to validate Equation (7) and is presented in Fig. 2. Results show that the lack of fit (LOF) was not significant. Thus the model is valid for end milling of titanium alloy, Ti-6Al-4V using TiAlN coated carbide tools under wet conditions with the following range of respective cutting speed V, feed per tooth f_z and radial rake angle γ_o: $130.00 \le V \le 160.00$ m.min^{-1}; $0.03 \le f_z \le 0.07$; $7.0 \le \gamma_o \le 13.0$ (^{o}).

Response: Surface Ra Transform: Natural log Constant: 0.00000
ANOVA for Selected Factorial Model
Analysis of variance table [Partial sum of squares]

Source	Sum of Squares	DF	Mean Square	F Value	Prob > F	
Model	0.71059	4	0.17765	30.143	0.00041094	significant
A	*0.13915*	*1*	*0.13915*	*23.612*	*0.0028252*	
B	*0.45208*	*1*	*0.45208*	*76.708*	*0.00012270*	
C	*0.026899*	*1*	*0.026899*	*4.5641*	*0.076532*	
AB	*0.092459*	*1*	*0.092459*	*15.688*	*0.0074445*	
Curvature	0.011311	1	0.011311	1.9193	0.21524	not significant
Residual	0.035361	6	0.0058935			
Lack of Fit	*0.011124*	*3*	*0.0037080*	*0.45897*	*0.73055*	*not significant*
Pure Error	*0.024237*	*3*	*0.0080790*			
Cor Total	0.75726	11				

Fig. 2 ANOVA for the 3F1-surface roughness model using TiAlN coated carbide tools.

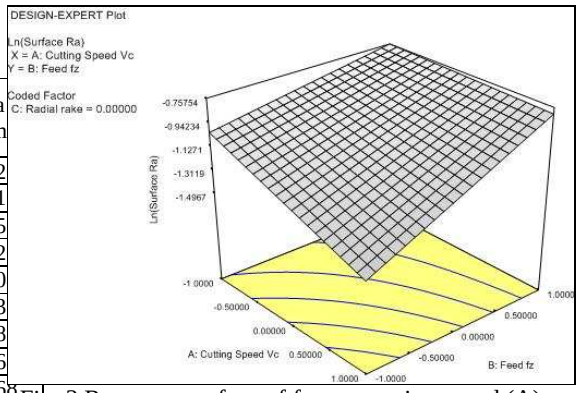

Fig. 3 Response surface of factors cutting speed (A) and feed (B) for the 3F1 surface roughness model using TiAlN coated carbide tools.

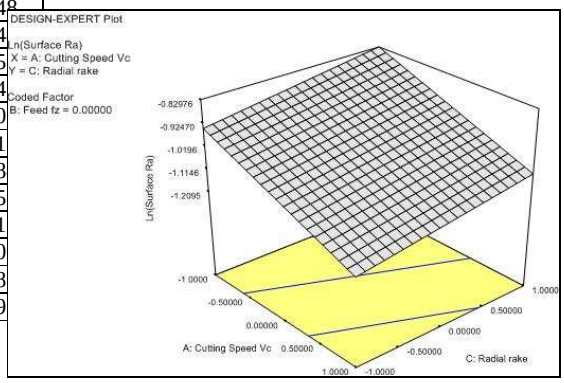

Fig. 4 Response surface of factors cutting speed (A) and radial rake angle (C) for the 3F1 surface roughness model using TiAlN coated carbide tools.

The response surface of Equation (7) is shown in Fig. 3 to Fig. 5. It was found that the most significant factor was feed per tooth followed by cutting speed and radial rake angle. From these response surfaces, it can be observed that the minimum surface roughness can be achieved when employing a combination of highest cutting speed, lowest feed per tooth and radial rake angle. In contrary, the maximum surface roughness can be obtained when using the lowest cutting speed combined with the highest feed per tooth and radial rake angle.

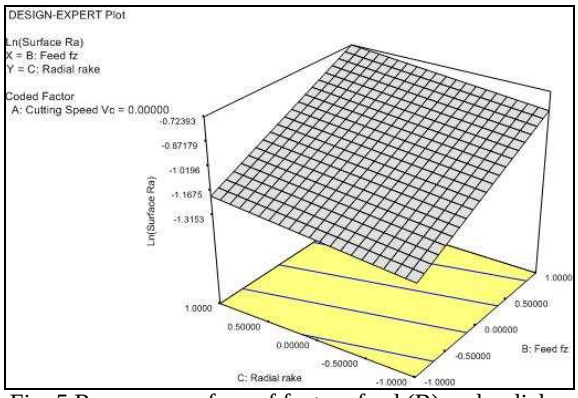

Fig. 5 Response surface of factors feed (B) and radial rake angle (C) for the 3F1 surface roughness model using TiAlN coated carbide tools.

In order to widen the point of view, additional observation on the 2nd order CCD surface roughness has to be investigated. From the analysis, the 2nd order surface roughness model can be formulated as follows:

$$\hat{y}_2 = -1.0810 - 0.12272x_1 + 0.23941x_2 + 0.71218x_3 + 0.10751x_1x_2 - 0.016614x_1x_3 - 0.020616x_2x_3 - 0.072385x_1^2 + 0.12822x_2^2 + 0.009294x_3^2$$

Response: Surface Ra Transform: Natural log Constant: 0.00000

ANOVA for Response Surface Quadratic Model

Analysis of variance table [Partial sum of squares]

Source	Sum of Squares	DF	Mean Square	F Value	Prob > F	
Block	0.00034835	1	0.00034835			
Model	1.6742	9	0.18603	55.274	< 0.0001	significant
A	*0.24096*	*1*	*0.24096*	*71.596*	*< 0.0001*	
B	*0.91709*	*1*	*0.91709*	*272.50*	*< 0.0001*	
C	*0.081153*	*1*	*0.081153*	*24.113*	*0.00028473*	
A^2	*0.062876*	*1*	*0.062876*	*18.682*	*0.00082835*	
B^2	*0.19729*	*1*	*0.19729*	*58.621*	*< 0.0001*	
C^2	*0.0010362*	*1*	*0.0010362*	*0.30788*	*0.58840*	
AB	*0.092459*	*1*	*0.092459*	*27.472*	*0.00015921*	
AC	*0.0022081*	*1*	*0.0022081*	*0.65610*	*0.43252*	
BC	*0.0034000*	*1*	*0.0034000*	*1.0103*	*0.33319*	
Residual	0.043752	13	0.0033655			
Lack of Fit	*0.0097086*	*4*	*0.0024272*	*0.64167*	*0.64621*	*not significant*
Pure Error	*0.034043*	*9*	*0.0037826*			
Cor Total	1.7183	23				

Fig. 6 ANOVA for the 2nd order CCD-surface roughness model using TiAlN coated carbide tools.

To prove the adequacy of the surface roughness model, ANOVA was carried out and results are listed in Fig. 6. ANOVA results indicated that LOF was not significant. Thus model or Equation (8) is valid for end milling Ti-6Al4V using TiAlN coated carbide tools under wet conditions with the following range of respective cutting speed V, feed per tooth f_z and radial rake angle γ_o: $124.53 \le V \le 167.03$ m.min^{-1}; $0.025 \le f_z \le 0.083$; $6.2 \le \gamma_o \le 14.8$ (^{o}).

From the following figures (Fig. 7 and Fig. 8), it is obvious to recognize that even the 3F1-surface roughness model is the most accurate model, it can't describe extended observation region with adequate accuracy (see standard order 13 to 24 in Fig. 7). In contrary, the 2nd order CCD-surface roughness model, which is less accurate than 3F1-surface roughness model, can represent extended range of observation better than 3F1-model (see standard order 13 to 24 in Fig. 8). It has proven the validity of each model for particular observation field.

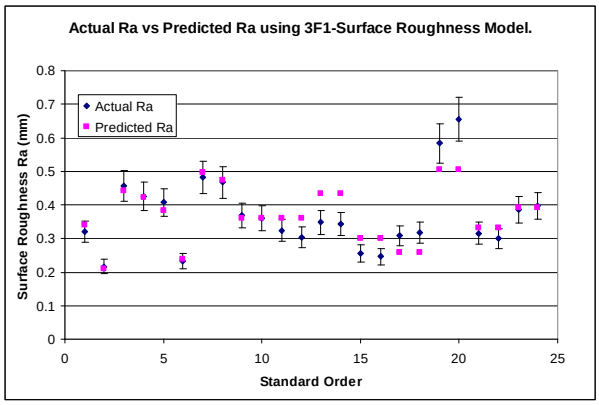

Fig. 7 Comparison actual surface roughness value with predicted surface roughness value using 3F1-surface roughness model for TiAlN coated carbide tools.

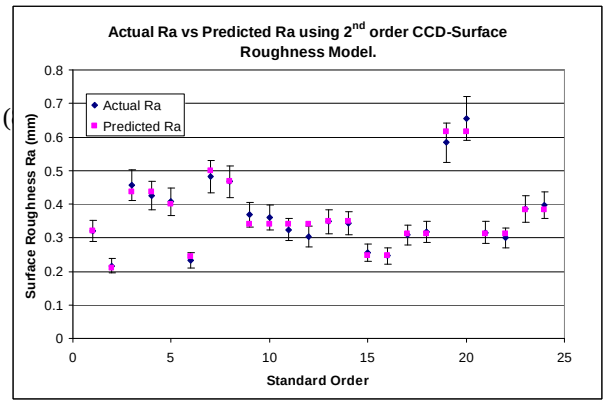

Fig. 8 Comparison actual surface roughness value with predicted surface roughness value using 2nd order CCD-surface roughness model for TiAlN coated carbide tools.

Based on the most accurate surface roughness model (3F1-surface roughness model), optimum cutting conditions for a minimum surface roughness value is to be investigated.

From Fig. 9 and Fig. 10, optimum cutting conditions were revealed according to their constraint. First optimum cutting condition was when end milling using V = 159.81 m/min; $f_z \approx 0.031$ mm/tooth, $\gamma_o \approx 7.3$ (^{o}). Another optimum cutting condition shown in Fig. 10 was V = 160.00 m/min; $f_z \approx 0.054$ mm/tooth, $\gamma_o \approx 7.0$ (^{o}).

Constraints

Name	Goal	Lower Limit	Upper Limit	Lower Weight	Upper Weight	Importance
Cut. Speed V	is in range	130.00	160.00	1.0000	1.0000	3
Feed fz	is in range	0.03	0.07	1.0000	1.0000	3
Radial rake	is in range	7.0	13.000	1.0000	1.0000	3
Surface Ra	minimize	0.216	0.482	1.0000	1.0000	3

Solutions

Number	Speed V	Feed fz	Radial rake	Surface Ra	Desirability	
1	159.81	0.030769	7.2706	0.21583	1.0000	Selected
2	159.80	0.030534	7.2046	0.21472	1.0000	
3	159.94	0.030110	7.9957	0.21595	1.0000	
4	159.91	0.030098	7.9370	0.21579	1.0000	
5	159.76	0.030017	7.7664	0.21528	1.0000	
6	159.89	0.030074	7.7355	0.21493	1.0000	
7	160.00	0.030000	8.2375	0.21636	0.99792	
8	160.00	0.030000	11.145	0.22887	0.92790	
9	160.00	0.030000	12.644	0.23559	0.89182	
10	160.00	0.030000	12.999	0.23722	0.88327	

10 Solutions found

Fig. 9 Possible solutions for 3F1-surface roughness model using TiAlN coated end mill with $n_c = 4$ when V and f_z are in range

Constraints

Name	Goal	Lower Limit	Upper Limit	Lower Weight	Upper Weight	Importance
Cut. Speed Vc	maximize	130.00	160.00	1.0000	1.0000	3
Feed fz	maximize	0.03	0.07	1.0000	1.0000	3
Radial rake	is in range	7.0	13.0	1.0000	1.0000	3
Surface Ra	minimize	0.216	0.482	1.0000	1.0000	3

Solutions

Number	Speed Vc	Feed fz	Radial rake	Surface Ra	Desirability	
1	160.00	0.053894	7.0001	0.31909	0.67458	Selected
2	160.00	0.054074	7.0001	0.32008	0.67457	
3	160.00	0.054130	7.0259	0.32055	0.67428	
4	160.00	0.053949	7.2041	0.32065	0.67242	
5	159.58	0.054670	7.0000	0.32435	0.66954	
6	160.00	0.051871	8.2546	0.31570	0.66058	
7	160.00	0.052709	10.918	0.33722	0.63218	

7 Solutions found

Fig. 10 Comparison actual surface roughness value with predicted surface roughness value using 2nd order CCD-surface roughness model for TiAlN coated carbide tools.

V. CONCLUSIONS

There were three surface roughness models that satisfied for describing the surface roughness values when end milling Ti-6Al4V, namely 3F1-model, 1st and 2nd order CCD models. The most accurate among them was the 3F1-surface roughness model. The 2nd order surface roughness model described better in the extended observation region than the 3F1-model.

According to optimization processes, two optimum cutting conditions were discovered for two different objectives of constraints, when end milling Ti-6Al4V using TiAlN-coated carbide tools.

ACKNOWLEDGMENT

The authors wish to thank the Research Management Center, UTM and the Ministry of Science, Technology and Innovation Malaysia for their financial support to the above project through the IRPA funding Vote no. 74545.

REFERENCES

[1]. J.I. Hughes, A.R.C. Sharman and K. Ridgway, "The effect of cutting tool material and edge geometry on tool life and surface integrity, *Proceeding of the Institution of Mechanical Engineers,* vol. 220, B2, pp.93-107, 2006.

[2]. E.O. Ezugwu, J. Bonney and Y. Yamane, "An overview of the machinability of aeroengine alloys", *Journal of Materials Processing Technology,* vol. 134, pp. 233-253, 2003.

[3]. R.R. Boyer, "An overview on the use of titanium in the aerospace industry, *Materials Science Engineering,* A213, pp. 103-114, 1996.

[4]. A.K.M. Nurul Amin, A.F. Ismail, M.K. Nor Khairusshima, "Effectiveness of uncoated WC-Co and PCD inserts in end milling of titanium alloy-Ti-6Al-4V, *Journal of Materials Processing Technology,* vol. 192-193, pp. 147-158, 2007.

[5]. J.I. Hughes, A.R.C. Sharman and K. Ridgway, "The effect of tool edge preparation on tool life and workpiece surface integrity, *Proceeding of the Institution of mechanical Engineers,* vol. 218, no. 9, pp. 1113-1123, 2004.

[6]. M. Dumitrescu, M.A. Elbestawi, T.I. El-Wardhany, "Mist coolant applications in high speed machining of advanced material", *In Metal Cutting and High Speed Machining,* Edited by D. Dudinzski, A. Molinari, H. Schulz, Kluwer, pp. 329-339, 2002.

[7]. M. Alauddin, M.A. El-Baradie, M.S.J. Hasmi, "Optimization of surface finish in end milling Inconel 718", *Journal of Materials Processing Technology,* vol. 56, no. 1, pp.54-65, 1996

[8]. I.A. Choudhury, M.A. El-Baradie, "Machinability assessment of Inconel 718 by factorial design of experiment coupled with response surface methodology", *Journal of Materials Processing Technology,* vol. 95, no. 1, pp. 30-39, 1999.

[9]. A. Mansour and H. Abdalla, "Surface roughness model for end milling: a semi free cutting carbon case hardening steel (EN32) in dry condition", *Journal of Materials Processing Technology,* vol. 124, no. 1-2, pp. 183-191, 2002.

[10]. Y. Sahin and A.R. Motorcu, "Surface roughness model for machining mild steel with coated carbide tools, *Materials & Design,* vol. 26, no.4, pp. 321-326, 2005.

[11]. M.Y. Noordin, V.C. Venkatesh, S. Sharif, S. Elting, A. Abdullah, "Application of response surface methodology in describing the performance of coated carbide tools when turning AISI 1045 steel", *Journal of Materials Processing Technology,* vol. 145, no. 1, pp. 46-58, 2004.

[12]. N.S. K. Reddy, P.V. Rao, "A Genetic algorithmic approach for optimization of surface roughness prediction model in dry milling", *International Journal of Machining Science and Technology,* vol. 9, no. 1, pp. 63-84, 2005.

[13]. N.S.K. Reddy, P.V. Rao, "Selection of optimum tool geometry and cutting conditions using a surface roughness prediction model for end milling", *The International Journal of Advanced Manufacturing Technology,* vol. 26, no. 11-12, pp. 1202-1221, 2005.

[14]. S. Sharif, A.S. Mohruni, M.Y. Noordin, V.C. Venkatesh, "Optimization of surface roughness prediction model in end milling titanium alloy (Ti-6Al-4V)", *Proceeding of International Conference on Manufacturing Science and Technology (ICOMAST),* 28-30 August, Melaka, Malaysia, pp. 55-58, 2006.

[15]. Design Expert Software 6.0, User's Guide, Technical Manual, Stat-Ease Inc. Minneapolis, MN, 2000.

[16]. D.C. Montgomery, "Design and Analysis of Experiments, 5th ed. Wiley, New York, 2001.

[17]. S. Sharif, A.S. Mohruni, M.Y. Noordin, "Modeling of tool life when end milling on titanium alloy (Ti-6Al-4V) using response surface methodology, *In Proceeding of 1st International Conference & 7th*

AUSN/SEED-Net Fieldwise Seminar on Manufacturing and Material Processing, 14-15 March, Kuala Lumpur, pp. 127-132, 2006.

ISSN: 1411-1284

Comparison of Ascorbic Acid and Zinc Polyphospate as a Corrosion Inhibitor in Secondary Cooling System

Yunita Sadeli, Shanti Perwitasari, Nandyo Alpalmy

Department of Metallurgy & Materials Engineering, Faculty of Engineering, University of Indonesia, Kampus UI, Depok 16424
Email : exclusive303@yahoo.com

Abstract - **Inhibitors that is the most commonly used to prevent corrosion of low carbon steel in secondary cooling system is Zinc Polyphospate.Pitting corrosion is happen mostly in the surface of low carbon steel so that zinc polyposphate is used in order to decrease corrosion rate. This substance considers to be effective if used as a corrosion inhibitor, despite it's negative effects to the environment. In order to reduce the risk of damage of the environment, another inhibitors must be found. From the previous experiment, it is found that Ascorbic Acid (familiar as Vitamin C) may be used as a corrosion inhibitors in stainless steel. The use of vitamin C as a corrosion inhibitors may reduce the risk of damage of environment and the costs are relatively cheap. This experiment is conducted to compare the inhibition capability from vitamin C and also Zinc polyphospate, held at room temperature and used linear polarization and potentiodynamic polarization as it's methodology. The results of this experiment is that the addition of 50 ppm of vitamin C can decrease corrosion rate to 3,59 mpy with 69,47% of efficiency, while zinc polyphospate can only decrease the corrosion rate to 5,8 mpy at concentration of 40 ppm with 50,68% of efficiency.**

Keywords: Low carbon steel, Ascorbic acid (Vit C), Zinc Polyposphate, Linear Polarization, Potentiodinamic polarization.

I.INTRODUCTION

Cooling system plays an important role in a nuclear reactor since its main function in transfering heat during operation. Common nuclear reactor consists of two coling system, primary one and secondary one e.g G.A Siwabessy Reactor at BATAN. Primary cooling system uses stainless steel in its pipe while the secondary one uses low carbon steel in its pipe. Fluids that flow in primary cooling system is free-mineral water while raw water flows in secondary one. Consequently, corrosion becomes a problem since many corrosive substances and unsure exist in raw water.

In order to overcome this corrosion process, Zinc Polyphospate is used as a corrosion inhibitor. Besides, natrium hypochloride is also added in order to prevent the growth of microorganisms. Previous experiment stated that zinc polyphospate can reduce the corrosion rate in a 64.28% value of efficiency. But according to USEPA (United States Environmental Protective Agency) and also EECD (European Economics Community Directive), Zinc regarded as substances that are hazardous to the environment. For this reason, this experiment was done in order to find new corrosion inhibitors that are harmless to the environment and also high in efficiency to reduce corrosion rate. Issao Sekine in his experiment said that ascorbic acid can be used efficiently to inhibit corrosion in neutral pH and 30^0 – 80^0 C of temperature. This indicates that ascorbic acid can be used as corrosion inhibitors to replace zinc polyphospate.

II.BASIC THEORY

Corrosion is a degradation of material due to reaction with environment.Corrosion mechanism in aquatic environment affected with the electrochemistry theory which involves electrical current in a surface of a metal (anode) to another area (cathode) through electrolite solution.
Generally corrosion reaction can be written as follows:

Oxidation : $M \rightarrow M^{2+} + 2e^-$
Reduction : $O_2 + 2H_2O + 4e^- \rightarrow 4OH^-$
$2H^+ + 2e^- \rightarrow H_2$

Prevention of corrosion could be done in following methods:

a. Use high purity of metals
b. Alloying the metals
c. Proper Design
d. Cathodic Protection
e. Inhibitors
f. Coating

The cheapest method is by using an inhibitor. Inhibitor is a substant that can reduce the corrosion rate in a few additon to corrosive environment.Inhibitor classified in three categories:
1. Anodic Inhibitors
2. Cathodic Inhibitors
3. Mix Inhibitors

Performance of inhibitors can be measure with its efficiencies in reducing corrosion rate. Efficiencies can be measure using following equation.

$$E = \frac{CR_0 - CR_1}{CR_0} x100\% \quad (1)$$

E = Efficiency value
CR_0 = Corrosion rate before addition of inhibitor
CR_1 = Corrosion rate after addition of inhibitor

While corrosion rate can be measured in two methods:

1. Weight Loss

In order to gain the value of corrosion rate, immersion of the sample to corrosive media is needed.Weight differences after immersion considered as a weight loss due to corrosion process.Equation that is used in weight loss methods is as follows.

$$mpy = \frac{534w}{DAT} \quad (2)$$

W is a weight loss(weight differences) ; D is a density of a sample(gr/cm^3); A is cross section of sample(sq.in) dan T is immersion time(hour).

2. Electrochemistry

This method based on electrochemical reaction from the corrosion process.This method has some advantages: fast measurement and accurate data. There are two ways in measuring corrosion rate using this method:

2.1 Tafel Extrapolation

To measure corosion rate, tafel area is extrapolated to corrosion potential while cutting point between the two curves shows the value of corrosion current (i_{corr}).The value then used in following equations.

$$mpy = \frac{0{,}13.i_{corr}.BE}{D} \quad (3)$$

I_{corr} is a corrosion current density ($\mu A/cm^2$) ; BE is equivalent weight (BA/n) dan D is a density of a metal (g/cm^3).

2.2 Linear Polarization

Also called with polarization resistance.Polarization resistance shows the inhibition from corrosion process.Equation is as follows.

$$i_{corr}(\mu A) = \frac{\beta a.\beta c}{2{,}3.(\beta a + \beta c)(A)(Rp)} \quad (4)$$

βa, βc is a tafel number for cathodic and anodic ; Rp is polarization resistance (k-ohm/cm^2).

III.EXPERIMENTAL RESULTS

Following tables shows the results of the corrosion rate measurements of low carbon steel in raw water.Value of corrosion current is gained from the polarization curve.Corrosion rate is measured using equation (3) and (4).

Tabel 1. Results of the measurement using potentiodynamic polarization

Results	
E (I=0)(mV)	-513.65
I_{corr} ($\mu A/cm^2$)	25.6
Corr rate (mpy)	11.92

Tabel 2. Results of the measurement using linear polarization

Results	
E (I=0)(mV)	-515.62
Cathodic tafel (mV)	820.15
Anodic tafel (mV)	422.68
I_{corr} ($\mu A/cm^2$)	28.19
Corr rate (mpy)	13.12
Pol Res (kOhm/cm^2)	4.2958

Since using either potentiodynamic or linear polarization methods resulting same tendencies, so the authors use only one of them in three times measurements.Relations between concentration and corrosion potentials is shown in figure (1) and (2) below.

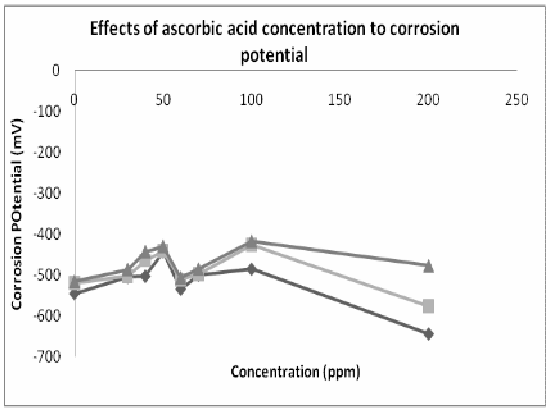

Fig 1.Relations between ascorbic acid concentrations and corrosion potentials

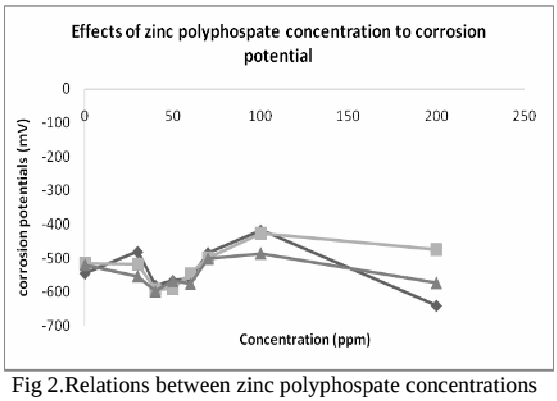

Fig 2.Relations between zinc polyphospate concentrations and corrosion potentials

Basically, corrosion current and corrosion potentials will be changed due to an addition of inhibitors.This changes will depend on the type of inhibitors that is used in a system.Addition of ascorbic acid until 50 ppm will cause corrosion potential to increase. This shows us that ascorbic acid belongs to anodic inhibitors.While addition of ascorbic acid until 60 ppm and more than 100 ppm will cause corrosion potential to decrease. In a system using zinc polyphospate, corrosion potential also changed due to the change in concentration. Zinc polyphospate belongs to cathodic inhibitor. Adding concentration up to 40 ppm will cause corrosion potential to decrease.Decrease in corrosion potentials is caused by the form of protective film in cathodic area and caused the oxygen reduction to resist.Thus, electron accumulated in a metal surface causing corrosion potential to be negative.Relations between concentration addition and corrosion rate shown in figure (3).For ascorbic acid, minimum corrosion rate (3.69 mpy) is reached in a 50 ppm of concentration. Further addition will cause corrosion rate to increase.For zinc polyphospate, minimum corrosion rate (5.8 mpy & 3.92 mpy) is reached in 40 ppm and 100 ppm of concentration. Further addition will increase in corrosion rate.

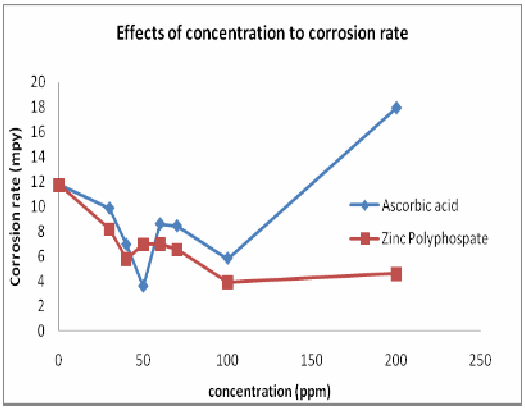

Fig.3 Relations between concentration and corrosion rate

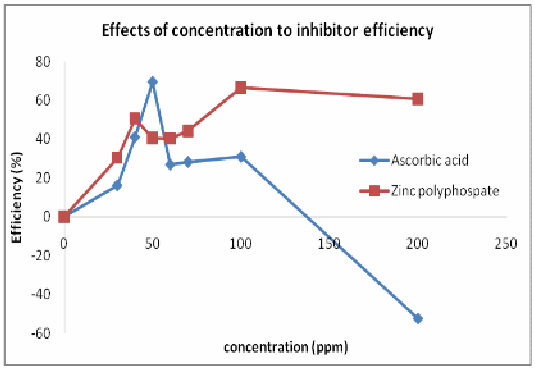

Fig.4 Relations between concentration and efficiency

The highest efficiency for ascorbic acid (69.47 %) is reached in 50 ppm of concentration.As explained before that further addition of ascorbic acid will increase the corrosion.Increase in corrosion rate will led to the decrease in inhibitor efficiency (fig.4). While highest efficiency for zinc polyphospate is reached in 40 ppm of concentration and will be decrease in further addition.Since both inhibitor could produce high efficiency so both of them consider effective as a corrosion inhibitor.Zinc polyphospate can produce higher efficiency (66.67%) in a 100 ppm but this higher concentration will harm the environment (hazardous).

Metallographic examination was also done in order to observe the destruction of a metal surface due to corrosion process. Metallographic examination was conducted using SEM (Scanning Electron Microscope). It can be seen from the figure below that pitting corrosion is happen on a metal surface.Either in ascorbic acid or zinc polyphospate,corrosion process on metal surface

using these inhibitor will decrease until maximum concentration is reached then increase in more inhibitor addition.

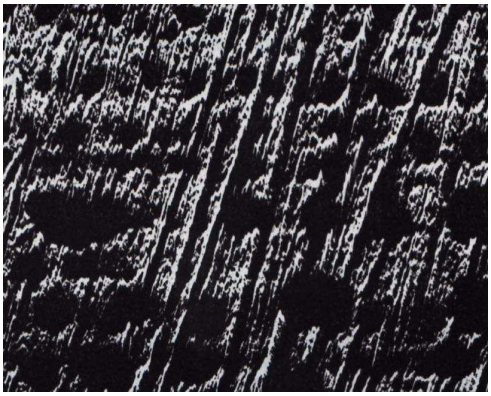

Fig.3 Metal surface condition in raw water

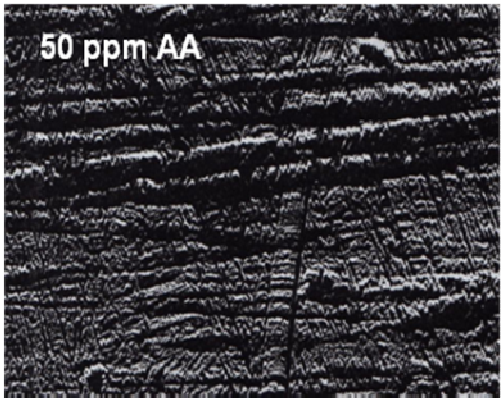

Fig.4 Metal surface condition in 50 ppm ascorbic acid

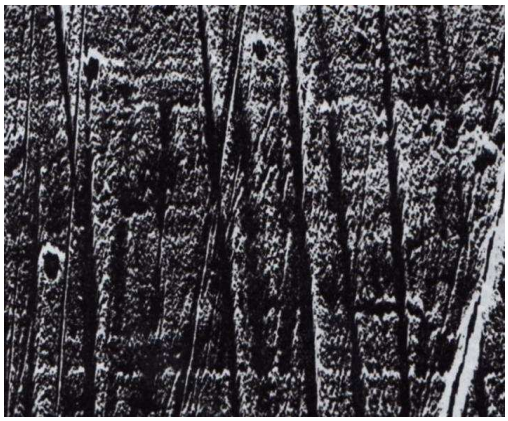

Fig.5 Metal surface condition in 40 ppm zinc polyphospate

IV. CONCLUSIONS

1. The use of 50 ppm ascorbic acid could decrease corrosion rate in low carbon steel from 11.72 mpy (without inhibitor) to 3.59 mpy.
2. The use of 40 ppm zinc polyphospate could decrease corrosion rate in low carbon steel from 11.72 mpy (without inhibitor) to 5.8 mpy.
3. Inhibitor efficiency at maximum concentration of ascorbic acid (50 ppm) is 69.87% and 50.68% in a 40 ppm of zinc polyphospate.
4. Corrosion that occured on a metal surface is pitting corrosion then decrease with an addition of inhbitor until its maximum concentration.

REFERENCES

[1]. Susilawati, Dewi Ika, *Studi Awal Asam Askorbat (Vit.C) Sebagai Inhibitor Korosi Pada Baja Tahan Karat Jenis AISI 304 Dalam Sistem Pendingin*,not published, FTUI, Depok 1992.

[2]. L,Valek,dkk. *Ascorbic Acid as Corrosion Inhibitor for Steel in AlkalineMedia Containing Chloride Ion*. Chem.Biochem.Eng.Q.**21**(1) 65–70 (2007).

[3].Tosun,Ayse dan Mubeccel ergun, *Protection of Corrosion of Carbon Steel by Inhibitors in Chloride Containing Solutions.* G.U. Journal of Science 19(3): 149-154 (2006).

[4].Franklin, James A., *Atlas of Electrochemical Equilibrium in Aqueous Solution (terj.).*, Pourbaix, Marcel, NACE, USA, 1974

[5]. Perwitasari, Shanti, *StudiPerbandingan Penggunaan Asam askorbat dan Seng Polipospat Sebagai Inhibitor Korosi Pada Baja Karbon Rendah*, not published, FTUI, Depok 1993.

[6].Uhlig, H.H. Revie.R.W., *Corrosion And Corrosion Control*, John Wiley and Sons Inc., Singapore, 3rd.ed., 1985.

ISSN: 1411-1284

Analysis of 32” Pipe Weld Crack on Gas Transmission Pipeline

Winarto, Deni Ferdian, Muhammad Anis
Department of Metallurgy & Materials Engineering, University of Indonesia
Kampus Baru UI Depok – 16424
Email: winarto@metal.ui.ac.id

Abstract— **Weld joint crack were found at several pipe joint of a new constructed gas transmission pipeline. The entire crack observed is a longitudinal crack. The welding process was performed by two welders using internal clamping. The crack was taken place at the fusion line of the weld and the centerline root weld. Microstructure and SEM examination of the sample revealed that the crack was propagated along the weld fusion line, followed the fusion line curve and then turn direction perpendicular to the weld centerline. The centerline crack was propagated with no significant change in crack direction. The significant hardness value was different between the root pass and capping weld. This created a residual stress to the weld joint along with additional stresses implied upon removal of the internal clamp and lifting of the pipe. Therefore, the cracks were occurred before hot pass performed or during the deposition of hot pass and movement of the pipe which subsequently propagates to the lower strength of the weld root and the bottom of the fusion line**

Keywords—Gas pipeline, Longitudinal crack, Internal clamp, Residual stress

I. INTRODUCTION

A constructed new pipeline was encounter longitudinal weld crack. The cracks running at the root pass either at the fusion line or at the root center. Position of the crack is at the bottom (6 o’clock) region of the weld, where two welders with the direction of vertical down meet each other and completed the pass. Radiographic interpretation of the weld joint resembles indications of hot cracking (multiple lines of crack along the root).

The weld consists of several pass with the root pass using E 6010 electrode and for filler and capping pass using E 8010G electrode with no preheat and no post weld heat treatment (PWHT).

Further investigation is needed to investigate that causes the weld crack, and to make recommendations for preventive action to this problem.

Figure 1. Picture of 42” pipeline rupture in weld join area.

II. METHODOLOGY

The visual and stereoscopic examinations were carried out on the failed weld joint. The chemical composition of the base material, cap and root weld was analyzed by emission optical spectrophotometer. Sectioned weld pipe joint then prepared for metallurgical evaluation.

The specimens were prepared using standard metallographic sample preparation techniques, and Nital 2% was used as an etchant to reveal the microstructure. Hardness profile measurements were performed in micro Vickers method. SEM equipped with EDX analysis was used for surface fractography and microanalysis examination of the failed section.

III. RESULTS & DISCUSSION

Chemical Analysis/Identification

The chemical analysis of the failed pipe sample is tested by spark-spectrometry and the result is shown in table 1. This result is conform to the specification of API 5L Gr X65 PSL 2. [1] API 5L required for PSL 2 has a mandatory requirement for carbon equivalent. Analysis of carbon equivalent calculation CE (pcm) from base metal is 0.146% (Ito-Bessyo formula was used for carbon less than 0.12%). No conclusion was made as inappropriate material selection could be possible cause of the crack.

Table 1. Chemical Composition Results **[1]**

Material	%C	%Si	%Mn	% P	% S	% Ti
API 5L – X65	0.22 max	-	1.45 max	0.025 max	0.015 max	0.06 max
Sample	0.06	0.269	1.318	0.008	.006	0.01

Visual Examination

The visual examination showed that most of the sample crack occurred at the weld fusion line of pipe, which is the border line between HAZ and the weld metal. From four of the sample received, one of the samples has the crack at the center of the weld

Metallography Examination

Macro-structures of the pipe were taken at the cross section area under magnification of 7X. The cutting area of pipe weld joint were taken into two areas, first, at location of the non-crack area as seen in Figure 2 and at location of crack area as seen in Figure 3 and 4

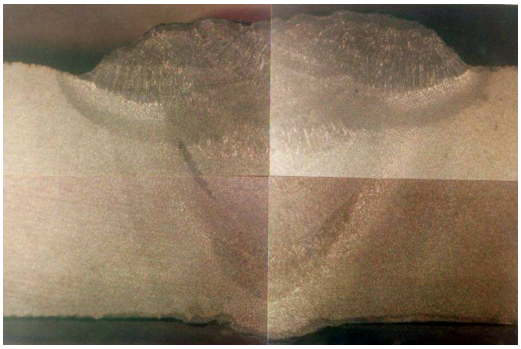

Figure 2. The macro-structure of non-fractured weld joint area, etched with 2 % Nital, magnification of 7 X

Figure 3. The macro-fractography of fracture surface sample A where the crack appears at fusion line of the root weld joint, 7 X

The results of macrostructure in Figure 2 show the typical of weld cross section, with good metal fusion and weld pass noticeable clearly. The macrostructure in Figure 3 and 4 which taken from sample A and B, was revealed the condition of the weld crack. For Figure 3, the crack took place along the weld fusion line, follow the fusion line curve and then turn direction perpendicular to the weld centerline.

Figure 4. The macro-fractography of fracture surface sample B where the crack appears at the center line of the root weld joint, 7 X

Figure 4 showed the crack propagated to the weld center with no significant change in crack direction. Those crack then further examined using SEM. Moreover, microstructures of the pipe were also taken at cross section area under magnification of 100 and 500 X.

The results of microstructure investigation can be seen in Figure 5 to Figure 7. The microstructure is dominantly consisted ferrite matrix of low-alloy carbon steel. The shape of grains also appeared elongated. The microstructure examination of the crack revealed no indication of martensite or bainite in close proximity to the weld crack.

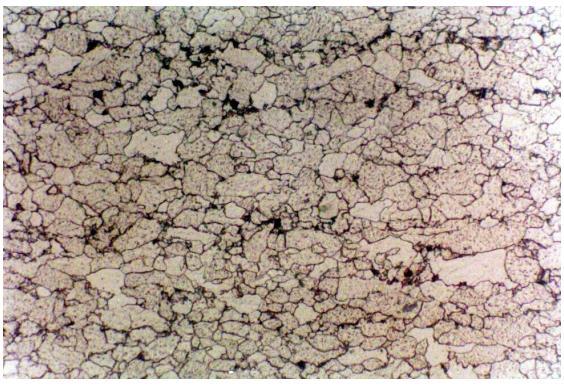

Figure 5. The microstructure of base metal shows ferrite & pearlite structure, etched with 2 % Nital, 500X

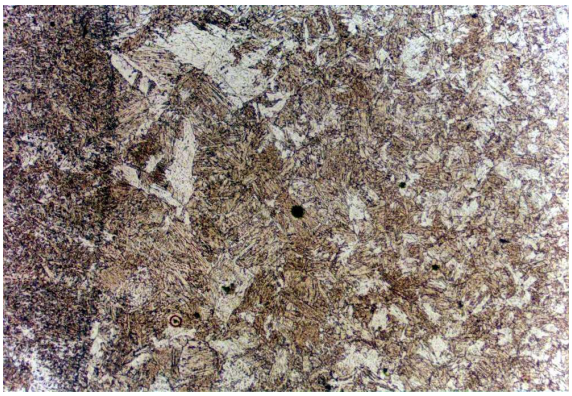

Figure 6. The microstructure of HAZ, etched with 2 % Nital, 100X

Figure 7. The microstructure of weld metal, etched with 2 % Nital,100X.

Micro-hardness Testing

The hardness of a transverse weld section that had been cut and polished to remove cutting effects was carried out in accordance with Vickers hardness testing method. [2] The location of indentations was subjected in three areas such as base metal, HAZ and weld metal. The schematic location can be seen in Figure 8.

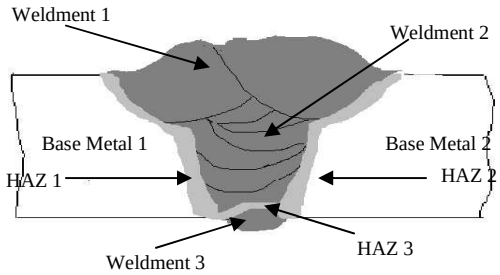

Figure 8. Schematic location of hardness test

The differentiation in hardness value in Table 1 above was probably caused by the variation in the microstructure along the weld cross section area. The differentiation between the weldment 1 and 2 compared to the weldment 3 is a result of different type of filler metal used. The weldment 1 and 2 (filled and capping pass) used filler metal E8010 G and for weldment 3 (root pass) used E6010. [3]

Table 1. Hardness value of the weld pipe cross section

No.	Location	Hardness (HV)
1.	Base Metal 1	234
2.	HAZ 1	194
3.	Base Metal 2	254
4.	HAZ 2	229
5.	Weldment 1	226
6.	Weldment 2	232
7.	Weldment 3	182

Vickers hardness test also performed at the area adjacent to the crack of the sample A. The measurements were taken 500 micron from the surface (pipe inner surface) with 500 micron distance between them. The result as seen in Table 2 showed no unusual hardness value which indicated no high hardness microstructure such as martensite or bainite.

Table 2. Hardness profile of the crack area cross section.

Indentation	Vickers Hardness (HV)	Remarks
I	190	Load = 25 gr. distance = 500 µ
II	181	
III	206	
IV	199	
V	217	
VI	181	
VII	184	
VIII	187	
IX	187	

Micro-Fractography Examination

In order to provide more information, failed part of the pipe fracture surface subjected to SEM for close examination. Unfortunately, the crack surfaces were covered with paint, and SEM macro-fractography cannot provide more information to reveal the crack origin, as seen in Figure 9.

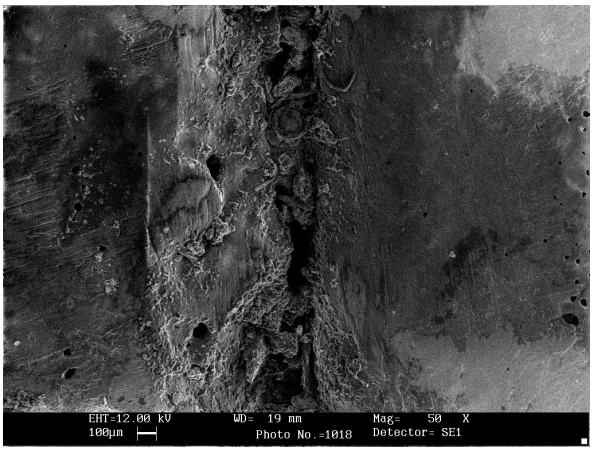

Figure 9. SEM Photographs of sample A taken at the surface of failed weld joint pipe consisting of some corrosion products (scale), SE detector 100X

Furthermore, fractography is carried out for the cross section of the failed area as seen in Figure 10. SEM examination of the weld crack showed a combination of trans-granular and inter-granular crack.

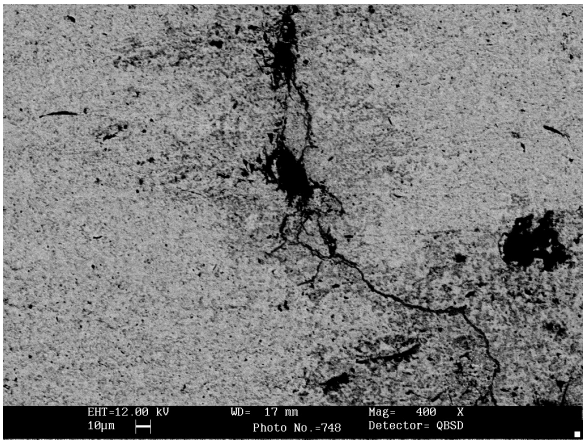

Figure 10. SEM Photographs of sample B taken at crack (scale), QBSD detector, 100X

EDX analysis of the failed revealed no significant element or compound can contribute to the weld pipe failure.

The weld crack of the pipeline can be classified as longitudinal crack or bead cracks. This crack runs in the direction of the weld axis, regardless the location in the weld metal or the fusion line. This type of crack can be divided as hot cracks and cold cracks. They are often caused by using the wrong filler alloy, poor edge preparation or poor clamping of the weld joint. Any combination of the joint design, welding conditions and welding techniques that results in a weld bead with an excessively concave surface and stress concentrations can promote such type of cracking. If the weld joint is clamped too much, the stresses developed around the weld may cause weld bead cracking. [4]

Microstructure examination of the sample revealed that the crack propagate along the weld fusion line, follow the fusion line curve and then turn direction perpendicular to the weld centerline. Another sample showed the crack propagated to the weld center with no significant change in crack direction. Weld crack depth from the root surface is approximately 6.10 mm and 4.60 mm for the analyzed sample.

The weld crack of the pipe was initiated from the root weld of the pipe. However, hardness examination has no indication of high hardness microstructure. The used of filler E6010 as the root pass has an impact to the strength of the weld joint. Other than that, the use of E 8010 G as hot pass created a big difference in the hardness of the weld. The big difference in hardness created a residual stress at the weld joint [4], along with additional stresses implied upon removal of the internal clamp and lifting of the pipe.

Vertical down technique where the welder meet at the bottom of the pipe also contribute to the stress of the weld pool. Vertical down welding technique has potency possibility for slag intrusion to the weld pool.[5] The characterization of the slag which has the tendency to float as a result of the lower density compared to the weld metal. When the welding process took place at the bottom where the two welder meet there is always possibility for less weld deposited reducing the overall thickness (cross section) at the meeting point.

From the crack morphology, hypothesis can be drawn, that the first crack, where the crack propagate along the fusion line. As for the second crack, the crack propagated from the center of the weld. This can be concluded from the large gap of the crack, which larger at the center compared to the surface.

This is due to the fact that when 100% root completed, the internal clamp was removed, the welded pipe was slightly bended and the tensile stress occurred at the bottom of the root weld face (at 6 a clock position). This cause the cracks appear before hot pass performed or during the deposition of hot pass and movement of the pipe. The crack subsequently propagates to the lower strength of the weld root and the bottom of the fusion line.

V. CONCLUSION

Based on data from investigation as well as testing results, several conclusions are drawn as follows:

1. The weld crack of pipeline is initiated by the stress at root weld when the internal clamp was removed immediately after completion of 100% root pass.

2. The analysis result found that the base material and weld metal are free from any extragenous material for crack initiation and the microstructure and hardness analysis also ensured it.

REFERENCES

[1]. API 5L, Specification for Line Pipe, 43rd Edition, **American Pipeline Institute Standard**, 2004

[2]. ASTM E384-04, Test Method for Microhardness of Materials, **American Standard for Testing Material Book**, 2004

[3]. AWS A5.1/A5.1M, Specification For Carbon Steel Electrodes For Shielded Metal Arc Welding, **American Welding Society Standard**, 2000

[4]. Kou, Sindo., Welding Metallurgy, **John Wiley & Son**, 1987.

[5]. Essab, Pipelines Welding Handbook**, Essab-Sweeden**, 2002

ISSN: 1411-1284

Failure Analysis of Motor Bike Steering Shaft

Winarto, Zulkifli and Dwi Marta Nurjaya
Department of Metallurgy & Materials Engineering, University of Indonesia
Kampus Baru UI Depok – 16424
Email: winarto@metal.ui.ac.id

Abstract— **Steering shaft which is one of motor bike parts is broken (failure) at the time of pre-delivery checking (PDC). The material of the steering shaft is made of steel. The sample of steering shaft was characterized and analyzed to find the main cause of the failure. The material characterization and analysis were started from visual test, examination of the fractography, metallography examination, hardness testing, charphy-impact testing, chemical composition testing, SEM examination and finally chemical analyzed by EDX. The results show that the failure of steering shaft was caused by torsion and high speed (sudden) load during services. The initiation of crack started from inner diameter which is due to the cold expanding process during manufacturing of steering shaft component.**

Keywords—Failure Analysis, Steering Shaft, Cold Expanding, High Speed Loading, Torsion

I. INTRODUCTION

Motor bike steering shaft is an important component in motorcycle (Figure 1). This steering shaft has fracture after through waving road. Figure of steering shaft after fracture can be seen below:

Figure 1. photographs of steering shaft after fracture.

This steering shaft was made of steel alloy and has experienced to be cold expanding process before it assembly.

Due to inadequate information to assess the reliability of the fracture steering shaft reporting, no assumption was made about the history of fracture steering shaft serviceability.

The failure analysis assessment was carried out in order to determine the main cause of the fracture steering shaft based on the metallurgical aspects, and followed by the conclusion according to the laboratory testing results.

II. METHODOLOGY

Investigation and analysis of steering shaft fracture are to find the main cause the fracture according to metallurgy aspect with laboratory testing and then make conclusion and recommendation. [1]

The procedure of failure analysis based on the following stages such as: [1,2]

1. Visual examination of general physical features
2. Chemical analysis / identification (by Sparks Spectrometer and EDS)
3. Mechanical properties: hardness testing
4. Microstructure (Metallography) analysis
5. Fractography examination
6. Discussion and conclusion

III. RESULTS & DISCUSSION

Visual Examination of General Physical Features

Parts of steering shaft which have fractured were visually examined. The two part of steering shaft which broken are observed as soon as received, as can be seen in Figure 2. The observation results are:

A. There are no visible cracks on the inner or outer of steering shaft, as seen in Figure 3.

B. Mode of fracture surface is dominated brittle fracture with bright appearance which is usually happened in tensile test, as seen in Figure 3.

C. There is an earring at the outer side of surface fracture, which is indicated as torsion load.

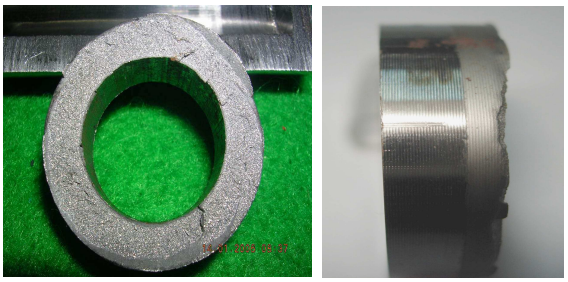

A B

Figure 2. Fracture surface of steering shaft. A) vertical appearance, B) horizontal appearance.

Chemical Analysis/Identification

In order to compare its chemical composition, part of steering which is not fracture was subjected chemical analysis using spark emission spectrometer. The result can be seen in Table 1.

Table 1. Chemical composition of steering shaft [3]

Material	% C	% Si	% Mn	% P	% S	% Cu	% Cr
JIS S 20 C	0.18-0.23	0.15-0.35	0.3-0.6	0.03 max	0.035 max	-	-
Sample	0.230	0.230	0.40	0.01	0.004	0.22	0.1

Chemical analysis result revealed that this steering shaft is conform to its specification which is JIS S20 C. Steering shaft material is classified as low carbon steel with carbon content maximum 0.23 %. Because chemical composition conform to its specification, no conclusion was made as in appropriated material selection could be as possible causes of the failure.

Mechanical Testing (Hardness & Impact Test)

The hardness was performed on the fracture steering shaft accordance with Vickers hardness testing [4]. The measurements were taken at the fracture area and far from fracture area. The result is summarized in Table 2.

Table 2. Hardness testing result using Vickers hardness method (VHN).

Indentation	Fracture area (VHN)	*Inner 1* (VHN)	*Inner 2* (VHN)	*Outer* (VHN)	*Center* (VHN)
1	**244**	**354**	**317**	**235**	**233**
2	**241**	**348**	**323**	**234**	**234**
3	**242**	**356**	**318**	**235**	**233**
4	**242**	**347**	**322**	**235**	**231**
5	**240**	**346**	**323**	**234**	**234**
Mean	**242**	**350**	**320**	**235**	**233**

The result show hardness value at the fracture area is 242 VHN. That hardness value is not different between the center and the outer diameter of *steering shaft*. However, the hardness at inner diameter was higher than fracture area and also at the middle area (center). This higher hardness indicated that material was subjected to strain hardening which is resulted from the cold expanding process.

In addition, Impact testing was also performed to steering shaft in order to compare impact value [5]. The result of impact testing can be seen in Table 3.

Table 3. Charpy-Impact Testing Result of Steering Shaft

Material	Impact Value (Joule/mm^2)
Standard	1.841
sample	1.195

The result of impact testing revealed that steering shaft which is failed has lower impact value than standard steering shaft. This indicated that failed steering shaft has a lower resistant to sudden load (shock load).

Metallography Examination

The microstructures of steering shaft were taken, which are shown in Figure 4. Microstructure of steering shaft was taken under magnification 500X. The result showed a normal microstructure of low alloy carbon steel with ferrite and pearlite structure. This microstructure is a normal microstructure; therefore, improper heat treatment and a poor microstructure were eliminated as possible causes of the failure.

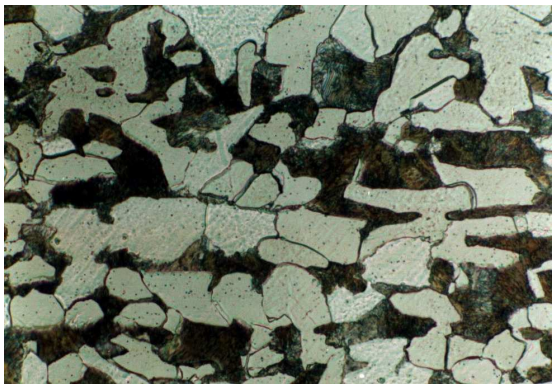

Figure 4. Microstructure taken at the base metal consisted of pearlite (black) and ferrite (white). Nital etched, magnification of 500 X.

Fractography Examination

In order to provide more information surface and damaged area were examined using optical microscope and scanning electron microscope (SEM).

Macro-fractography examinations clearly showed that the fractures had occurred in a brittle manner (Figure 2), and no ductile appearance. This fracture happened suddenly (sudden fracture) so there is no possibility deformation can occur.

Figure 5 shows a location of fracture area which is examined by optical microscope & scanning electron microscope.

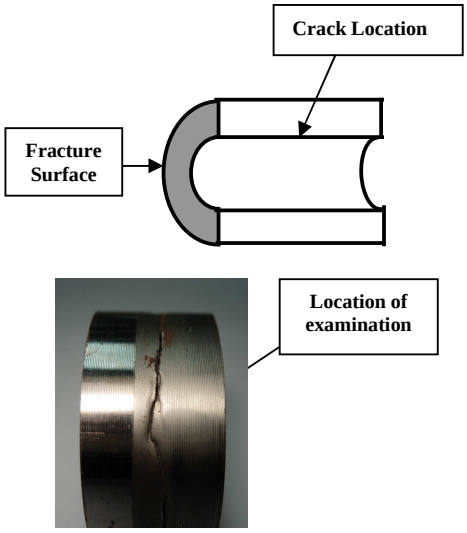

Figure 5. Location of microstructure and SEM examination

Figure 6 shows a microstructure of outer area of fracture steering shaft which is mating sample. The line direction appears in the photograph which is indicates the fracture because of torsion load.

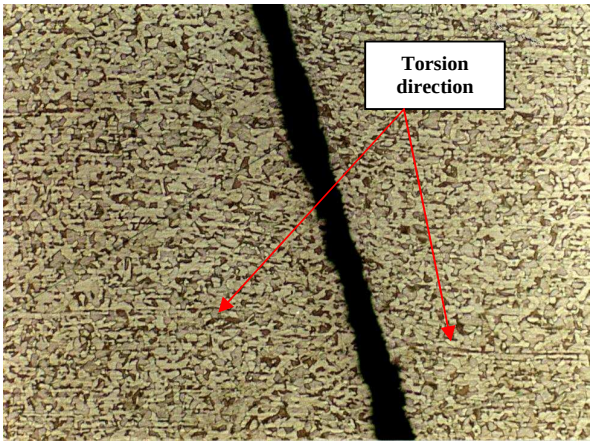

Figure 6. Microstructure of fracture which show direction of torsion. Picral etched. Magnifications 50X.

Figure 7 shows clearly the cause of torsion on the grain structure where the grain is not in its original position (not in straight-line position).

In inner diameter of steering shaft were found some crack. These cracks can be seen in Figure 8 and 9. With SEM, the length of crack can be measured and one of that cracks has length 460 µm, as seen in Figure 8. Most of these cracks are growth in trans-granular, which is shown in Figure 9.

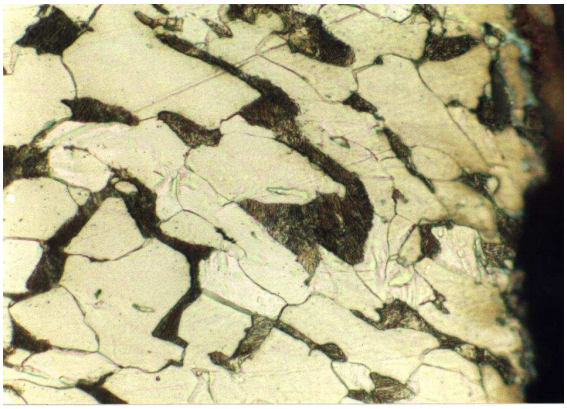

Figure 7. Microstructure of fracture show grain is not in original position. Nital etched. Magnifications 500X.

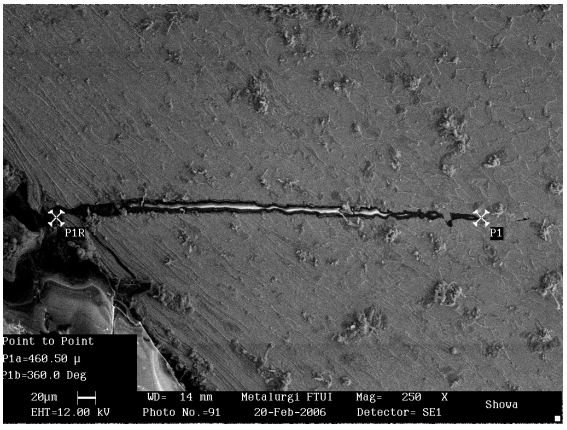

Figure 8. Micrograph shows the length of crack. Magnifications 250X

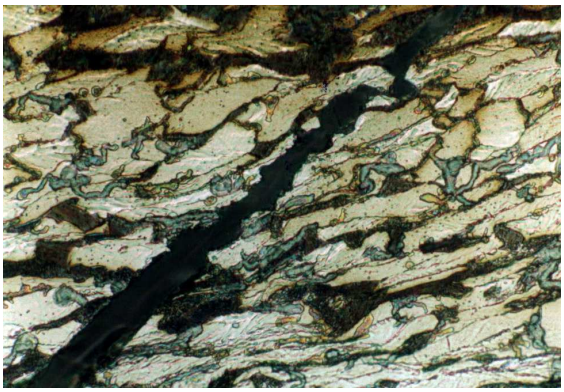

Figure 9. Microstructure show crack is growth trans-granular. Nital etched. Magnifications 500X

Steering shaft is a component part of motorcycle. Steering shaft was manufactured using expanding process which is enlarging inner diameter of steering shaft at room temperature (cold working).

Crack is not found at the outer diameter and there was not hardness differential between fracture area and center area of steering shaft. However, it was found some crack in inner and outer of steering shaft which has higher hardness compared to fracture area and the center area of steering shaft. The higher hardness is caused by expanding process (cold working). [6]

The presence of crack at inner diameter of steering shaft is very high risk in manufacture parts. The measurement of crack dimension has 460 µm in length, close to 0.5 mm, which is categorized as a very long size.

The steering shaft can be initiated by crack in inner diameter and then with the presence of impact (shock) load can cause sudden fracture.

Shock load failures are identified as "catastrophic" because there may be no warning signs such as distortion prior to the final fracture, and these failures may cause substantial collateral damage. Shock load can cause brittle fracture of ductile material. The mechanism of torsion load was showed in Figure 10. The presence of crack in inner diameter of steering shaft made the fracture faster.

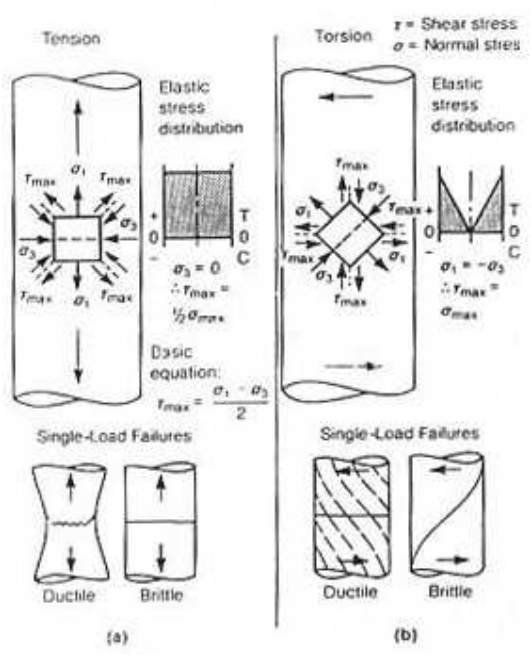

Figure 10. The mechanism of Torsion Fracture.[6]

V. CONCLUSION

Based on data from investigation as well as testing results, several conclusions are drawn as follows:

1. The main cause of steering shaft fracture is high speed overload (shock load) with torsion mode.
2. Crack growth was initiated from inner diameter of steering shaft due to the cold expanding process.

REFERENCES

[1]. ASM Metals Handbook Vol. 10, Failure Analysis and Prevention, American Society for Metals, Metals Park Ohio, 1987.

[2]. E. P. Polushkin, Defects and Failures of Metals, Elsevier Publishing, Amsterdam, 1956.

[3]. JIS G 4051, Specification for Carbon Steels for Machine Structural Use, **Japan Industrial Standard**, 2001.

[4]. ASTM E384-04, Test Method for Microhardness of Materials, **American Standard for Testing Material Book**, 2004

[5]. ASTM E23-04, Standard Test Methods for Notched Bar Impact Testing of Metallic Materials, **American Standard for Testing Material Book**, 2004

[6]. Wulpi DJ. Understanding how component fail. **Metals Park (OH): ASM**; 1985. p.117

ISSN: 1411-1284

Development of Nodular Indefinite Chilled Iron (NICI) by Combination of Controlled Cooling Heat Treatment and Copper Alloying

Y. Prasetyo, S. K. Lee, E.R. Baek

Department of Advanced Materials Sci. & Eng. Yeungnam University,
214-1 Dae-dong, Gyeongsan-si, Gyeongsangbuk-do, 712-749, Korea
Tel.82-53-8103976, Fax. 82-53-811-4133 E-Mail: yustenite@yahoo.com

Abstract– **Nodular infinite chilled iron (NICI) contents with nodular graphite, cementite and ausferrite phases was successfully developed for roll material using low nickel content (2.0~2.5) and cheap alloying element such as copper (~ 2.0%). Hot shakeout of CO_2 sand mold of as-cast iron was conducted to increase the cooling rate and then isothermal heating in muffle furnace in temperature 300 ^{0}C in 6 hours to achieve ausferritic transformation. By achieving the ausferrite phase in as-cast condition, the structure will be free of crack and thermal stress that usually occurred in austempered ductile iron (ADI). It was confirmed by optical microscope and electron microscope (SEM) observations that with the small addition of copper, the amount of pearlite was decreased, but with further addition of copper, the amount of martensite was increased.**

Keywords– NICI, Ausferrite, Controlled cooling, Roll material

I. INTRODUCTION

The general term of nodular indefinite chilled cast iron (NICI) is specifically as ductile cast iron that produced in high cooling rate in its solidification with various matrix microstructures such as pearlite, martensite and ausferrite that related to alloying elements and cooling condition with the present of cementite that required to increase the hardness properties that will enhance the wear properties. NICI was usually applied as work roll in continuous casting hot-rolled steel billet or plate. Since the condition of rolling condition was extremely at high temperature and high loading pressure, high mechanical and fatigue properties was required to prolong the lifetime of work roll.

It already well known that pearlites and martensites have low mechanical properties compared to ausferrite phase. With respect of this idea, the development of work roll will focused on the introduction of ausferrite phase (composed of bainitic ferrite and retained austenite) as a matrix structure with the present nodular graphite and cementite phase. Another consideration of the work roll development is the high alloying cost by the addition of nickel (4.0~5.0%) and molybdenum (~1.0%). The addition of nickel and molybdenum are effectively increasing the hardenability to avoid the pearlitic transformation, but the alloying cost will be high. Another possibility to increase the hardenability was the introduction of cheap alloying element such as copper (~2.0%). With the addition of copper and manganese, it will possible to decrease the amount of nickel to level ~2.5% and molybdenum to level ~0.5% [1].

II. BASIC THEORY

Ausferrite phase was produced in bainitic region by isothermal treatment at sufficient time to accommodate bainitic transformation. Ausferrite was composed of high carbon retained austenite and bainitic ferrite. The banitic ferrite was a bainite phase without carbide precipitation because of high content of silicon in irons as can be seen in Figure.1.

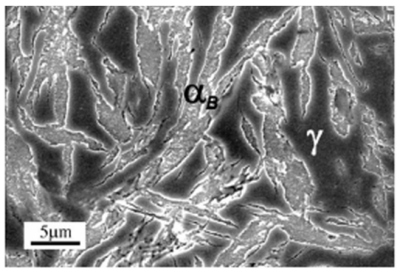

Fig. 1. Scanning electron micrograph of ausferrite phase that consist of bainitic ferrite (light region) and high carbon retained austenite (dark region) [2]

The general transformation sequences in as cast ductile iron are [2]:

$$L\ (\text{liquid}) \rightarrow \gamma + L \rightarrow \gamma + G_f\ (\text{graphite}) \rightarrow \alpha + P\ (\text{pearlite}) + G_f \quad (1)$$

However, with the present of alloying element, the transformation will change as:

$$L\ (\text{liquid}) \rightarrow \gamma + L \rightarrow \gamma + G_f\ (\text{graphite}) \rightarrow \gamma_{(\text{High carbon})} + \alpha_B + G_f \quad (2)$$

Proper alloying element was the key point to achieve the bainitic transformation. As can seen in Figure 2. molybdenum, copper and nickel are effective alloying element to increase the hardenability of iron. At low level of alloying, molybdenum have the strongest effect on hardenability. At range 1 to 2%, the Cu and Ni have quite similar effect on hardenability, but above 2%, the Ni has the strongest effect on hardenability.

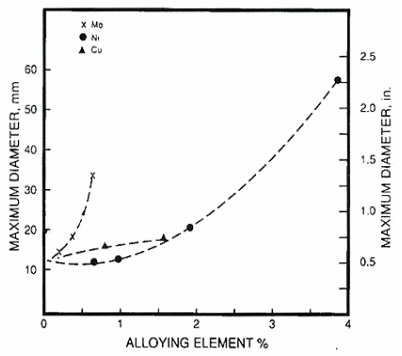

Fig. 2. Effect of alloying element on iron hardenability [3]

Another concern in ausferritic transformation is to prevent the martensitic transformation because martensite is brittle phase. As we are conducting high level alloying element, the γ phase are so stable and it will produce martensite phase and retained γ in as cast microstructure. In iron, typically plate martensite was formed due to the bainitic transformation was not completed during isothermal condition.

III. EXPERIMENTAL RESULTS

The iron, melted in 10 kw induction furnace with capacity 3 kg, was produced from charge of Sorel metal and steel scrap. Sorel metal was supplied from KT Roll, South Korea. Magnesium was added by plunging technique with a 5% magnesium-containing ferrosilicon. Silicon was added by using 75% foundry grade ferrosilicon after magnesium addition. Copper was added in range from 0 - 2.0 % to observed the effect of copper. As much as 2.5 kg of melted iron was poured into 25 mm thick CO_2 sand Y-block. After the as-cast iron reaches 900 ^oC in mold cooling, the mold was shaked out to increase the cooling rate. With isothermal temperature 300 ^oC and isothermal time 6 hour, it will achieve ausferrite phase in the microstructure. After the temperature for isothermal holding was achieved, the specimen was held in muffle furnace for 6 hours and then takes out to air cooling. The chemical composition of five alloy with variation of copper was shown in Table 1. Microstructures of all the samples were examined by optical
Microscopy and SEM after polishing and etching with 2% nital solution. Phase volume fraction was calculated using optical microstructure based on pixel percentage using Image-Pro Plus software. X-ray diffraction (XRD) analysis was performed to estimate the austenite content following the procedure of Rundman and Klug [4]. XRD was done using a monochromatic copper Kα radiation at 40 kV and 100 mA. A Rigaku rotating head anode diffractometer was used to scan the angular 2θ range from 72–92° at a scanning speed of 5°/min. The volume fraction of austenite (γ) was determined by the direct comparison method using the integrated intensities of the above planes [5].

Table 1. Chemical composition of the NICI

Alloy	C	Si	Mn	Mo	Cr	Ni	Cu	Fe
1	3.30	2.02	0.37	0.25	1.36	2.57	0.02	Bal.
2	3.36	2.05	0.38	0.25	1.44	2.54	0.52	Bal.
3	3.37	2.00	0.36	0.28	1.35	2.48	0.98	Bal.
4	3.32	1.98	0.36	0.29	1.36	2.49	1.45	Bal.
5	3.32	2.02	0.39	0.26	1.42	2.57	2.02	Bal.

III. a. Copper effect on microstructure

Copper was known as austenite stabilizer in ductile iron. Small amount of copper usually added to refine the pearlite in pearlitic grade ductile iron. In this experiment, copper greatly have effect to increase the graphite volume fraction as much 72.8% from 3.79% in alloy 1 (0.02 %Cu) to 6.55% in alloy 5 (2.02% Cu), which have significant effect to decreased the cementite volume fraction as much as 61.5%. as can be seen in Table 2.

Table 2. Volume fraction of NICI

Phase Volume fraction (%)						Isothermal Condition		Hardness
Alloy	Graphite	Cementite	Pearlite	Martensite	Ausferrite	Temperature (°C)	Time (h)	(HRC)
1	3.79	21.43	2.42	0	72.18	300	6	48.05
2	4.88	15.71	1	10	69.41	300	6	46.25
3	5.40	13.91	0	55.69	15	300	6	45.95
4	5.76	13.60	0	72.64	6	300	6	47.75
5	6.55	8.24	0	84.26	1	300	6	51.65

The microstructure of alloy 1 and alloy 5 was shown in Figure 3. Microstructural observation revealed that with small addition of 0.52 % Cu (alloy 2) was decrease the amount of pearlite to 1.0 %, from 2.42 % and with addition of 0.98 % Cu, the pearlite phase was not present which mean that copper was increase the iron hardenability by sift the pearlitic nose. It was also observed that copper also increase the martensite volume fraction as much as 82.26 % within 2.02 % Cu and decrease the ausferrite volume.

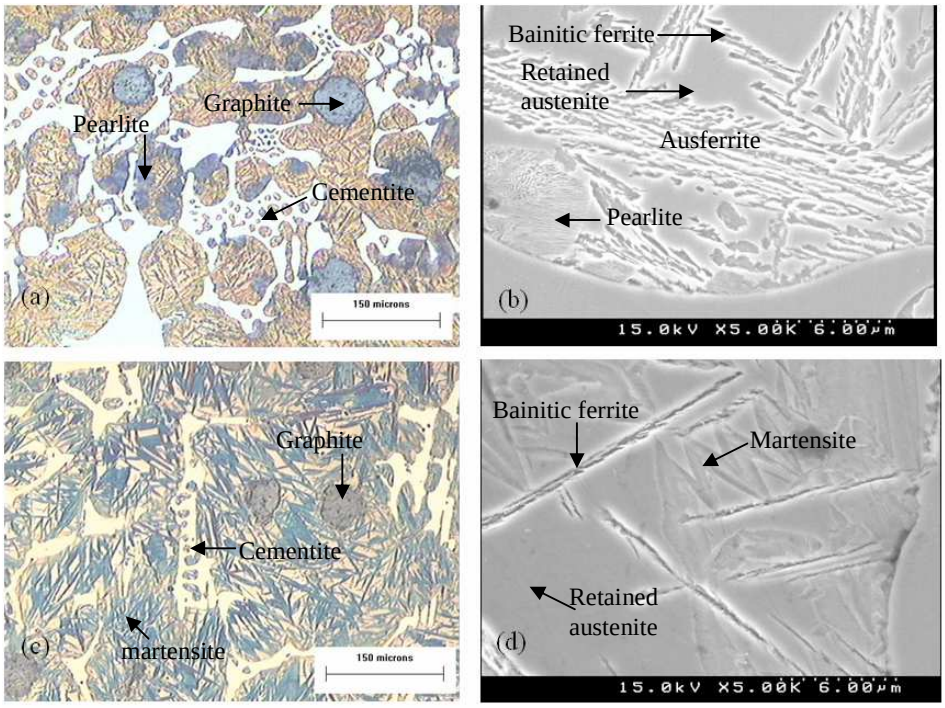

Fig. 3. Microstructures of sample by isothermal temperature 300 ^{o}C in 6 hours. (a) Optical microstructure of 0.02% Cu, (b) SEM micrograph of 0.02% Cu, (c) optical microstructure of 2.02% Cu and (d) SEM micrograph of 2.02% Cu . Nital Etched.

fraction to 1.0 % which mean that copper also greatly sift the bainitic transformation nose to the right. Within the shift of bainitic transformation, the transformation bainitic ferrite was delayed, and need prolong the isothermal to completed transformation. The schematic illustration of CCT diagram of NICI alloyed with copper was shown in Figure 4.

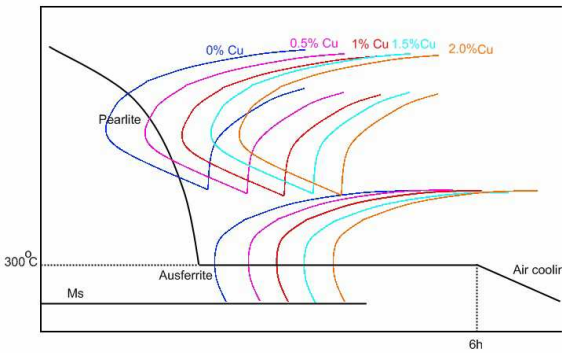

Fig. 4. Schematic illustration of CCT curve.

III. b. Retained austenite anlysis

XRD analysis revealed the retained austenite volume fraction by direct comparison method using the integrated

intensities of the above planes. Specific plane was used to count the volume fraction as can be seen in Figure 5.

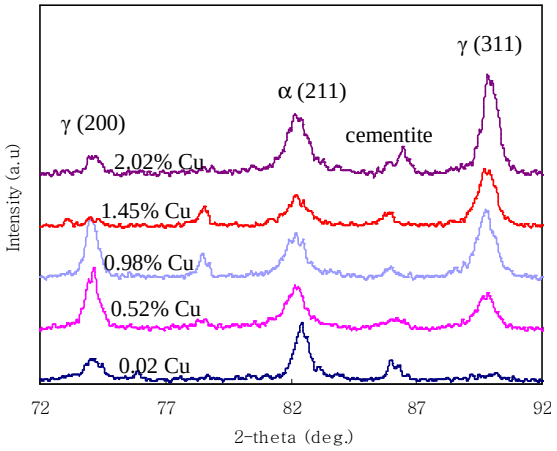

Fig. 5. XRD profile of NICI alloyed with copper

The result of retained austenite calculation was shown in Table 3. As can be seen in Table 3. that copper will increase the retained austenite volume fraction due effect that soluble cooper will attract the atom carbon to austenite
during solidification. With copper addition 2.02%, the retained austenite was increased 22.2% compared to without copper addition. By further increasing the carbon content in retained austenite by copper addition, the bainitic ferrite was having difficulty to form and grow because bainitic ferrite must transfer atom carbon to retained austenite that already enrich with carbon because copper addition which can be seen on low ausferrite content (1.0%) in 2.02% Cu. The high

carbon retained austenite will transform into martensite during air cooling

Tabel 3. Retained austenite calculated using XRD profile

Cu content (wt.%)	Retained austenite (%)
0.02	8.28
0.52	9.47
0.98	9.66
1.45	9.77
2.02	10.12

III. c. Mechanical Properties

Hardness and tensile strength was measured to find the optimum mechanical properties due to copper effect on microstructure evolution as can be seen in Fig. 6. As mentioned before that copper will increase the graphite volume fraction and decrease the cementite volume fraction and will have impact to decrease the hardness value as much as 4.37% from 48.05 HRC to 45.95 HRC. By further increase the copper content of, the martensite content will increase and will have effect to increase the hardness as much as 12.40% to 51.65 HRC. The tensile strength was significantly dropped due to copper addition which is indicated of high martensite content and low ausferrite content. Based on mechanical consideration, it is still difficult to find the optimum mechanical properties due to copper effect that have inverse effect to prevent the pearlite formation but promote martensite formation. Copper introduction in NICI can be applied by considered the effect in specific application in condition that wear properties was the main consideration.

1.

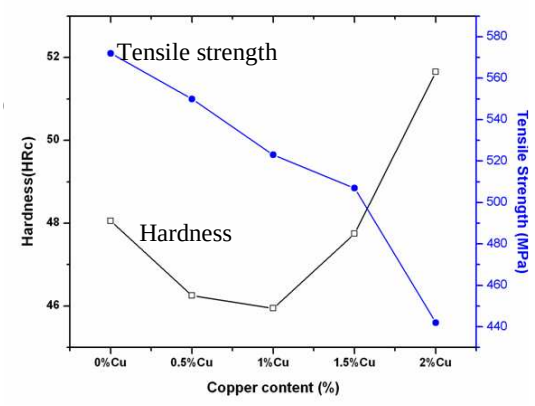

Fig. 6. Hardness and tensile strength of NICI alloyed with copper

from 3.79% in alloy 1 (0.02 %Cu) to 6.55% in alloy 5 (2.02% Cu)

2. Pearlitic transformation was successfully avoided but martensite volume fraction was increased and follow the decreased of ausferrite volume fraction with copper addition as much as 0.98%.
3. Mechanical properties shown that hardness value was decrease within 0.52% Cu addition due to decreased cementite volume fraction. With further addition of copper addition to level 2.02%, the hardness value was significantly increase, but the tensile strength was decreased due to massive formation of martensite.

REFERENCES

[1] R. B. Gundlach, C. R. Loper, B. Morgensteren, *Ductil e Iron Handbook. Composition of Ductile Irons, Ducti le Iron Handbook*, ed. by M. Burditt, AFS, Illinois, (1992), 19 7.M. F. Burditt, Ductile Iron Handbook

[2] W. Xu, M. Ferry and Y. Wanga, *Influence of alloying elements on as-cast microstructure and strength of gr ay iron*, Materials Science and Engineering A 390 (20 05) 326–333.

[3] E. Dorazil, *High Strength Austempered Ductile Cast I ron*, New York: Ellise Horwood, 1991

[4] K.B. Rundman, R.C. Klug, AFS Trans. 90 (1982) 499–508

[5] B.D. Cullity, *Elements of X-ray Diffraction*, Addison-Wesley, Reading,MA, 1974,

ISSN: 1411-1284

Application of Response Surface Methodology in the Development of Tool Life Prediction Models when End Milling Ti-6Al4V.

A.S. Mohruni[*], S.Sharif[**], M.Y. Noordin[**], V.C. Venkatesh[***]

*Faculty of Engineering, Sriwijaya University, Jl. Raya Prabumulih Km.32, Indralaya, 30662
Tel. +62-711-410745 email : mohrunias@yahoo.com, mohrunias@unsri.ac.id
[**]Faculty of Mechanical Engineering, Universiti Teknologi Malaysia, 81310-UTM Skudai, Johore, Malaysia
[***]Faculty of Engineering and Technology, Multimedia University
75450, Melaka, Malaysia

Abstract– **This paper deals with development of prediction models for tool life when end milling titanium alloy, Ti-6Al4V using TiAlN-coated solid carbide tools under flood condition. Primary machining parameters such as cutting speed, feed and radial rake angle were used as independent variables. Three main models such as 3F-model, 1st CCD-model and 2nd CCD-model, were observed using response surface methodology (RSM) in determining the optimum cutting conditions for a particular tool life interval. ANOVA was applied to prove adequacy of the predictive models.**

Keywords– Tool life models, End milling, Titanium Alloys, Response Surface Methodology.

I. INTRODUCTION

The trend in using titanium as aerospace materials in the airframe structure is increasing, mainly due to its great resistance to oxidation at elevated temperature, in addition to its low weight-to-strength ratio. Previous studies have shown that titanium and its alloys are considered as difficult to machine material, regardless of the type of tool materials used. This has been attributed to their low thermal conductivity which concentrates heat in the cutting zone (typically less than 25% that of steel), retention of strength at elevated temperatures and high chemical affinity for almost all cutting tool materials [1]-[11].

Machinability of materials provides an indication of its adaptability to be manufactured by a machining process. In general, machinability can be defined as an optimal combination of factors such as low cutting force, high material removal rate, good surface integrity, accurate and consistent workpiece geometrical characteristics, low tool rate and good curl or chip breakdown of chips [12].

Investigations in machinability studies used quite extensive statistical design of experiments (DOE). The DOE refers to the process planning of the experiments so that appropriate data can be analyzed using statistical method, which results in valid and objective conclusions [13]. A large number and a separate set of tests are required for each and every combination of cutting tool and workpiece materials, in order to establish an adequate functional relationship between the tool life and the cutting parameters (cutting speed, feed, and radial rake angle) [14].

The tool deterioration phenomena in end milling cutter is discussed in detail in ISO 8688-2 [16], which was used as reference to determine the tool life criteria. Two categories of cutting conditions in end milling may be considered, which are: (i) cutting condition as a results of which tool deterioration due to wear; and (ii) cutting conditions under which tool deterioration is due to other phenomena such as edge fracture or plastic deformation [17].

Traditionally, investigation of the effect of various cutting parameters on tool life was carried out using one variable at a time approach. However, this study takes other approach which used simultaneous variation of speed, feed and radial rake angle to predict the tool life model when end milling Ti-6Al4V. This approach which was pioneered by Wu [18] is known as response surface methodology (RSM), where the response of the dependent variable (tool life) is presented as a surface.

II. DEVELOPMENT OF THE MATHEMATICAL MODEL USING RSM

For this purpose, the mathematical model relating to the machining responses and their factors were developed to facilitate the optimization of the machining process.

II.1 POSTULATION OF THE MATHEMATICAL MODELS

It is assumed that the proposed model for the tool life is merely a function of cutting speed V, feed f_z and radial rake angle γ_o. Other factors such as machine tools, stability, entry and exit condition etc are kept

constant. Thus the proposed tool life model in end milling Ti-6Al4V can be expressed as

$$T = C.V^{k} f_z^{l}.\gamma_o^{m}.\varepsilon^{'} \quad (1)$$

where T is the experimental (measured) tool life according to tool life criteria (min^{-1}), V is the cutting speed ($m.min^{-1}$), f_z is the feed per tooth ($mm.tooth^{-1}$), γ_o is the radial rake angle (^{o}), $\varepsilon^{'}$ is the experimental error and C, k, l, m are parameters to be estimated using experimental data.

In order to facilitate the determination of constants and exponents, the mathematical model will have to be linearized using logarithmic transformation, and equation (1) can be converted into first order polynomial as

$$\ln T = \ln C + k \ln V + l \ln f_z + m \ln \gamma_o + \ln \varepsilon^{'} \quad (2)$$

which can also be formed as

$$y = b_0 x_0 + b_1 x_1 + b_2 x_2 + b_3 x_3 + \varepsilon \quad (3)$$

and finally can be written as

$$\hat{y}_1 = y - \varepsilon = b_0 x_0 + b_1 x_1 + b_2 x_2 + b_3 x_3 \quad (4)$$

where y is the experimental measured tool life on a natural logarithmic scale, $\hat{y}_1$ is the natural logarithmic value of predicted (estimated) tool life, x_0 = 1 (a dummy variable), x_1, x_2 and x_3 are the coded value (natural logarithmic transformation) of V, f_z and γ_o respectively, ε is the natural logarithmic transformation of experimental error ε' and b_0, b_1 and b_3 are the model parameters to be predicted using the experimental data [19].

To investigate the extended observation region, the second order model is also useful when the second order and interaction effect of V, f_z, γ_o are significant. The first order model in equation (4) can be extended to the second order model as

$$\begin{aligned}\hat{y}_2 &= y - \varepsilon \\ &= b_0 x_0 + b_1 x_1 + b_2 x_2 + b_3 x_3 \\ &\quad + b_{12} x_1 x_2 + b_{13} x_1 x_3 + b_{23} x_2 x_3 \\ &\quad + b_{11} x_1^2 + b_{22} x_2^2 + b_3 x_3^2 \end{aligned} \quad (5)$$

where $\hat{y}_2$ is the predicted response based on the experimental measured tool life on a natural logarithmic scale and b values are the parameters, which are to be estimated by method least squares method.

Analyzing of the experimental results was conducted by means of Design Expert 6.0 software [20], while validity of the resulted prediction models, which is used for optimizing the machining process, has to be tested using analysis of variance (ANOVA).

III. EXPERIMENTAL WORKS

Before commencing the experimental tests, a well planed experimentation was essential in order to acquire the relevant data for the development of the mathematical model. Using design of experiments (DOE) the development of mathematical model were started with 2^k-factorial design and stepwise extended to central composite design.

III.1 EXPERIMENTAL DESIGN

First step in developing mathematical model is to consider the 2^k-factorial design with replicated center points as screening tests of the experiments, which employed the first 12 experiments as shown in Fig. **1** [13].

An extended design of 2^3-factorial design is called a second order central composite design (CCD), which was augmented with replicated stars point as shown in Fig. **1**. The number of such repeated measurements affects the distance of the "axial star points" with the factor space. According to previous study [19], the distance of axial star points to the center points α is 1.4142.

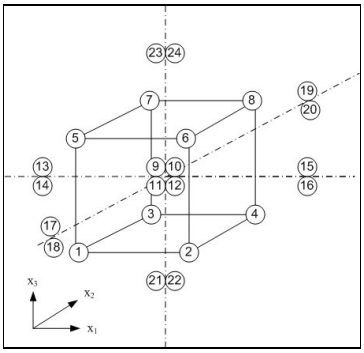

Fig. 1 Design of experiments used in developing mathematical models.

III.2 CODING OF INDEPENDENT VARIABLES

Further step in developing the mathematical models is coding of independent variables by taking into consideration the capacity and limiting cutting conditions of milling machine. The following transforming equation was used.

$$x = \frac{\ln x_n - \ln x_{n0}}{\ln x_{n1} - \ln x_{n0}} \quad (6)$$

where x is the coded variable of any factor corresponding to its natural x_n, x_{n1} is the natural value at the +1 level and x_{n0} is the natural value of the factor

corresponding to the base or zero level [14] - [19]. The level of the independent variables and coding identification are illustrated in Table 1.

Table 1 Levels of independent variables for end milling Ti-6Al4V

Independent Variable	Level in coded form				
	-α	-1	0	+1	+α
V (mm.min^{-1}) x_1	124.53	130	144.22	160	167.03
f_z (mm.tooth^{-1}) x_2	0.025	0.03	0.046	0.07	0.083
γ_o (^{o}) x_3	6.2	7.0	9.5	13.0	14.8

III.3 EXPERIMENTAL SET-UP

The tests were carried out with a constant a_a (axial depth of cut) 5 mm and a_e (radial depth of cut) 2 mm under flood conditions with a 6% concentration of water base coolant using MAHO 700S CNC machining center for side milling operation. The grade K-30 solid carbide end mill cutters, with PVD-TiAlN coated which were prepared with different radial rake angle according to DOE, were used for experimentation.

The reference workpiece material was a rectangular bar (110 x 110 x 270 mm) of Ti-6Al4V. Tool life criteria used were $VB_{max} \geq 0.25$ mm, chipping ≥ 0.20 mm and catastro-phic failure.

Tool wear was measured using a Nikon tool makers' microscope with 30x magnification. The measurements of tool wear according to [16] were carried out for each cutting edge at initial cut and continuously after a particular length of cut (depend on wear progressive of each tool) until the end of tool life was achieved.

IV. EXPERIMENTAL RESULTS AND DISCUSSIONS

The tool life experimental results of TiAlN-coated carbide tools are shown in Table 2. The major contributor for wear occurred in end milling Ti-6Al4V were flank wear of the end of the cutting edge and chipping.

IV.1 DEVELOPMENT OF THE TOOL LIFE MODEL USING 2^K-FACTORIAL DESIGNS.

The first 12 trials obtained in Table 2 (see also Fig. **1**) were used for generating the 3F1-model as a screening tests.

Using Design Expert software with ln transformation, the developed 3F1-tool life model in coded factor can be written as follows

$$\hat{y} = 1.3332 - 0.3643x_1 - 1.5032x_2 + 0.2002x_3 + 0.0764x_2x_3 \quad (7)$$

From Equation (7), it can be recognized that the most significant factor which influenced the tool life, is the feed followed by cutting speed and lastly the radial rake angle. From the ANOVA results shown in Fig. 2, it can be seen that the lack of fit (LOF) of the model is not significant. Thus indicating that Equation (7) was valid for the given cutting conditions, which is side milling of Ti-6Al4V using TiAlN-coated solid carbide tools under flood conditions with the following ranges of cutting speed V, feed per tooth f_z and radial rake angle γ_o : $130 \leq V \leq 160$m.min^{-1}; $0.03 \leq f_z \leq 0.07$ mm.tooth^{-1}; $7 \leq \gamma_o \leq 13$ (^{o}) respectively.

Table 2 Tool life results for TiAlN-coated carbide tools

Std. Order	Type	Cutting Speed V (m.min^{-1})	Feed per tooth (mm.th^{-1})	Radial rake angle (^{o})	Tool Life (min)
1	Factorial	-1	-1	-1	20.81
2	Factorial	1	-1	-1	10.91
3	Factorial	-1	1	-1	0.89
4	Factorial	1	1	-1	0.46
5	Factorial	-1	-1	1	29.08
6	Factorial	1	-1	1	12.81
7	Factorial	-1	1	1	1.65
8	Factorial	1	1	1	0.75
9	Center	0	0	0	5.09
10	Center	0	0	0	5.86
11	Center	0	0	0	5.26
12	Center	0	0	0	4.48
13	Axial	-1.4142	0	0	11.43
14	Axial	-1.4142	0	0	11.36
15	Axial	1.4142	0	0	3.54
16	Axial	1.4142	0	0	3.58
17	Axial	0	-1.4142	0	13.79
18	Axial	0	-1.4142	0	14.03
19	Axial	0	1.4142	0	0.21
20	Axial	0	1.4142	0	0.22
21	Axial	0	0	-1.4142	5.20
22	Axial	0	0	-1.4142	5.23
23	Axial	0	0	1.4142	8.78
24	Axial	0	0	1.4142	8.48

Response: Tool Life TL Transform: Natural log Constant: 0
ANOVA for Selected Factorial Model
Analysis of variance table [Partial sum of squares]

Source	Sum of Squares	DF	Mean Square	F Value	Prob > F	
Model	19.50	4	4.88	604.15	< 0.0001	significant
A	*1.06*	*1*	*1.06*	*131.51*	*< 0.0001*	
B	*18.08*	*1*	*18.08*	*2239.61*	*< 0.0001*	
C	*0.32*	*1*	*0.32*	*39.71*	*0.0007*	
BC	*0.047*	*1*	*0.047*	*5.78*	*0.0530*	
Curvature	0.25	1	0.25	30.86	0.0014	significant
Residual	0.048	6	8.071E-003			
Lack of Fit	*0.012*	*3*	*3.912E-003*	*0.32*	*0.8129*	*not significant*
Pure Error	*0.037*	*3*	*0.012*			
Cor Total	19.80	11				

Fig. 2 ANOVA for 3F-model of TiAlN coated end mill with $n_c = 4$.

IV.2 DEVELOPMENT OF THE TOOL LIFE MODEL USING 2nd CCD

Another development of the higher order model was conducted employing the CCD, which utilizes 24 experimental results.

The result of the second order model analysis in coded variables is given below,

$$\hat{y} = y - \varepsilon$$
$$= 1.6383 - 0.3878\,x_1 - 1.4887\,x_2 + 0.1891\,x_3$$
$$+ 0.07637\,x_2x_3 + 0.10684\,x_1^2 - 0.5451\,x_2^2 + 0.1327\,x_3^2$$

Result obtained from Equation (8) strengthen the previous effect revealed in Equation (7) that the most significant factor, which influenced the tool life, is the feed followed by cutting speed and radial rake angle. Similar result for the 3F1-model was recorded for the interaction effect and additional quadratic effect occurred in second order CCD model.

ANOVA for Response Surface Reduced Quadratic Model
Analysis of variance table [Partial sum of squares]

Source	Sum of Squares	DF	Mean Square	F Value	Prob > F	
Block	5.1801E-006	1	5.1801E-006			
Model	43.456	7	6.2081	1443.3	< 0.0001	significant
A	*2.4061*	*1*	*2.4061*	*559.41*	*< 0.0001*	
B	*35.461*	*1*	*35.461*	*8244.5*	*< 0.0001*	
C	*0.57214*	*1*	*0.57214*	*133.02*	*< 0.0001*	
A^2	*0.13686*	*1*	*0.13686*	*31.820*	*< 0.0001*	
B^2	*3.5661*	*1*	*3.5661*	*829.09*	*< 0.0001*	
C^2	*0.21139*	*1*	*0.21139*	*49.146*	*< 0.0001*	
BC	*0.046664*	*1*	*0.046664*	*10.849*	*0.0049213*	
Residual	0.064518	15	0.0043012			
Lack of Fit	*0.025895*	*6*	*0.0043159*	*1.0057*	*0.47692*	*not significant*
Pure Error	*0.038623*	*9*	*0.0042915*			
Cor Total	43.521	23				

Fig. 3 ANOVA for second order CCD-model of TiAlN coated end mill with n_c = 4.

To check the adequacy of Equation (8), ANOVA was carried out and results are shown in Fig. 3. It is obvious that the LOF of the proposed model is not significant. This implies that Equation (8) is valid for side milling of titanium alloy Ti-6Al4V using TiAlN coated carbide tools under flood conditions with the following ranges of cutting speed V, feed per tooth f_z and radial rake angle γ_o: $124.53 \le V \le 167.03$ (m.min^{-1}); $0.025 \le f_z \le 0.083$ (mm.tooth^{-1}); and $6.2 \le \gamma_o \le 14.8$ (^{o}) respectively.

IV.3 DEVELOPMENT OF THE TOOL LIFE MODEL USING 1st CCD

The second option of tool life for the CCD model is the linear CCD model. The factorial data from Table 2 which is identical with the data for 3F1-model were used to construct this model. This approach was adopted to avoid the accumulative error when too many unused data were taken into account while computing the data.

The first order model resulted from the CCD analysis in coded variables is as follow,

$$\hat{y} = 1.4351 - 0.3643x_1 - 1.5032x_2 + 0.2002x_3 \quad (9)$$

Equation (9) can be transformed using Equation (6), which resulted in the predictive tool life as

$$\hat{T} = 653.113V^{-3.50897} f_z^{-3.54822} \gamma_o^{0.64681} \quad (10)$$

where $\hat{T}$ is the predicted tool life in (min).

Response: Tool Life TL Transform: Natural log Constant: 0.00000
ANOVA for Response Surface Linear Model
Analysis of variance table [Partial sum of squares]

Source	Sum of Squares	DF	Mean Square	F Value	Prob > F	
Model	19.458	3	6.4860	150.77	< 0.0001	significant
A	*1.0614*	*1*	*1.0614*	*24.673*	*0.0010969*	
B	*18.076*	*1*	*18.076*	*420.18*	*< 0.0001*	
C	*0.32053*	*1*	*0.32053*	*7.4506*	*0.025863*	
Residual	0.34416	8	0.043020			
Lack of Fit	*0.30747*	*5*	*0.061495*	*5.0283*	*0.10706*	*not significant*
Pure Error	*0.036689*	*3*	*0.012230*			
Cor Total	19.802	11				

Fig. 4 ANOVA for first order CCD-model of TiAlN coated end mill with n_c = 4.

For validation of equation (10), the ANOVA was used. From the ANOVA shown in

Fig. **4**, the LOF is not significant but the model is significant. It implies that the model can represent the experimental data with acceptable mean square error (MSE). This equation is valid for side milling of Ti-6Al4V using TiAlN-coated solid carbide tools under flood conditions with the following ranges of cutting speed V, feed per tooth f_z and radial rake angle γ_o : $130 \le V \le 160$m.min^{-1}; $0.03 \le f_z \le 0.07$ mm.tooth^{-1}; $7 \le \gamma_o \le 13$ (^{o}) respectively.

Constraints

Name	Goal	Lower Limit	Upper Limit	Lower Weight	Upper Weight	Importance
Cut. Speed Vc	is in range	130.00	160.00	1.0000	1.0000	3
Feed fz	is in range	0.030000	0.070000	1.0000	1.0000	3
Radial rake	is in range	7.0000	13.000	1.0000	1.0000	3
Tool Life TL	maximize	5.0000	29.081	1.0000	1.0000	3

Solutions Number	Cutting Speed Vc	Feed fz	Radial rake	Tool Life TL	Desirability	
1	130.10	0.030001	13.000	27.716	0.97268	Selected
2	130.00	0.030002	12.927	27.695	0.97227	
3	130.00	0.030000	12.261	26.947	0.95672	
4	130.35	0.030000	12.357	26.825	0.95414	
5	130.00	0.030000	12.056	26.721	0.95192	
6	130.00	0.030000	11.935	26.588	0.94909	
7	130.00	0.030000	11.739	26.373	0.94449	
8	130.00	0.030000	8.6531	23.220	0.87217	

8 Solutions found

Fig. 5 Possible solutions for 3F1-tool life model using TiAlN coated end mill with n_c = 4 when V and f_z are in range.

IV.4 OPTIMUM CUTTING CONDITIONS FOR A PARTICULAR TOOL LIFE RANGE USING 3F1-MODEL

To determine which model should be chosen from the three types of obtained tool life models, in finding the optimum cutting conditions for a particular tool life range. It is essential to select the most accurate model gained from the analysis based on the MSE of the three models. It was found that the 3F1-tool life model is the most accurate model compared to others models. Based on the 3F1-tool life model, the possible solutions for the end mill having tool life greater than

5 minutes when cutting speed V and feed f_z is kept in range, are illustrated in

Fig. **5**. From the results, it is recognized that the optimum cutting condition for end milling Ti-6Al4V, which fulfill the given constraint, was cutting speed V 130.10 m.min^{-1}, feed per tooth f_z 0.03 mm.tooth^{-1} and radial rake angle γ_o 13^o.

Constraints

Name	Goal	Lower Limit	Upper Limit	Lower Weight	Upper Weight	Importance
Cut. Speed Vc	maximize	130.00	160.00	1.0000	1.0000	3
Feed fz	maximize	0.030000	0.070000	1.0000	1.0000	3
Radial rake	is in range	7.0000	13.000	1.0000	1.0000	3
Tool Life TL	maximize	5.0000	29.081	1.0000	1.0000	3

Solutions

Number	Speed V	Feed fz	Radial rake	Tool Life TL	Desirability	
1	153.56	0.038009	13.000	8.8544	0.37094	Selected
2	153.75	0.037974	13.000	8.8351	0.37093	
3	154.06	0.037907	13.000	8.8122	0.37089	
4	151.27	0.038560	13.000	9.0000	0.37000	

4 Solutions found

Fig. 6 Possible solutions for 3F1-tool life model using TiAlN coated end mill with $n_c = 4$ when V and f_z are maximized.

Another optimum cutting condition for end milling Ti-6Al4V with the following constraints; tool life greater than 5 minutes and cutting speed V and f_z are maximized, which are appropriate for industrial needs, is illustrated in

Fig. **6**. Results show that the optimum cutting condition for end milling Ti-6Al4V, which satisfy the specified constraint, was cutting speed V 155.56 m.min^{-1}, feed per tooth f_z 0.038 mm.tooth^{-1} and radial rake angle γ_o 13^o.

V. CONCLUSIONS

Three tool life prediction models were satisfied for describing the tool life when end milling Ti-6Al4V, namely 3F1-model, 1st and 2nd order CCD-models. The most accurate among them was the 3F1-tool life prediction model.

Main effects in linear observation region, which described by 3F1- and 1st order CCD models, showed the same contribution to tool life as compared to the 2nd order CCD tool life model.

Based on the optimization processes, two optimum cutting conditions are revealed for two different objectives of constraints, when end milling Ti-6Al4V.

ACKNOWLEDGMENT

The authors wish to thank the Research Management Center, UTM and the Ministry of Science, Technology and Innovation Malaysia for their financial support to the above project through the IRPA funding Vote no. 74545.

REFERENCES

[1]. W. Koenig, "Applied research on the machinability of titanium and its alloys", *Proceeding 47th Meeting of AGARD Structural and Materials Panel, Florence, AGARD CP256, London*, pp. 1-10, 1979.

[2]. R. Komanduri and W.R. Reed, "Evaluation of carbide grades and new cutting geometry for machining titanium alloy", *Wear*, vol. 92, pp. 113-123, 1983.

[3]. P.A. Dearnley and A.N. Gearson, "Evaluation of principal wear mechanism of cemented carbides and ceramics used for machining titanium alloy IMI318", *Materials Science and Technology*, vol. 2, pp.1986.

[4]. M. Wang and Y. Zhang, "Diffusion wear in milling titanium alloys", *Mterial Science and Technology*, vol.4, pp 548-553, 1988.

[5]. A.R. Machado and J. Wallbank, "Machining of titanium and its alloys-a review", *Proceeding of the Institution of Mechanical Engineers*, vol. 204, pp.53-59, 1990.

[6]. A. Jawaid, C.H. Che Haron, A. Fallah, "Tool wear in machining of titanium alloy Ti 6242", *Proceeding of the 3rd International Conference on Progress of Cutting and Grinding, Osaka, Japan, Nov.*, pp. 126-131, 1996.

[7]. E.O. Ezugwu and Z.M. Wang, "Titanium alloys and their machinability – a review", *Journal of Materials Processing Technology*, vol.68, pp.262-274, 1997.

[8]. A. Jawaid, S. Sharif, K. Koksal, "Evaluation of wear mechanism of coated carbide tools when face milling of titanium alloys", *Journal of Materials Processing Technology*, vol. 99, no. 1, pp. 266-274, 2000.

[9]. H. Niemann, Ng. Eu-gene, H. Loftus, A. Sharman, R. Dewes and D. Aspinwall, "The effect of cutting environment and Tool coating when high speed ball nose end milling titanium alloy", *In Metal Cutting and High Speed Machining*, edited by D. Dudzinski, A. Molinari, H. Schulz, pp. 181-189, 2002.

[10]. J.I. Hughes, A.R.C. Sharman and K. Ridgway, "The effect of tool edge preparation on tool life and workpiece surface integrity, *Proceeding of the Institution of Mechanical Engineers*, vol. 218, no. 9, pp. 1113-1123, 2004.

[11]. A.K.M. Nurul Amin, A.F. Ismail, M.K. Nor Khairusshima, "Effectiveness of uncoated WC-Co and PCD inserts in end milling of titanium alloy-Ti-6Al-4V, *Journal of Materials Processing Technology*, vol. 192-193, pp. 147-158, 2007.

[12]. M.Y. Noordin, V.C. Venkatesh, S. Sharif, S. Elting, A. Abdullah, "Application of response surface methodology in describing the performance of coated carbide tools when turning AISI 1045 steel", *Journal of Materials Processing Technology*, vol. 145, no. 1, pp. 46-58, 2004.

[13]. D.C. Montgomery, "Design and Analysis of Experiments, 5th ed. Wiley, New York, 2001.

[14]. I.A. Choudury, M.A. El-Baradie, M.S.J. Hasmi, "Tool life prerdiction model by design of experiments for turning high strength stell (290 BHN)", *Journal of Materials Processing Technology*, vol. 77, no. 1-3, pp. 319-326, 1998.

[15]. I.A. Choudury and M.A. El-Baradie, "Prediction of tool life in end milling by response surface methodology", *Journal of Materials Processing Technology*, vol. 77, no. 1-3, pp. 319-326, 1998.

[16]. ISO 8688-2, Tool life testing in milling, Part 2: End Milling, (E) 1-26, 1989.

[17]. M. Alauddin, M.A. El-Baradie, M.S.J. Hasmi, "Prediction of tool life in end milling by response surface methodology", *Journal of Materials Processing Technology*, vol. 71, no. 1, pp. 456-465, 1997.

[18]. S.M. Wu, "Tool life testing by response surface methodology, part I and part II", transc. ASME, vol. 86, pp. 105-116, 1964.
[19]. S. Sharif, A.S. Mohruni, M.Y. Noordin, "Modeling of tool life when end milling on titanium alloy (Ti-6Al-4V) using response surface methodology, *In Proceeding of 1st International Conference & 7th AUSN/SEED-Net Fieldwise Seminar on Manufacturing and Material Processing*, 14-15 March, Kuala Lumpur, pp.127-132, 2006.
[20]. Design Expert Software 6.0, User's Guide, Technical Manual, Stat-Ease Inc. Minneapolis, MN, 2000.

ISSN: 1411-1284

On The Estimation of Visco-elastic Properties for Nylon and GFRP Materials

Gatot Prayogo, Danardono A.S

Mechanical Eng. Department, Fac.of Engineering, University of Indonesia
Kampus Baru UI, Depok 16424, Indonesia
Tel. 021-7270032, fac. 0217270033, e-mail: gatot@eng.ui.ac.id

Abstract-**In order to determine visco-elastic properties of Nylon and GFRP materials, Dynamic Mechanical Properties Testing in tensile oscillation and frequency of 100 Hz. was carried out for Nylon and GFRP materials. Specimen for this testing is rectangular cross section with dimension of 70.0 mm length, 3.0 mm thickness, and 7.0 mm width. The range of testing temperature was selected between 20°C to 31°C. This attempt is aimed to estimate viscoelastic data as a requirement for ANSYS (LS-DYNA) constitutive materials, indicated as Short time shear modulus (G_0), Long time shear modulus (G_∞), and Decay constant (β). Experimental data from Dynamic Mechanical Properties testing shown as tensile storage and loss moduli was converted to shear storage and loss moduli based on principle corresponding between Young's modulus, shear modulus and Poison's ratio. Furthermore, shear relaxation modulus (G_t) for both materials, Nylon and GFRP materials in above condition can be predicted and discussed.**

Keywords- Visco-elastic, Nylon, GFRP, Impact, Shear modulus.

I. INTRODUCTION

Composite materials posses high specific strength, stiffness and excellent resistance against fatigue. Unfortunately, the materials are very sensitive to impact damage due to impingement of raindrops, hailstones, debris, and tools dropped by maintenance personnel. These impacts can cause significant damage in composite materials called Barely Visible Impact Damage (BVID). When the long term usage of structures fabricated by composite materials is considered, an impact of single raindrop at velocity of 200 m/sec may produce no damage but repetition of the raindrop impact will bring about erosion on the materials [1)].

An experimental research of repeated raindrop impacts using nylon beads as impactor and GFRP as target materials has been conducted [2)]. Damage generated from that experiment is ring crack at front surface of specimen, star crack at back surface of specimen, and internal damage showing as debonding, matrix cracking, and delamination.

In order to analyze above impact damage, a series of attemps should be conducted. One of those attempts is to do impact simulation to get internal and surface transient stresses , contact duration, etc., using specific engineering software for impact collision like LS-DYNA. Since, Nylon and GFRP materials behave as viscoelastic materials at high strain rate deformation such as at high or moderate impact velocity, therefore it is necessary to select viscoelastic type of materials as a constitutive materials during simulation.

There are numerous viscoelastic model for this condition, however in this research work it will be matched to Hermann and Peterson model used in computational software, LS-DYNA [3)]. Therefore, the objective of this attempt is to estimate suitable viscoelastic data will be used as constitutive material during computation using LS-DINA.

II. MATERIALS AND MEHOD

In this research work, there are two main activities i.e. experimental and computational work. Experimental work was performed to get viscoelastic data shown as tensile storage modulus, tensile loss moduli and tan δ. Computational work was done to get viscoelastic data shown as shear storage modulus and shear loss modulus which match ANSYS LS-DYNA constitutive materials for linear viscoelastic.

SPECIMEN

There are two type of materials used in this experiment, Nylon and GFRP materials. The specimen was prepared by cutting of Nylon and GFRP sheets. According to ASTM standard used for this viscoelastic testing [4)], Its dimension is 70.00 mm length, 3.0 mm thickness, and 7.0 width. Glass Fiber Reinforced Plastic (GFRP) materials used in this test was fabricated from commercial CSM (Chopped Strand Mat) fiber glass and resin (UP)

as matrix materials. Volume fraction of fiber glass (V_f) is 33 wt %. Its density (ρ) and Poison's ratio (ν) are 1.44 gr/cm^3 and 0.3 respectively. The detailed fabrication method of GFRP sheet materials was shown in [2]. Nylon materials used in this specimen is Nylon 6.6. Its density (ρ) and hardness are 1.14 gr/cm^3 and R118, respectively.

EXPERIMENT

Dynamic mechanical properties testing was carried out based on ASTM Standard D 4065-1 using Visco-elastometer. Selected frequency for this testing is 10 Hz and 100 Hz, and the range of testing temperature is between 15°C to 150°C. A typical data of tensile storage mudulus and tensile loss modulus for nylon and GFRP materials can be seen in Fig.1 and Fig.2, respectively, as shown below.

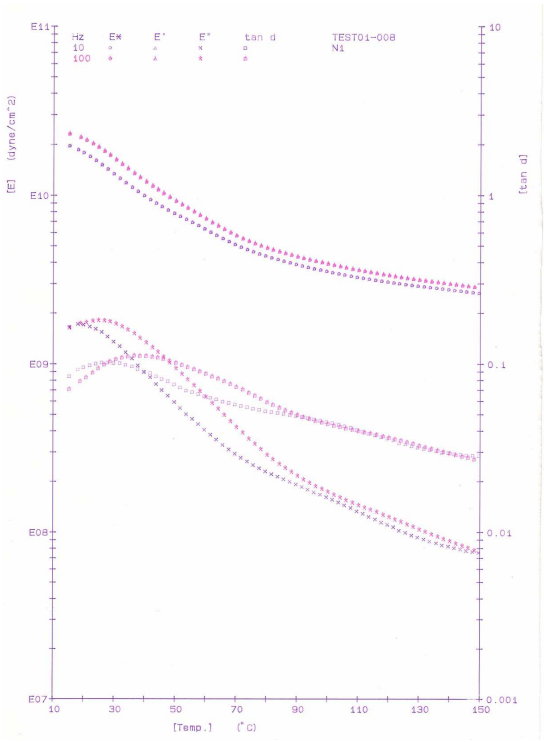

Fig. 1, Storage and loss tensile moduli of nylon materials

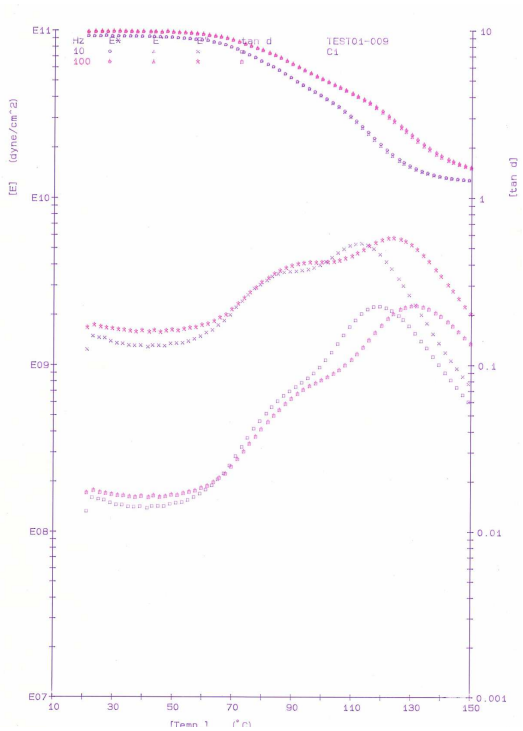

Fig. 2, Storage and loss tensile moduli of GFRP materials

DETERMINATION OF SHEAR STORAGE MUDULUS AND SHEAR LOSS MODULUS

Viscoelactic properties i.e shear storage modulus (G_0) and shear loss modulus (G_∞), can be estimated from tensile storage and loss moduli based on correspondence principle as discussed by Sogabe Y. et.al [5]. We have :

$$G' = \frac{E'}{2(1+\nu)} \qquad G'' = \frac{E''}{2(1+\nu)} \qquad \text{,and}$$

The value of G_0 is comparable to G' , and G_∞ is comparable to G".

Furthermore, a part of those data as shown in Figure 1 and 2, that is for 100 Hz and temperature range of 20°C to 30°C will be processed and analyzed as a requirement in research work. Linear viscoelastic model introduced by Hermann and Peterson [3] assumed that the model is deviatoric behavior, and the shear relaxation modulus (G_t) is given by :

$$G_t = G_\infty + (G_O - G_\infty)e^{-\beta t}$$

.

Where, G_o is short time shear modulus, G_∞ is long time shear modulus, β is decay constant which is equal to G_o/G_∞ .

III. RESULT AND DISCUSSION

As shown in Figure 3, complex shear modulus (G*) and storage shear modulus (G') for nylon materials have very similar value. The value is about 8.1E+08 Pa. at 20°C, and It decrease gradually became about 6.23E+08 Pa. at 30°C. This common phenomena shows that shear elastic modulus decrease with increasing temperature. Shear loss modulus at 20°C is about 6,77E+07 Pa, and 6,65E+07 Pa at 30 °C. This shows that the value of shear loss modulus is relatively constant at temperature range between 20 °C to 30 °C.

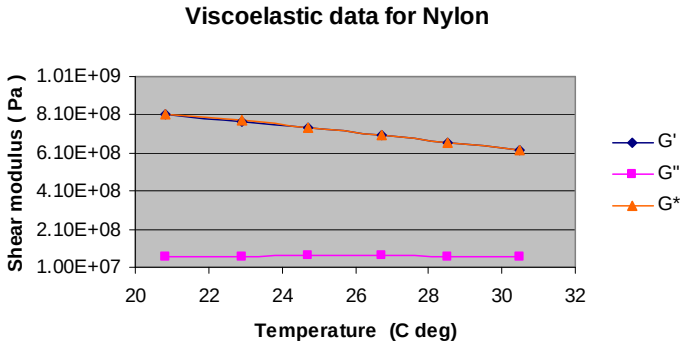

Fig. 3. Viscoelastic data for nylon materials.

As shown in Figure 4, complex shear modulus (G*) and storage shear modulus (G') for GFRP materials have very similar value. The value is about 3,76E+09 Pa. at 20°C, and It is relatively contant became about 3,79E+09 Pa. at 30°C. This phenomena shows that shear storage elastic modulus of GFRP materials does not change significantly by small increasing temperature from 20 °C to 30 °C. Shear loss modulus at 20°C is about 6,38E+07 Pa, and 6,23E+07 Pa at 30 °C. This shows that the value of shear loss modulus is relatively constant at temperature range between 20 °C to 30 °C.

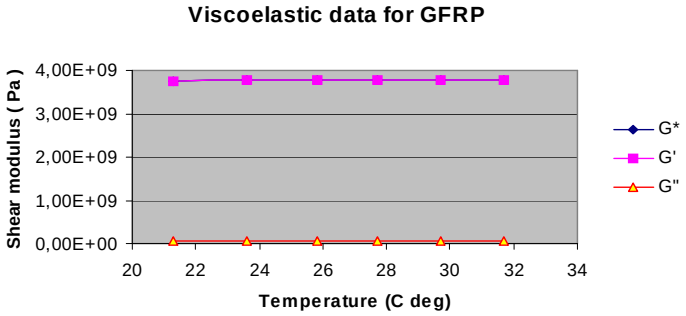

Fig. 4 Viscoelastic data for GFRP materials

Figure 5 and 6 show relaxation mudulus for nylon and GFRP materials respectively which are predicted from Eq. (2) above, and shape of the curve appear to be very similar to the curve of viscoelastic model for 3-parameter solid (spring-dashpot arragement)[7,8]. The curve show that the relaxation modulus seem decrease linierly or exponentialy, since the relaxation time is very short. Complete relaxation for those materials do not occur eccept for much longer time scale. This mean that both, nylon and GFRP materials, still behave as solid materials

during viscoelastic testing. This condition is very similar to that during impact testing.

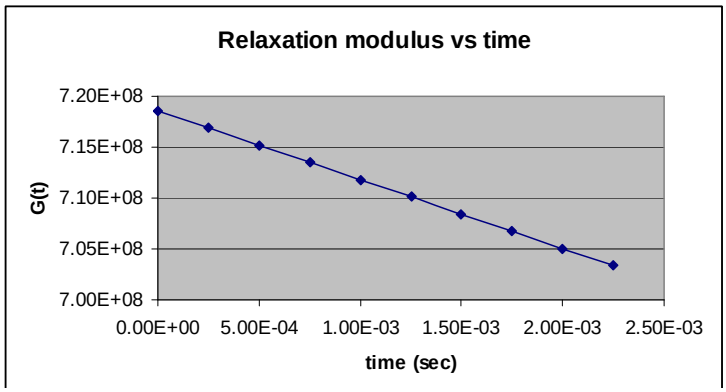

Fig. 5. Relaxation modulus vs time for nylon materials

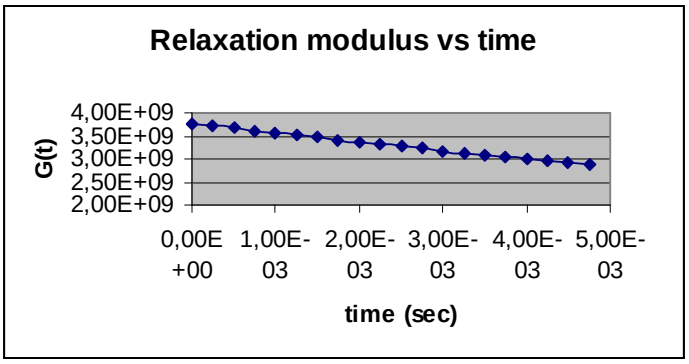

Fig. 6. Relaxation modulus vs time for GFRP materials

IV. CONCLUSION

Finally, it can be concluded as follows :

1. Viscoelastic properties of nylon and GFRP materials
   was predicted at temperature range between 20 °C to 30 °C. This range of temperature is reasonable condition which is representative temperature during impact testing.
2. For nylon materials, average value of short time shear modulus (G_o) is $7{,}19.10^8$ Pa , and average value of long time shear modulus (G_∞) is $6{,}84.10^7$ Pa, decay constant (β) is about 10.5.
3. For GFRP materials, average value of short time shear modulus (G_o) is $3{,}78.10^9$ Pa , and average value of long time shear modulus (G_∞) is $6{,}40.10^7$ Pa, decay constant (β) is about 59.0.

ACKNOWLEDGEMENT

Dynamic mechanical properties testing was performed at Industrial Research Institute, Aichi Prefecture Government, Nishishinwari, Hitotsugi-cho, Kariya City 448, Aichi Prefecture, Japan. Thanking you very much for this experimental work.

V. REFERENCES

[1] Zukas J.A., Limitations of Elementary Wave Theory, in ed. Zukas J.A., et.al, Impact Dynamics, John Wiley & Sons, 1982, USA.

[2] Gatot Prayogo, Hiroomi Homma, Yasuhiro Kanto, Repeated Rain-drop Impact Damage in Glass-Fibre Reinforced Plastics, 2nd ISIE (International Symposium on Impact Engineering), Beijing, China, 1996

[3] ANSYS LS-DYNA User's Guide

[4] Standard Practice for Plastics : Dynamic Mechanical Properties: Determination and Report of Procedures, ASTM D 4065-01.
[5] Sogabe Y., Tsuzuki M., Senda T., Kishida K., Viscoelastic Properties of CFRP Subjected to Impact Load, Macro- and Micro- Mechanics of High Velocity Deformation and Fracture edited by Kawata and Shioiri, Springer Verlag (1987).
[6] Marker Bradley N., Ferencz Robert M., Hallquist John O., NIKE3D User's Manual, November, 1990.
[7] Flugge Wilhelm, Viscoelasticity, Blaisdell Publishing Company, 1967.
[8] Gibson, Ronald F., Principles of Composite Materials Mechanics, McGraw-Hill series in Aeronautical and Aerospace Engineering, 1994.

Interfacial Shear Strength and Debonding Mode between the Ramie (*Boehmeria nivea*) Fiber Surface and Polymers Matrix

E. MARSYAHYO*
PhD Student, Postgraduate School, Gadjah Mada University
Yogyakarta; Department of mechanical Engineering, National Institute of Technology, Malang

R. SOEKRISNO. H.S.B ROCHARDJO, JAMASRI
Department of Mechanical and Industrial Engineering, Faculty of Engineering,
Gadjah Mada University Yogyakarta

ABSTRACT. Treatment the ramie fibers is a must to obtain optimal wettability and also intimate contact as a lock and key mechanism between the fiber surface and polymer resin. Comparison of wetting process between polypropylene (PP) and epoxy resins were also provided by investigation of the interfacial shear strength measurement using the pull-out test method. In the pull-out test, the fiber embedded in epoxy and polypropylene with embedded length 1 and 2 mm showed that epoxy matrix has a lower interfacial shear strength (ISS) than PP. Ramie treated-PP matrix had ISS around 5 to 11 MPa and ramie embedded in epoxy had ISS 2 to 7 MPa in average. Fiber-matrix pull-out fracture mechanism indicated from SEM proved that fiber embedded in PP matrix has better bonding-ability except for untreated fiber-PP. It was also found that fiber pull-out in epoxy matrix with embedded length 1 and 2 mm due to weaker bonding interaction between fiber and epoxy matrix. It was a proved that hydrophilic ramie fiber and hydrophobic polymeric materials can be combined properly and interact together to build an intimate contact due to fiber surface topography and chemical/physical interaction to the polymeric matrix.. Ramie fiber had critical length less than 1 mm and indicated to be able utilized for reinforcement material both discontinuous and continuous form in composite system.

KEYWORDS: ramie fiber, pull-out, interfacial shear strength, debonding mode

INTRODUCTION

The application of natural fibers reinforced composite has attracted substantial issues on their compatibility aspects such as adhesive bonding and wettability. Adhesive bonding and wettability are variables to be optimized in order to get the best properties and performance in composite materials. Fiber surface treatment and characterization of several natural cellulose fibers are necessary to predict the properties and performance of composite [1-3]. Ramie (*Boehmeria nivea*) fiber was believed as the strongest fibers in term of tensile strength and Young's modulus compare to other natural cellulose fibers available today[4-5]. Utilizing and modifying ramie as reinforcement fiber in polymer composites material become an essential in order to improve mechanical properties of the composites.

This paper is focused on surface porosity and contact angle between ramie treated fiber and epoxy and polypropylene liquid droplets. Surface porosity of the fiber affected surface roughness in which the matrix can flow and fill the porous to build mechanical interlocking [6],[9]. Adhesion and wettability are the main key of interfacial strength of the composite. Epoxy and PP liquid droplets were used to examine contact angle between the fiber surface and the droplets. Contact angle measurement is one of the simplest method to determine and understanding relationship between hydrophilic and hydrophobic materials n the creation of a beneficial fiber-matrix relationship [7-8]. Interactions between fiber surfaces and matrix also can be evaluated using single fiber pull-out method to determine interfacial shear strength and

* Author to whom correspondence should be addressed. Dept. of Mechanical and Industrial Engineering, Faculty of Engineering, Gadjah Mada University, Jl. Grafika no.2-Yogyakarta, Indonesia. Email: marsyahyo@yahoo.co.uk

bonding fracture modes between fiber and matrix in interface region in which the fiber is embedded [11].

Figure 1 interpret the forces acting on the fiber surface and the matrix when load applied (P). The pull-out test is considered to be the best method of evaluating the interfacial shear load as it can directly measure the ISS between the fiber and matrix.

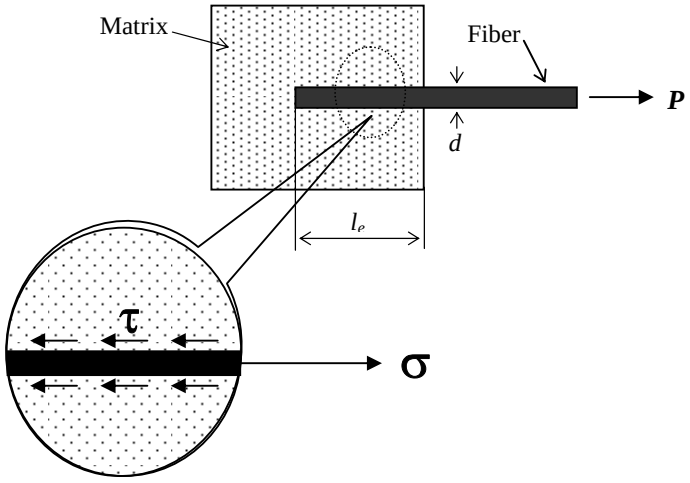

Figure 1. Interaction forces of the fiber surface-matrix in equilibrium fiber pull-out

The interfacial shear strength (ISS) are calculated from force equilibrium equation for the maximum pull-out load (σ_f) obtained from the test results with embedded length l_c .

$$\sigma_f \frac{\pi d^2}{4} = \tau_i \pi d (l_c) \quad (1)$$

$$\tau_i = \frac{(\sigma_f) d}{4 l_c} \quad (2)$$

Fiber debonding can occur easily when embedded fiber length in the matrix is less than critical fiber length (l_c) and due to poor fiber-matrix interfacial bonding. Moreover, debonding failure modes is also mainly governed by fiber breakage and matrix fracture.

EXPERIMENTAL

Materials

Ramie fibers were decorticated from Garut, West Java Indonesia. The fibers were prepared and pretreated using 5% NaOH boiling solution for 1 hour. Washed by distilled water until pH=7. and dried at room temperature for 20 hour and continued to oven heating 110^0 for 1 hour. After pretreatment, the fibers were grouped into four samples and immersed in ethanol, acetone, MEK and silane for 180 minutes at ambient temperature. Allowing oven-dried 110^0 for 1 hour and calculated the weight differences before and after treatment. Fibers were kept at vacuum sealed bag before surface porous characterization and applied to epoxy and PP liquid droplets. Ethanol, acetone and MEK were bought from Merck Indonesia. Silane (trimethoxymethylsilane) was from Fluka-Sigma Aldrich Corp. Epoxy was obtained from Bratachem, Bandung. Recycling disposal grade 5 uniform PP was used and melted by electric solder as liquid droplets .

Methods

Pull-out test was conducted in Mesdan-Tensolab strength tester with 100 N load cell and lowest test speed 7 mm/min. The pull –out specimens were attached using special jig and the fibers above the matrix were glued to paper board as seen in figure 2.

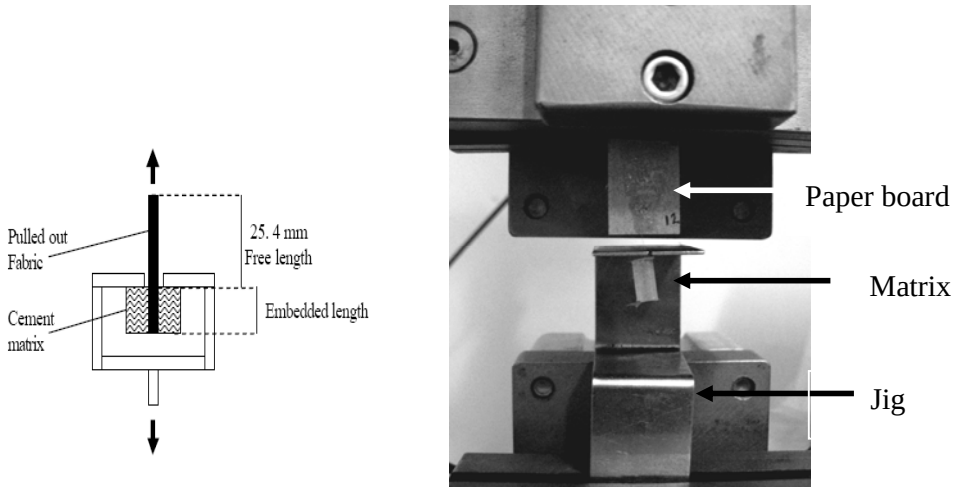

Figure 2. Fiber-matrix pull-out test and the specimen's jig

RESULT AND DISCUSSION

Assuming that lateral stresses were constant along the fiber embedded length so the ISS of ramie fiber-PP had higher ISS than ramie-epoxy. This is oversimplified calculation from the force balanced equation because the matrix properties did not include as for first approximation only [11]. Figure 3 showed comparison of the ISS ramie treated both embedded in epoxy and PP matrix with the embedded length of 1 and 2 mm.

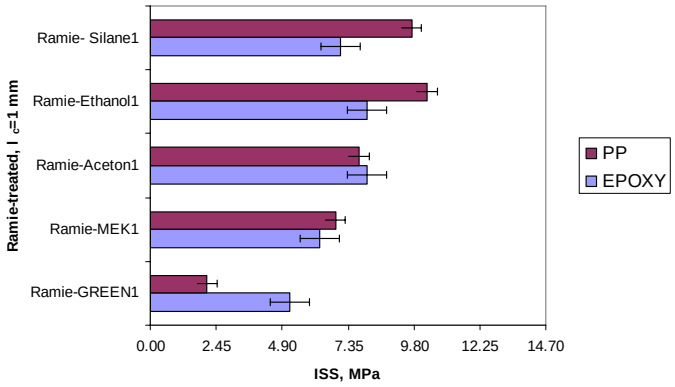

(a) ISS Ramie-matrix with embedded length l_c= 1 mm

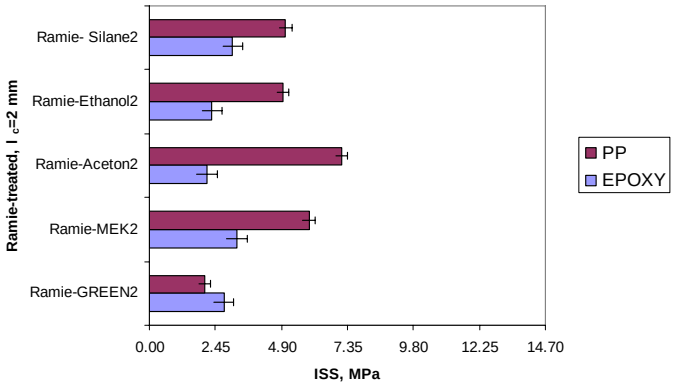

(b) ISS ramie-matrix with l_c= 2 mm

Figure 3. ISS ramie both embedded length 1 and 2 mm in epoxy and PP matrix

Ramie-silane1 and ramie-ethanol1 both embedded in epoxy and PP matrix showed the optimum ISS value for 1 mm embedded length. ISS of ramie-silane1-PP was 9.72 ±0.37 MPa and ramie-ethanol1-PP was 10.28 ± 0.45 MPa compared to ramie-silane1-epoxy and ramie-ethanol1-epoxy with the ISS 7.09 ±0.69 and 8.05 ±0.72 MPa lower than ramie fiber embedded in PP matrix. For embedded length 2 mm, ramie-acetone2-PP had the highest ISS about 7.14 ±0.23 MPa and ramie-MEK2-epoxy had ISS 3.24 ± 0.31 MPa.

From SEM analysis (fig.4), the fracture modes of fiber pull-out showed that ramie-PP has better fiber surface and matrix interaction with no pull-out occurred and except for ramie-Green-PP. In epoxy matrix, fiber pull-out from matrix was founded at embedded length 1 and 2 mm.

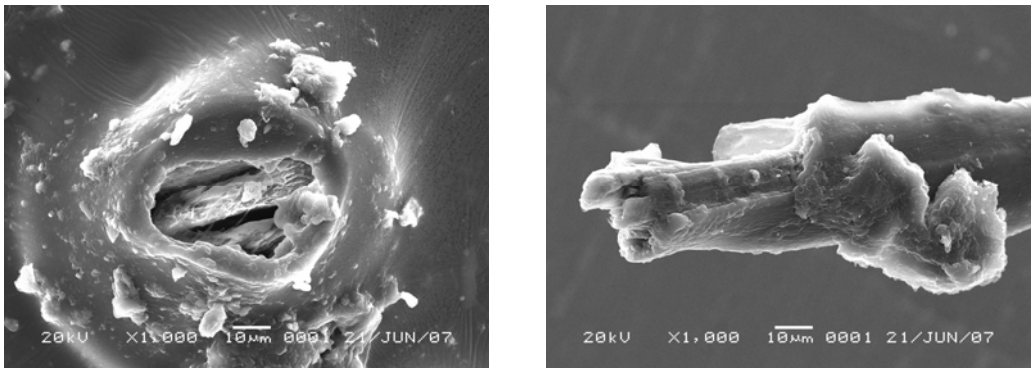

(a) Ramie-Green1-epoxy shows fiber pull-out and there is no epoxy still sticked on the fiber end surface. It seems to be pull-out easily from the matrix.

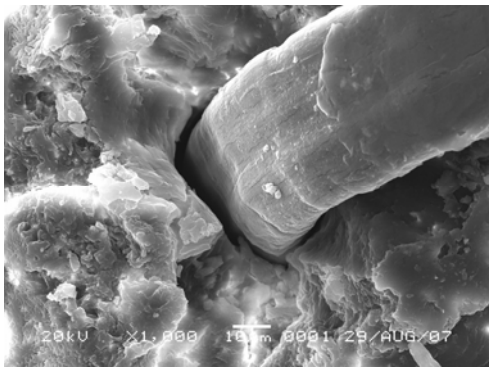

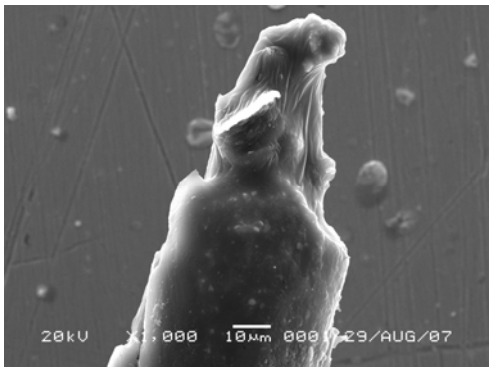

(b) Ramie-Green1-PP showed no pull-out but the region around embedded fiber and matrix surface indicated debonding between two surfaces due to pull-out load and arising broken fiber only.

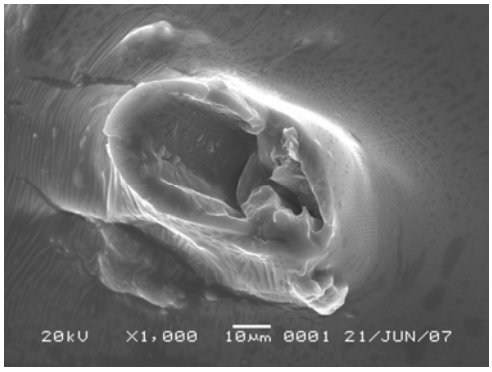

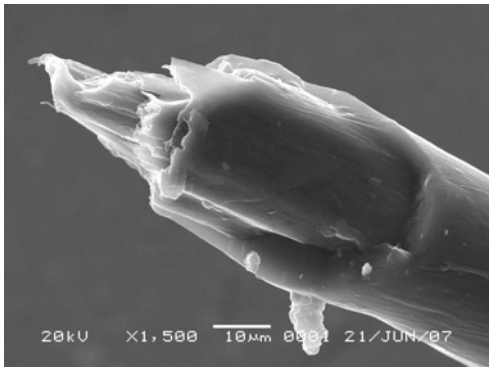

(c) Ramie-silane1- PP has a good bonding mechanism indicated by fracture of embedded fiber. The fiber was still embedded on the matrix surface and look alike the matrix was covered the broken fiber surface area.

Figure 4. Pull-out fracture mechanism of ramie fiber embedded in epoxy and PP matrix.

From the point of view, PP matrix has more optimum wettability than epoxy matrix. The ISS ramie-PP showed a better compatibility and bonding performance dominate by mechanical interlock and may also chemical interaction on the fiber-matrix interface.

CONCLUSIONS

This paper presented some unique surface topography of ramie fibers surface treatment. If ramie fiber to be used for reinforcement in polymer composite materials, they should be treated properly and investigate in term of their compatibility to combine with polymer material to build up better wettability and adhesion performances. In average, the rami-PP showed higher ISS than ramie-epoxy due to PP matrix has a better wetting capability to fiber surface and the fracture mechanism indicate that rami-PP had no fiber debonding from the the matrix because of intimate contact in the fiber surface more optimum than rami-epoxy. The knowledge of the ramie fiber surface topography and interaction to the polymer matrix is important as representing the key in fiber performance in the sense of composite system. From the point of view, ramie fiber had critical length less than 1 mm and this indicate that ramie fiber can be utilized for reinforcement in polymer composite in the form of discontinuous and continuous fiber.

ACKNOWLEDGEMENT

We would like to thanks to the head of *Sentra Ramie Terpadu Koppontren Darussalam* Garut-West Java-Indonesia, Mrs. Aminah Mussadad, for her patience during the periode we learned about ramie plant and its morphology and supporting ramie material in this research is also greatly acknowledged.

REFERENCES

1. Bismarck, A, Askargota, I.A., Springer, J., Lampke, T., Wielege, B., Stamboulis, A., Shenderovich, I., Limbach, H. (2002). Surface Characterization of flax, hemp and Cellulosic; Surface properties and the Water uptake Behavior, Polymer Composites, vol. 23., no.5., pp. 872-894
2. Eichhorn, S.J, Baile, C.A., Zafeiropoulos, N., Mwaikambo, L.Y., Ansell, M.P., Dufresne, A., Entwistle, K.M., Franco, P.J.H., Escamilla, G.C., Groom, L., Hughes, M, Hill, C., Rials, T.G., Wild, P.M. (2001). Review Current International Research into Cellulosic Fibres and Composites, J. of Materials Science, vol.36, pp. 2107-2131
3. Feng, D., Caufield, D.F., Sanadi, A.R. (2001), Effect of Compatibilizer on the Structure Property Relationship of Kenaf Fiber/Polypropylene Composites, Polymer Composites, vol. 22., no. 4
4. Feresenbet, E., Raghavan,D.,Holmes,G.A. (2003). The Influence of Silane Coupling Agent Composition o the Surface Characterization of Fiber and on Fiber-Matrix Interfacial Shear Strength, The J. of Adhesion, vol.79, pp. 643-665, Taylor&Francis.
5. Belgacem, M.N., Gandini, A.(2005). The Surface Modification of Cellulose fibers for Use as Reinforcing in Composite materials, Composite interfaces, vol.12, pp, 41-75, VSP publ.
6. Drzal, L.T. (2003), ASM Handbook:Composite Interface, Interfaces and Interphases, FB MVU, online:www.mb.hs_wismar.de/interfaces.
7. Mihranyan, A. (2005). Engineering of Native Cellulose Structure for Pharmaceutical Application, thesis report, Uppsala Univ., ISBN 91-554-6130-1, Sweden.
8. Marsyahyo, E., Soekrisno, Rochardjo, H.S.B., Jamasri. (2006). Investigation of Chemical Surface Treatment of Ramie Fiber (Boehmeria nivea) on Surface Morphology, Tensile Strength and Single Fiber Fracture Modes, International Conference Product design and development, 12 December 2006, Gadjah Mada University.
9. Vick, C.B. (1999). Adhesive Bonding of Wood Materials, Wood Handbooks-Wood as Engineering Materials, ch.9, pp.1-23. Forest Product laboratory, Madison.
10. Rochery, M. Vroman, I., Campagne, C. (2006). Coating of Polyester with Poly(dimethylsiloxane) and Poly(tetramethylene oxide) based Polyurethane, J.of Industrial Textiles, vol.35, no. 3, pp. 227-238.
11. Li, Y., Mai, Y.M., Ye, L., (2005). Effects the Fibre Surface Treatment on Fracture-Mechanical Properties of Sisal Fibre Composites, Composites Interfaces, vol.12, no. 1-2, pp. 141-163., VSP publ.

ISSN: 1411-1284

Fabrication of CuO Added-$BaTiO_3$ Ceramics for NTC Thermistor

Dani Gustaman Syarif

Nuclear Technology Center for Materials and Radiometry – BATAN
Jl. Tamansari 71, Bandung 40132, Indonesia.
Telp.: 62-22-2503997, Fax.:62-22-2504081, Email:danigustas@batan-bdg.go.id

Abstract-**This work was dealing with a fabrication process of a new material for negative thermal coefficient (NTC) thermistor using $BaTiO_3$ as base material. It is required to modify the $BaTiO_3$ ceramic due to its very high electrical resistivity to produce the NTC ceramic. Here, CuO was used as an additive to get the $BaTiO_3$ based-NTC ceramics. The NTC ceramics were produced as follow. Powder of $BaTiO_3$ and CuO (with concentration of 0 – 40 mole %) were mixed together homogeneously. The mixed powder was pressed with pressure of 4 ton/cm^2 into green pellets. The green pellets were sintered at 1100^{o}C for 2 hours in air. Electrical characterization was done by measuring electrical resistivity of the sintered pellets after coating them with silver paste. An X-ray diffraction (XRD) and microstructural analyses (using SEM) were carried out to know phases within the sintered ceramics. It was known that the electrical resistivity of the CuO added-$BaTiO_3$ ceramics decreased with the increase of CuO concentration where the optimal concentration was in between 5 and 10 mole %. Thermistor constant (B) of the CuO added-$BaTiO_3$ ceramics was relatively large and the value of the electrical resistivity of the ceramics was within the market application range, making the ceramics were applicable as the NTC thermistor. The XRD and SEM data showed the presence of second phase responsible for the NTC ceramic formation.**

Key words : $BaTiO_3$, thermistor, NTC, CuO.

I. INTRODUCTION

Negative thermal coefficient (NTC) thermistors (thermistor is acronym of thermally sensitive resistor [1]) are widely used in many fields such as instrumentation, medical, food processing and automotive [2]. The thermistor can be applied in some devices such as electric current limiter, catheter, flowrate sensor, pressure sensor and human body thermometer. It is well known that thermistors are generally made of transition metal oxide spinel ceramics in the form of AB_2O_3 where A is the ion in octahedral position and B is the ion in tetrahedral position[2,7-10].

It is required to find another material for diversification. Some ceramics may be chosen as the NTC material and one is $BaTiO_3$. Unmodified $BaTiO_3$ is an insulator so some efforts have to be done to produce the NTC ceramics from $BaTiO_3$. Here, a new material made of $BaTiO_3$ and CuO for the NTC thermistor was proposed. This material was made based on a hypothesis that CuO may form a conductive material within the $BaTiO_3$ as the base-material and change the electrical characteristic. This work studied about the effect of CuO addition on the electrical characteristics of the $BaTiO_3$ ceramic and the possibility of the ceramic to be an NTC thermistor.

II. METHODOLOGY

Powder of $BaTiO_3$ and powder of CuO, where the concentration of CuO powder was 0, 5, 10, 20, 30 and 40 mole %, were mixed homogeneously in a mortar agate. The powder of $BaTiO_3$ was synthesized from $BaCO_3$ and TiO_2 by mixing them and calcining the mixture at 1100^{o}C for 4 hours in air. The mixed powder was then pressed with pressure of 4 ton/cm^2 into green pellets. The green pellets were sintered at 1100^{o}C for 2 hours in furnace air. The sintered pellets were analyzed using x-ray diffraction (XRD) to know crystal structure and phases within the pellet. The microstructure of the fracture surface of the pellets was observed by using a scanning electron microscope (SEM).

Electrical characterization of the sintered pellets was carried out by measuring electrical resistivity at different temperatures with interval of 5^{o}C using a two-point method. Before electrical measurement, the pellets were coated with silver paste and baked at 600^{o}C for 6 minutes. The electrical resistivity and temperature data was plot into ln resistivity vs 1/T curves. The curve was made by referring to an Arhenius equation of equation 1 below [1,3,7,8, 10-13]:

$$\rho = \rho o \, Exp. \, (B/T) \qquad (1)$$

where, ρ is electrical resistivity at temperature T, ρo is a constant or the electrical resistivity at infinite temperature, B is thermistor constant and T is temperature in Kelvin. From this curve the electrical

characteristics were determined. The gradient of the curve is the thermistor constant (B). From data of B, the sensitivity (α) was calculated using equation 2 [2]:

$$\alpha = B/T^2 \qquad (2)$$

where, α is sensitivity at temperature T, B is thermistor constant and T is temperature in Kelvin. From data of B, the activation energy Ea was calculated using equation 3 [8,11] :

$$Ea = B.k \qquad (3)$$

where, Ea is the activation energy, B is the thermistor constant and k is the Boltzmann constant.

III. RESULTS AND DISSCUSION

III.1 XRD data

Fig.1 shows the XRD profile of $BaTiO_3$ ceramic without any addition. Fig. 2, 3, 4 and 5 are the XRD profiles of the $BaTiO_3$ ceramics added with 10, 20, 30 and 40 mole % CuO. It is clearly seen the presence of additional peaks other than main peaks from $BaTiO_3$ in the XRD profiles of Figure 2 until 5. This additional peaks come from a second phase. However, it was difficult to identify the second phase. The second phase may be more than one compound. One is a reaction product containing Ba and Cu. So, the materials may be $BaCuO_2$, unreacted CuO (becomes Cu_2O) and segregated TiO_2. The formation of $BaCuO_2$ is possible because this material can be formed at temperature lower than 1100^{o}C [14].

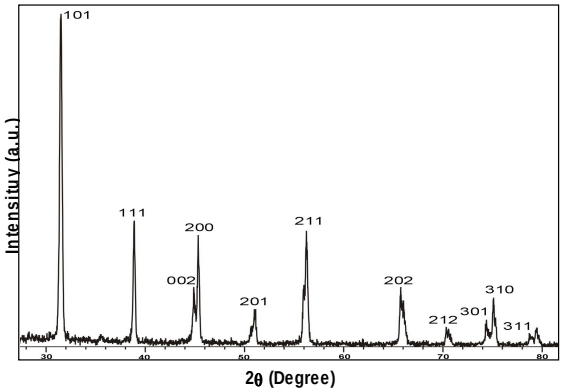

Fig.1. XRD profile of $BaTiO_3$ ceramic without addition of CuO.

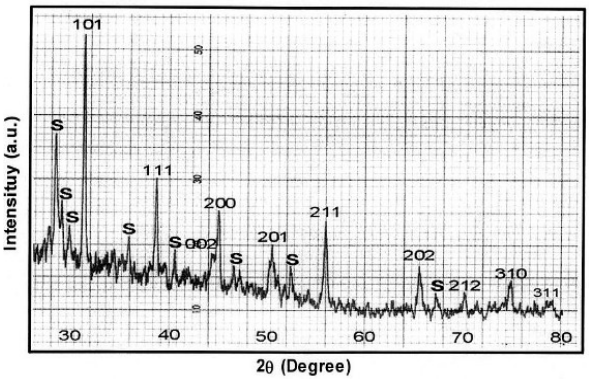

Fig.2. XRD profile of $BaTiO_3$ ceramic added with 10 mole % CuO.

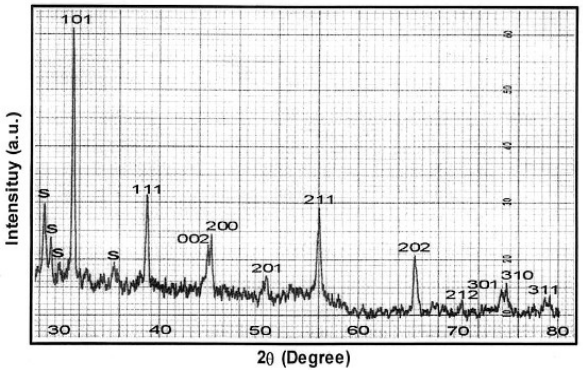

Fig.3. XRD profile of $BaTiO_3$ ceramic added with 20 mole % CuO.

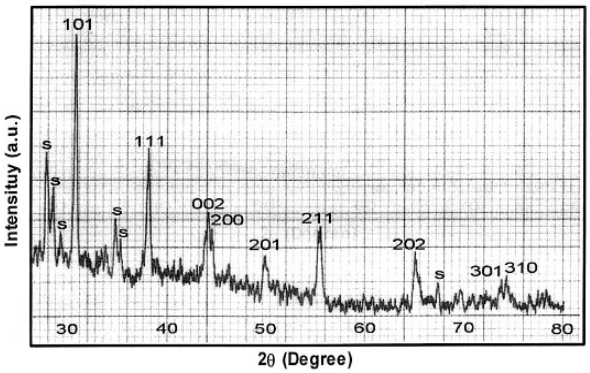

Fig.4. XRD profile of $BaTiO_3$ ceramic added with 30 mole % CuO.

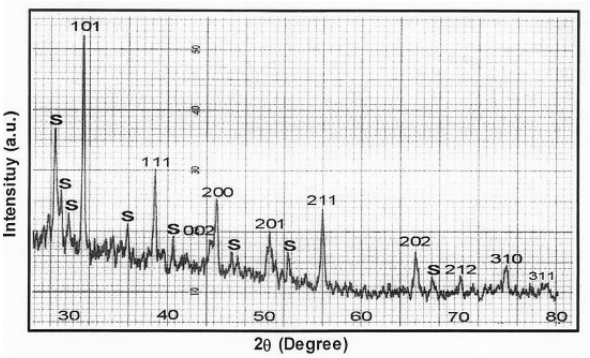

Fig.5. XRD profile of $BaTiO_3$ ceramic added with 40 mole % CuO.

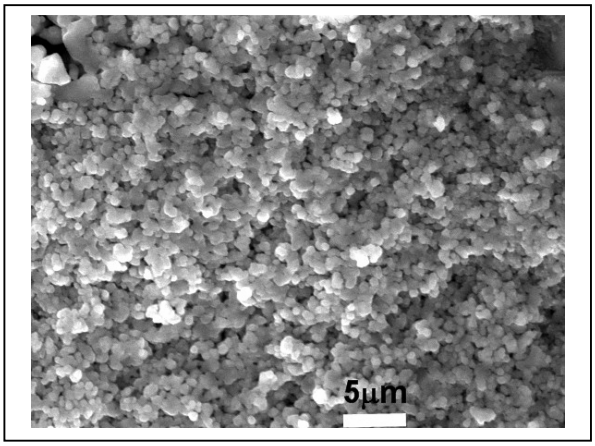

Fig.6. Microstructure (taken using SEM) of $BaTiO_3$ ceramic without addition of CuO. Containing no second phase.

III.2. Microstructure

Fig. 6 – 9 are microstructures of the $BaTiO_3$ ceramic without addition of CuO and those added with 10, 30 and 40 mole % CuO. As shown in Figure 7 - 9, the ceramics added with CuO consist of two phases namely $BaTiO_3$ as the main phase and the second phase. The amount of the second phase increases with the increase of CuO additive. The second phase segregates at grain boundaries. Considering the microstructures of Fig. 6-9, the prominent effect of the addition of CuO is largering grains of the $BaTiO_3$ ceramic remarkably. The additive of CuO promoted grain growth of the $BaTiO_3$ ceramic during sintering.

Usually a substitution of host cation by ion of additive can promote the sintering since the ion of additive can be accommodated through a solid solution formation. In this case the solid solution formation compensated through substitution of Ba or Ti ions with that having higher valence resulting in defect of cation vacancy. However, the additive used here is CuO having valence of 2. The substitution of Ba and Ti ions by Cu^{2+} ion will not produce cation vacancy. The possibility of the substitution of Ba and Ti ions by Cu^{2+} ion is also very small to occur since the ionic radii of the ions is considerd. Considering the ionic radii of Cu^{2+}, Ba^{2+} and Ti^{4+} namely 87 pm, 149 pm and 74,5 pm [15], respectively, it is very difficult for Cu^{2+} to substitute either Ba^{2+} or Ti^{4+}. So, the mechanism of promoting grain growth in this case is grain boundary activated sintering. During sintering, the additive of CuO reacted with either Ba or Ti containing material, resulting in a liquid phase. Then the liquid phase activates the sintering. The possible grain boundary material is that containing Ba and Cu which melts at temperature below 1100^{o}C.

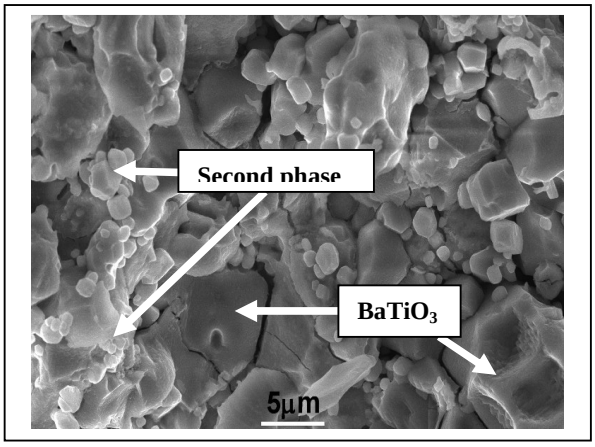

Fig.7. Microstructure (taken using SEM) of $BaTiO_3$ ceramic added with 10 mole % CuO.

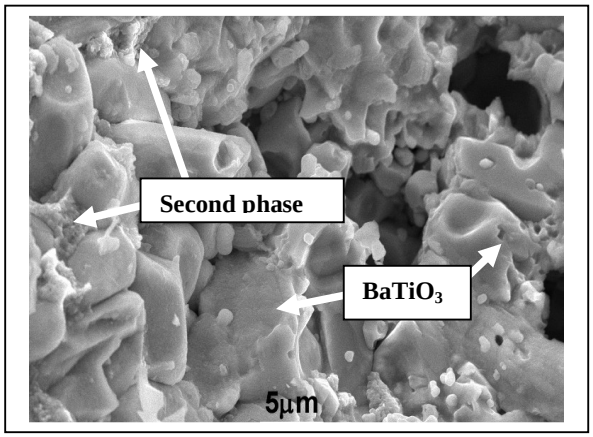

Fig.8. Microstructure (taken using SEM) of $BaTiO_3$ ceramic added with 30 mole % CuO.

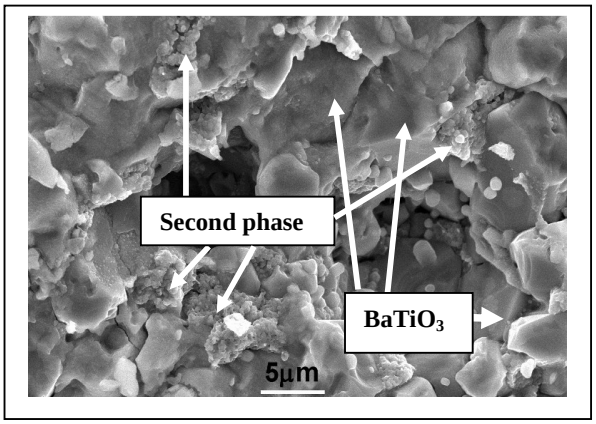

Fig.9. Microstructure (taken using SEM) of $BaTiO_3$ ceramic added with 40 mole % CuO.

III.3. Electrical Characteristics

Electrical data of the CuO added-$BaTiO_3$ ceramics is shown in Fig. 9 and Table 1. The value of sensitivity α (alpha) was calculated using equation (2) and the activation energy was calculated using equation (3). The electrical data of Fig. 9 shows that the electrical characteristic of the ceramics follows the NTC tendency expressed by an Arrhenius equation of eq. 1 [11].

As shown in Table 1 and Fig. 11, the resistance of the ceramic decreases with the increase of CuO concentration. Since the resistivity of the pure $BaTiO_3$ is very large, the responsible for decreasing resistivity and thermistor constant is the presence of CuO additive. The CuO forms a second phase inside the $BaTiO_3$ ceramic. This second phase should be conductive because the $BaTiO_3$ is resistive. Another mechanism in lowering the resistance of the $BaTiO_3$ ceramic is by substitution of Ba or Ti ions with that having higher valence which is compensated by formation of electron. The additive used here is CuO having valence of 2. Compensation by creating additional electron for conduction band is not possible when Cu^{2+} ion substitutes either Ba ion or Ti ion. Considering the ionic radii of Cu^{2+}, Ba^{2+} and Ti^{4+} namely 87 pm, 149 pm and 74,5 pm [15], respectively, it is very difficult for Cu^{2+} to substitute either Ba^{2+} or Ti^{4+}. So, the possible mechanism in lowering resistance is growing the grains of the $BaTiO_3$ ceramic and embedding material having lower resistance at the grain boundaries of the $BaTiO_3$ ceramic as the matrix. The presence of the second phase at the grain boundaries also eliminates the PTC effect of the $BaTiO_3$, at least till 100°C.

The large the concentration of CuO, the large the concentration of the second phase is. The increase of the amount of the second phase followed by lowering the resistivity of the ceramics. The addition of CuO also decreases the thermistor constant (B) and the activation energy for electrical conduction of the sensor ceramic (Ea). Comparing to the value of B and α for the industry (where B and α are equal or larger than 2000K and 2.2%/K, respectively), the B and α of the ceramic which fit the requirement are those from ceramic added with 5 mole % CuO, however, the resistivity of this ceramic is too large compared to the required one (1 Mohm-cm). So, the optimum concentration of the added CuO is between 5 and 10 mole % namely 7,6 mole % as calculated from Fig.10.

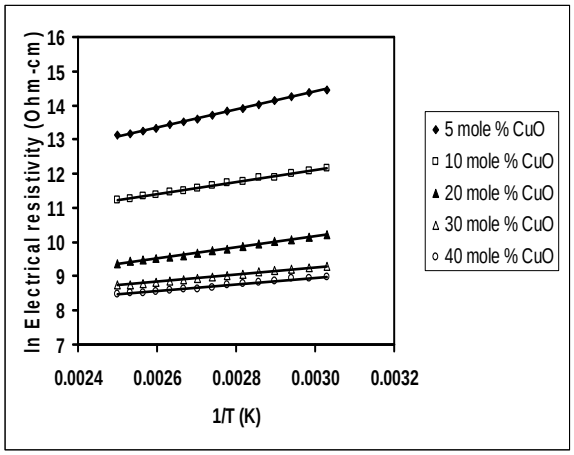

Fig.10. Ln Electrical resistivity as a function of 1/T of $BaTiO_3$ ceramics added with CuO.

Table 1. Electrical characteristics of $BaTiO_3$ ceramic added with CuO.

No.	CuO (mole %)	ρRT (Ohm-cm)	B (K)	α (%/K)	Ea (eV)
1.	5	4260939	2613	2.90	0.225
2.	10	327814	1773	1.97	0.153
3.	20	44160	1589	1.77	0.137
4.	30	14652	1044	1.16	0.089
5.	40	10917	1002	1.11	0.086

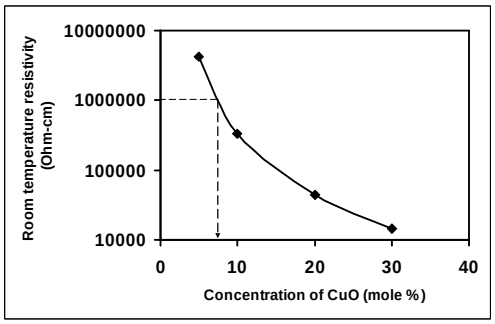

Fig.11. Electrical Resistivity of the $BaTiO_3$ ceramics as a function of CuO concentration.

IV. CONCLUSION

A new ceramic base on $BaTiO_3$ for NTC thermistor has been produced by CuO addition. The responsible material within the ceramic for the NTC thermistor formation is a reaction product mainly containing Ba and Cu which tends to segregate at grain boundary and melts during sintering. The reaction product is a conductive material. The grain boundary material activates the sintering of $BaTiO_3$ resulting in large grains and decreasing the resistance of the ceramic. The optimum concentration of CuO for resulting in good thermistor fitting the industry requirement is about 7,6 mole %. The addition of CuO eliminates the PTC effect of the $BaTiO_3$.

ACKNOWLEDGMENT

The author thanks to Mr. Yudi Setiadi from Materials Physics Group of PTNBR BATAN for providing the XRD data and Setiani Ibrahim from UNJANI for providing the SEM data.

REFERENCES

[1]. M. Parlak, T. Hashemi, M.J. Hogan, A.W. Brinkman, "Electron beam evaporation of nickel manganese thin film negative temperature coefficient thermistors", Journal of materials science letters, Vol.17, p.1995, 1998.

[2]. BetaTHERM Sensors [on line]. Available: http://www.betatherm.com.

[3]. Eun Sang Na, Un Gyu paik, Sung Churl Choi, "The effect of a sintered microstructure on the electrical properties of a Mn-Co-Ni-O thermistor", Journal of Ceramic Processing Research, Vol.2, No. 1, 2001, p 31-34.

[4]. Yoshihiro Matsuo, Takuoki Hata, Takayuki Kuroda, "Oxide thermistor composition", US Patent 4,324,702, April 13, 1982

[5]. Hyung J. Jung, Sang O. Yoon, Ki Y. Hong, Jeon K. Lee, "Metal oxide group thermistor material", US Patent 5,246,628, September 21, 1993.

[6]. Kazuyuki Hamada, Hiroshi Oda, "Thermistor composition", US Patent 6,270,693, August 7, 2001.

[7]. K. Park, "Microstructure and electrical properties of $Ni_{1.0}Mn_{2-x}Zr_xO_4$ ($0 \le x \le 1.0$) negative temperature coefficient thermistors", Materials Science and Engineering, B104, 2003, p. 9-14.

[8]. K. Park, D.Y. Bang, "Electrical properties of Ni-Mn-Co-(Fe) oxide thick film NTC thermistors", Journal of Materials Science: Materials in Electronics, Vol.14,2003, p. 81-87.

[9]. Shopie Gulemet Fritsch, Jaouad Salmi, Joseph Sarrias, Abel Rousset, Shopie Schuurman, Andre Lannoo, "Mechanical properties of nickel manganites-based cermics used as negative temperature coefficient thermistors", Materials Research Bulletin, Vol. 39, 2004, p. 1957-1965.

[10].R. Schmidt, A. Basu, A.W. Brinkman, "Production of NTCR thermistor devices based on $NiMn_2O_{4+\delta}$", Journal of The European Ceramic Society, Vol. 24, 2004, p. 1233-1236.

[11]. K. Park, I.H. Han, "Effect of Al_2O_3 addition on the microstructure and electrical properties of $(Mn_{0,37}Ni_{0,3}Co_{0,33-x}Al_x)O_4$ ($0 \le x \le 0.03$) NTC thermistors", Materials Science and Engineering, B119, 2005, p. 55-60.

[12].The Effect of TiO_2 Addition on the Characteristics of $CuFe_2O_4$ Ceramics for NTC Thermistors, International Conference on Mathematics and Natural Sciences (ICMNS) 2006, ITB, Bandung, October 2006.

[13].Dani Gustaman Syarif, "Fabrication of thick film ceramics for NTC thermistor using Fe_2O_3 derived from mineral", International Conference on Instrumentation, Communication and Information Technology (ICICI 2007) Proc., 271-274, 2007.

[14].Winnie Wong-Ng, Lawrence P. Cook, Liquids diagram of the Ba-Y-Cu-O system in the vicinity of the $Ba_2YCu_3O_{6+x}$ phase field", Journal of Research of the National Institute of Standards and Technology 103, 1998, pp.379-418.

[15].Michel Barsoum, "Fundametals of Ceramics", McGraw Hill, NY, 1997.

ISSN: 1411-1284

Structure and Properties of $Cu(In_{1-x}Al_x)Se_2$ Thin Films Grown by RF Magnetron Sputtering For Solar Cells Applications

Badrul Munir [a*] and Kyoo Ho Kim [b]

[a] Department of Metallurgy and Materials Engineering University of Indonesia
Kampus UI Depok 16424 Indonesia
* Corresponding author email : bmunir@metal.ui.ac.id
[b] School of Materials Science and Engineering Yeungnam University
214-1 Dae-dong Gyeongsan 712-749 Republic of Korea

Abstract - **Thin films based on $CuInSe_2$ (CIS) have been considered as one of the most promising absorber layers for solar cells, approaching 20% efficiencies using Ga addition to form $Cu(InGa)Se_2$. However, low cost technology and materials are essential to reduce the manufacturing cost of solar cells. Addition of aluminum to the CIS films is a viable alternative to reduce the usage of expensive indium and gallium as well as to improve the band gap of CIS solar cells by forming $Cu(In_{1-x}Al_x)Se_2$ (CIAS). CIAS thin films were prepared using single step sputtering on corning glass substrates. All films have good adhesion to the substrate and show strong (112), (220)/(204) peaks. By varying Al content, the optical band gap of the films were estimated to be in the range 1.05 ~ 1.75*eV*, which is suitable for applications as an absorber layer in solar cells.**

Keywords: Thin Films, Solar cells, $CuInSe_2$, sputtering, properties

I. INTRODUCTION

Polycrystalline thin films based on $CuInSe_2$ (CIS) have been considered as one of the most promising absorber layers for solar cells approaching 20% laboratory efficiencies after Ga addition which replaces part of In in the CIS system to form $Cu(InGa)Se_2$[1]. The merits include high optical absorption coefficient, suitable band gap and long-term stability. However, there is still a need to reduce the manufacturing cost of solar cells by employing low cost technology and materials. CIS band gap (*Eg*) is 1.04 eV, still lower than solar spectrum energy and optimum *Eg* for solar cell absorber (1.1~1.3eV). Increasing absorber layer *Eg* will result in a higher open circuit voltage of the solar cells although to some extent will lower the short circuit current. However In and Ga are considerably expensive. Addition of aluminum to the CIS films is form $Cu(In_{1-x}Al_x)Se_2$ (CIAS) is a viable alternative to improve the *Eg* as well as to reduce the usage of expensive indium and gallium of CIS solar cells. It requires relatively smaller amount of Al alloy concentration than Ga to achieve a comparable *Eg*. Although a high 16% efficiency has been recorded on CIAS using co-evaporation method [2-4], there have been limited literatures on alternative production routes. While co-evaporation has the ability to control stoichiometry of the films, practically, it requires complex control of heating systems, relatively high amount of materials and high degree of chamber contamination. RF magnetron sputtering offers a viable alternative for producing thin films at low cost. It has been employed successfully to produce CIS thin films for solar cells application through selenization of sputtered precursors.

This paper explores the possibility to grow CIAS thin films by a simple one-step sputtering deposition from binary selenides.

II. EXPERIMENTAL DETAILS

CIAS thin films were deposited on corning glass 1737 substrates by means of RF magnetron sputtering from a 2-inches single target. Substrates were cut in $50x15cm^2$ and subsequently cleaned ultrasonically in soap water and organic solutions (acetone, ethanol) and de-ionized water prior to loading into the deposition chamber. The sputtering target was compacted from a mixture of bindary selenides of CuSe, InSe and additional Al powders. Powders with at least 4N purity were used as starting materials. After initial chamber evacuation by turbo molecular pump reached 10^{-5} Torr, depositions were carried out

at 40 mTorr working pressure using Ar sputtering gas flowing at 2.2 sccm. Substrate to target distance was kept constant at 50mm. To study the effect of deposition temperature, substrates were heated up at different temperature ranges from no intentional heating (RT) until 200^{0}C. Films with different Cu/(In+Al) and In/Al as well as Metal/Se ratios were obtained by varying the target compositions, mainly the InSe and Al (up to 10 wt-%) content as Al addition is designed to replace part of In. To preserve the same condition for every deposition the target was remixed and pressed after every deposition process. The average film thickness is 1.5 μm resulted from 3 hours total deposition time using 75W RF power (deposition rate 1.38 Å/s).

All of the deposited films were characterized to study their stoichiometry, structural and optical properties as well as the type of conductivity. X-Ray diffractometer (Rigaku DMax 2500) was used to examine the films' crystallinity by Cu-Kα radiation (λ=1.5405Å). The surface morphology of the films was observed by scanning electron microscope (Hitachi S-4100) while the chemical composition of the films were measured by energy dispersive x-ray spectroscopy (EDX) attached to the SEM equipment, in which the standard of the measurement was calibrated by wavelength dispersive spectroscopy [6]. Cary Varian UV-Vis spectrophotometer was employed to observe the optical properties of the films. The films conductivity were examined using Van der Paw method at 300 K (ECOPIA HMS-3000, USA).

III. RESULTS AND DISCUSSION

First depositions were carried out to produce CIS films using sputtering target composed of finely mixed CuSe and InSe powder (1:1 mole ratio) at different deposition temperatures from without intentional heating (RT) to 200^{0}C. Deposition at higher substrate temperature is needed to improve the crystallinity of the films.

Fig 1 shows that the ratio of Cu:In:Se in the films could be maintained near stoichiometry up to 125^{0}C deposition. Above that temperature, In and Se content in the film decreased rapidly due to loss during deposition. Therefore all the subsequent depositions for producing CIAS thin films specimens were carried out at 125^{0}C.

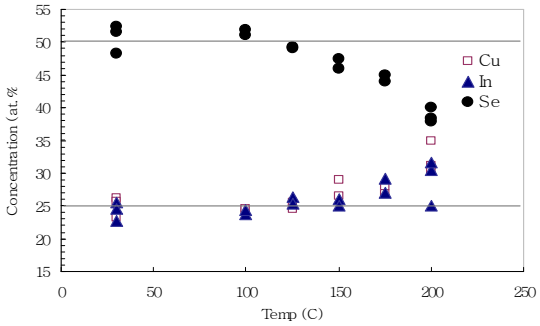

Fig. 1. Stoichiometry of CIS films at various deposition temperatures.

The graph also revealed the narrow variation in elemental concentration of Cu and In for every deposition temperature except for deposition above 150^{o}C where the Se content decreased abruptly. It was also noted that the average ratio of Cu/In in the films is slightly lower than 1.0. A Cu-poor film is favored to make a *p*-type solar cell absorber. However chalcopyrite materials especially CIS is widely known for its tolerance to stoichiometry variation without affecting much of its structural properties.

Table 1 shows the chemical composition of films before and after Al addition in the target deposited at 125^{0}C as observed by EDX bulk analysis. Apart from CIS films (marked as CIAS-0), two groups of specimens were prepared from target with addition of 3, 6 and 10 wt-% Al powder, denoted as CIAS-3, CIAS-6 and CIAS-10, yielding films with x value from 0 ~ 0.34. All of the observed films shows only slightly deficient in Se between 45.95 ~ 48.22 at-%, which is found to be better compared to the similar films produced by two-step selenization of sputtered metallic precursors [7].

Table 1. EDX analysis of films deposited at 125^{0}C (concentration in at-%)

Target	Cu	In	Se	Al	*x*
CIAS-0	25.19	26.59	48.22	0	0
CIAS-3	24.89	22.69	47.88	4.54	0.17
CIAS-6	23.77	22.24	47.23	6.68	0.23
CIAS-10	21.92	21.05	45.95	11.08	0.34

Increasing the deposition temperature and addition of Al increases the ratio of Cu/(In+Al) as well as the loss of Se. It is understandable since the Al is added in pure form, not in a binary selenide and at higher temperature In and Se are vaporized faster. Further selenization process can be employed to achieve complete stoichiometric composition of CIAS films. The average amount of Cu in the films is

27 at-%, which seems relatively high compared to the one reported by Marsillac, et.al. (around 23.5 at-%) [2]. This can be anticipated by adjusting the CuSe/InSe ratio in the target as the sputtering yield of Cu is higher than In.

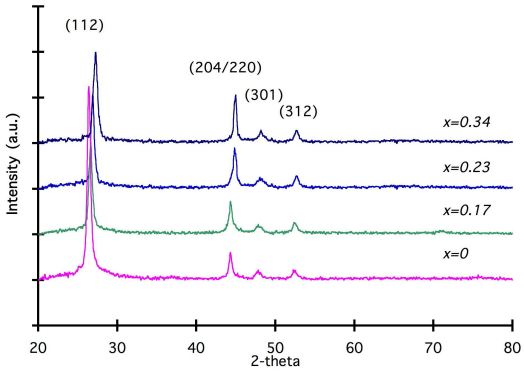

Fig. 2. XRD spectra of films at different Al contents and deposition temperatures

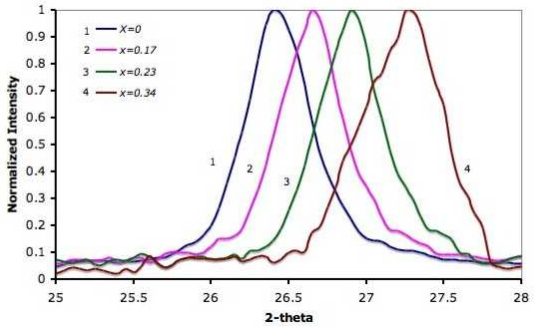

Fig. 3 Normalized XRD spectra showing the shift of (112) peak with the increase of Al content in CIAS films.

The XRD spectra analysis for CIAS films is shown in Fig 2. All of the films shows strong CIS peaks, mainly shown by (112), (204/220) and (312) orientations. From the spectra, the films were found to be single phase and polycrystalline chalcopyrite structure. Compared to RT deposition, the heating of substrate during film deposition led to increasing crystallinity of the films. One specific feature was the growth of (301) orientation at higher substrate temperature, which could not be seen in CIS film grown without intentional substrate heating. As shown in Fig 3, the addition of Al in the films shifts (112) peaks towards higher 2θ, as previously reported by Itoh, et.al. (1998) and Paulson, et.al. (2002). This is an indication that can result in higher band gap as the lattice constant of the films decreased [3,4].

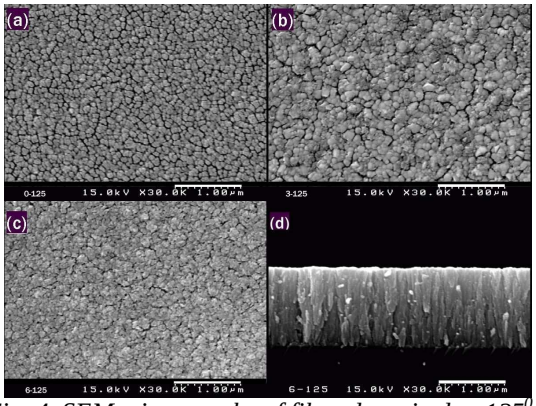

Fig. 4. SEM micrographs of films deposited at 125^{0}C (a) CIAS-0 (b) CIAS-3 (c) CIAS-6 (d) cross section of CIAS-6

Fig. 4 depicts surface morphology and cross section of the films showing relatively smooth surfaces with an increase in the grain size along the addition of Al. Compared to films produced via co-evaporation or two-stage process (i.e. by precursors deposition and selenization), films produced by one-step sputtering deposition method have smaller grain size which is understandable as deposition took places at lower temperature and due to the nature of sputtering process.

Further annealing and/or selenization process may be employed to improve the grain size and the stoichiometry of Se in the films. There is no sign of secondary phase presences in the surface as confirmed by XRD analysis. All of the films show uniform and columnar grains as clearly represented in Fig. 3d. Columnar structure is preferred and necessary to facilitate current transport across the films. A rather densely packed microstructure free of pinholes and micro-cracks were also observed from the cross section image. Generally, all of the films show strong adhesion to the substrates, which highlights the advantage of sputtering deposition over two-step process.

The transmittance spectra of the films were determined by UV-Vis spectrophotometer in the range 400-2500 nm wavelength. The optical band gap is determined from the transmission spectra correspond to the equation:

$$\alpha = A (h\nu - E_g)^n / h\nu \qquad (1)$$

where A is a constant (which is equal to about 10^5 $cm^{-1}eV^{-1}$ at n=2). The exponent n (usually 1/2 ~ 3) depends on the nature of the optical transition whether direct allowed, direct forbidden, indirect allowed or indirect forbidden, respectively Film

without addition of Al shows 1.05*eV* optical band gap, while films with Al addition yield 1.35*eV* for CIAS-3, 1.55*eV* for CIAS-6 and 1.75*eV* for CIAS-10 respectively. These values are in good agreement with optical band gap of CIAS films produced by co-evaporation method as by Paulson, et al. and Reddy, et.al. [3,8].

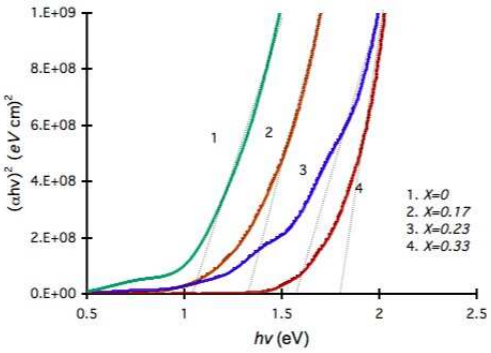

Fig. 5 Projected optical band gap of CIAS films.

IV. CONCLUSION

P-type $Cu(In_{1-x}Al_x)Se_2$ thin films with Al content x=0, 0.17 and 0.34 were deposited on glass substrates using one-step deposition by RF magnetron sputtering at 125^0C. Films with good substrate adhesion, smooth surfaces, columnar structure and free from secondary phases were grown successfully. The films were found to be near stoichiometry, single phase and polycrystalline with chalcopyrite structure, dominated by strong (112) and (204/220) chalcopyrite orientation peaks. As the Al content in the film increases from 0 to 34 at-%, the optical band gap of the films were estimated to be in the range 1.05 ~ 1.75*eV*, which is suitable for applications as an absorber layer in solar cells.

REFERENCES

[1] M. A. Contreras, K. Ramanathan, J. AbuShama, F. Hasoon, D.L. Young, B. Egaas and R. Noufi; Prog. Photovolt: Res. Appl. 2005:13 209-216

[2] S. Marsillac, P.D. Paulson, M.W. Haimbodi, R.W. Birkmire and W. Shafarman; Appl. Phys. Letters 81 No. 7 (2002) 1350-1352

[3] P.D. Paulson, M.W. Haimbodi, S. Marsillac, R.W. Birkmire and W. Shafarman; J. Appl. Phys. 91 No. 12 (2002) 10153-10156

[4] F. Itoh, O. Saitoh, M. Kita, H. Nagamori, H. Oike, Sol. Energy Mater. Sol. Cells 50 (1998) 119-125

[5] K.T.Ramakrishna Reddy, I. Forbes, R.W. Miles, M.J. Carter, P.K. Dutta; Materials Letters 37 (1998) 57-62

[6] A. Brummer, V. Honkimaki, P. Berwian, V. Probst, J. Palm, R. Hock; Thin Solid Films 437 (2003) 297-307

[7] B. Munir, R.A. Wibowo, E.S. Lee and K.H. Kim; in Proceedings of the IUMRS-ICA-2006 (2006)

[8] Y. Bharath Kumar Reddy, V. Sundara Raja, Physica B 381 (2006) 76–81

ISSN: 1411-1284

Amorphous TiO_2–PMMA nanohybrids thin films of highly ordered TiO_2 nanoparticle arrays in PMMA matrix and a novel technique to enhance its nanocrystallinity

A.H.Yuwono [1], Y. Zhang [2], B.H. Liu [2], Ji Wei [3], John Wang [2]

[1]Department of Metallury and Materials Engineering, Faculty of Engineering, University of Indonesia, Indonesia.

[2] Department of Materials Science and Engineering, Faculty of Engineering, National University of Singapore, Singapore

[3] Department of Physics, Faculty of Science, National University of Singapore, Singapore

Email: ahyuwono@metal.ui.ac.id

Abstract– **A systematic investigation has been conducted into TiO_2−PMMA nanohybrid thin film derived from copolymer templating, aimed at understanding the mechanisms responsible for the occurrence of the largely amorphous TiO_2 nanoparticles, which cannot be avoided under the conditions tolerable by the polymer matrix. While the assembling by copolymer templating leads to a highly organized nanostructure, the largely amorphous TiO_2 state is shown to relate to the fast development of stiff Ti–OH networks during hydrolysis and condensation, assisted by the entrapment of the rigid polymer matrix. A post-hydrothermal treatment involving high-pressure water vapor has been successfully devised to enhance the nanocrystallinity of TiO_2 nanoparticles.**

Keywords– Nanohybrids, TiO_2 nanoparticles, Enhanced Nanocrystallinity.

I. INTRODUCTION

Functional nanohybrid thin films consisting of inorganic nanoparticles in polymer matrix promise several potential applications in optoelectronic devices [1]. For instance, nonlinear optical switching devices in photonics and real-time coherent optical signal processors would benefit from the development of fast, low optical loss materials with large values of third-order nonlinear susceptibility,$\chi^{(3)}$ [2]. Our previous study has shown that titania-poly(methylmethacrylate) or TiO_2–PMMA nanohybrids derived from *in-situ* sol-gel polymerization route can fulfill such requirements since they exhibit a very fast recovery time of ~1.5 picoseconds and large optical nonlinearities up to 1.93 x 10^{-9} esu [3,4]. However, the condensation reaction of hydrolyzed TiO_2 precursors involved in the *in situ* sol–gel polymerization takes place in random locations in the amorphous polymer matrix, leading to a lack of uniformity in the inorganic-organic nanostructures. It is therefore of considerable interest to synthesize nanohybrid thin films of highly ordered TiO_2 nanoparticle arrays in PMMA. To realize the structure, a diblock copolymer consisting of hydrophobic PMMA and hydrophilic PEO domains is considered as an appropriate template. However, a desired micellization cannot be easily obtained by simply dissolving PMMA−PEO diblock copolymer in tetrahydrofuran (THF), toluene and acetone. This is mainly due to the strongly swollen PMMA chains of high mobility in these commonly available solvents. Therefore, the present work is firstly aimed at investigating into suitable solvating medium and templating conditions leading to the formation of the desired nanostructure arrays. Moreover, our further concern is to enhance the nanocrystallinity of TiO_2 phase and maintain the integrity of polymer matrix in the resulting nanohybrids.

II. EXPERIMENTAL PROCEDURE

The synthesis process involves the dissolution of PMMA−PEO block copolymer ((Polymer Sources Inc; M_n PMMA: PEO = 1700: 3500 g/mol and polydispersity of 1.1) in a mixture of deionized water and THF (99%, Acros), followed by incorporation of titanium tetra-isopropoxide (TTIP, 98%, Acros) into hydrophilic PEO sites. Vigorous stirring for 24 hours was conducted to complete the dissolution of the precursors, resulting in a yellowish transparent solution. The nanostructure of the resulting nanohybrids was studied by using a high-resolution transmission electron microscope (HRTEM, JEOL−3010, operated at 300 keV and with a resolution of 0.14 nm). TEM samples for investigation were prepared by dropping a

small amount of the solution onto a carbon-coated copper grid placed on tissue paper, leaving behind a thin film on the copper grid which was then annealed at desired temperature, heating rate and holding time.

III. EXPERIMENTAL RESULTS

Solution modification. One of the preliminary concerns in this project is to find a suitable solvent enabling the use of PMMA−PEO diblock copolymer as a template for the formation of TiO_2 nanoparticles. The desired micellization was realized when dissolving this diblock copolymer in a modified mixture solvent containing deionized water and THF in a proportional volume ratio of 50%. This is in a good agreement with results of small-angle neutron scattering (SANS) studies by Edelmann and coworkers [5] who demonstrated that a synergistic micellization among PMMA−PEO chains can be obtained when a large amount of water (~40−60 vol %) was involved. This is due to the reduced swelling and thus reduced mobility of PMMA, together with an increase in PEO mobility. We observed that an acidic environment is essential for stabilizing TTIP due to its highly water-sensitive nature and susceptibility to a premature macro-precipitation. On the basis of this consideration, it is of further interest to obtain an optimum processing condition by adjusting the pH value of solution. Figures 1a and 1b show TEM images for nanohybrid thin films on the carbon-coated copper grid, derived from dissolution of PMMA−PEO diblock copolymer in 50 vol % THF and 50 vol % water at pH values of 1.20 and 0.33, respectively. Prior to TEM investigation, both films were annealed in air at 150 ^{o}C for 48 hours at a heating rate of 1 ^{o}C/min. It is apparently seen that nanohybrid derived from solution at the pH value of 1.20 (Fig. 1a) consists of clusters of titania particles formed outside the spherical PMMA domains. Although the onset of arrangement had been shown, however, there existed locations where the titania nanoparticles were distributed rather unevenly. This suggests that, at a high water content of 50 vol %, which is in fact essential for micellization, the concentration of HCl in the solution was insufficient for a complete protonation on titanium alkoxide, resulting in so called micro-aggregates to occur. The average size of these aggregates was estimated to be 9 $\pm$ 1.5 nm. By contrast, the nanohybrid derived from solution at the pH value of 0.33 shows no particle aggregation (Fig. 1b). The film provides a highly dense and much more regular structure consisting of hexagonal-like arrays of PMMA cores and very fine titania nanoparticles of less than 2 nm in size. The inorganic phase creates an interconnected network rather than discrete nanoparticles (shown as darker areas in the inset of Fig 1b).

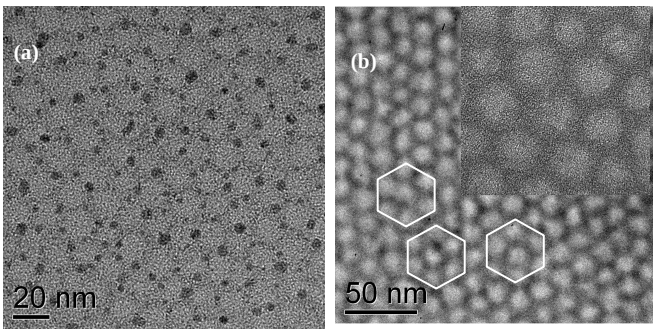

Fig 1. TEM micrographs of the nanohybrid thin films, containing titania nanoparticles derived from dissolution of PMMA−PEO diblock copolymer in 50 THF vol % and 50 vol % water at the pH value of (a) 1.20 and (b) 0.33, respectively.

X-ray diffraction for phase identification performed on the thin films coated on glass/quartz substrates did not show any noticeable peaks for titania in the 2θ angle of 20−70^{o}. This indicates that the nanocrystallinity of these fine TiO_2 nanoparticles is of short-range order. Therefore, further confirmation on the nanocrystallinity of titania nanoparticles was provided by Raman spectroscopy, as shown in Fig. 2.

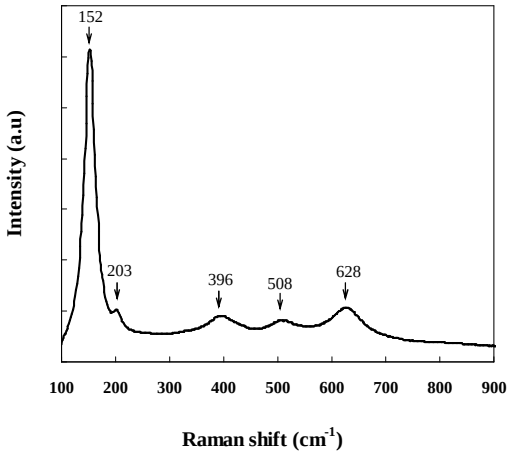

Fig. 2. Raman spectroscopic spectrum of the nanohybrid thin film containing titania nanoparticle arrays in PMMA matrix, derived from the solution with water content of 50%v and pH 1.20.

A considerably intense peak at 152 cm^{-1} is shown for the nanohybrid thin film, followed by four weak peaks at 203, 396, 508 and 628 cm^{-1}, respectively. The first two and fifth peaks are in agreement with the E_g Raman active mode of anatase phase (144, 197 and 639 cm^{-1}), while the third and fourth peaks can be assigned to the B_{1g} and A_{1g} or B_{1g} modes (399 and 513 or 519 cm^{-1}), respectively [6]. On the one hand, the well-resolved peak of the E_g mode at 152 cm^{-1} arises from the external vibration of anatase structure [7],

confirming that fine anatase crystallites have indeed been formed in the nanohybrid structure. On the other hand, the intrinsically weak peak at 203 cm^{-1} and the broad bands at 396, 508 and 628 cm^{-1} agree with what has been shown by the XRD phase analysis, *i.e.*, the crystallinity of the fine anatase particles is of short range. There is also a shift in wavenumber of the E_g mode to 152 cm^{-1}, with a broadened full width at half-maximum (FWHM) of 24 cm^{-1}, in comparison to 144 cm^{-1} and 7 cm^{-1} in line width for single crystal anatase [7,8].

Post-hydrothermal treatment. Concerning the lack of nanocrystallinity for the TiO_2 nanoparticles assembled in a polymer matrix, Brinker *et al.* [9] and Langlet *et al.* [10] have suggested that the largely amorphous nature is related to the high functionality of the titanium alkoxide precursor favoring the fast development of a stiff Ti–O–Ti network via condensation. In this connection, further studies by Matsuda *et al.* [11] and Kotani *et al.* [12] suggested that structural changes in the TiO_2 thin films derived from sol-gel process could be induced by the treatment in a high humidity environment at temperatures above 100 ^oC. Further investigation by Imai *et al.* [13,14] confirmed that the exposure of sol-gel derived TiO_2 films to water vapor triggered rearrangement of Ti–O–Ti network leading to formation of anatase phase at relatively low temperature (180 ^oC). On the basis of this understanding, we have investigated the feasibility of enhancing the nanocrystallinity of TiO_2 phase assembled by diblock copolymer templating by a post hydrothermal process. For this purpose, the thin films spin-coated on glass substrates were first annealed at 150 ^oC for 48 hours, and then exposed to the treatment by high pressure water vapor in a Teflon-line stainless steel autoclave (Parr, Moline, Illinois) at 150^oC for 24 hours. A specially designed stand was placed inside the Teflon tube in order to prevent the samples from direct contact with liquid water. A high magnification TEM micrograph for the post-hydrothermally treated film is given in Fig. 3a. The film clearly shows crystallites with well-established lattice fringe. The *d*-spacing of the lattice fringe is measured to be 0.352 $\pm$ 0.008 nm, which is in good agreement with the *d*-value of the (101) crystal plane in anatase titania. According to Imai's model [13,14], the enhancement in TiO_2 crystallinity involves the cleavage of strained Ti–O–Ti bonds by water molecules, resulting in the formation of much more flexible Ti–OH leading to the rearrangement and densification of Ti–O–Ti bonds. As a consequence of the crystallite growth, the well organized arrays of individual core-corona structures in the hexagonal-like configuration have undergone some re-arrangement. However, when observed at low magnification (Fig. 3b), it is obviously seen that the orderly arrangement by diblock copolymer templating can be maintained at large scales, where the TiO_2 nanocrystallites are dispersed quite uniformly in the polymer matrix. This suggests that under a well controlled post-hydrothermal treatment condition, it would be possible to obtain nanohybrid thin film containing highly ordered arrays of TiO_2 nanoparticles in the hexagonal-like configuration, while at the same time they are of enhanced crystallinity.

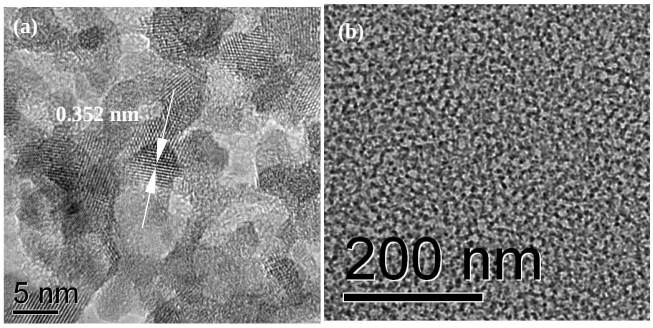

Fig. 3. TEM micrographs of the nanohybrid thin film containing titania nanoparticle arrays derived from the solution with water content of 50 vol % and pH 0.33 upon post-hydrothermal treatment showing (a) well-dispersion of TiO_2 nanocrystallites in the PMMA matrix and (b) well-established lattice fringe in the crystallites.

Figs. 4a and 4b show the high resolution XPS spectra of O1s region for the conventionally annealed and post-hydrothermally treated nanohybrid samples, TEM micrographs of which have been shown in Figures 1b and 2a, respectively. Both spectra demonstrate broad and asymmetric signals ranging from ~526 to 536 eV indicating the coexistence of different chemical environments on the titania nanoparticle surfaces. Each spectrum can be fitted into three peaks located at ~ 529.5-530, 531.5 $\pm$ 0.5, 533 $\pm$ 1 eV, attributed to oxygen in the metal oxide component (*i.e.* O^{2-} bound to Ti^{4+} in TiO_2 lattice), oxygen in the hydroxyl groups (–OH) or defective oxides, and physisorbed or chemisorbed molecular water, respectively [15]. The last two species are mainly associated with the TiO_2 surfaces. In the conventionally annealed sample (Fig. 4a), the estimated area percentage under the metal oxide peak was ~23.0%, which is considerably lower than that of the hydroxyl groups/defective oxides (~63.5%). This is in agreement with the fact that the TiO_2 phase in this sample is still largely amorphous, as has been shown by the XRD and TEM studies. Due to the strained characteristics of Ti–O–Ti bonds contained in the hydroxyl groups as well as non-stoichiometric nature of the defective oxides, a retardation towards formation of a well crystallized TiO_2 phase is therefore expected. On the other hand, when the hydrothermal treatment was applied to the thin film sample, the percentage of metal oxide peak increases significantly up to ~49.0%, accompanied by a decrease in the hydroxyl-defective oxides peak down to ~42.3% (Fig. 4b). This confirms the effectiveness of high pressure water vapor in converting the surface states of TiO_2 nanoparticles to less-defective ones, promoting the crystallinity. Similar results on the role of water vapor in removing the surface defects

have been reported for bulk TiO_2 (110) surfaces by Wang *et al*. [16]. It is also observed that there occurs a reduction of chemisorbed water content from 13.5% to 8.7%, which is believed to be a consequence of the involvement of water molecules in the cleavage of the strained Ti–O–Ti bonds and their rearrangements into nanocrystalline TiO_2 phase.

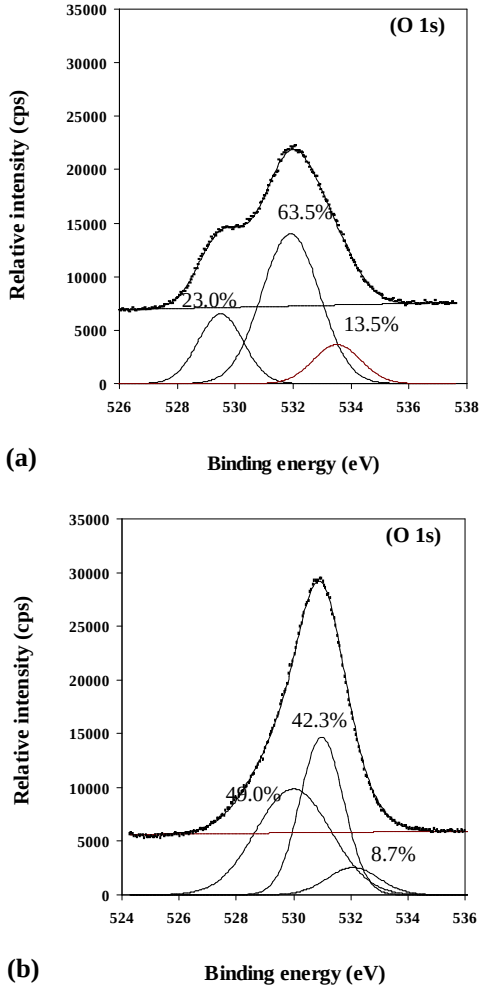

Fig. 4. XPS high resolution O 1s spectra of (a) the conventionally annealed and (b) the post-hydrothermally treated nanohybrid thin films containing titania nanoparticle arrays in PMMA matrix, derived from the solution with water content of 50 vol % and pH 0.33.

Further confirmation on the post-hydrothermal treatment in promoting the nanocrystallinity of nanohybrid film is given by FTIR results in Fig. 5. The hydroxyl groups of Ti–OH in the spectra of the conventionally annealed and post-hydrothermally treated samples are observed as a broad absorption band in the range of ~3400–3500 cm^{-1} [17], while the characteristic peak for TiO_2 phase is indicated by a vibration band of Ti–O–Ti groups at 900–400 cm^{-1} [18]. Apparently, the conventionally annealed thin film shows a more intense Ti–OH band than that of the post-hydrothermally treated sample, while on the other hand the latter demonstrates a stronger intensity for Ti–O–Ti band than the former. This is consistent with the results of TEM and XPS studies, showing that the post-hydrothermally treated sample exhibits an enhanced nanocrystallinity of TiO_2 phase.

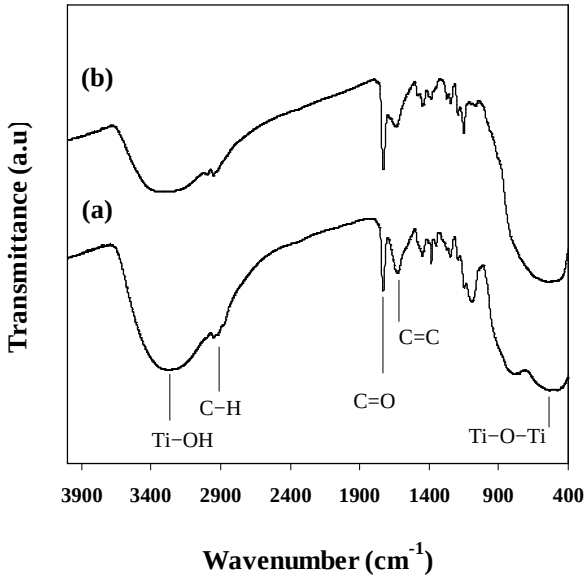

Fig. 5. FTIR spectra of (a) the conventionally annealed and (b) the hydrothermally treated nanohybrid thin films, derived from the solution with water content of 50 vol % and pH 0.33.

From the surface profiler measurement, it was observed that there was a change in film thickness. It was initially 36 nm for the conventionally annealed sample, while the post-hydrothermal treatment reduced it to 24 nm upon. This indicates that part of the film surface has been leached out by the water molecules at high vapor pressure. On the other hand, however, it was also observed that the stretching vibration bands of C=O and C–H in the PMMA segments at 1730 and 2950 cm^{-1} on both samples are almost the same in intensity. It suggests therefore that the internal integrity of the polymer chains in the PMMA matrix is successfully retained. A longer duration (48 hours) for the initial conventional annealing prior to hydrothermal treatment was able to stabilize the polymer chains in the nanohybrid thin film.

IV. CONCLUSIONS

A solvent modification has been successfully performed for enabling the use of PMMA–PEO diblock copolymer as a template for synthesizing nanohybrid thin film containing

highly ordered arrays of TiO_2 nanoparticles in PMMA matrix. A mixture solvent consisting of 50 vol % water in THF, maintained at a pH level of 0.33 is the appropriate condition for micellization of the block copolymer. This gave rise to a nanohybrid thin film consisting of PMMA domains in highly ordered arrays of hexagonal-like configuration surrounded by very fine titania nanoparticles of ~2 nm in size. Raman spectroscopy confirms the formation of anatase as the predominant inorganic phase in the nanohybrid, although the crystallinity of these fine anatase particles is of short range. The low nanocrystallinity of anatase phase is due to the occurrence of stiff Ti−O−Ti networks which cannot further dense into nanocrystalline TiO_2 phase. A post-hydrothermal treatment in high pressure water vapor significantly enhances the crystallinity of TiO_2 nanoparticles. This involves the cleavage of strained Ti–O–Ti bonds by water molecules, resulting in the formation of much more flexible Ti–OH leading to the rearrangement and densification of Ti–O–Ti bonds. By properly controlling the post-hydrothermal parameters including temperature and time, nanocrystalline TiO_2 dots in well preserved configuration promise for enhanced properties in optoelectronic applications.

REFERENCES

1. B. Wang, G.L. Wilkes, J.C. Hedrick, S.C. Liptak, and J.E. McGrath**,** *Macromolecules*, Vol 24, pp 3449-3450, 1991.
2. G.L. Fischer, R.W. Boyd, R.J. Gehr, S.A. Jenekhe, J.A. Osaheni, J.E. Sipe, and L.A.Weller-Brophy, *Phy.s Rev. Lett.*, Vol 74 (10), pp 1871-1874, 1995.
3. A.H. Yuwono, J.M. Xue, J. Wang, H.I. Elim, W. Ji, Y. Li, and T.J. White, *J. Mater. Chem.*, Vol 13**,** pp 1475-1479, 2003.
4. H.I. Elim, W. Ji, A.H. Yuwono, J.M. Xue, and J. Wang, *Appl. Phy.s Lett.*, Vol 82 (16), pp 2691-2693, 2003.
5. K. Edelmann, M. Janich, E. Hoinkis, W. Pyckhout-Hintzen, and S. Höring, *Macromol. Chem. Phys.*, Vol 202 (9), pp 1638-1644, 2001.
6. H.C. Choi, Y.M. Jung, and S.B. Kim, *Vibrational Spectroscopy*, Vol 37, pp 33, 2005.
7. W.F. Zhang, Y.L. He, M.S.Zhang, Z. Yin, and Q.Chen, *J. Phys. D : Appl. Phys*., Vol 33, pp 912, 2000.
8. D. Bersani, P.P.Lottici, and X.Z. Ding, *App. Phys.Lett*., Vol 72, 73, 1998.
9. C.J. Brinker and A.J. Hurd, *J. Phys. III France*, Vol 4**,** pp 1231-1242, 1994.
10. M. Langlet, M. Burgos, C. Couthier, C. Jimenez, C. Morant, and M. Manso, *J. Sol-Gel Sci Technol.*, Vol 22 (1-2), pp 139-150, 2001.
11. A.Matsuda, Y. Kotani, T.Kogure, M. Tatsumisago, and T.Minami, *J. Am. Ceram. Soc*., Vol 83 (1), pp 229, 2000.
12. Y.Kotani, A.Matsuda, T.Kogure, M.Tatsumisago, and T. Minami, *Chem. Mat*., Vol 13, pp 2144, 2001.
13. H. Imai and H. Hirashima, *J. Am. Ceram. Soc*., Vol 82 (9), pp 2301-2304, 1999.
14. H. Imai, H. Moromoto, A. Tominaga, and H. Hirashima, *J. Sol-Gel Sci. Technol.*, Vol 10, pp 45-54, 1997.
15. R. Sanjines, H. Tang, H. Berger, F. Gozzo, G. Margaritondo, and F. Levy, *J. App. Phys.*, Vol 75 (6), pp 2945-2951, 1994.
16. L.Q. Wang, D.R; Baer, M.H. Engelhard, and A.N Shulz,. *Surf. Sci*., Vol 344, pp 237, 1995.
17. L.H. Lee and W.C. Chen, *Chem. Mater.*, Vol 13 (3), pp 1137-1142, 2001.
18. S.X. Wang, M.T.Wang, Y. Lei, and L.D. Zhang, *J. Mater. Sci. Lett*., Vol 18, pp 2009, 1999.

ISSN: 1411-1284

Deposition of SnO_2 Tansparent Conducting Oxide Films and Their Characterization

Dwi Bayuwati and Syuhada

Research Centre for Physics, Indonesian Institute of Science
(Pusat Penelitian Fisika-LIPI),
Kawasan Puspiptek Serpong, Tangerang 15314
Tel. 021-7560-556/570, fax. 021-7560-554 email : dwitomi@cbn.net.id

Abstract– **We present the deposition of transparent conducting oxide (TCO) films using ultrasonic spray pyrolysis technique. Several SnO_2-TCO films on glass substrate have been deposited at various temperatures and spray time using $SnCl_4.5H_2O$ solution as precursor and N_2 as carrier gas. The deposition temperature was varied from 300°C to 370°C and the deposition time was from 8 minutes. The optical, electrical and structural properties of the SnO_2 - TCO films were investigated. From optical spectrometer, we obtained that the films are quite high transparent (>70%) in visible ranges. The electrical properties measurement with four point probe showed that these films behave as n-type semiconductors with resistivity value of about 1.402 x 10^{-2} Ω-cm. Structural examination using SEM shows mean grain size of 0.5 um. The XRD study confirms the formation of polycrystalline phase of SnO_2 film and the degradation of crystallographic phases at lower temperature.**

Keywords– SnO_2, transparent conducting oxide.

I. INTRODUCTION

Transparent conducting oxide (TCO) plays important role in silicon substrate based thin film as well as other thin films solar cells [1]. Ideally, it is highly conductive and transparent to visible light and also reflects infrared radiation; to make them applicable as energy conserving heat reflective coatings on windows and as one of transparent surface electrodes for solar cells. Several TCO materials have been developed for solar cells for example Indium Tin Oxide (ITO), Tin Oxide (SnO_2) dan Zinc Oxide (ZnO) [1-4]. Various methods have been used to prepare the TCO thin film such as e-beam and vacuum evaporation, RF and DC sputtering, laser pulse ablation, chemical vapour deposition, spray pyrolisis and so on [1-4]. In this paper, we use ultrasonic spray pyrolysis technique because of its simplicity in operation and low investation (compared with other techniques mentioned before), and less pressure also less overspray with unclog nozzle (compared with ordinary spray pyrolysis technique). In this technique, ultrasonic wave is generated from an ultrasonic fogger to vibrate and break the reactant solution into fog to be sprayed to the substrate at certain temperature and time deposition. Several Tin Oxide/SnO_2 films on glass substrate - TCO have been deposited at various temperatures and spray time using $SnCl_4.5H_2O$ solution as precursor and N_2 as carrier gas. The optical, electrical and structural properties of the SnO_2 - TCO films were investigated using optical spectrometer, four point probe; x-ray diffractometer/XRD and scanning electron microscope/SEM; respectively.

II. EXPERIMENTAL DETAILS

The deposition set up as shown in Figure 1, consists of of an ultrasonic generator and a pyrolysis region. The pyrosol generator includes a pot containing the solution reactant which is to be nebulized by an ultrasonic fogger (piezoelectric crystal) which is immersed on it [4,5].

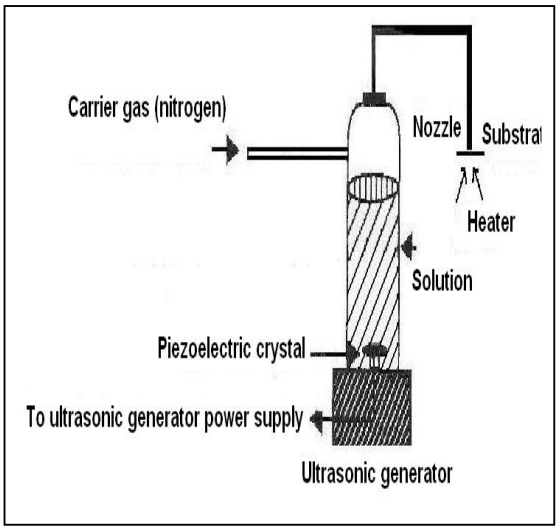

Fig.1. The TCO deposition set-up [4].

The solution reactant is nebulized by ultrasonic foggers to be fog. The fog formed in the pot was carried out by a carrier gas (nitrogen) to react with a heated substrate in the furnace or heater area via a glass nozzle.

The solution reactant consists of the mixture of ($SnCl_4.5H_2O$ + alcoholic liquid + H_2O) with Fluorine as the dopant. Before the deposition process, the solution reactant was first nebulized for 30 minutes to form homogeneous fogs. The deposition process was conducted in a chamber with an exhaust system to blow out the unnecessary gas.

The tin oxide layer will be formed on the glass substrate according to the chemical reactions [4]. The first stage of chemical reaction for the mixed solution is as bellows [4]:

$$SnCl_4.5H_2O + 2CH_3OH \rightarrow SnCl_4.2CH_3OH + 5H_2O \quad (1)$$

$SnCl_4.5H_2O$ complexes transform into $SnCl_4$ according to the following reaction:

$$SnCl_4.2CH_3OH \rightarrow SnCl_4 + 2CH_3OH \quad \ldots\ldots\ldots\ldots (2)$$

The following reaction takes place on the substrate surface:

$$SnCl_4 + H_2O \rightarrow SnO_2 + 4HCl \quad \ldots\ldots\ldots\ldots (3)$$

Before the deposition process, the glass substrate (microscope glass slides) was first cleaned with alcohol liquid and deionized water and then dried using nitrogen gas. The deposition process was conducted at temperature 300-370^{0}C and deposition time 8 minutes. The nitrogen gas flow was kept constant at about 300ml/minute.

The quality of the formed layer depends on particle size, temperature and time deposition and also on the nitrogen gas flow. The velocity of the formed films can be expressed as [6]:

$$V_f = k_g [SnCl_4] B (g) \ldots. (4)$$

where g = gas phase, k_g = mass transport coefficient and $[SnCl_4]$ B (g) is concentration of $SnCl_4$ at vapor phase. The mean of fog particle size can be expressed as [7]:

$$d_a = 0.73 \sqrt[3]{\frac{T}{\rho f^2}} \quad (5)$$

where T is surface pressure, ρ liquid density and f frequency of ultrasonic fogger.

The TCO films were characterized on its electrical and optical properties using four point probe and optical spectrometer, respectively. The measured electrical properties are resistivity and semiconductor type of the deposited films. For optical measurement, we only examine the transmission curve of the samples at visible range. All these measurement were done at room temperature. The crystal structure was examined using XRD and surface morphology was studied using SEM.

III. EXPERIMENTAL RESULTS

3.1. Optical characterization.

Using JASCO V-570 optical spectrometer, we measured the transmission spectral response of the SnO_2-TCO films at wavelength range of 200-800 nm, for films with various experimental conditions. The experimental conditions (T_d=deposition temperature and t=deposition time) of each samples are: sample G1(T_d=300^{0}C, t=8 minutes), G2 (T_d=350^{0}C, t=8 minutes) and G4 (T_d=370^{0}C, t=8 minutes). The TCOs are quite high transparent (>70%) in visible ranges as shown in Figure 2.

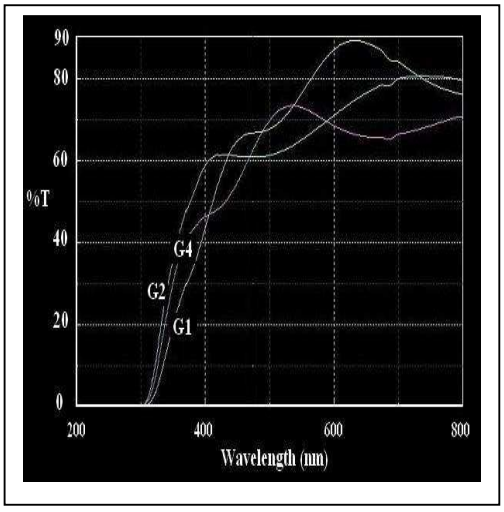

Fig.2. The optical transmission spectra of SnO_2 TCO layer.

3.2. Electrical characterization.

The electrical properties measurement with four point probe showed that these films behave as n-type semiconductors with resistivity value in the order of about 1.402 x 10^{-2} Ω-cm. This value is good enough but for solar cell application a reduction of resistivity into order of 10^{-3} Ω-cm will result in better solar cell efficiency.

3.3. Structural characterization.

Structural behavior of the SnO_2-TCO films on glass substrate has been studied with x-ray diffractometer for the G1, G2 and G4 glass samples. The XRD study confirms the formation of polycrystalline phase of SnO2 film at deposition temperature > 300^0 C and shows the degradation of crystallographic phases at lower temperature as shown in Figure 3, Figure 4 and Figure 5.

The amorphous phase was seen from the XRD curve of SnO2-TCO deposited at 300^0 C with deposition time 8 minutes (see Figure 3). At this temperature, the preheating of the fog is not sufficient and it remains wet. At Figure 4 and Figure 5, we can see that the deposited films started to form polycrystalline structure. At this temperature (>300^0 C), the

preheating is enhanced and chemical reaction occur as SnO_2 is generated near the substrate. The higher temperature the degree of crystalline is rising.

Better crystal grade will be seen at higher temperature but not exceed 550 ^{0}C, because there will be loss of carrier density at the grain boundary and the possibility of the diffusion of the impurities from the substrate [3].

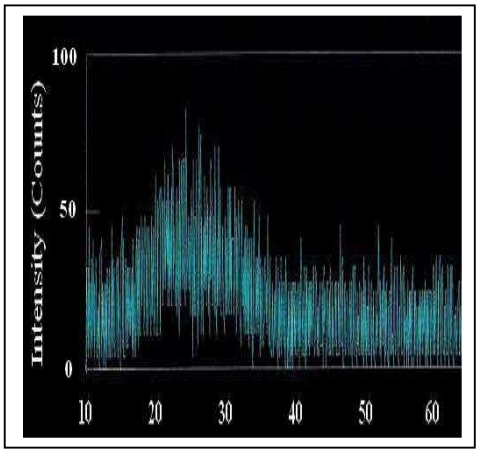

Fig.3. The XRD curve of SnO_2 TCO film at T_d=300^{0}C and t= 8 minutes.

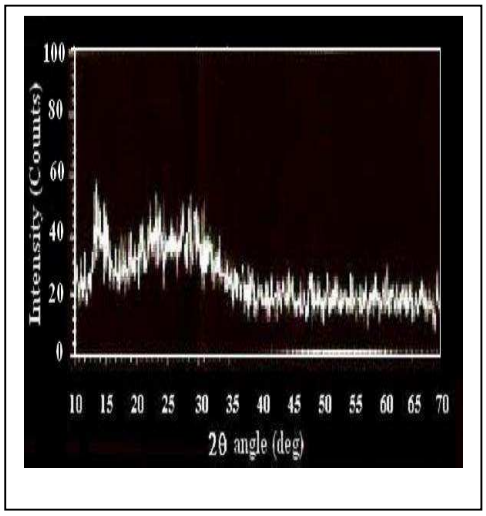

Fig.4. The XRD curve of SnO_2 TCO film at T_d=350^{0}C and t= 8 minut

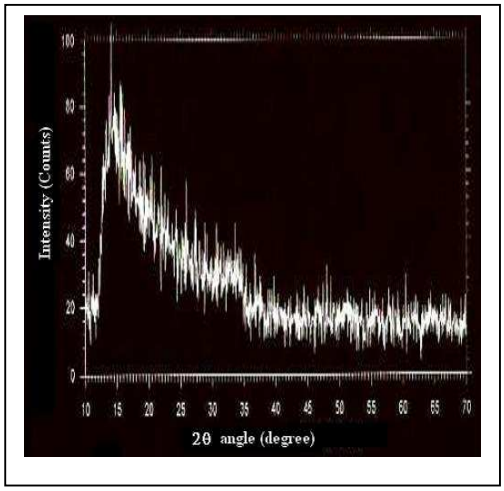

Fig.5. The XRD curve of SnO_2 TCO film at T_d=370^{0}C and t= 8 minutes.

3.4. Morphology characterization.

Examination of surface morphology using SEM shows mean grain size of about 0.5 um as can be seen in Figure 6, for G4 sample. We only present the SEM image for G4 sample because there was no noted difference in form and size of the grain at various selected temperature mentioned before because the temperature variation range is not wide enough; caused by the limited availability of the heater provided.

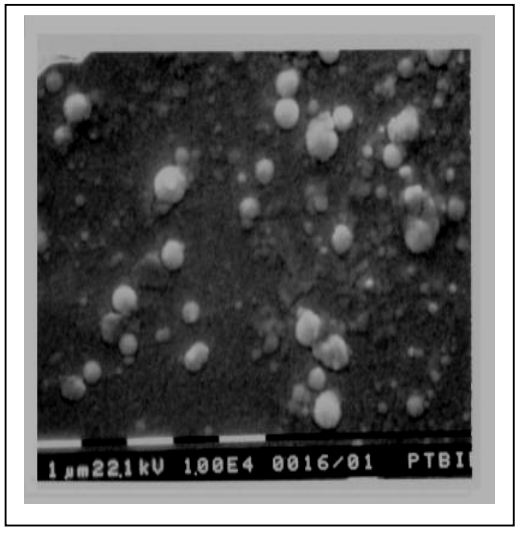

Fig.6. The surface morphology of the SnO_2 TCO film.

Based on these results, we conclude that to get high quality of TCO films, we need to optimize the temperature and time of deposition as well as the flow

of the carrier gas. The thickness of the films should also been studied by varying the deposition time. The choosen range of temperature variation was not wide enough to study the degree of crystallinity as well as the morphology of the films. The precursor solution should also be investigated for example by varying the concentration of the starting solution ($SnCl_4.5H_2O$, alcoholic liquid and H_2O); because it also affects the properties and morphology of the deposited films.

IV. CONCLUSIONS

The deposition of transparent conducting oxide (TCO) using ultrasonic spray pyrolysis technique has been described. Several SnO_2–TCO films on glass substrate have been deposited using $SnCl_4.5H_2O$ solution as precursor and N_2 as carrier gas.

From optical spectrometer measurement, we obtained that the films are quite high transparent (>70%) in visible ranges.

The electrical properties measurement with four point probe showed that these films behave as n-type semiconductors with resistivity value of about 1.402 x 10^{-2} Ω-cm.

Structural examination using SEM shows mean grain size of about 0.5 um and no noted difference in form and size for all samples deposited at different deposition temperature (300-370^{0}C).

The XRD study confirms the formation of polycrystalline phase of SnO_2 film at temperature > 300 ^{0}C and shows the degradation of crystallographic phases at lower temperature.

In conclusion, we still need to find the optimum characteristics of the SnO_2-TCO films, to get high transmission spectra in visible range with good crystalline phase and low resistivity value to get best performance of the TCO for solar cell application.

To get high quality of TCO films, we need to optimize the temperature and time of deposition as well as the flow of the carrier gas. The temperature variation should be wide enough, if possible until about 550^{0}C. The precursor solution should also be investigated because it also affect the properties and morphology of the deposited films.

Several improvement in experimental set-up is being conducted to have a stable high temperature heater and homogen-output spray-nozzle system.

ACKNOWLEDGEMENT

The authors would like to acknowledge Research Centre for Physics – Indonesian Institute of Science (Pusat Penelitian Fisika-LIPI) for funding the research.

REFERENCES

[1] S. Shanthi, et. al., "Effect of Fluorine Doping on Structural, Electrical and Optical Properties of Sprayed SnO_2 Thin Films", Journal of Crystal Growth 194, 1998, 369-373.

[2] Z.B. Zhou et. al., "Preparation of Indium Tin Oxide Films and doped Tin Oxide Films by an Ultrasonic Spray CVD Process", Applied Surface Science, Vol. 172, 2001, 242-252.

[3] D. Zaouk et. al., "Fabrication of Tin Oxide (SnO_2) Thin Film by Electrostastic Spray Pyrolysis", Microelectronic Engineering, Vol. 51-51, 2000, 627-631.

[4] J. Dutta, J. Perrin, T. Emeraud, J.M. Laurent, A. Smith, "Pyrosol Deposition of Fluorine-doped tin dioxide thin films", Journal of Material Science, Vol. 30, 1995, 53-62.

[5] http://www.infoscantech.com/support/fogger1.html

[6] B. Correa-Lozano, C.H. Comninellis, A De Battisti, "Preparation of SnO_2-Sb_2O_5 by the Spray Pyrolysis Technique", Journal of Applied Chemistry, 26, 1996, pp. 83-89.

[7] www.sono-tek.com

ISSN: 1411-1284

Development of Multi-Axis Force Detector for 5-DOF Articulated Robot

Gandjar Kiswanto, Aji Sambodo

Laboratory of Manufacturing Technology and Automation
Department of Mechanical Engineering – University of Indonesia
gandjar_kiswanto@eng.ui.ac.id, gandjar.kiswanto@ui.edu

Abstract-***Robots give an opportunity for increasing the rapidity of manufacturing processes with fewer error levels. Most industrial robots in the use today, which are the articulated robot with numerically position controlled, still have a trouble for identifying the changes in its environments. This characteristic have created a limitation for the application of robot in the manufacturing processes that need the sense of force such as deburring, polishing, and precision assembly process. Multi Axis Force Detector System permit an articulation robot for detects the force at the end effectors in the x, y, and z direction relative to end effectors. In this research, the Multi Axis Force Detector is specially designed for the RV-M1 5 Articulated Robot, one of the facilities in the Manufacturing Laboratory, Mechanical Engineering Department University of Indonesia. The main device for force detection is the strain gage. Focuses on this research are in the mechanical transducer design, Wheatstone bridge configuration for optimum works of strain gage, signal conditioning, and data acquisition of Multi Axis Force Detector. There is also a trial for the prototype, to obtain the equation that converts the output voltage to force at the end effectors in x, y, and z directions; and analyze what actually take place in the force detection processes. The trial section was using the calibrated mass.***

Keywords: *articulated robot, multi-axis force,*

1. INTRODUCTION

Demand of a product with high precision and accuracy is difficult to reach by numerically position controlled robot applied nowadays. So that the otomation and robotics technology growth have to be sustained by sensor and measurement technology as a very important input parameter in manufacturing process. Robot's sense system was made with a basic idea like human sense but with specified ability and higher resolution. One of significant system detector to the increasing of robot's ability is a multy axis force's detector. Input given by sensor to robot's controller will be used as a feedback to correct errors which happen in manufacturing process.with the force detector development system, robot can do manufacturing processes which need human sense *deburring*, *polishing*, *high precision assembly*; *self calibration*; *invers kinematics*; and the making of contour follower robot's movement line [1].

The research about multy axis force detector prototype system will be used in 5 degree of freedom articulated robot for a research about contour follower line. As its application,the amount of axis used are 3 which are x, y and z relative to *end effector* robot coordinate. Work principle about the making of line movement for articulated robot with force detector system is by using force actuator which will get the value of parameters and the direction of reaction force caused by its contact to the contoured object. Direction parameters and reaction force value will be the input in robot algorithm to make decision about movement direction so that end effector still can touch the object.

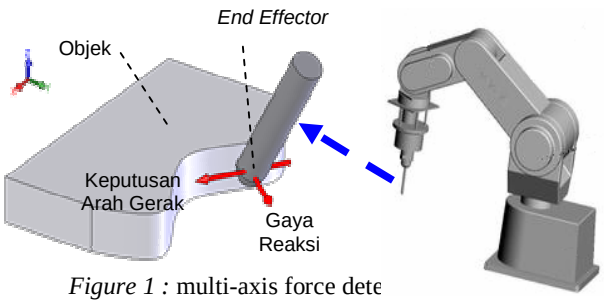

Figure 1 : multi-axis force dete
countored follower application.

2. DESIGN OF TRANSDUCER

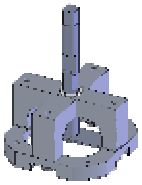

Figure 2: multi-axis force detector tranducer system

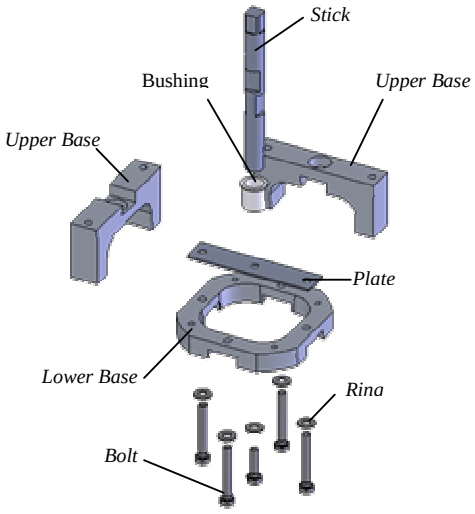

Figure 3: Parts of mult-axis force detector tranducer

In order to to detect force in 3 different direction, it needs at least 3 strain gages location which are independent to each other. The designed locations are on *tranducer*, *stick part* and *plate*. Because of the strain gages are placed on these 2 parts, so *stick* and *plate* are the most important things which have an extra attention in design. Adhesif material of Both strain gage component is stainless steel, according to strain gage material.. While other components like *bushing*, *upper base 1*, *upper base 2*, and *lower base are* produced with mildsteel material which is easy to get, so that its more economic and its coated by chrome in order to increase its resistance to corrosion. It's work principle in detecting forces in 3 different axis is explained in figure 4.

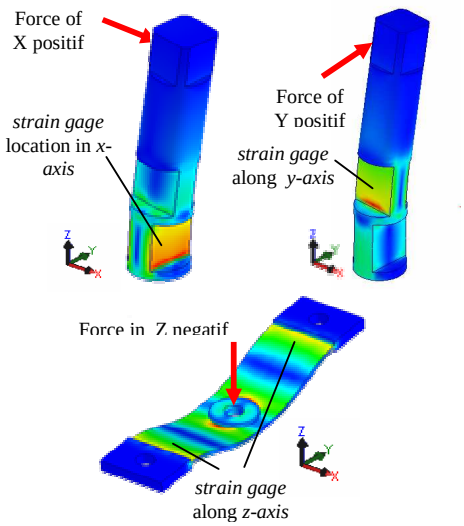

Figure 4: work principle and strai gage location.

The following is a figure of moment and moment equation along stick component axis and plate when force is applied:

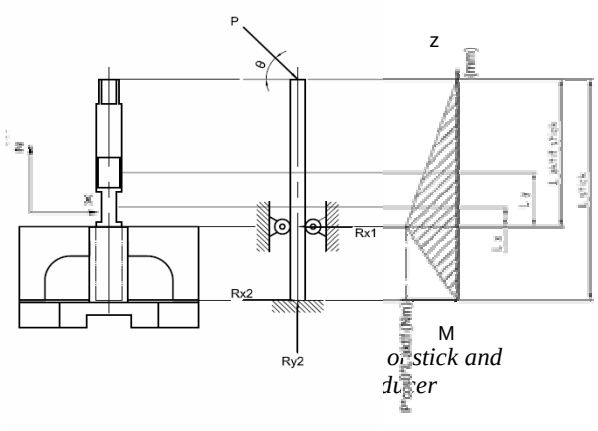

of stick and lever

3. STRAIN GAGES and WHEATSTONE-BRIDGE SERIES

Strain Gage used in this research is uniaxial type with 120Ω of first resistance and 2,11±1,0% of gage factor. Figure 6 shows strain gage configuration in wheatstone bridge series which is applied in this research.

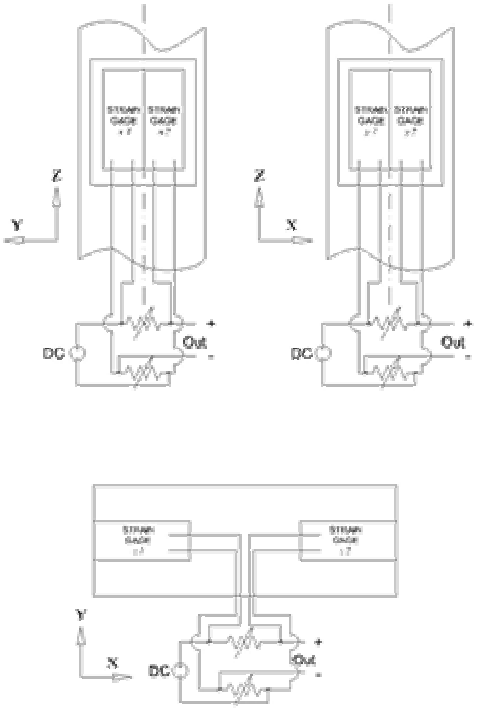

Figure 6 : strain gage schematic configuration of multy axis force detector system at stick and plate components.

The output voltage equation from wheatstone bridge series to the strain according to Figure 6 can be formulated as the following [3] :

$$e = \frac{1}{4} K(\varepsilon_1 + \varepsilon_2)E \qquad (1)$$

where e is an output voltage of wheatstone bridge; K is a gage factor of strain gage; ε_n is a strain that experienced by n strain gage; and E is an excitation stress which has a value of 3,333 volt.

4. SIGNAL CONDITIONING and DATA ACQUISITION

Signal conditioning used in this application is as follows [4]:

1. Stabilization of excitation voltage
   3,333 volt of excitation voltage.
2. Amplification : *Amplification Gain* is 500.
3. Filtering
4. insulation
5. Offset nulling
   a. Hardware compensation
   b. Software compensation

The configuration of data acquisition which is applied at interface software shall be as follows:

Table 1 : Data acquisition Configuration of multi-axis force detector system

No	Item	Specification	Note
1	Resolusion	12 bit	Std. Specification DT3010
2	Channel-Gain List	Entry 0 Entry 1 Entry 2	Channel 0 gain 1 Channel 1 gain 1 Channel 2 gain 1
3	A/D Source sample clock	Internal	Std. Specification DT3010
4	A/D Frequence sample clock	1200 Hz	Entry number multiplication entry
5	Analog input Conversion Method	*Continuously-Paced Scan*	
6	Trigger source	Software	
7	Trigger acquisition	Pre-trigger	
8	Data Format	bipolar	- 5 volt - 5 volt
9	Buffer size	4	> 3
10	Buffer wrap mode	multiple	

5. TESTING

There are 2 methods that are used when doing calibration:

1. the increasing of constant load
2. hysterisis analyse.

the increasing of constant load is aimed to see data output linearity; While the hysterisis analyse methode aimed to see hysterisis that might happen along measuring process. Force measurement is done for each methode with 6 different direction, which are x positive, x negative , y positive, y negative, z positive, dan z negative axis relative to mechanic actuator of *end effector*.

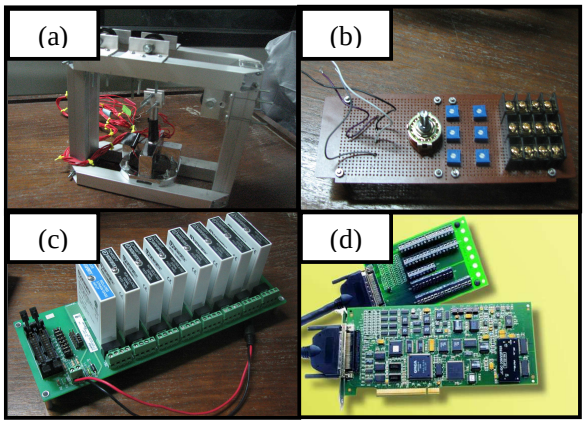

Figure 7. Testing tools in multi-axis force detector system, a)Tranducer callibration fixture, b) Wheatstone bridge series and 3-channels and 4-poles Switch, c) Signal conditioning, d)Data Acqusition Board

The obtained force of *end effector* basicaly comes from string attraction which is bounded on the tip of mechanics actuator. That string attraction comes from load wheigt and a place which is sustained by string. To vary that forces directions, 3 pulley which are passed by string are placed on the rig. Where the string line on pulleys and mechanic actuator position on the rig are arranged to get 6 different string direction

6. COMPARISON OF THEORITICAL OUPUT VOLTAGE TO ACTUAL OUTPUT

As comparison, actual value of output voltage is representated with voltage value that comes from equation of linear result of the increasing

of constant load methode and hysterisis methode data.

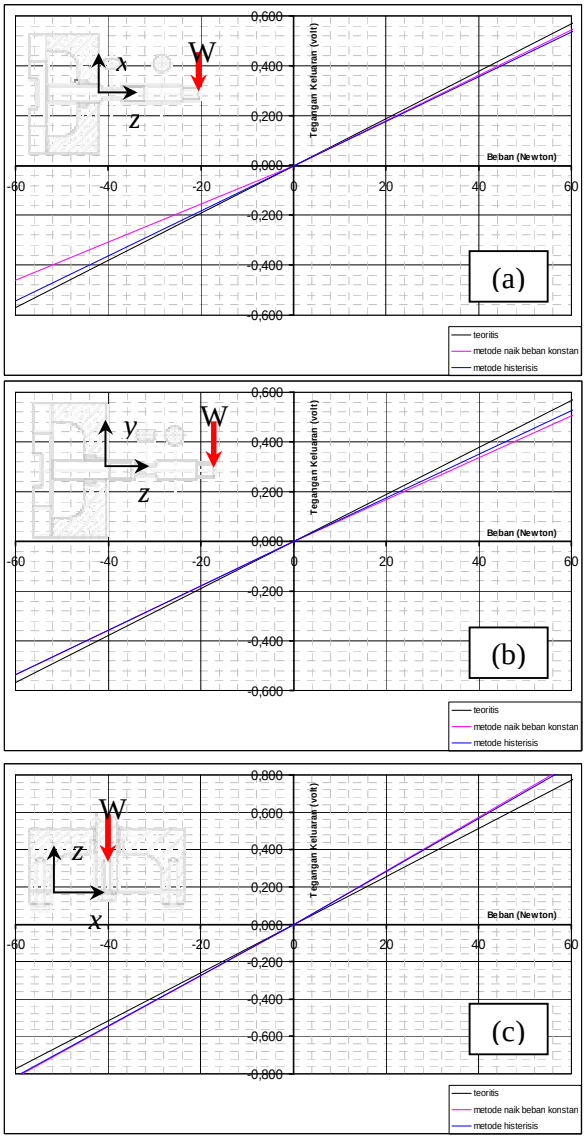

Figure 8 : Comparison between theoritical output voltage to linear equation of regression result testing data :

(a) for X force detector area
(b) for Y force detector area
(c) for Z force detector area

In Figure *8* (a) dan (b) seems that the gradien of linear equation from actual data regession result is lower than teoriticall gradient. it shows that disturbance happened along load convertion process, so it becomes output voltage of data acquisition device From load convertion to material strain, Disturbance which is caused by inappropiate geometry of actual stick due to design, or stick material which not homogeneous or different material properties between actual and teoriticall. Other disturbances could happen during strain convertion to inner resistance of the straingage. These disturbance are missalignment of straingage installation, imperfect adhesion of straingage that caused by the thickness of adhesif material is scraggly on strain gage's base

the different result between the comparison of actual gradient to teoritical one happens in z force detector area. contrary to previous force detector area, z force detector area or plate component has higher actual gradient than teoritical one. It is caused by concentrated strain of straingage in plate component which is caused by ring addition in installation of plate to lower base. It gives conclusion that imperfect geometry factor needs to be calculated in teoritical prediction and it can affects output voltage with more than 1 factors. Other possibility is plate material which not appropiate to spesification, but this factor cannot be confirmed because there is no metalugical data analyzing to multy axis force detector system

7. CONCLUSION

Figure 9 is a mapping of unit convertion in multy axis force detector system and its disturbance's causes that might happen.

According to actual data, it can be conclude that teoriticall output equation need to be completed by correction factors which can change the value of equation gradient. Next is a general teoriticall voltage output equation of multy axis force detector system and the table as an example of correction value of each measurement axis as a testing result of multy axis force detector system.

$$e = \frac{1}{4} j_G j_V j_A GK(\varepsilon_1 + \varepsilon_2)E_{exc} \quad (8)$$

where:

j_G is a geometry correction factor and component material, and it can has a value of > 1;

j_V is a correction factor of voltage drop,caused by inner resistance of the series, ambient temperature,heat *generation*, have value in the range of $0 \le j_V \le 1$;

j_A is a correction factor of strain gage misalignment and strain gage adhesif condition to material. Have value in the range of $0 \le j_V \le 1$;

G is a gain from amplification facility of signal conditioning device.;

K is a gage factor of strain gage.

$\varepsilon_{1,2}$ is a strain that experienced by strain gage 1 and 2;

E_{exc} is an excitation voltage which is suplied by signal conditioning device.

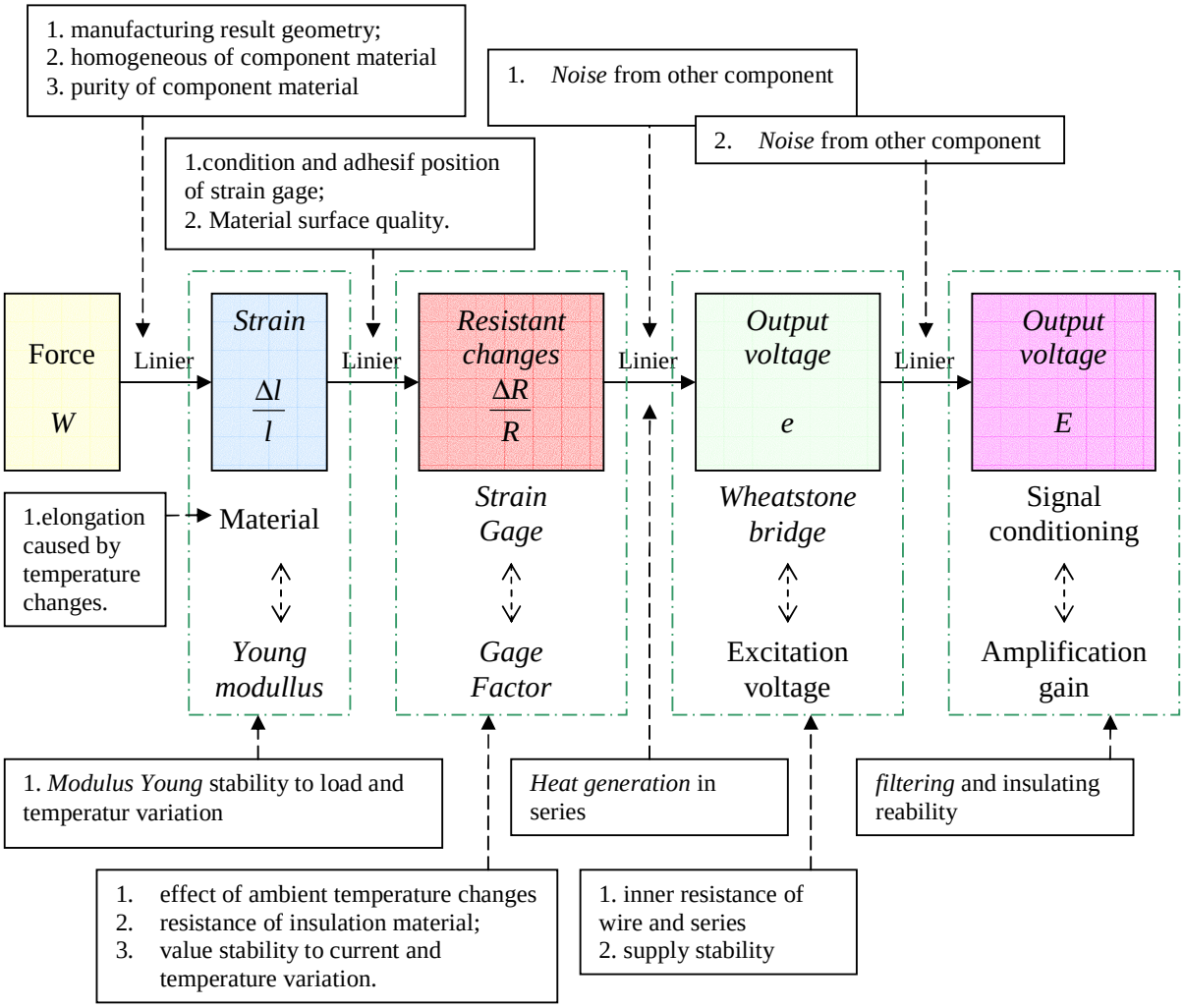

Figure 9: maping of conversion unit in multi-axis force detector system.

REFERENCES

[1] BL Autotec Ltd., *BL Sensor Multi-axis Force/Torque Sensor* (Kobe: BL Autotec Ltd., 2006). Diakses 26 Februari 2007 dari BL Autotec. http://www.bl-autotec.co.jp/english/pdf/BL-RJ-006E.pdf

[2] Bernard J. Hamrock, Bo Jacobson, Steven R. Schmid, *Fundamentals of Machine Element* (Singapore: McGraw-Hill, 1999), hal. 140-161

[3] Kyowa Electronic Instrument co., LTD., *How Strain Gages Work* (Tokyo : Kyowa Electronic Instrument co., LTD., 2006). accessed 27 Januari 2007 from Kyowa Sensor System Solutions. http://www.kyowa-ei.co.jp/english/product/gages/pdf/howsgw.pdf.

[4] Data Translation Inc., *DT3010 Series User's Manual* (Locke Drive Marlboro: Data Translation, Inc., 2006) hal 135-162. Diakses 27 Januari 2007 dari Data Translation Inc. http://ftp.datx.com/Public/DataAcq/DT3010Series/Manuals/um3010.pdf

ISSN: 1411-1284

The Development Of Portable Blood Carrier By Using Thermoelectrics And Heat Pipes

Nandy Putra, Hiban Hardanu, Parlin Adi Sugiarto

Heat Transfer Laboratory
Department of Mechanical Engineering, University of Indonesia
Kampus Baru UI Depok
E-mail : **nandyputra@eng.ui.ac.id**

Abstract-The malnutrition is a chronic epidemic and commonplace spreads mostly at the suburb area and rural. Recently, it emerges because of the unmonitored nutrient's growth for the society living in these areas. Taking the blood sample is a common method to observe this epidemic, especially anemia. These samples are taken from the societies living at cites, suburbs, and rural areas. This must be supported by good blood storages to avoid the blood's destruction and to generate the accuracy of test's results at the laboratory. The common storage is an ice box that uses iced pack as a cooler mediator. Unfortunately, some shortcomings of this ice boxes -as the blood carrier- are their high dependency on the iced pack -that firstly must be cooled at a refrigerator/cooler-, not exactly measured of its cold endurance, and the limited capacity to keep the optimum temperature, about 4-6^{0}C. The objective of this research is to develop a blood carrier prototype cooled by double peltier element and heat pipe in order to follow the standard procedure of blood transportation. The blood carrier may facilitate researchers to get the well-maintained blood sample especially from the suburbs and rural areas. Basically, this prototype might also properly be used for the research of mammalian, viruses, and others medical purposes. The developed prototype was tested and the result showed that the cabin's temperature could reach the desired temperature.

Keywords: Heat pipe, Blood carrier, Peltier Element, Thermoelectric

1. Introduction

The agreement of Millennium Development Goals (MDGs) consist of 8 goals, 20 targets, 48 indicators, where the first goal is every countries should eradicate extreme poverty and hunger, with reduce by half the proportion of people living on less than a dollar a day and reduce by half the proportion of people who suffer from hunger in 2015. Two of five indicators of the first goals are the lower of malnutrition at children under five (forth indicators) and lower of inhabitant with energy deficit (fifth indicators). While in Indonesia, malnutrition at children under five increase rapidly as reported recently by national newspaper especially in NTB. Other indicator, based on Human Development Index (HDI), Indonesia is at 112 ranks in the world, and it is also possible to be worse if the government is not enough fast to handle this problem [1].

Most people are not aware whether one's suffering malnutrition or not. For example a student who unable to study well at school might be caused by the insufficient of certain nutrient such as iodine and ferric. About 50% population of Indonesia suffer malnutrition, the impact are the higher mother and children mortality rate and decrease the human productivity. It will decrease society's welfare. The most forms of malnutrition are the lack of protein, vitamin A, Iodine, and ferric [2].

The malnutrition, especially anemia can be detected by taking some blood samples at some areas -include cities, suburbs, and rural area-. This process is supported by a blood carrier in the form of ice pack as a cooler. A good blood's storage treatment is needed to avoid blood destruction and to generate accuracy data. The shortcomings of this blood carrier are: its dependence on the iced pack – that firstly must be cooled at a cooler or refrigerator -, not exactly measurement of its cold endurance, and the limited capacity to keep the optimum temperature about 4-6^{o}C.

These shortcomings are unable the blood carrier to be used at the optimum capacity especially when the blood is taken at the suburb or rural area. That's why WHO stated that basically the blood carrier used at the developing country is not specifically designed as media for blood storage. It does not fulfill the basic requirements, such as no monitoring temperature, audiovisual alarm and other insufficient storage's standards [3]. A better blood carrier must be designed to overcome these shortcomings. It must be easy to be brought, saving energy, and fulfill the blood's storage standards. These all in order to support the

data monitoring of malnutrition happens in most area, so the government can be able to take a fast and proper policy to overcome malnutrition.

Thermoelectric modules are friendly to the environment as CFC gas or any other refrigerant gas is not used. Thermoelectric module could operate at different temperature at hot and cold side until -20 ^{o}C at cold side. Thermoelectric devices can be called as solid state devices, because they do not use mechanical moving parts and have no noise or vibration, therefore need substantially less maintenance. They have small size and are light in weight. Thermoelectric coolers are appropriate for niche applications (under 25 W) [4]. Besides that the easy installation make thermoelectric module to be the one of suitable alternative to maintain the optimal blood temperature's cabin at 4-6 ^{o}C [5].

Due to all the above advantages, thermoelectric devices have found very extensive applications in wide areas, such as military, aerospace, instrument and industrial or commercial products in the past decades [6]. According to the working modes, these applications can be classified into three categories, which are coolers (or heaters), power generators or thermal energy sensors [4]. The aim of the present study is to design and build blood carrier which easy to bring, have aesthetic value, light in weigh, saving energy, selling value and to test the performance of prototype by using thermoelectric cooler and heat pipes.

2. Thermoelectric and Heat pipe for cooling system

A thermoelectric has two sides which are called as hot side and cold side. All thermoelectric coolers (TECs) need heat sinks in order to dissipate or absorbed the energy at the two junctions. A Peltier cooling unit is therefore composed of three basic components, the Peltier module, the heat dissipater or heat sink at the hot side of the module and the cooling component or cold sink at the cold side of the module, as shown in Fig. 1.

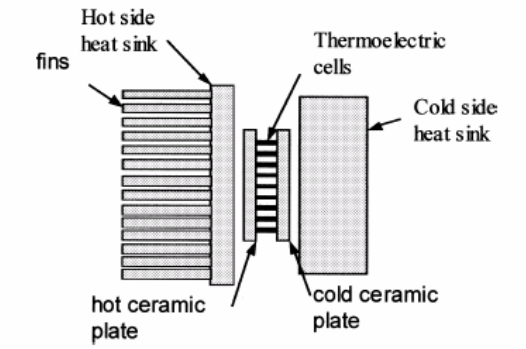

Figure.1 The components of thermoelectric cooling system [7]

The object to be cooled may be direct contact with the cold side of the thermoelectric module, or may be cooled indirect contact through a heat exchanger using either a liquid flow or forced air. The generated heat from the hot side may also be dissipated to the ambient either by natural or forced convection, or removed using a heat exchanger. Fig. 2 illustrates various combinations for heat transfer modes for each side [7].

Any thermoelectric has a maximum temperature difference between hot side and cold side with the maximum electrical current. In order to have maximum temperature difference of thermoelectric module, the use of heat or cold sink plays an important rule. For this reason, the design or selection of a heat sink is crucial to the overall operation of a thermoelectric system. For having the better heat transfer in the device, the heat sink should be designed well to minimize the thermal resistance. This could be achieved by several ways such as maximizing the exposed surface area or by

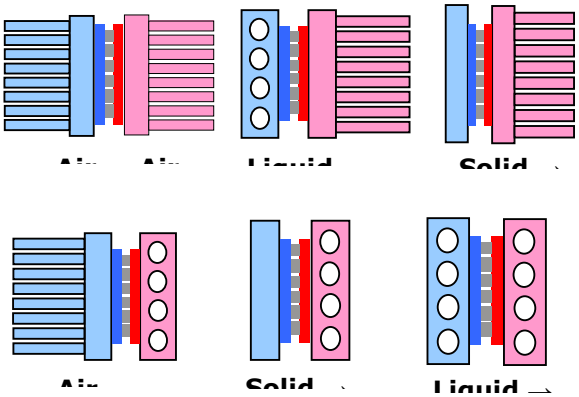

using heat pipes to enhance the heat transfer.

Fig. 2 Different arrangement heat transfer of cold and heat sink on the thermoelectric module [7]

Heat pipes are devices with a very high thermal conductivity and typically consist of a sealed tube with an internal wick. Heat pipes are devices with a very high thermal conductivity and typically consist of a sealed tube with an internal wick, as shown in figure.3.

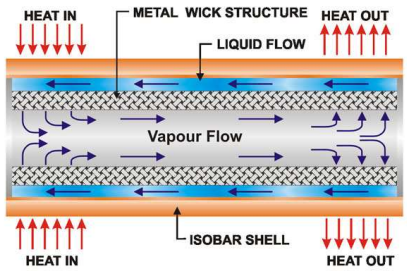

Fig.3 Schematic of heat pipe system [8]

Heat pipe has 3 main components [8]:

- Container (cylinder)

Container shape basically is closed cylinder that could isolate work fluid to not reacted with outside environment and could keep the different pressure (system – environment), and have a great thermal conductivity to absorb and release heat from work fluid. The common material that used is copper, aluminum, and stainless steel.

- Wick Structure (capillarity)

In the inner side of casing wall there is a hollow structure component. This side is called capillarity structure or wick. The main function of this component is just like pump to flowing the work fluid that condensate in condenser edge so that the work fluid could go back to evaporator edge to absorb heat from heat source. This component work by capillarity pressure from work fluid so there is no need of power to flow the work fluid.

- Work Fluid

Work fluid function is to carrying heat from heat source to be released to environment. Most of the heat pipe manufacturer using water, methanol, or alcohol as work fluid. This work fluid always operated near its boiling temperature. So the higher latent heat from work fluid, the more heat that could be absorbed, and that kind of heat pipes are more efficient.

3. Design of blood carrier prototype

The design of the prototype can be seen in Fig 4. The prototype is designed to carry 50 tubes of blood samples (3 ml each tube) and can maintain their temperature between 4-6^{o}C. The dimension of the blood carrier is 454 x 209 x 264 mm. and made of acrylic. To avoid more head load from the outside of the box, Styrofoam isolation material was used and placed inside the box. The cooling systems were installed on the right and left side of the box. Each cooling system consists of two Peltier elements, heat pipe and heat sink fan. In the prototype, two commercially available 40 X 40 mm thermoelectric modules were cascaded and connected electrically in series. This way was chosen in order to have higher temperature difference between hot side and cold side of the thermoelectric module. A metallic space block made of aluminum was positioned between the cold side of the thermoelectric modules and the cold side heat sink. To minimize the thermal contacts between the thermoelectric module and cold sink, a thin film of silicon thermal paste were used. The commercial heat pipe was mounted on the hot side of thermoelectric to release more heat and to keep at the certain temperature on that surface. Fins made of aluminum were attached on condensation side of heat pipe horizontally then a small fan was mounted directly on the fins to provide forced air convection to the hot side heat sink of heat pipe. The blood carrier is equipped with a temperature control not only to maintain the setting temperature but also to reduce energy supply when the setting temperature has been reached.

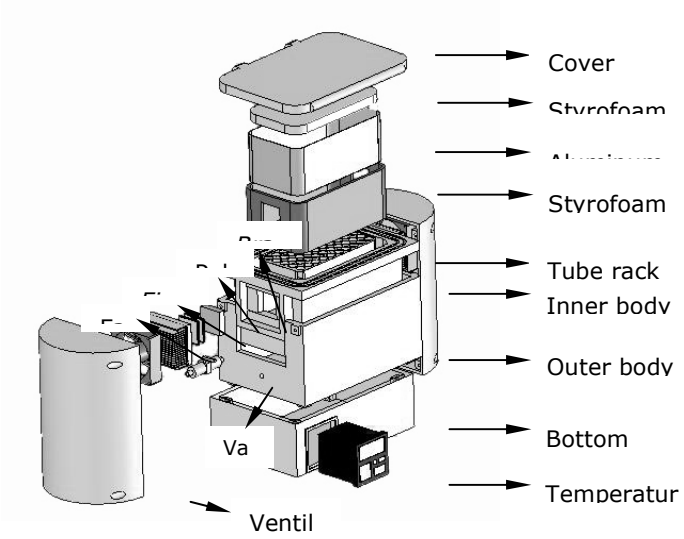

Fig.4 Prototype of blood carrier

4. Experimental setup

Figure 5 shows the experimental setup for testing the performance of the designed blood carrier. Thermocouple type K are used and placed on the several points such as on cold and hot side of peltier elements, and in the compartment. All the thermocouples are connected to data acquisition then the measured temperatures can be stored to the computer. DC power supplies were used to supply electrical energy input to the thermoelectric modules and fans. The input power (voltage and current) are recorded from its LCD display.

Since the aim of the testing was to know the performance of blood carrier by using thermoelectric and heat pipe as cooling system, the system was tested with the variation of power supply. The purpose was also to use heat pipe on the hot side of peltier element. For this reason, tests were also carried out with the heat pipe 2 pipes and 4 pipes and no heat pipes only heat sink fan, to investigate its effect on the performance of the thermoelectric cooling system. Then the system was tested with, and without load, in order to evaluate the effect of load on the performance of the cooling system.

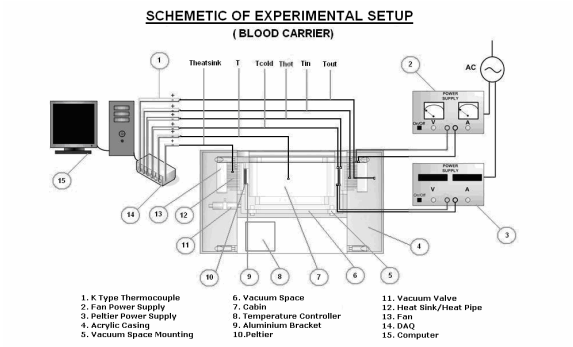

Fig 5 Schematic of experimental setup

5. Results and discussion

For the several of power supply, 24, 27, 30 Watt were applied in this testing. According to graphic shown in Fig 6, it can be seen that the variation of power supply did not give the different data even though the lowest cold side temperature is occur in 27 W of power supply. But there is important information, that the temperature on cold side of the peltier element for all power supply showed similar trend, drops rapidly at the initial time, then to be constant after 30 minutes of the operation. The minimum temperature can be reached for all testing was -5 ^{o}C. For the next testing, the power supply 27 was applied.

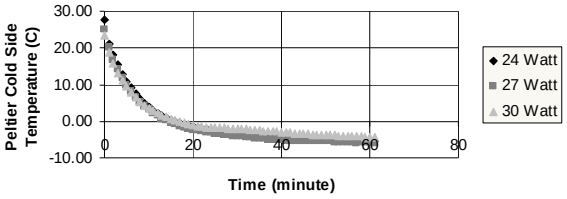

Fig 6 Comparation of double peltier power supply

In order to investigate the effect of heat pipe on the performance of the thermoelectric cooling system, the experiment was prepared in condition without load, using parallel double peltier connected with 27 W power supply for each side (1 set parallel double peltier). The testing with 4 heat pipe, 2 heat pipes and without heat pipe (only heat sink fan) on the hot side of peltier element were carried out. According to graphic shown in Fig 7, can be seen that heat pipe cooling performance is better than the system only used heat sink fan and using more Heat Pipe will give better performance in cooling the peltier's hot side. Because the liquid in heat pipe can absorb more heat, that is rejected from the hot side of peltier element. It affected the higher temperature difference between hot side and cold side temperature. From previous study confirmed that the double peltier can created difference between hot side and cold side temperature around 40ºC [9], thus if the hot side temperature can be maintained as low as possible, then the cold side temperature will be decrease and that makes cabin temperature become decrease as well. Detail data shows in figure 7 that after 5.5 hour operation the temperature in the cabin were: $T_{heat\ sink}$ = 3.49ºC ; $T_{heat\ pipe\ [2]}$ = -0.09ºC ; $T_{heat\ pipe\ [4]}$ = -1.57ºC

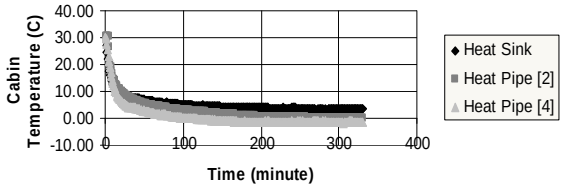

Fig 7 Comparation performance of heat sink and heat pipes

With the intention of evaluate the effect of load on the performance of the cooling system, then the system was tested with, and without load. The experiment was done in condition with and without load, using parallel double peltier connected with 27 W power supply for each side (1 set parallel double peltier), using 4 heat pipe as cooler for peltier hot side. Figure 8 depicts the cabin's temperature comparison between the system with and without load. It can be seen that by adding the load (50 tube 3ml full of water) will give a significant effect in decreasing the acceleration of cooling process. With load the temperature decreased slowly and after 5 hour it reached below 10 ^{o}C. It means that the system has not worked effective yet. Therefore the icepack or phase change material is needed to accelerate cooling in the cabin.

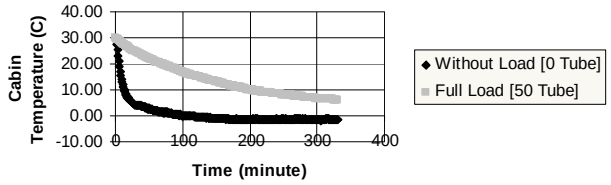

Fig 8 Comparison of cabin temperature while without loaded and fully loaded

6. Conclusion and recomendation

The prototype of blood carrier with thermoelectric and heat pipe as cooling system has been designed and tested. The Placement of heat pipe combined with the conventional heat sink

system, gave an improvement in the performance of the thermoelectric cooling system but the cooling system needs longer time to reach the desired temperature in the cabin temperature 4-6ºC when the load was applied.

The use of a Phase Change Material can provide a bigger cold storage capacity, which helps to overcome peak loads. It is therefore recommended that further tests should be carried out to investigate the role of Phase Change Material and its effect on the performance of the thermoelectric cooling system.

Acknowledgements

The authors would like to thank *Riset Unggulan Universitas Indonesia* 2007 for funding this project.

References

[1] Nurpudji A Taslim, "Kontroversi seputar gizi buruk : Apakah ketidak berhasilan Departemen Kesehatan?" http://www.gizi.net/Makalah-artikel. Download tanggal 21 Maret 2007

[2] Azrul Azwar, "Kecenderungan Masalah Gizi dan Tantangan di Masa Depan" Pertemuan advokasi Program Perbaikan Gizi Menuju Keluarga sadar Gizi, Jakarta 27 September 2004.

[3] www.who.org, Download 20 Maret 2007

[4] S.B. Riffat, Xiaoli Ma (2003).Thermoelectric: a review of present and potential applications. Journal of Applied Thermal Engineering, 23 (2003)913-935.

[5] Martindale, the extra pharmacopoeia, London, 30th Edition. Pharmaceutical Press 1982.

[6] Nandy Putra, Aziz Oktarianto, Idam Bariyanto, Fery Yusivar,"Penggunaan heat sink fan sebagai pendingin sisi panas elemen peltier pada pengembangan vaccine carrier", in press di Jurnal Teknologi FTUI, Depok, 2007.

[7] S.B. Riffat, Xiaoli Ma (2003). A novel thermoelectric refrigeration system employing heat pipes and a phase change material: an experimental investigation. Journal of renewable energy 23 (2001) 313-323.

[8] www.acrolab.com, download 20Maret 2007

[9] Nandy Putra, Uji Unjuk Kerja Kotak Vaksin berbasis Elemen Peltier Ganda, Seminar Nasional Perkembangan Riset dan Teknologi di Bidang Industri Universitas Gajah Mada Yogyakarta, 27 Juni 2006. ISBN 979-99266-1-0

ISSN: 1411-1284

Object Recognition Based on Its Features for Human Robot Dialog

Rahmadi Kurnia

Dept. Electrical Engineering, Andalas University, Kampus Baru Limau Manis Padang, West Sumatra.
Tel. +62-751- 72584
Fax + 62 -0751- 72566
e-mail : rahmadi_kurnia@ft.unand.ac.id

***Abstract*—There are many methods that can be used to evaluate human robot dialog for object recognition. The appropriateness of those methods depends on basic knowledge of the robot, robot sensor and the real condition of the target object. In this paper we focus to determine and generate what is the content and the kind of questions users need to effectively, efficiently and continently interact with a robot that has not any prior basic knowledge of the target object in real condition . The system commonly will ask the user by using yes/no question if it finds some ambiguous objects then restore it for its dynamic knowledgebase. The robot will think and ask like human mind about missing information.**

Keywords-component; Objects feature , feature characteristic.

I. INTRODUCTION

Human-computer interaction is a discipline concerned with the design, evaluation and implementation of interactive computing systems for human use and with the study of major phenomena surrounding them [1]. One goal for interaction between people and robots is based on conversation about tasks that a person and a robot can undertake together. Not only does this goal require linguistic knowledge about the operation of conversation, and real world knowledge of how to perform tasks jointly but the robot must also interpret and produce behaviors that convey the intention to maintain the interaction or to bring it to a close

Human-robot interaction currently takes many forms. This interaction can be done by verbal and non verbal behavior [2]. For verbal behavior, there are some issues such as unknown words, dialog generation and robot knowledge to be settled. Some attempts are made for dealing with unknown words. Danmati[3] and Nagata[4] estimated a class (a part of speech or text) of unknown word in a speech and text. Takizawa [5] made maximum probability of unknown words that was formulated as finding registered words. Takahashi [2] generated a dialogue by extracting all of situation and process it as a working memory. He focused to find some objects which were recognized before by the robot.

Other human robot interaction can be done though integrating visual auditory information with the idea of integration of visual and audio sense by relaxation method and intend to construct audio visual conversation system that consist of combination conversation and gesture [6].

This paper focuses about human – robot interaction by dialog. When the robot is commanded to find a required object in the complex scene, it will ask to the user about missing information. The main purpose of this paper is to formulate an effective, efficient and convenient dialog in human-computer interaction. We minimize unknown word to simplify dialog process and convenient interaction's purpose. User answers the question of robot by choosing "*yes or no*" for almost all of the conditions. We generate several rules to make most effective, effective and convenient dialog. This method has three advantages. *First*, the robot can avoid mistakes to interpret all things of the answer from the human. *Second*, the system provides some convenient dialogs to the user by describing the current situation. *Third*, the robot can learn various things by its previous work experiences. It records all important information of previous tasks into its dynamic knowledgebase for executing the task in next duty.

II. SYSTEM CONFIGURATION

Figure 1 shows the configuration of the system. An input scene is segmented and labeled by using image processing process to find the features of objects. If the segmentation and labeling process result is unrecognizable for the robot, it will ask to the user. The system obtains an effective and efficient question by processing this result according to general rule and dynamic database that obtained from specific characteristic of each features and some stored previous outputs.

A. Image Processing Part.

Color segmentation. We use robust analysis of features space method for color image segmentation [7]. This method reduces the number of color in the image and divide image to several region. For getting a best result, we merge some nearest color region by using hue method in HSI color space. [8]. The *HSI* system separates color information of an image from its intensity information. Color information is represented by hue and saturation values, while intensity describes the brightness of an image, is determined by the amount of the light. Hue represents basic colors,

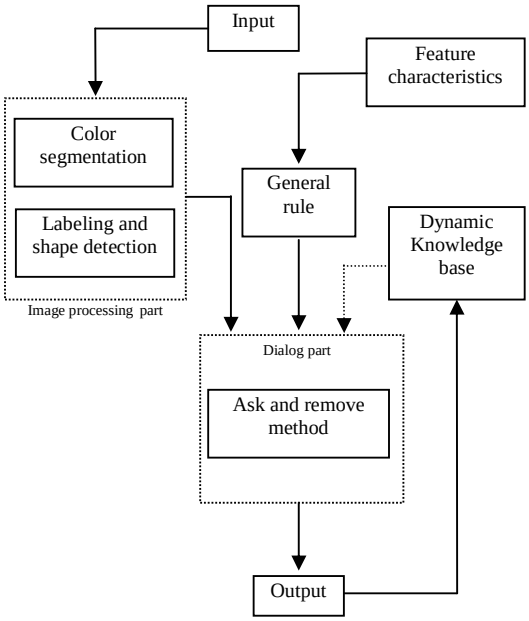

Figure 1. Configuration System

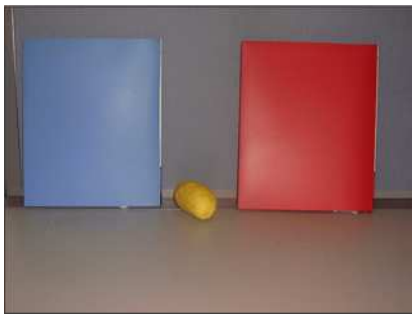

(a)

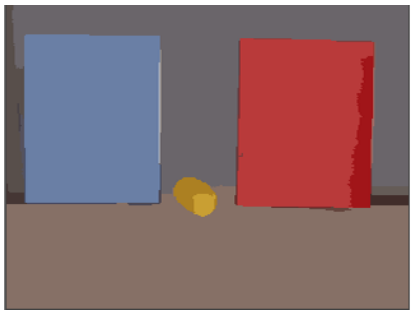

(b)

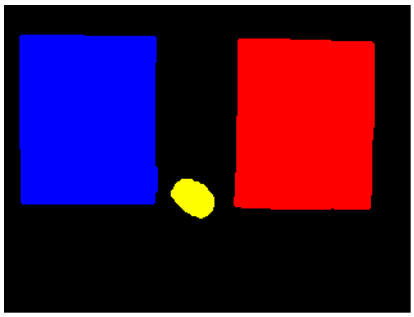

(c)

Figure 2. Color segmentation result .(a) Original Image. (b). Segmentation results (c) HIS result after segmentation process

and is determined by the dominant wavelength in the spectral distribution of light wavelengths. Some threshold of hue value is determined or to remove background and merging of nearest color for achieving small number region. Figure 2 shows an original image (a), a color segmentation result image (b) and HIS results of image after segmentation processes (c). In this paper we fix some threshold of hue value that estimated from 0^0 to 360^0. For example, blue is 240^0, yellow is 60^0, green is 120^0, red is 0^0 magenta is 300^0 etc.

Labeling and shape detection. Some values are put to the image to label the similar color in one region for detecting the number of object(s). The shape of object is detected by determine its size, area, surrounding by using curve ratio equation. [9]. We get some curve ratio is specific for each standard shape objects from experiments. For example, the curve ratio of circle is 0.8, square is around 0.79, rectangular is 0.7, triangle and other irregular shape are less than 0.58

B. Feature Characteristics and General Rule

Object feature is a most important thing for pattern object recognition. Object feature can be used to recognize in single or cluster object. In this paper, four features (size, color, position and shape) are used to analyze, describe and search the target object. All of the features are sorted related on their special characteristic in any condition. By groping this feature into some general characteristic and manipulated them like human thinking, the general rule can be obtained for any condition of objects for making efficient and effective question to the user.. Four general characteristic which cover these feature are: Vocabulary representative, objects distribution, uniqueness, objectivity / subjectivity.

There are general characteristic of each features that are explained below:

General characteristic of objects:

1. *Vocabulary representative*
   The feature of object has some vocabularies to be described to the user. The system has several exact words to describe all condition of objects. Color, size and position are included in this characteristic. Color has some vocabularies like red, yellow, blue, green, cyan, magenta, brown, white, black etc. The expressions of position are left, right, up side and under side. Big and small are the exact words for size feature. Even though this feature only has two terminologies but both of them are representative words. The feature of shape is excluded of this characteristic because some of its shape is irregular and indefinable.

2. *Object Distribution*
   The feature of object is recognizable for any kind of distribution objects.
   Shape, color and size are easy to be described for any distribution objects because their feature independents of the objects location. For position, the expression of its word will be difficult to define if the objects flock together

3. *Uniqueness*
   There is one peculiar feature belonged to each object. This feature of one object is unique and is differed each other. The feature of position is covered by this characteristic. In the real condition there is only one specific location of each object in the scene. Their position can be described by side direction or specified by detail using x-y coordinate.

4. *Objectivity/subjectivity*
   Objectivity: The feature of object is independent of other objects. Shape and color are included in this characteristic.
   Subjectivity:
   In real condition, we will incapable to assure the feature of one object if they haven't seen the other object(s) in advance. We are in doubt to state one objects is big or small and in the left or right side before we know the location and size of other(s).
   In this paper we sort the size base like human thinking. From any experiment result we get conclusion that human can clearly and surely distinguish the size of two objects if the minimum of difference of the biggest object and the smallest one is equal as a doubled smallest object. .

   The grouping of size can be explained as :

   for Max size $\geq$ 4 * Min size
   if size $\geq$ Max size - Min size
   Word size = big
   else if size $\leq$ 2 * Min size
   Word size = small
   else
   Word size = unpredictable

   where Max size = maximum size
   Min size = minimum size

   Objects position can be recognized by dividing them into two opposite group's side especially for multiple objects. Sorting multiple objects location based on the distance of furthest object in each group. In this paper, the barrier of groups should conform to equation [] for recognizable.

$$d_{side} \geq 2 * d_{max} \quad (1)$$

where d_{side} = distance of two furthest objects sides in each group..
d_{max} = maximum of distance in one group.

The relation of features and their characteristic is shown in table 1.

In this paper, when several candidate target objects are detected, the robot will ask the user to ensure an exact one. Robot reduces unnecessary objects by referring of user's answer to simplify the scene. The system analyzes each question which can remove most unnecessary objects to determine their priority. The highest priority's question will be asked to the user in any cases for obtaining most efficient and convenient dialog. We call this method as Ask and Remove (AaR) method.

Table 1. Feature and its characteristics

Characteristic	Color	Size	Position	Shape
Vocabulary representation	√	√	√	○
Object distribution	√	√	○	√
Uniqueness	○	○	√	○
Objectivity	√	○	○	√

In AaR method, the number of total objects is divided into two categories:

First, the number of total objects is less than four objects. The system will choose only subjectivity characteristic to determine a question by using. This characteristic consists of size and position which are very effective to describe some objects in limited number. The detail of each objects feature can be formulated easily by comparing one object volume, objects area and object location to other(s).

Second, the number of total objects is more than three objects. The system spelled out this condition to three intervals of similarity object characteristic number for formulating any cases. In this paper, we obtain the partition value of each interval from experimental results. The entire of interval are:

Identify applicable sponsor/s here. *(sponsors)*

a. Interval A: the number of objects that has similar characteristic is less than 30% of the total objects number.
b. Interval B: the number of objects that has similar characteristic is more than 30% but less than 70% of the total objects number.
c. Interval C: the number of objects that has similar characteristic is more than 70%of the total objects number.

All of the classification of these intervals is shown by figure 3.

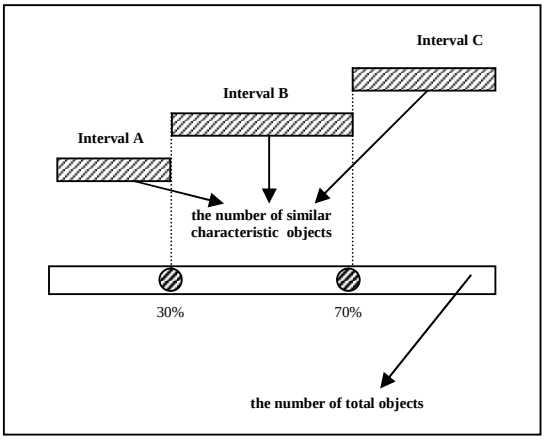

Figure 3. Interval condition of target objects

Table 2 shows all of cases that might be possible in real condition.

Table 2. All of condition of target objects

	The number of objects that has similar characteristic:			Event
	Interval A	Interval B	Interval C	
characteristic	*vocabulary*			*Case 1*
		vocabulary *objectivity*		*Case 2*
		objectivity	*vocabulary*	*Case 3*
		vocabulary	*objectivity*	*Case 4*
	objectivity			*Case 5*
			vocabulary *objectivity*	*Case 6*

From the table we get some cases:

Case 1:

The number of objects which has similar vocabulary's characteristic is less than 30% of the total objects. In this case we ignore other characteristics and their interval location because in interval A, vocabulary's characteristic has several exact expression word to define more than others. Therefore, "what question" is a best choice to make a dialog with the user. The system asks the user a question which contains these expression words then will remove unnecessary objects based on user's answer. In reality, even though in this characteristic consist of position color and size but in this case the most priority is color. Position and size has a couple depended expressions' word to define their feature. This condition means : the number of objects which has similar size and position can be less than 30% of the total objects but simultaneously, the number of objects which has similar opposite size and position will be more than 70%of the total objects. For case 1, position and size always located in two intervals. Therefore both of them are confusable for becoming a content of a question.

Color's feature is possible to be located in two interval (e.g. interval A and interval B) simultaneously, but all of its words expression independent each other

Case 2:

In this second case, the number of objects which has similar objectivity's characteristic or vocabulary's characteristic is between 30% and 70%of the total objects and more than 70%of total objects. This condition can be solved by determining a suitable feature, which is included in both of characteristics. We formulate that feature by using equation (1) and simulate it by Venn diagram as shown in figure 3.

$$CoQ_2 = V \wedge O \quad (2)$$
$$= color$$

where,

CoQ_2 = content of question for case 2
V = vocabulary
O = objectivity

From that equation we find the best feature is found by intersect both of the characteristics. In this case we get a color as a best feature to be asked to the user.

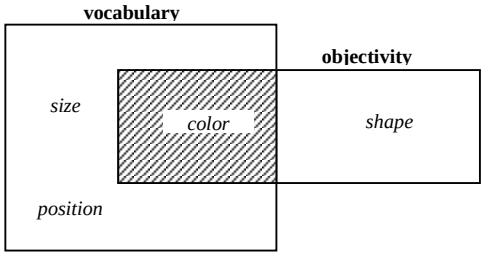

Figure [4]. Venn Diagram of vocabulary and shape intersection

Case 3:

The number of objects which has similar objectivity's characteristic is between 30% and 70%of the total objects and more than 70%of total objects have similar vocabulary's characteristic. In this case, vocabulary's characteristic is not effective to be asked to the user because there is too many similar objects' feature to used "ask and remove" method. Therefore, the priority for asking the user at the first time is objectivity characteristic. The content of feature of this characteristic which is asked can be formulated as:

$$CoQ_3 = O - V \quad (3)$$
$$= \text{shape}$$

where,

CoQ_3 = content of question for case 3

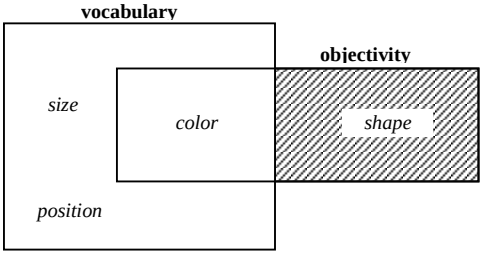

Figure[5]. Venn Diagram of Objectivity - Vocabulary

This result can be described by Venn diagram as shown in figure [5].

Case 4:

This case is an opposite of case 3. In this case, the number of objects that has similar vocabulary's characteristic is between 30% and 70%of the total objects and more than 70%of total objects have similar objectivity's characteristic.

This means that there are so many objects have similar feature for vocabulary's characteristic which lead to an inefficient and ineffective first question to be asked to the user. Therefore the objectivity's characteristic is more priority than other characteristics. The formulation of the features of this case is shown by equation (4).

The exactly feature this characteristic which is asked can be formulated as:

$$CoQ_4 = V - O \quad (4)$$
$$= \text{size and position}$$

where,

CoQ_4 = content of question for case 4

This equation obtains that size and position are two candidate features which can be chosen for containing the question as shown in figure 4. Both of them has a couple opposite word The estimation for choosing one of them based on whose feature can remove unnecessary object(s) after the robot get an answer from the user. The system will determine the number of objects in each word feature. Most of the number of unnecessary object can be removed if the number of objects in both of their word borders on balance.

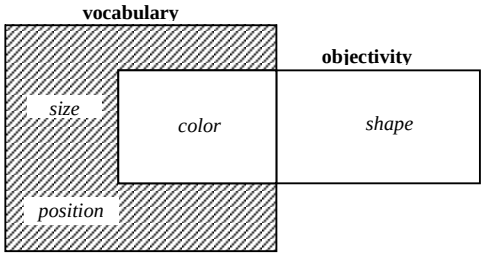

Figure 6.Venn Diagram of Vocabulary - Objectivity

Case 5:

The number of objects which has similar objectivity's characteristic is less than 30% of the total objects. The system will get some varieties of the object features by analyzing them independently. Each object features will be performing as a single object to recognize their feature. Therefore, position and size feature is unconcerned with the system.

In this case, one of two probabilities condition could be happened: *First*, there are several similar color objects and similar shape objects in the scene. In this case, the color will be chosen by the system because it has complete and definite word objects expression more than shape. *Second*, there are several similar shape including in interval A and several similar color objects belong to other interval. In this case shape will be a highest priority because it has the most varieties to be asked to the user.

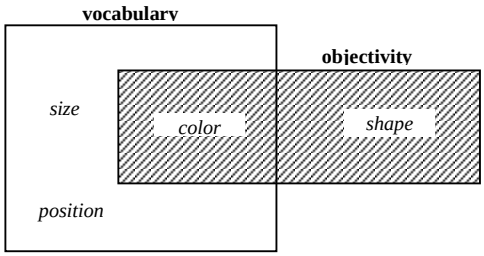

Figure[7]. Venn Diagram of Objectivity

Case 6:

In this case the number of objects which has similar objectivity's characteristic or vocabulary's characteristic is more than 70%of the total objects .For this specific condition, the system will specify the detail feature of each objects to get their uniqueness and their distribution. . The system manages a first question based on both of these characteristic.

Table 3 shows all of general rule of robot question in any cases.

Table 3. General rule

Condition	Question	
	Content	The Type
The total objects < 3	Subjectivity	"*yes/no*" question
Case 1	*Vocabulary*	"*what*" question
Case 2	*Vocabulary*	"*yes/no*" question
Case 3	Objectivity	"*yes/no*" question
Case 4	vocabulary	"*yes/no*" question
Case 5	Objectivity	"*what*" question
Case 6	uniqueness or object distribution	"*yes/no*" question

C. Dynamic Knowledgebase

The system records the results and their process to a dynamic database. This database contains some features of the objects. In this research, system can exactly record the result only for objective characteristic because subjective characteristic is not stable and relative. Position feature is usually changed for every case and size is dependent to other objects.

The knowledgebase of robot will be increased if it does a new task. This dynamic knowledgebase also become perfect if there are various feature in one objects. If the human command to the robot to bring an apple, the robot will know that the color of the apple is usually red and its shape is circle. This knowledge is never changed until the robot has a new task to bring green or yellow apple.

Having this dynamic knowledge, the robot will be helpful for human assistance in the future.

III. EXPERIMENTAL RESULT

For example, we have four objects which have 2 similar color and shape. We command the robot to bring a red apple which located among the objects. This example refers to case 2 at table (2).There are some steps in this experiment:

1. We segment an original image as shown in figure 8.
2. Merging nearest color region for removing background as shown in figure 9. In this step, the number of target objects(s), their size and shape are determined but not appeared.
3. The system asks a *yes/no* question that contain about color to the user.
4. The system removes unnecessary objects based on user answer and than thinks like human to formulate next question as shown in figure 10.
5. There are only two objects (less that 3) in the current scene. Therefore, the system makes a question based on subjectivity characteristic feature that have been explained before.
6. The system asks the second question and remove unnecessary object to get a real target objects. Figure 11shows the final result

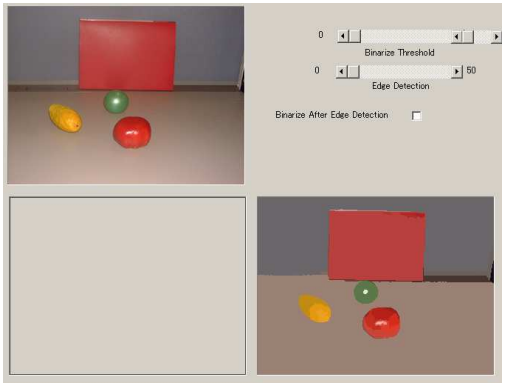

Figure 8.Segmentation result.

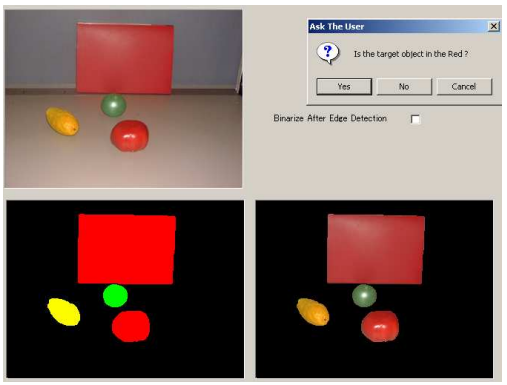

Figure 9.Merging nearest color region result

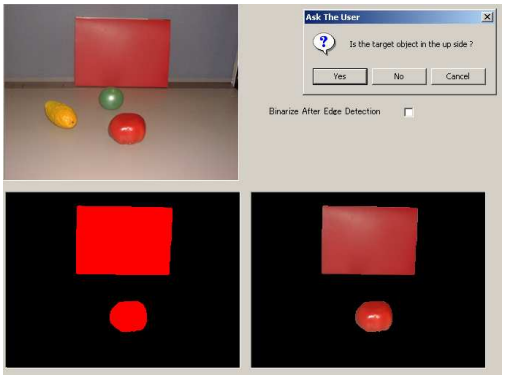

Figure 10.AaR method result

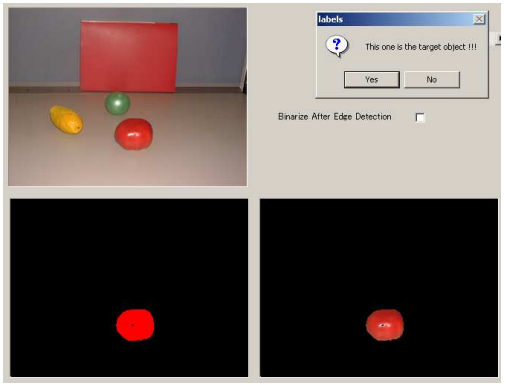

Figure 11.Final result

IV. CONCLUSION

We have explained and done some experiment to make an effective, efficient and convenient dialog of human user interaction. The system has been proved that the system can think not only like human mind but also it can record of each case in its memory for next same duty in the future.

REFERENCES

[1] Hewett, T., Baecher, R., Card, S., Carey, T., Gasen, J., Mantei, M., Perlman, G., Strong, G., and Verplank, W. (1992). "ACM SIGCHI curriculum for human-computer interaction." Report of the ACM SIGCHI Curriculum Development Group

[2] Takuya Takahashi, Satoru Nakanishi, Yoshinori Kuno and Yoshiaki Shirai,"Human Robot Intervace by Verbal and Nonverbal Behaviors,Henryk Palus and Damian Bereska," Region Based Colour Image Segmentation,"

[3] G. Damnati, F. Panaget, " Adding NewWords in a Spoken DialogueSystem Vocavulary Using Conceptual Information and Derived Class-based LM", Proceeding of Workshop on Automatic Speech Recognition and Understanding, 1999

[4] M. Nagata, "A Part of Speech Estimation Method for Japanese Unknown Word Using a Statistical Model of Morphology and Context" , 37th Annual Meeting of the Association for Computational Linguistic, pp. 277-278, 199

[5] Masao Takizawa, Yasushi Makihara, Nobutaka Shimada, Jun Miura and Yoshiaki Shirai, "A Service Robot with Interactive Vision- Objects Recognition Using Dialog with User".

[6] Tomohiro Kawaji, Kei Okada, Masayuki Inaba, Hirochika Inoue, " Human Robot Interaction through Intergrating Visual Auditory Information with Relaxation Method", Proceeding of IEEE International Conference on Multisensor Fusion on Integration for Inteligent Systems Tokyo, 2003 , pp 323 - 328.

[7] Comaniciu, D. and P. Meer," Robust Analysis of Feature Spaces: Color Image Segmentation" in Proceedings of 1997 IEEE Conference on Computer Vision and Pattern Recognition, San Juan , PR, 1997: p. 750-755.

[8] H.D. Cheng, X.H. Jiang, Y Sun, Jingli Wang," Color Image Segmentation : advances and prospects," Pattern Recognition Journal 34 (2001), pp. 2259 – 2251.

ISSN: 1411-1284

Development of Analytic Solution of Inverse Kinematics and Motion Simulation for 5-DOF Milling Robot

Gandjar Kiswanto, Hafid budiman

Laboratory of Manufacturing Technology and Automation
Department of Mechanical Engineering – University of Indonesia
gandjar_kiswanto@eng.ui.ac.id, gandjar.kiswanto@ui.edu

Abstract - **This research is about finding analytic solution of inverse kinematics of 5 degree of freedom milling robot. The simulation with GUI using MATLAB is also developed to verify the solution. In order to move the manipulator, the position and the manipulator parts (joint, link and end effector) need to be explained, and the FRAME is placed for each joint. The movement is actually a description change from the old frame to the new frame, and the process is called mapping. Mapping involves translation and rotation process, the frame position is changed by translation and the frame orientation is changed by rotation. The change of orientation uses roll and pitch calculation. The robot movement are based on points and orientation information of the CL-File (Cutter location file) generated in a CAM-system. The movement includes of 2 types, which are forward kinematics and inverse kinematics. The analytical solustion of inverse kinematics, the position and orientation are then changed into robot's joint angle, so that its possible for milling robot to move according to CL points and Orientation. The result shows the robot movement in multi-axis milling process, and how far the level of accuracy.**

Key words : Analytic solution, inverse kinematics, 5 DOF milling robot

1. INTRODUCTION

Industrial robot which commonly used is an arm (articulated) robot. The robot used in this research has 5 degree of freedom. The inverse kinematics solution is needed in order to command the robot to reach assigned destination (target) which are the position and orientation of the end-effector (cutting tool) within its working envelope. Therefore, this research is aimed to solve inverse kinematics analytically and to develop movement simulation for 5 degree of freedom robot, with all articulated joints, for multi-axis milling process. Milling robot will move according to position and orientation of target points along the machined part. The GUI is developed in order to have an easy implementation. The *inverse kinematics* is done by first doing the *forward kinematics*. This will result the value of *r11*, *r12,…*, *r33* and *x*, *y*, *z*. Then, these values are included into complete inverse kinematics calculation.

2. FORWARD KINEMATICS SOLUTION

The standard Denavit-Hartenberg (DH) method is used to solve the kinematics. The assigment of frame coordinates and DH parameter are shown in Figure 1 and Table 1. Based on DH method, the transformation matrices from joint *n* to the joint *n+1* is :

$$ {}^{i-1}_{i}T = \begin{bmatrix} C\theta_i & -S\theta_i & 0 & a_{i-1} \\ S\theta_i C\alpha_{i-1} & C\theta_i C\alpha_{i-1} & -S\alpha_{i-1} & -S\alpha_{i-1} d_i \\ S\theta_i S\alpha_{i-1} & C\theta_i S\alpha_{i-1} & C\alpha_{i-1} & C\alpha_{i-1} d_i \\ 0 & 0 & 0 & 1 \end{bmatrix} $$

Table 1. DH parameters

	α_{i-1}	a_{i-1}	d_i	θ_i
1	0	0	d_1=133	θ_1
2	-90	0	0	θ_2
3	0	a_2=250	0	θ_3
4	0	a_3=160	0	θ_4
5	90	0	d_5=72	θ_5

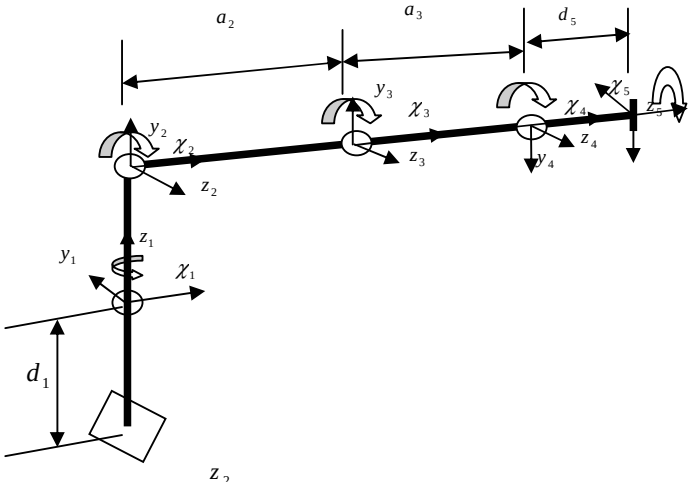

Based on the above table and the following calculation, the matrices transformation for forward kinematics are as follows :

$${}^{0}_{5}T = {}^{0}_{1}T\,{}^{1}_{2}T\,{}^{2}_{3}T\,{}^{3}_{4}T\,{}^{4}_{5}T$$

where

$$ {}^{0}_{5}T = \begin{bmatrix} r_{11} & r_{12} & r_{13} & p_x \\ r_{21} & r_{22} & r_{23} & p_y \\ r_{31} & r_{32} & r_{33} & p_z \\ 0 & 0 & 0 & 1 \end{bmatrix} $$

$$r_{11} = C_1C_5(C_{23}C_4 - S_{23}S_4) + S_1S_5 \quad (1)$$

$$r_{21} = S_1C_5(C_{23}C_4 - S_{23}S_4) + C_1S_5 \quad (2)$$

$$r_{31} = C_5(S_{23}C_4 + C_{23}S_4) \quad (3)$$

$$r_{12} = -C_1C_5(C_{23}C_4 - S_{23}S_4) + S_1C_5 \quad (4)$$

$$r_{22} = -S_1S_5(C_{23}C_4 - S_{23}S_4) + C_1C_5 \quad (5)$$

$$r_{32} = -S_5(S_{23}C_4 + C_{23}S_4) \quad (6)$$

$$r_{13} = C_1(-C_{23}S_4 - S_{23}C_4) \quad (7)$$

$$r_{23} = S_1(-C_{23}S_4 - S_{23}C_4) \quad (8)$$

$$r_{33} = -S_{23}S_4 + C_{23}C_4 \quad (9)$$

$$p_x = d_5C_1(-S_{23}C_4 - C_{23}S_4) + a_3C_1C_{23} + a_2C_1C_2 \quad (10)$$

$$p_y = d_5S_1(-S_{23}C_4 - C_{23}S_4) + a_3S_1C_{23} + a_2S_1C_2 \quad (11)$$

$$p_z = d_5(-S_{23}S_4 + C_{23}C_4) + a_3S_{23} + a_2S_2 + d_1 \quad (12)$$

$$S_i = Sin\theta_i \quad , C_i = Cos\theta_i$$

and can be simplified as follows :

$$\begin{bmatrix} r_{11} & r_{12} & r_{13} & p_x \\ r_{21} & r_{22} & r_{23} & p_y \\ r_{31} & r_{32} & r_{33} & p_z \\ 0 & 0 & 0 & 1 \end{bmatrix} = \begin{bmatrix} C\alpha C\beta & C\alpha S\beta S\gamma - S\alpha C\gamma & C\alpha S\beta C\gamma + S\alpha S\gamma & p_x \\ S\alpha C\beta & S\alpha S\beta S\gamma + C\alpha C\gamma & S\alpha S\beta C\gamma - C\alpha S\gamma & p_y \\ -S\beta & C\beta S\gamma & C\beta C\gamma & p_z \\ 0 & 0 & 0 & 1 \end{bmatrix} \quad (13)$$

where α , β and γ are the global orientation of Roll, Pitch dan Yaw, $C\alpha$ is short for Cos α, $C\beta$ for Cos β , and $C\gamma$ for Cos γ. Therefore, Roll, Pitch dan Yaw can be calculated as :

γ =0, α =0, β =Atan2(r_{13},r_{33}) (14)

3. ANALITICAL SOLUTION OF INVERSE KINEMATICS

This inverse kinematics analysis will be used implemented for 5 degree of freedom milling robot movement simulation. The result of inverse kinematics solution is:

$$\theta_1 = A\tan2(p_y, p_x)$$

$$\theta_3 = A\tan2(\pm\sqrt{1-C_3^2}, C_3)$$

$$\theta_{23} = A\tan2(S_{23}, C_{23})$$

$$\theta_2 = \theta_{23} - \theta_3$$

$$\theta_4 = A\tan2(S_4, C_4)$$

$$\theta_5 = A\tan2(S_5, C_5)$$

4. SIMULATION TEST AND RESULT ANALYSIS

4.2.1 Milling Robot Movement

A sculptured part was modeled in a CAD-system, then it was then transferred to the CAM-system to generate 5-axis tool paths. Based on this, milling of the part is conducted to produce the so called CL-file. The CL-file (*cutter location file*) is a file which contain the *position* (*x, y, z*) and *orientation* (*i, j, k*) of the milling cutter. This information is the fed to the developed software as a sequence of target points (end points). Then, by using *inverse kinematics solution*, target point and orientation are converted to the *joint values*, so that the milling robots moves to the ordered position and orientation. The simulation is shown in Figure 2.

4.2.2 Accuracy

Accuracy of end-effector to the target point is then analysed which could be affected by :

- **Orientation change and part position.**

Orientation change and part position will affect the accuracy and effector. It can be seen in Table 3, where the test had been done in 5 times with different position and part orientation.

Table 3. Average of the end effector difference and target points (mm)

	X-X'	Y-Y'	Z-Z'
Per 4	15.39163	34.17442	0
Per 5	11.74469	11.32833	0
Per 1	11.72044	10.84376	0

Per 2	11.72044	10.84376	0
Per 3	0	0	0

The differences above is caused by the change of end effector orientation that would change *r11,r12,...,r33 value.* It would affect *θ2* and *θ3* that will move the robot arms, as shown in Figure 3.

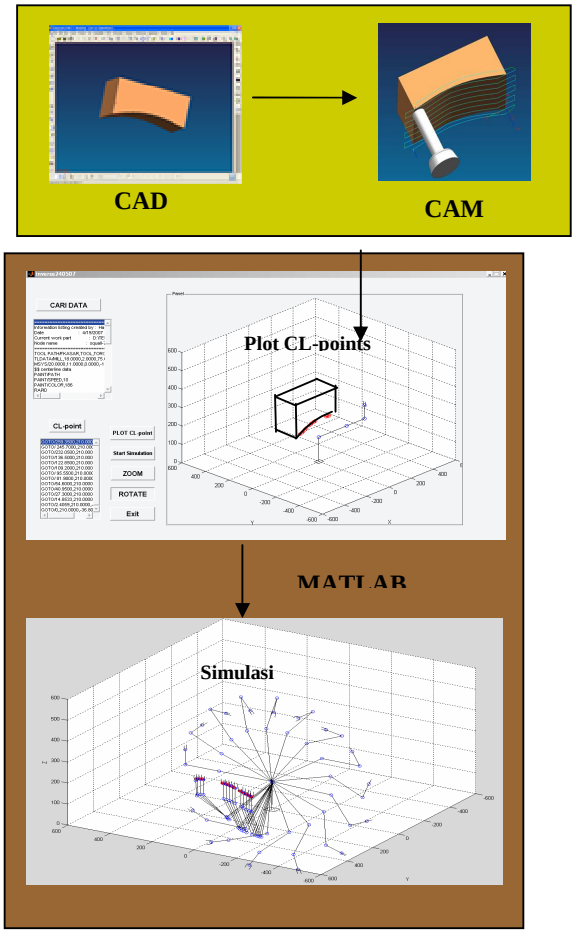

Figure 2. Process of milling robot's movement simulation

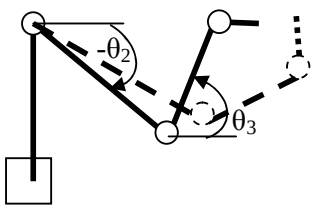

Figure 3. End effector differences after the change of orientation

- **Approach error**

A test is done to see the approach effect to the accuracy and effector to target point. The result is shown in Table 4.

Table 4. Relation between approach *and end effector position (mm)*

	Jumlah angka di belakang koma		
average	1	2	4
X'-X	23.7	15.45	15.8050
Y'-Y	20.9	21.88	22.1102
Z'-Z	45	8.18	0.3224

These approach differences occurred in sinus, cosinus, tangen value and also in significant value of π. π until 11 of significant value is 3.1428571248 if it is approximated into 2 significant value, it would be 3.1. The use of π in this research is very often in order to change the angle into radian. Since MATLAB cannot directly read the angle value in degree, so that it has to be convert into radian by using *(π/180)*degree.*

5. CONCLUSION

This research aimed to develop the system simulation of 5 degree of freedom milling robot movement. The simulation is done by placing the model of a part on robot working environment and the motion is done based on the information of cutter location point (CL-Point). This information is changed into joint angle by using analytic inverse kinematics. Based on the result, the orientation and the position from object is determining the end effector acuracy of milling robot, and the accuracy is also determined by *approach error*.

REFERENCES

1. Craig,, J. J., *Robotics Mechanic and Control*, Addison-Wasley, USA, 1986
2. John Q. GanDieter; Eimei Oyama; Eric M. Rosales; Huoshen Hu, *A complete analytical solution to the inverse kinematics of the Pioneer 2 robotic arm*, robotica(2005) volume 23 pp.123-129,2005
3. Duane, Hanslemen; Bruce, Littlefield, *Matlab Bahasa Komputasi Teknis*, Penerbit Andi, Yogyakarta, 1997
4. *Mitsubishi Industrial Micro-Robot System Model RV-MI MoveMaster EX technical Manual*, Mitsubishi Electric Corporation, Japan.
5. *Matlab Creating Graphical User Interfaces*, The MathWorks, Inc,2000-2006
6. Refaat Yousef Al Ashi; Ahmed Al Ameri, *Introduction to Graphical User Interface (GUI) MATLAB 6.5*, Uae University College Of Engineering Electrical Engineering Department Ieee Uaeu Student Branch.

7. Koren, Yoram, *Robotics for Engineers*,McGraw-Hill, Singapore, 1978
8. Dr. Ir. Gandjar K, M.Eng, *Diktat Kuliah: Otomasi dan Robotika*, Departemen Teknik Mesin Universitas Indonesia, 2006
9. Sciavicco, Lorenzo; Bruno Siciliano, *Modeling and Control of Robot Manipulators*, McGraw-Hill, Singapore, 1996.
10. Yuyut Wibowo, *Perancangan Frame koordinat joint dan simulasi robot artikulasi lima derajat kebebasan untuk web-based robot control*, Skripsi, Departemen Teknik Mesin Universitas Indonesia, 2006
11. Matriks Rotation. http://www.euclideanspace.com/maths/geometry/rotations , 5 januari 2007
12. Parthiban Delli, Ming Leu, *Unigraphics-NX3 For Engineering Design*, Department of Mechanical and Aerospace Engineering University of Missouri
13. Steven C. Chapra, Raymond P. Canale, *Metode numerik untuk teknik*, Penerbit Universitas Indonesia (UI-Press), 1991

ISSN: 1411-1284

Effects of Parallel and Zigzag Blade Configurations and Flow Passage in Casing Cover on Centrifugal Pump Peformance

Harinaldi* dan Sugeng Sunarto**

*) Departement of Mechanical Engineering
Faculty of Engineering University of Indonesia Kampus Baru-UI, Depok, Jawa Barat, 16424
E-mail: harinald@eng.ui.ac.id
**) Pump Division, PT. National Gobel, Jakarta

Abstracts-**This paper discusses a product design development of a commercial household waterpump. The pump is a turbine-impeller type centrifugal pump with an original total head 28 m and maximum capacity 30 l/min of water. The design development of the pump is conducted by considering the fluid dynamics aspects of the flow inside the pump while maintaining the same specific driving power to that of available commercial type. In order to do this, the blade configuration and the flow passage in the pump casing are modified. Two blade configurations i.e parallel and zigzag arragement are investigated and in each arragement three flow passage angles ($0,5^o$, $1,0^o$ dan $2,0^o$) of casing cover are used in the modified pumps and their peformance is experimentally determined. The pump test is conducted in a pump test-bench equipped with open-loop water channel driven by a single-phase condensor-run induction motor (125 W, 220 V/50 Hz) following the standard of Hydraulic Standard Institute by measuring the pressure at suction and discharge line, the angular speed, the power of driving motor and the time needed to fill a standard glass with water. Some results of common formance characteristics including the relations between water head, flow capacity, water horse power, break horse power and pump efficiency are then presented in characteristic curves of pump peformance to be further analysed. It is found that the variation of blade arrangements give less significant effects to the pump peformance compared to that of variation of flow passage in casing cover. The maximum pump efficiency up to 16% and larger capacity are obtained by using casing cover with flow passage angle 0.5^o. Meanwhile, maximum total head up to 31 m can be obtained by using casing cover with flow passage angle 1^o. With larger flow passage angle (2^o) both total head and pump efficiency decrease drastically. On the other hand, sound measurement shows more significant difference of noise level between the pump with parallel and zigzag arrangement of the blades for the same flow passage angle of casing cover.**

Key words :
Centrifugal pump, blade configurations, flow passage angle, pump casing, noise level

1. Introduction

Centrifugal pumps have been widely utilized for industrial as well as daily life purposes. The specifications and technological modes in such pumps have developed over the century so that nowadays there are more than enough choice for the user to find out suitable pumps to fit their needs. Especially for pump manufacturers, the development of pump design with better peformance and more efficient in energy consumption as well lower production cost has been the main interest. Some of the works on centrifugal pumps include those of Henshaw [1980] who patented his invention on modified volute pump casing claimed to reduce radial load by approximately 45% without significantly affecting capacity, head pressure or efficiency. In one aspect of the invention, he discovered that the loads imposed on the impeller shaft can be decreased when the centrifugal pump is operating below its best-efficiency-point capacity by increasing the casing flow area above that of a true volute casing in the area from just downstream of the cutwater towards a point generally opposite the cutwater. Meanwhile, Osborne, et.al [1988] investigated and patented his invention on low specific speed pump casing construction. The casing of an otherwise conventional low specific speed centrifugal pump was modified by enlarging its pump chamber and discharge passage, as compared to a like pump of a given output flow rate, and a restrictor was placed adjacent the outlet end of the discharge passage for purposes of throttling the flow

output from the pump to a value equal to such given flow rate. The interior of the pump casing was enlarged as required to reduce the flow velocity of pump fluid therewithin to an extent such that minor variations in size and surface finish occasion substantially less frictiion loss than encountered in a comparable pump having the same discharge flow rate. The required percentage increase in the size of the pump interior tend to increase, as specific speed decreases, in that interior flow velocities, and thus losses due to frictional effects tend to increase as the value of specific speed decreases. Tatebayashi and Tanaka [2005] investigated the various characteristics of screw-type centrifugal pumps both experimentally and numerically and found that three back flow regions existed in this type of pump. Among these, the back flow from the volute casing toward the impeller outlet was the most influential on the pump performance. Thus the most important factor to achieve higher pump performance was to reduce the influence of this back flow. One simple method was proposed to obtain the restraint of back flow and so as to improve the pump performance. This method was to set up a ringlike wall at the suction cover casing between the impeller outlet and the volute casing. Impellers with splitter blades have been used in turbomachinery design for centrifugal pumps by Usta and Pancar [2007]. In their study, impellers having a different number of blades (z=3, 4, 5, 6, and 7) with and without splitter blades (25, 35, 50, 60, and 80% of the main blade length) were tested in a deep well pump. The effects of the main blade number and lengths of splitter blades on the pump performance have been investigated. While the number of main blades and the lengths of the splitter blades of a principal impeller were changed, the other parameters such as pump casing, blade inlet and outlet angles, blade thickness, impeller inlet and outlet diameters, were kept the same. As the results it was found that increasing the number of blades increases the head of the pump, however, it causes a decrease in efficiency due to the blockage effect of the blade thickness and friction. The impellers with splitter blades between two long blades can be used to alleviate the serious clogging at the inlet of the impeller caused by more blades.

Considering the possibilities to improve pump peformance by variying some design parameter indicated by previous investigations, this work is aimed to improve the product design of a comercial household water pump of centrifugal type with turbine impeller design which has a specification of total head 28 m of water and maximum capacity of 30 l/min. Design improvement is conducted by considering the fluid dynamical aspect of water flow in the pump while maintaining the driving power to be similar to that of available comercial pump. This has been done by make some modification on the blade configurations and flow passage in the casing cover.

2. Experimental Method

The experimental work was conducted by following the standard of Hydraulic Standard Institute for pump testing. The test measured pressures at suction and discharge line, angular velocity, electric potential, current and power of driving motor as well as the duration to fill the standard glass of certain volume. The pump testing was done in a test-bench which consisted of an open loop water flow. The sketch of testing installation and apparatus is shown in Fig. 1.

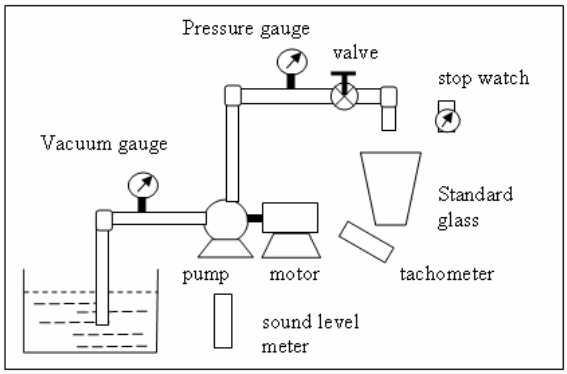

Figure 1. Schematic of Pump Testing Installation

The test bench was equipped with a single-phase condenser-run induction motor operate at 220V/50Hz and consume input power of 125 Watt. In the test, the motor shaft was directly coupled with pump shat so that loses in power transmission can be neglected. Measurement apparatus used in this experiment were well calibrated and included Bourdon type pressure gauge (Yamamoto, JIS B-7505), non-contact type digital tachometer (Line Seiki TM 1002), digital stopwatch, standard glass, sound level meter (Extech-407730) and JIS C1102 class 0.5 voltmeter, ammeter and wattmeter (Yokogawa). Using these instruments, the measurement uncertainties for pressure and flow capacity could be maintained below 1 % dan pump rotation of which were in the acceptable range suggested by the Hydraulic Standard Institute for maximum uncertainties of ± 2%, ± 2% for pressure and flow capacity measurement respectively. The tested pump was a commercial water pump turbine impeller type-centrifugal pump (National – GP-125JB) with original specification of total head 28 m and maximum flow capacity30 l/min. In this commercial version, the pump has standard construction of parallel blade arrangement between two faces of impeller and flat casing cover (0O flow passage along volute). In the current investigation, the pump was tested using two configurations of

blade arrangement i.e parallel (original one) and zig-zag (modified one). Besides the blade configuration, the flow passage angle in casing cover was also varied into three condition 0.5, 1 and 2 degree. Both impeller and casing were manufactured by an accurate machining process using CNC so that the required dimensional accuracy can be obtained. Figure 2 shows the detail dimension as well as the pictureof impeller and casing cover construction.

The pump testing with modified impeller arrangements and casing cover was done with constan pump rotation of ± 3000 rev/min. For each condition of discharge valve opening, the reading of where γ specific weight of water.

each measurement apparatus was done 7 times and time interval of each reading was set to 5 minutes. Measurement readings included suction (hgs) and discharge (hgd) pressures, flow capacity (Q), and motor power (Pm) and noise level. Hence, the total head (H), water power (Pw) and pump efficiency (ηp) could be determined with the following formulas:

$$H = h_{gd} - h_{gs} \quad (1)$$

$$P_w = \gamma QH \quad (2)$$

$$\eta_p = P_w / P_m \quad (3)$$

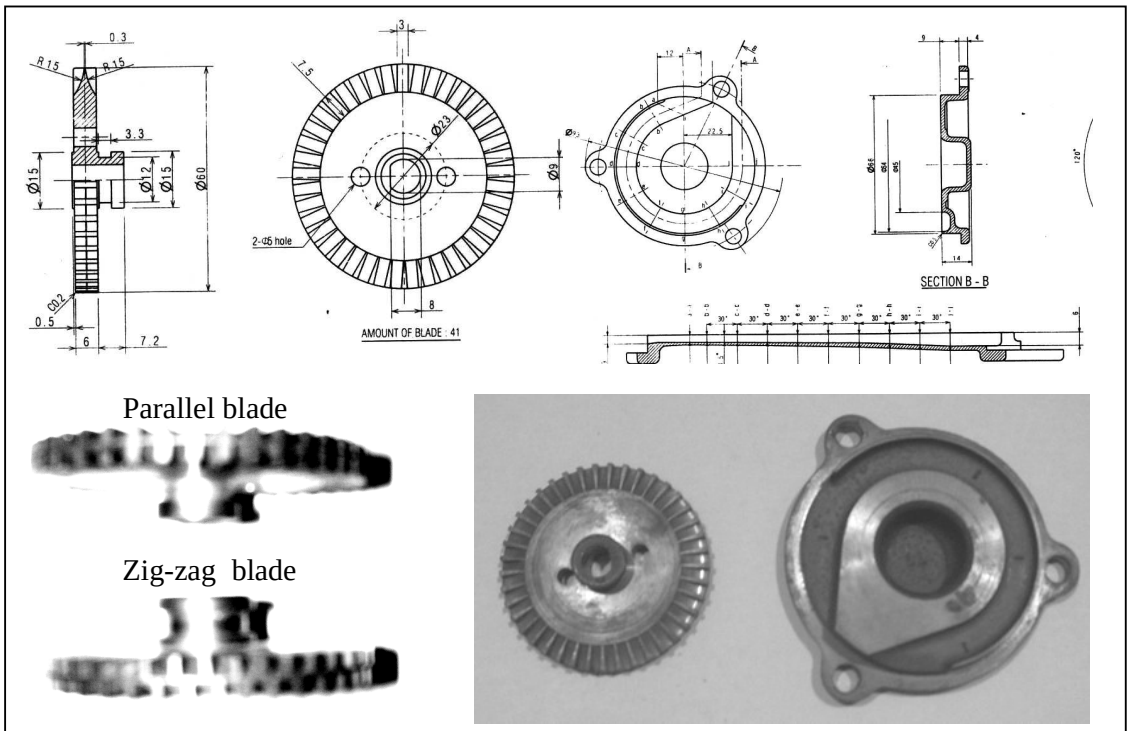

Figure 2. Impeller and casing cover construction

3. Results and Discussion

Some results of pump performance parameter including the relation between head, capacity, water power, motor power and pump efficiency are then presented in standard pump diagrams as shown in Figs. 3-5, and further analysed.

Figure 3 shows the Q-H curves for the tested pumps with (a) parallel blade arrangement and (b) zig-zag blade arrangement with all variations of casing cover used in the experiment. The curves are drawn for pumps operating at 3000 rev/min. It is clear from the figures that both blade arrangements show similar tendency with respect to the variation of cover casing. It can be observed that flow passage angle variation give significant effect to the pump peformance. Increasing the flow passage angle of casing cover up to 1o will increase the total head at the same pump capacity. A maximum total head up to 31 m can be obtained by using casing cover with flow passage angle 1o.This improvement is more significant in the lower range of pump capacity up to half of maximum capacity (± 15 l/min). For upper range of pump capacity, the effect becomes less significant and especially at pump with zig-zag blade arrangement this effect tends to vanish. However, further increase of flow passage angle of casing cover to 2o will give a very significant but opposite effect to the Q-H characteristics. The curve shift down below the other curves and the total maximum head can reach only 12 m with maximum capacity of 23 l/m.

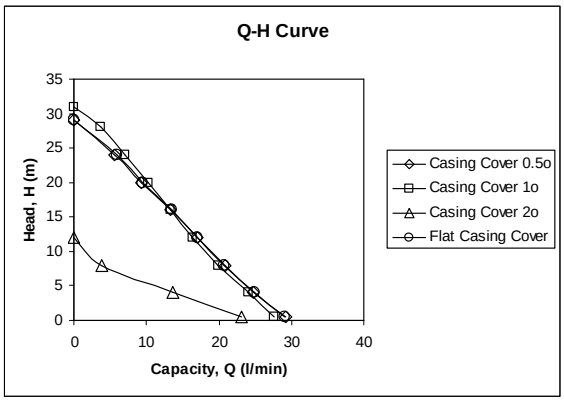

(a) parallel blade

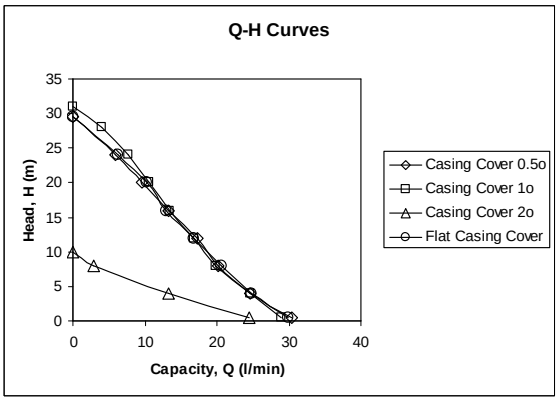

(b) zig-zag blade

Figure 3. *Q-H* curves of pump peformance (*n* = 3000 rpm) for (a) parralel and (b) zig-zag blade

Characteristics curves of pump water power, Pw - Q for the tested pumps with (a) parallel blade arrangement and (b) zig-zag blade arrangement with all variations of casing cover used in the experiment are shown in Fig. 4. For parallel blade arrangement, it is seen in Fig. 4(a) that the curves for the cases of flat casing cover and flow passage angle 0.5o almost coincide for the whole range of pump capacity with a slight higher value of the maximum water power for 0.5o casing cover. This maximum power is the highest for all the cases of parallel blade arrangement being tested. Meanwhile for zig-zag blade arrangement, the highest maximum water power is obtained with casing cover having flow passage angle 1o as shown in Fig. 4(b). For the case of casing cover with flow passage angle 2o, it is clear in both blade arrangements a similar tendency to the previous characteritics curve in which the increase of flow passage angle will reduce the water power drastically.

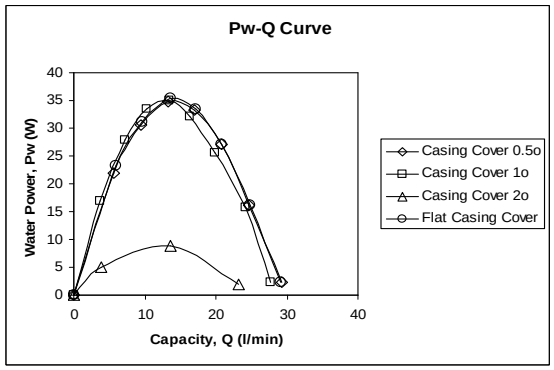

(a) parallel blade

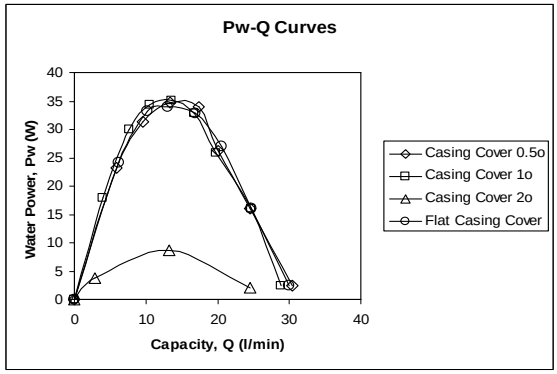

(b) zig-zag blade

Figure 4. *Pw-Q* curves of pump peformance (*n* = 3000 rpm) for (a) parralel and (b) zig-zag blade

Figure 5 shows the efficiency-capacity curves, η_p –*Q*, for the tested pumps with (a) parallel blade arrangement and (b) zig-zag blade arrangement with all variations of casing cover used in the experiment. For parallel blade arrangement, it is seen in Fig. 5(a) that the curves for the cases of flat casing cover and flow passage angle 0.5^o almost coincide for the whole range of pump capacity. The best efficiency point (BEP) for the curves are reached at the capacity around 16.3 l/min with a slight higher value of the BEP for 0.5^o casing cover. For all the case observed, the maximum efficiency up to 16.24% is obtained by using casing cover with flow passage angle of 0.5^o. Meanwhile for casing cover with flow passage angle 1^o, the efficiency curve shifts toward lower capacity value with BEP reached at 14 l/min. On the other hand, for zig-zag blade arrangement as shown in Fig. 5(b), all the efficiency curves but the case of flow passage angle 2^o almost collapse into single curve except in the region of BEP. For all the case observed, the maximum efficiency up to 16.40 % is obtained by using casing cover with flow passage angle of 0.5^o at the flow capacity of 17.4 l/min. Furthemore, just like two other characteristics curves, in case of flow

passage angle 2^o, it is clear that in both blade arrangements the pump efficiency decrease drastically.

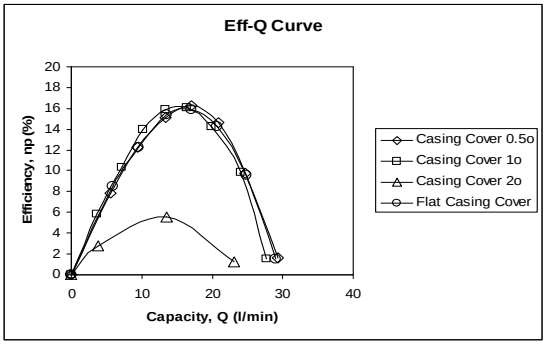

(a) parallel blade

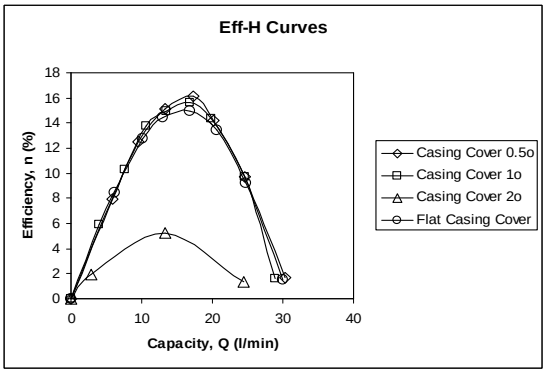

(b) zig-zag blade

Figure 5. *Eff-Q* curves of pump peformance (n = 3000 rpm) for (a) parralel and (b) zig-zag blade

Figure 6 shows the noise level ratio of the pump with zig-zag blade to the pump with parallel (I_z/I_p) arrangements. The noise level was measured with varied pump speed starting from low rotation until its operational speed of ± 3000 rev/min with half-opened discharge valve. The presented data in only for the case of casing cover with flow passage angle 0.5o since for other cases the tendency is similar. The figure indicates a more significant difference of noise level between the pump with zigzag and parallel arrangement of the blades for the same flow passage angle of casing cover. The pump with zig-zag blade arrangement tends to operate with less noise for all range of pump speed. The ratio of noise level is slightly increase as the pumps operate with higher speed.

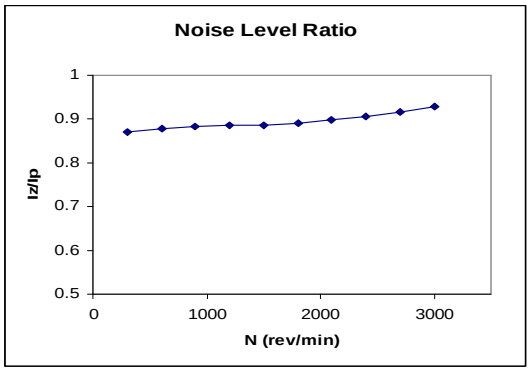

Figure 6. Noise level ratio of the pump with zig-zag blade to the pump with parallel arrangements.

Considering all the pump characteristics curves previously discussed, it can be seen that effort to improve pump peformance by varying either the blade arrangement or the flow passage angle can give prefered results under some certain conditions. It seems that the variation of blade arrangements give less significant effects to the pump peformance compared to that of variation of flow passage in casing cover. Increasing the flow passage angle up to 1^o can increase the total head up to 31 m which means significant increase of 10.7 % from the standard commercial design of flat casing cover. Meanwhile, although not too significant there is indeed around 3 % improvement of maximum efficiency when using casing cover with flow passage angle of 0.5^o. Further increase of flow passage angle in casing cover will decrease the whole peformance of the pumps drastically regardless the type of blade arrangement. The main reason to this significant decrease may be due to the change of flow pattern in the flow passage of casing volute having enlarged cross sectional area. The formation or backflow region reported by Tatebayashi and Tanaka [2005] which can influence the pump peformance could be the main mechanism responsible to the decrease of peformance of the pump with larger flow passage angle of casing cover. To elucidate this mechanism, in the future further investigations focussing on the diagnostic of detailed flow field inside the pump casing is needed.

4. Concluding Remarks

The characteristics of modified turbine-impeller type centrifugal pump has been investigated experimentally following the pump testing standard. The effect of blade configuration and flow passage angle variation in the casing cover to the total head developed by the pump, water power, pump efficiency and noise level of pump operation has been the focuss of the investigation. Some results show that the variation of blade arrangements give

less significant effects to the pump peformance compared to that of variation of flow passage in casing cover. The maximum pump efficiency up to 16.24 % and larger capacity are obtained by using casing cover with flow passage angle 0.5o. Meanwhile, maximum total head up to 31 m can be obtained by using casing cover with flow passage angle 1o. With larger flow passage angle (2o) both total head and pump efficiency decrease drastically. On the other hand, sound measurement shows more significant difference of noise level between the pump with parallel and zigzag arrangement of the blades for the same flow passage angle of casing cover. The pump with zig-zag blade arrangement tends to operate with less noise intensity.

Acknowledgement
Financial support of this work by Pump Division, P.T National Gobel, Jakarta is gratefully acknowledged.

References

Henshaw, T.L., 1980, "Modified Volute Pump Casing", United States Patent 4213742.

Hydraulic Institute, 1983, "Hydraulic Institute Standards for Centrifugal, Rotary dan Reciprocating Pumps", Ohio, USA.

Osborne, J.C, and Murphy P.T, 1988, " Low Specific Speed Pump Casing Construction", United States Patent 4789301

Tatebayashi, Y and Tanaka, K, 2005, "Pump Performance Improvement by Restraining Back Flow in Screw-Type Centrifugal Pump", Journal of Turbomachinery, Vol. 127, Issue 4, pp. 755-762

Usta, N and Pancar, Y., 2007, "Effects of Splitter Blades on Deep Well Pump Performance", Journal of Energy Resources Technology, Vol. 129, Issue 3, pp. 169-176

ISSN: 1411-1284

Determination of Flow Properties of Mud Slurry

Ridwan (*), Yanuar (**), Budiarso (**), and Raldi AK (**)

(*) Mechanical Engineering Department, Gunadarma University, Jakarta
E-Mail: ridwan@staff.gunadarma.ac.id
Telphone: (+62) 21 7888 1112
(**) Mechanical Engineering Department, University of Indonesia, Depok

Abstract-Although many types of viscometer are available, most of them are quite unsuitable for collecting scientific or engineering data. Due to various features of their construction make it impossible to determine both shear stress and shear rate at the same known point in the equipment. The flow curve therefore can not be constructed from data obtained with such devices. Most of these unsatisfactory instruments give complex reading functions of several type of fluid properties. The aim of this study to examine the viscous properties and to make curve of mud slurry by horizontal pipe as viscometer. These viscometer determine relationships between shear stress and shear rate. The diameter of pipe was 12,7 mm. The length of pipe was 1000 mm. Calculated the shear stress and the shear rate by measuring the pressure loss gradient and the gradient of velocity, respectively. Weight fraction of mud slurry were 20 %, 30 % and 45 %. The results indicated the apparent viscosity of mud slurry is not proportional to the shear stress and shear rate but the relationship could be approximated by power law's mode with the index n = 0.93 – 1.0

Keywords: shear stress, shear rate, flow curve, mud slurry, horizontal pipe, viscometer, apparent viscosity.

I. INTRODUCTION

The hydraulic transport of solids in pipes is economically attractive in comparison to transport by truck, railway or ship. The goods transported over long distances are mainly coal and iron ore and the carrier fluid is water. Since the longest pipelines for the hydraulic transport are about 400 km in length, by using drag reducing additives considerable energy saving should be possible in the hydraulic transport of solids. Mud slurry is essentially a mixture of solids and liquids. Its physical characteristics are dependent on many factors such as size of particles, concentration of solids in the liquids phase, size of the conduit, temperature and viscosity of the carrier [1]. The flow slurry in a pipeline is much different from the flow of a single-phase liquid. Theoretically, a single-phase liquid of flow absolute (or dynamic) viscosity can be allowed to flow at slow speeds from a laminar flow to turbulent flow. If the slurry's speed of flow is not sufficiently high, the particles will not be maintained in suspension. On the other hand, in the case of highly viscous mixture will be too viscous and will resist flow. The flow regimes were classified into six categories: homogeneous flow, heterogonous flow, fully moving bed, part stationary bed and stationary bed, and the empirical formulations to estimate the pressure drop in two phase flow was obtained. [6]

The aim of this study to examine the viscous properties and to make curve of mud slurry by horizontal pipe as viscometer. These viscometer determine relationships between shear stress and shear rate.

II. BASIC THEORY

The Pressure drop flow throught a section of pipe a constant diameter between two location 1 and 2 can be write: [1]

$$F_{12} = \frac{\pi}{4} D^2 (P_1 - P_2)$$

This force is balanced by the friction Force, Fr

$$F_r = \tau_w \pi D L$$

Where L is the distance between point 1 and 2

$$\frac{\pi}{4} D^2 (P_1 - P_2) - \tau_w \pi D L = 0$$

or

$$\tau_w = \frac{D(P_1 - P_2)}{4L} = \frac{D\Delta P}{4L} \qquad (1)$$

where D is pipe inner diameter, and τ_w wall shear stress.

For a Newtonian fluid the shear stress is proportional to the velocity gradient (shear rate), can be write: [2,3,4]

$$\tau_w = \mu \frac{\partial u}{\partial y} \quad (2)$$

Where ϑu/ϑy is Shear rate (velocity gradient). The constant of proportionality (μ) is called the Newtonian viscosity. The Newtonian viscosity depends only on temperature and pressure and is independent of the rate of shear. The diagram relating shear stress and rate of shear the so – called flow curve, see fig.1

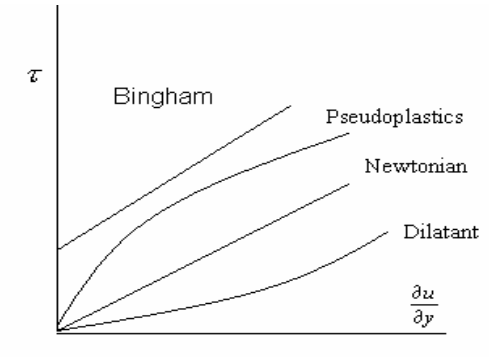

Fig 1. Flow curves
Newtonian and non-Newtonian Fluids [1],[7]

Non Newtonian fluids (Bingham, Pseudoplastics, and dilatants) are those for which the flow curve is not linier. The "viscosity" of a non Newtonian fluids is not constant at a given temperature and pressure but depends on other factors such as the rate of shear in the fluids. Non-Newtonian fluids may be described by rheological equation of the form: [5,7]

$$\tau_w = \mu_a \left(\frac{\partial u}{\partial y} \right)^n = \mu_a (\gamma)^n \quad (3)$$

where μ_a is apparent viscosity, 'n ' is power law Index, and γ shear rate

Power Law Index (n), can be write from equation:[10]

$$n = \frac{Log \frac{\tau_1}{\tau_2}}{Log \frac{\gamma_1}{\gamma_2}} \quad (4)$$

The relationship between volume percent solids, solids specific gravity of the suspending medium, and the weight percent concentration of solids is given as follows: [7,8]

$$Cw = \frac{Cv\rho_s}{Cv\rho_s (100 - Cv)} = \frac{Cv\,\rho_s}{\rho_m} \quad (5)$$

where Cw is weight percent solids, Cv is Volume percent solids, ρs density of solids, and density of mixture.

III. EXPERIMENTAL SETUP

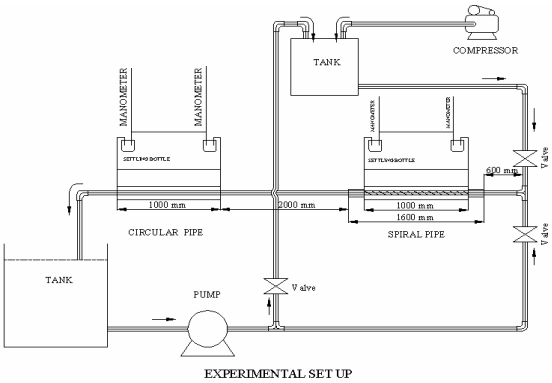

Fig.2. Experimental Set Up

The experimental set up was shown in fig.2. The mud slurry were circulated by pump and collected in tank where they were mixed to uniform concentration. The pressure drop was measured at 1000 mm length between each pressure tap by manometer through a settling bottle. The inner diameter of test pipe was 12,7 mm. The shear stress and the shear rate can be obtained by measuring the pressure loss gradient and the gradient of velocity, respectively. Weight fraction (Cw) of mud slurry was 20 %, 30 % and 45 %. The temperature was keep at 27 ^{o}C.

III. RESULTS AND DISCUSSION

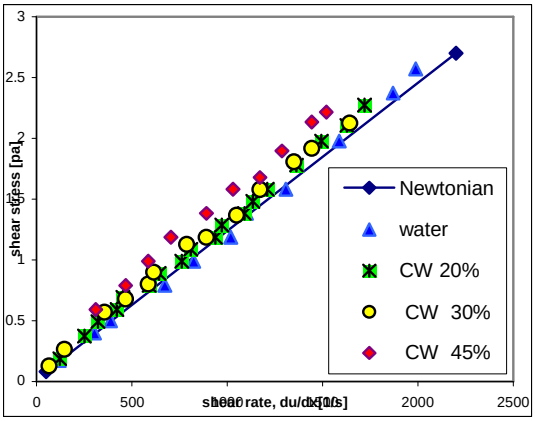

Fig.3. Flow curve of mud slurry

Fig.3 shows the flow curve of the mud slurry solution measured using a horizontal pipe. The temperature of mud slurry was maintained at T = 27 ± 0.5 ^{o}C throughout the experiments because the mud slurry rheology is temperature dependent. The effect of mud slurry degradation on the result was examined by means of pipe friction loss measurement at the start and end of the experiment. The plot data for Cw = 45 % is not linier, indicating that the material is a power law fluid over this range of shear stress.

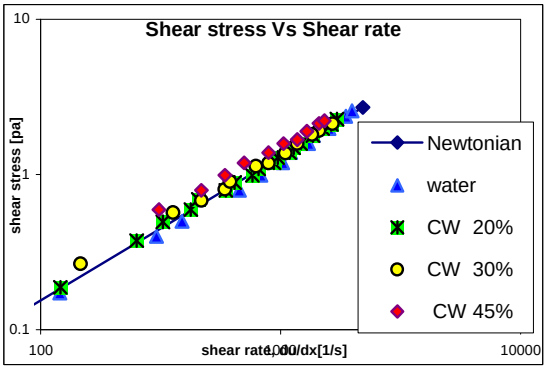

Fig.4. Flow curve of mud slurry (log-log)

In Figure 4. Using standard tangent-drawing procedures, tangents are drawn to the curve at various 8V/D, to obtain corresponding value of n from the tangent slop K from the tangent intercept at 8V/D equal to unity. The flow curve shear Stress τ is plotted against shear rate, du/dx for mud slurry.

The plot is linier, indicating that the material of mud slurry is a power law fluids over this range of shear stress. Since the value from all there weight fraction of solution on the same single curve, the value of power law index for mud slurry were n = 0.93 – 1.0.

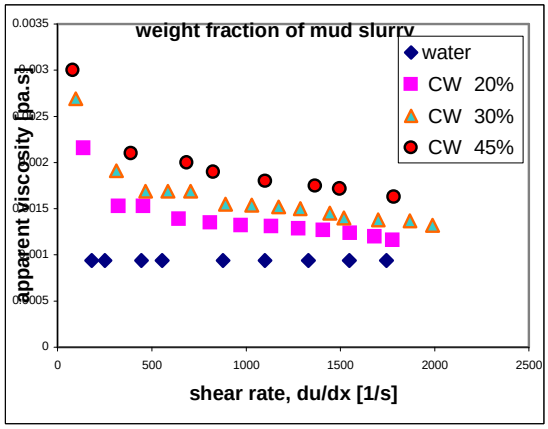

Fig.5. Apparent Viscosity of mud slurry

Measurement of the viscosity of mud slurry was carried out by horizontal pipe viscometer, and the data of 20 %, 30 %, and 45 % weight fraction of mud slurry, Cw solution are presented apparent viscosity versus shear rate in fig.5. It can be seen that the viscosity increased with decreasing shear rate although tended to a constant value in the high shear rate region. The viscosity differed with the type of viscometer and the hysteresis of the viscosity occurred. Because the viscosity of mud slurry was complicatedly depend on many parameters, the generalized Reynolds numbers was calculated using the apparent viscosity of mud slurry.

IV. CONCLUSIONS

Curve flow characteristics of mud slurry were measured by horizontal pipe viscometer and calculated the shear stress and shear rate at the wall by the measurement of flow rate and the pressure loss. The results are summarized follows:

The mud slurry behaves as the Newtonian fluids for Cw 20 %, 30 % and the shear thinning fluid (pseudoplastics fluid) for Cw = 45 %. The power law model describes approximately the behavior of mud slurry and the range of the power law fluids index is n = 0.93 ~ 1.0.

List of Symbols

Cw = weight percent solids (%)
Cv = Volume percent solids (%)
D = Pipe inner diameter (m)
K = Power Law coefficient
L = length (m)
n = Power Law index (-)
U = Mean velocity (m/s)
τ_w = wall shear stress (Pa)
ρ = density [kg/m^3]
γ = du/dx = shear rate (1/s)
γ = 8 U/D
μ_a = Apparent viscosity (Pa.s)

τw = wall shear Stress (Pa)
ρ_s = density of solids (kg/m^3)
ρ_m = density of mixture (kg/m^3)

REFERENCES

1. Abulnaga, "Slurry Handbook", McGraw-Hill, 2002
2. Monji H, Matsui, G, and Saito, T, "Pressure drop Reduction of Liquid-Particles Two-Phase flow with nearly equal Density". Proceeding of the 2 nd International comprence on Multiphase flow. Kyoto. Japan. 1995
3. Shah, S.N, Lord, D.L. "*Critical velocity correlation for slurry transport with non-Newtonian Fluids",*. AIChE Journal, Vol.37. No.6. 1991
4. Usui, H, Et.all. "*Viscosity Prediction of Dense Slurries Prepared by Non-Spherical Solid Particle"*. Journal of Chemical Engineering of Japan, Vol 34, no.3 pp 360 – 368. 2001
5. Usui, H. "*Prediction of Dispersion Characteristics and Rheology in Dense Slurry"*, Journal Of Chemical Engineering of Japan, Vol 35, no.9 . pp 815 – 829.2002
6. Watanabe, K. "*Drag Reduction on Fly Ash Slurries in a Spiral Tube"*.Elsevier science Publishing company, Inc. Pp 693 – 700. 1988.
7. Wasp, J.E, Kenny P.J, Ghandy, R.L. "*Solid –Liquid flow Slurry Pipeline Transportation",* Trans Tech Publication. Clausthal, Germany. 1977
8. Weir, "*Pumping Non-Newtonian Slurries"*. Technical Bulletin, no. 14. 2007
9. Yanuar dan Damawidjaya. "*Koefisien gesek aliran dua fase pada Pipa Spiral"*. SNTTM V. UI. Depok. .2006
10. Yanuar. "Kurva Aliran dengan Koaksial Silinder Putar". Jurnal teknologi. UI. No.2 . Hal 121-123. 2007

ISSN: 1411-1284

Development of Prototype of Hybrid Vehicle Controller

Gandjar Kiswanto, Danardono AS, Endiandika TP, Pranadityo

Laboratory of Manufacturing Technology – Mechanical Engineering,
University of Indonesia, UI New Campus, Depok - Indonesia
gandjar_kiswanto@eng.ui.ac.id, endiandika@gmail.com, pranadityo@gmail.com

*Abstract-**Hybrid vehicle use two types of engine for the propulsion, a gasoline engine and an electric engine. A controller is needed to make this hybrid system going well. Microcontroller is used to process the digital data that came from the input parameters. The vehicle parameters used by the microcontroller as an input are engine rotation (RPM), vehicle speed (km/h), and vehicle angle position. This parameter can be detected using encoder as sensor. Encoder counts the engine revolution that is converted into RPM and vehicle speed. It also can be used to determine angular position of the vehicle using mechanism attached to the encoder**.*
Keywords :Hybrid controller, control system

1. INTRODUCTION

Energy crisis become one of the serious problem that happens in the latest century. It focused on the lack supply of oil and gas being used in many industry and transportation vehicle as an energy source (fuel). There are many solutions for this problem, but the important things are to make energy source based on hydrocarbon, and more economical [1]. Along with the technology research, nowadays many vehicles are built based on the hybrid technology. A Hybrid Technology in a car or any others vehicle can be described as a vehicle that use two types of engine as a propulsion, electric motor engine and gasoline engine.

The hybrid vehicle can decrease the fuel consumption and increase the mileage. Thus, they are lowering the air pollution.

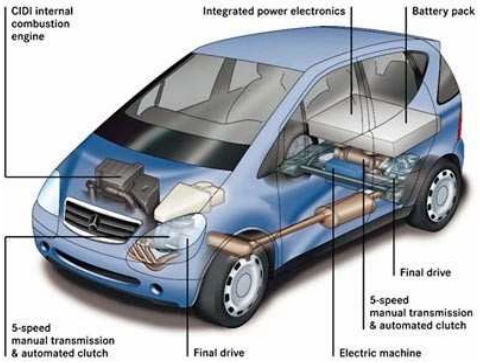

Pic 1. Hybrid Car[2]

Two types of engines in a hybrid car are working related to the conditions of the vehicle such as speed, torque, vehicle position in a road, and cruising. When the vehicle cruises with speed that is lower than 20 Km/h, the electric motor will be active. Higher than 20 Km/h, the gasoline engine will start to give some torque power, and the electric motor will shut down. If acceleration needed, the electric motor will turn on for a while giving additional torque for the vehicle. And also if the vehicle is decelerated, energy from the wheel will be converted into the potential energy to charge the battery.

Another example : a hybrid car can save a lot of fuel by shutting down the gasoline engine and only use the electric motor while the vehicle stop temporarily [3].

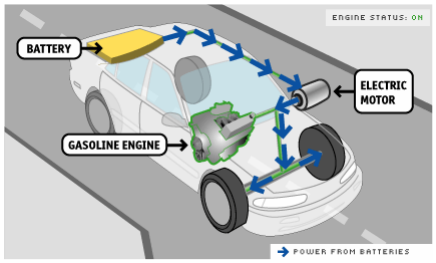

Pic 2. Hybrid car when cruising lower than 20 Km/h [3]

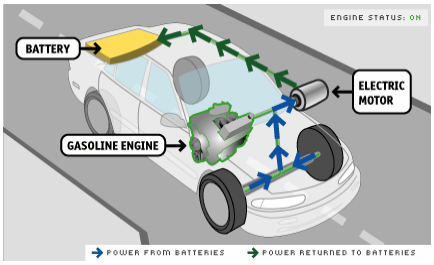

Pic 3. Hybrid car when re-generative breaking [3]

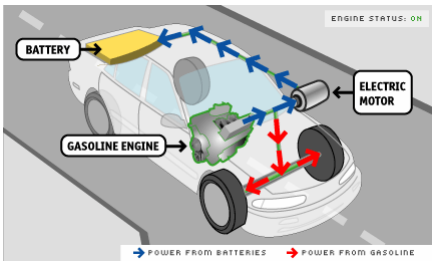

Pic 4. Engine configuration while the vehicle is accelerating [3]

2. CONTROLLER DESIGN AND METHODS

Microcontroller can be used to control the mechanism of the vehicle. Microcontroller will detect the input parameter and decide the operating mode for the vehicle such as speed controlling, charging the battery, and increasing the efficiency of gasoline engine.

All of these actions depend on the condition like engine RPM, engine vehicle, acceleration, speed vehicle, and road condition [4].

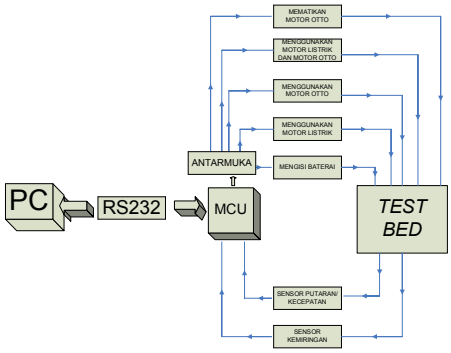

Pic 5. Hybrid control scheme

By identifying the sensors as an input, the microcontroller will give an artificial intelligence to the system.

These sensors will transmit the digital and analog signal into the microcontroller that have an equivalent value as the condition.

3. EXPERIMENTAL TEST BED DESIGN for HYBRID CONTROLLER

These characteristics will be simulated in a test bed, including the simulation of the engine RPM, vehicle speed, and also the position of the vehicle by measuring the angle related to the road or ground.

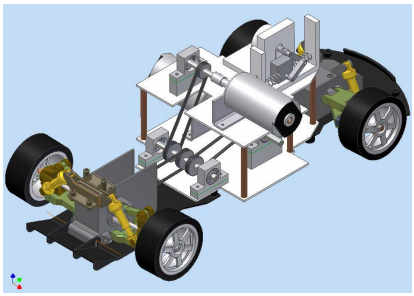

Pic 6. Prototype of the hybrid test bed

The engine RPM and the vehicle speed will be detected using an encoder as a rotary sensors. By using the same method as an engine RPM, the angle position can be measured by giving mechanism that attached to the encoder.

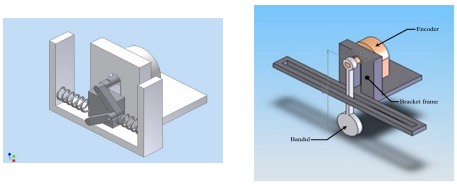

Pic 7. Prototype of the angle sensors

These two sensors and other parameter will be used as an input for the microcontroller to determine which operating mode will be used for the vehicle.

4. RESULT

Some of the vehicle mode with a different characteristic can be explained as follow:

- Silent Mode

The vehicle use electric motor connected to a battery as main propulsion. This mode only limited for a speed not more than 20 km/h. If the vehicle speed is increasing (more than 20 km/h), the vehicle will change to the next operating mode.

- Gasoline Mode

When the vehicle speed is more than 20 km/h, the vehicle will start the gasoline engine and turn off the electric motors.

- Acceleration/Climb Mode

Both engines will start to give enough torque for the vehicle when accelerating.

- Decelerate/Descend Mode

The electric motor will change as a generator to charge the battery.

All of this mode will be simulated into project test bed, which represents the real configuration of hybrid car, which are RPM and speed detection, and angle position detection.

These are photos from the latest progress of the project :

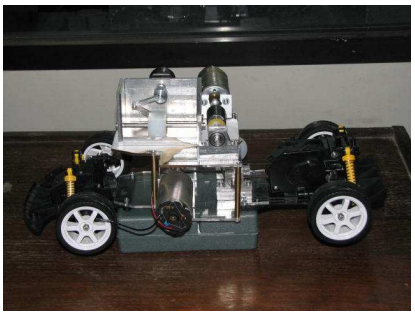

Pic 8. Experimental test bed (left)

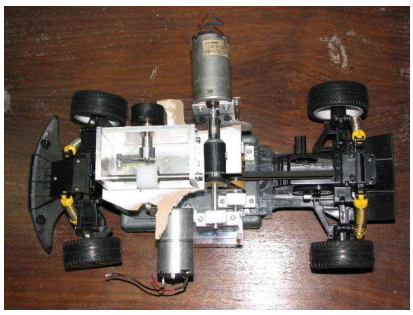

Pic 9. Experimental test bed (top)

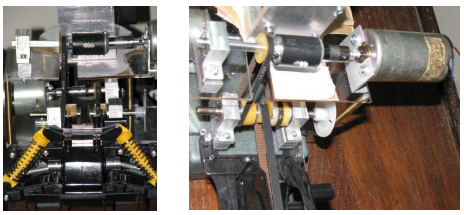

Pic 10. Drive train

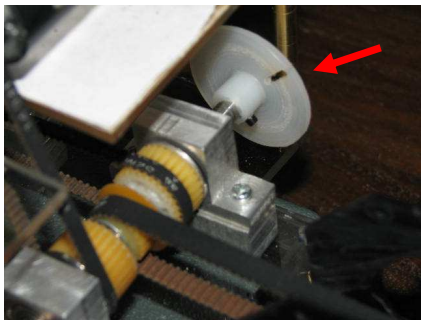

Pic 11. Encoder disc

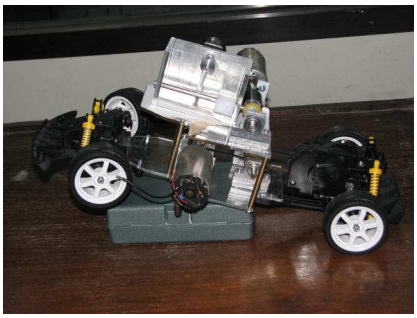

Pic 12. Climbing position

Pic 13. Descending osition

5. CONCLUSIONS AND FUTURE WORKS

The prototype of hybrid vehicle controller has been developed. The logic (and algorithm) functions for controlling shows an expected response to the input values and conditions. The prototype will be further tested on real enggagement of combustion engine and AC-motor which .

REFERENCES

[1] _____. 2004. *Kebijakan Energi Nasional 2003-2020 : Kebijakan Energi Yang Terpadu Untuk Mendukung Pembangunan Nasional Berkelanjutan*. Jakarta : Departemen Energi Dan Sumber Daya Mineral.

[2] _____. 2005. Bluerpint *Pengelolaan Energi Nasional 2005-2025*. Jakarta : Departemen Energi Dan Sumber Daya Mineral.

[3] Layton, Julia., dan Nice, Karim. 2007. *"How Hybrid Cars Work"*. Pada

http://auto.howstuffworks.com/*hybrid*-car.htm/printable, Tanggal 3 Maret 2007, pukul 10.25.

[4] _____. 2005. "*How Hybrids Work*". Pada http://images.google.co.id/imgres?imgurl=http://reviews.cnet.com/i/ct/hcbg/*hybrid*_braking.gif&imgrefurl=http://reviews.cnet.com/4520-10845_7-6212547-1.html&h=255&w=428&sz=23&hl=id&start=3&tbnid=jLhaxAcof9-tiM:&tbnh=75&tbnw=126&prev=/images%3Fq%3D*hybrid*%2Bcar%26gbv%3D2%26svnum%3D10%26hl%3Did%26sa%3DG, Tanggal 3 Maret 2007, pukul 11.33.

[5] Wong, William. 2005. "*Smart Motion Makes For a Smarter design*". Pada http://www.elecdesign.com/Articles/Print.cfm?ArticleID=11294, Tanggal 3 Maret 2007, pukul 10.25.

ISSN: 1411-1284

Role of fibres on the shear strength of peat Case: Tampan-Riau Peat

Wiwik RAHAYU
Department of Civil Engineering , Faculty of Technology - University of Indonesia,
Kampus UI Depok, 16424 – Indonesia, Fax. 62 21 7270028,
e-mai: wrahayu@eng.ui.ac.id

Abstract, *Peat soils are fragmented organic materials that undergo continuous chemical and biological changes, associated with further decomposition of the organic constituents. Consolidation time and rate is therefore of primary importance in their mechanical properties. The shear strength is a fundamental property in the analysis of soil stability during construction, as well as at the end of construction under the loads of structure. The paper presents results from an experimental study on the fibrous peat of Tampan-Riau, (Sumatra, Indonesia). Consolidated undrained triaxial tests on undisturbed samples were made under different conditions of strain rates and consolidation times to analyse the long-term shear strength of peat. The frictional character of the fibrous peat is highlighted by the high value of the friction angle (□') with a negligible value of the cohesion (c'). In order to examine the role of the fibres, the same tests were made on smaller samples from which the fibres had been removed. The comparison of the results between the two types of samples shows that the removal of the fibres gives the material behaviour similar to that of an overconsolidated clay. The role of the fibres in the shear behaviour of the remoulded peat still remains. The presence of the fibres in the initial state leads to a high value of the friction angle, as well as an important reduction in void ratio during consolidation. A scanning electron microscope was used to obtain high resolution observations of the peat, its composition, made after triaxial and consolidation tests to study the degradation of the fibres during the tests.*

KEY-WORDS : peat, triaxial, shear strength, consolidation, strain rate, SEM

1. Introduction

The variability of peat can be important, depending on the decomposition of the organic components. Geotechnical engineers classify peats into two types: the mud, which is called amorphous peat, and the woody mesh, fibrous peat. Fibrous peats feature a dual porosity structure composed of macro pores forming a very open network between the largest fibres, and micropores in the mud and between the smallest fibres. The major part of the moisture content of peats comes from the free water filling the macropores as the quantity of water adsorbed in the micropores is very small.

The shear strength of fibrous peats is very much influenced by the presence of the fibres. In a first phase, consolidation of the macro pores leads to a large decrease in void ratio and an increase in shear strength, as in other fine grained soils. In a second phase, if the consolidation time is large enough, consolidation of the micro pores will occur, resulting in a further increase in shear strength. Moreover, because of the orientation of the fibres during the tests, the shear strength continues to develop up to large deformations without showing a maximum (Lechoviscz 1993).

The peat is a frictional material with a very high internal friction angle compared to that of non organic soils. The value of the effective friction angle (') can reach 50° and 51°, respectively for undrained and drained triaxial tests on a finely- woody fibrous peat, and 48° in undrained tests on a rather fibrous peat. Edil and Dhowian (1981) obtained values of 50° for ' for an amorphous peat and 53° to 57° for a fibrous peat. Extensive experimental studies were also carried out by Soepandji et al. (1996) on Indonesian fibrous peats. The results show that the shear behaviour of the Indonesian fibrous peat is rather variable from one place to another, but that the material keeps a high friction angle ', ranging from 39 ° to 44°.

The prediction of peat behaviour is becoming important because of development projects in some areas of Indonesia which are formed of large deposits of peat. According to Rieley et al. (1996), Indonesia contains the largest area of peat in the tropical zone and is the third country in the world whose surface is

covered by peat. In this paper, the mechanical behaviour of a fibrous peat from Sumatra (Indonesia), derived from Consolidated Undrained (CU+u) triaxial tests, will be presented. The role played by the fibres in the mechanical behaviour will be highlighted by comparing the behaviour of the undisturbed material (with fibres) with that of the remoulded material from which the largest fibres had been removed. Observations of peat specimens with a scanning electron microscope (SEM) have been carried out to understand the effect of stress on both the fibrous parts and amorphous parts of the soil. The objective of the tests campaign is to improve the knowledge of peat behaviour and its modelling. The influence of such factors as the consolidation time and compression rate is studied.

2. Material and experimental method

The undisturbed samples were taken at depths of 0.50 m to 1.0 m in peat deposits of the Tampan-Riau area in Sumatra, by pressing a thin-walled sampler quickly and continuously into the soil on the base of a shallow pit. Tubes with sharp cutting edges and large diameters were used to reduce remoulding disturbance during sampling. As a sample with a diameter of 10 cm is required for the triaxial test, it was found that the use of tube with sharp cutting edge of 20 mm length enabled the tube to penetrate more easily into the soil.

The soil sample used is a dark brown fibrous peat. Like most peaty or organic soils, this material is normally acid and has high water content as well as high organic content and low bulk density, as shown in table 1 presenting the physical properties of Tampan-Riau peat. As comparison, usual values of the physical properties of peat have also been reported. The results of the chemical analyses are presented in Table 2. The high organic content is shown by the value of ignition loss which is about 75%. The SiO_2 content is unusual for peaty soil. That is probably due to the existence of sandy particles in our samples.

To study the effect of consolidation time, two series of tests were carried out as follows: (i) a series of tests with 4 days of consolidation and 1 %/h strain rate, (ii) a series of tests with 12 days of consolidation and 1 %/h strain rate. To study the role of the fibres, remoulded samples were prepared by removing most of the fibres: The peat was first dried, then crushed and passed through a 0.08 mm sieve; afterwards, the dry powder was mixed up with water, up to a water content of 573 %. Then, the specimens were consolidated in a small tube under vertical stresses increasing up to 100 kPa and placed in the triaxial cell. The triaxial tests were performed on the small samples, 35 mm in diameter and 70 mm in height (H/D = 2), with the same procedure as that of the tests on the undisturbed samples.

Table 1. Physical Properties of Tampan-Riau peat*, compared with the other Indonesian peat**

Physical Properties	Value*	Value**
Natural water content, w (%)	551	19 to 688
Apparent density, $_{.}$ (Mg/m^3)	0.95	1.03 to 1.28
Dry density, $_{d}$ (Mg/m^3)	0.16	0.16 to 0.35
Organic content, C_{MO} (%)	76	64 to 85
Density of solid particles, $_{s}$ (Mg/m^3)	1.51	1.37 to 1.87
Degree of acidity, pH	3.60	3.30 to 6.47
Liquid Limit, w_L (%)	414	177 to 441
Plastic Limit, w_P (%)	303	129 to 377

Table 2.Chemical content of Tampan – Riau peat

Chemical species	weight (%)
ZnO	0.068
BaO	0.004
SiO_2	22.565
Fe_2O_3	0.478
MgO	0.157
TiO_2	0.131
CaO	0.586
Al_2O_3	1.353
K_2O	0.026
Na_2O	0.020
Ignition loss	74.612

3. Test Results

3.1. Effect of the consolidation time

The effect of the consolidation time on the shear behaviour of the peat results from the comparison between the two series of test, with 4 days and 12 days of consolidation, at 1%/h strain rate. For 4 days consolidation time, the results have been presented in figure 1. In the case of 12 days consolidation, tests were carried out under different lateral confining pressures up to 300 kPa. The results are presented in figure 2.

In the [$_1$, q] plane, the stress deviator remains constant for deformations larger than 5%. The curve corresponding to the highest stress (300 kPa) presents a maximum: the stress deviator increases up to a deformation of 3%, then decreases to reach a constant value which is close to that for the 250 kPa confining stress. The shape of this curve is probably due to the formation of a discontinuity surface caused by the reorientation of the particles, including the fibres, during the compression, which practically results in a reduction of shear strength. In the [p', q] plane, the stress paths reach the perfect plasticity line, with a slope M of 1,54.

The change in pore water pressure with deformation is marked, under the highest stresses, by the continuous increase of the curves without the appearance of a plateau, even for deformations of 15 %. The lower the stress, the more stabilised the curve tends to be. The reduction of void ratio during consolidation is important, especially under the highest stresses, as shown in the [p', e] plane: . e varies between 3.87 and 5.60.

By comparing figure 1 with figure 2, we note that, when the consolidation time is increased, the beginning of the curve is stiffer. The strain-stress curves increase more quickly to reach higher values of the deviator, especially under 100 kPa and 200 kPa confining stresses. For higher consolidation stresses, the effect of the consolidation time on the maximum value of the deviator is not very significant. The effect of the consolidation time on the stress path is important, as shown by the value of the slope M. For 4 days consolidation, the slope M is 1.42 (' = 35°) whereas, for a longer time (12 days), it reaches 1.54 (' = 38°).

The consolidation time also influences the evolution of the pore water pressure during the test: for 12 days consolidation, the pore water pressure increases more quickly to reach a higher value, especially under the 100 kPa and 200 kPa confining stresses. The same trend is observed in the strain-stress curves, except for the 300 kPa stress, where the reduction of the stress deviator is accompanied by an increase in pore water pressure. Concerning the volume changes during the consolidation phase, an important decrease in void ratio is observed in the tests with the longest consolidation time. As the consolidation time is long, the reduction of voids in the specimens becomes important: the void ratio at the beginning of the compression is much decreased compared with that for shorter consolidation time. For example, under the same isotropic stress of 100 kPa, 4 days of consolidation time leads to a decrease in the void ratio from 9.03 to 8.4, while for 12 days of consolidation the decrease in void ratio reaches 7.2.

3.2. Tests on remoulded samples

To determine the effect of fibres on peat behaviour, triaxial tests were performed at various strain rates after a consolidation phase of about 4 days for all the tests on remoulded samples, the fibrous parts of which had been removed by passing the material through a 0.08 mm sieve.

Although the fibres were removed, the reduction of void ratio during the consolidation is still remarkable (figure 3). After the removal of the fibrous parts, the reduction of void ratio (e) in the remoulded samples varies between 1.20 and 2.33 during the consolidation phase. The void ratio decreases from 5.0 to 3.8 under a consolidation stress of 100 kPa, while under 300 kPa of consolidation stress, it is reduced to 2.67.

4. Effect of the fibres on the shear strength behaviour of the peat

By comparing the results of the triaxial tests on undisturbed samples of Tampan-Riau peat (at the rate of 1 %/h for 12 days of consolidation) with those on remoulded samples (at the rate of 0.2 %/h), under different isotropic stresses (100 kPa, 200 kPa and 300 kPa), it is possible to assess the role of the fibres (figure 4).

First, the shape of the strain-stress curves q($_1$) is completely different: the curves for the undisturbed samples reach a constant value while those of the remoulded samples continuously increase. Concerning the stress paths in the [p', q] plane, the way in which they reach the failure criterion is also different. However, the values of the slope M are very similar, equivalent to an effective friction angle (') of 37°.

The evolution of pore water pressure under the isotropic stress of 100 kPa, shown in the [$_1$, u] plane, is not very different. Under the 200 and 300 kPa confining stresses, the increase in pore water pressure is larger in the undisturbed samples and the beginning of the curves is stiffer. As previously noted, the reduction of the void ratio during consolidation in the remoulded samples, in the [p', e] plane, is still very large. The removal of the fibrous parts results in a critical state line of the remoulded samples completely different from that of the undisturbed samples under the same consolidation stresses. That is probably due to the effect of a more homogenous material which has a behaviour similar to that of an over-consolidated clay. Thus, the critical state lines are almost parallel with the consolidation line, contrary to those of the undisturbed samples that are more heterogeneous.

5. Observation with SEM

The nature of the degradations and physicochemical transformations of the organic matter in peat soils were the subject of many SEM-based studies (Bourdon 1999; Laggoun-Défarge et al. 1999; Bourdon et al. 2000). Most of the organic compounds cannot be observed under conventional scanning electron microscope (SEM) because they are unstable and rich in water. They need to be cryofixed before observation (Défarge 1997). This cryo-SEM is equipped with a field emission gun. It allows high resolution observations of the natural fabric of organic-rich and highly hydrated specimens under low voltage conditions.

From these results, it appears that the structure of the peat contains a great number of pores: pores related to the amorphous mass, pores remaining between and inside the fibres whose dimension is more important. As the plant cell walls are much more resistant, the degraded walls are well preserved, as well as the pores inside the walls.

To study the affect of the fibres on the peat micro texture (spatial relationships between organic constituents), cryo-SEM observations were also performed on remoulded samples from which the fibrous parts larger than 0.08 mm had been removed by wet sieving. Figure 6 shows photos of the initial remoulded sample. As expected, the remoulded peat samples are mainly composed of a more homogeneous amorphous organic material (figure 6a) compared to undisturbed peat specimens (figure 5a). The mean porosity ranges from 1 to 10 µm and is similar to that of amorphous undisturbed peat.

After the triaxial test under a confining stress of 100 kPa, no noticeable reduction of porosity is visible in the samples. This is probably due to the fine fibres which are still present and recognisable in the samples. Concerning the two types of specimen that were studied, it appears that the removal of the fibres gave the remoulded samples a structure similar to that of an amorphous peat. After the triaxial tests, the material looks like a compacted amorphous mass. However, even in that case, preserved fibrous parts still have

an influence on the shear behaviour. To relate the results of cryo-SEM observation to those of triaxial tests, we suppose that the reduction in porosity of the peat corresponds to the reduction in the void ratio resulting from the consolidation phase in the triaxial tests.

6. Conclusion

The study of the behaviour of undisturbed and remoulded specimens of Tampan-Riau peat on consolidated undrained triaxial path leads to the following conclusions:

The increase in consolidation time leads to a higher value of the slope M of the failure criterion. For 4 days of consolidation, the value of the slope M is 1.42 while, for 12 days of consolidation, this value is 1.54. This corresponds to an increase in the effective friction angle (') from 35° to 38°.

The undrained triaxial tests on the remoulded samples from which the fibrous parts had been removed clearly show the role of the fibres in the shear behaviour of peat. The effect of this removal results in a behaviour similar to that of an over-consolidated clay. However, in all the cases, the presence of fibres in the initial state leads to a high value of the friction angle, as well as an important reduction in void ratio during consolidation. The frictional character of the fibrous peat is confirmed in this study by the value of ' which varies between 35° and 38°, with a negligible value of cohesion (c').

Because of the natural condition of peat at high water contents, which is very soft and very compressible, the preparation of the samples influences the obtained results, both with respect to the strength of the material and its shear parameters. The comparative study with other fibrous peats shows large variations of the behaviour on triaxial paths from one case to another because of the heterogeneity of these materials, related to their different degrees of humification.

The results of the SEM observations showed that the removal of the fibrous parts gave the remoulded samples a structure similar to that of an amorphous peat, more homogenous than that of the fibrous peat. We suppose that the reduction in the porosity of the peat corresponds to the reduction in the void ratio resulting from the consolidation phase. However, it is difficult to quantitatively relate the porosities at the microscopic and macroscopic levels.

REFERENCES

Bourdon S 1999. Approches micromorphologiques et moléculaires de la diagenèse précoce de la matière organique dans une tourbe à Cypéracées en milieu tropical (Tritrivakely, Madagascar). Implications paléoenvironnementales. PhD Thesis University of Orleans.

Défarge C 1997. Apports du cryo-microscope électronique à balayage et du microscope électronique à balayage haute résolution à l'étude des matières organiques et des relations organo-minérales naturelles. Exemple des sédiments microbiens actuels. C.R. Académie des Sciences Paris, Sciences de la terre et des planètes 324, 553-561.

Edil TB & Dhowian AW 1981. At rest lateral pressure of peat soil. Journal of Geotechnical Engineering Division, Proceeding of the American Society of Civil Engineers, ASCE, GT2, 201- 217.

Lechovicz Z 1993. An evaluation of the increase in shear strength of organic soils. In: Advances in Understanding and Modelling the Mechanical Behaviour of Peat, Balkema, Rotterdam, pp 167-178.

Rieley JO Page SE & Setiadi B 1996. Distribution of peatlands in Indonesia. In: Global peat resources, Lappalainen E (Ed.) Publisher International Peat Society pp 169-177.

Soepandji BS Setianto A & Wungkana RF 1996. Stress path analysis according to critical state concept using triaxial data in CU & CD conditions of South of Sumatra and Riau peat soil. Proceeding of technical Seminar - Peat Study for Engineering Purposes, Indonesia pp 31-39.

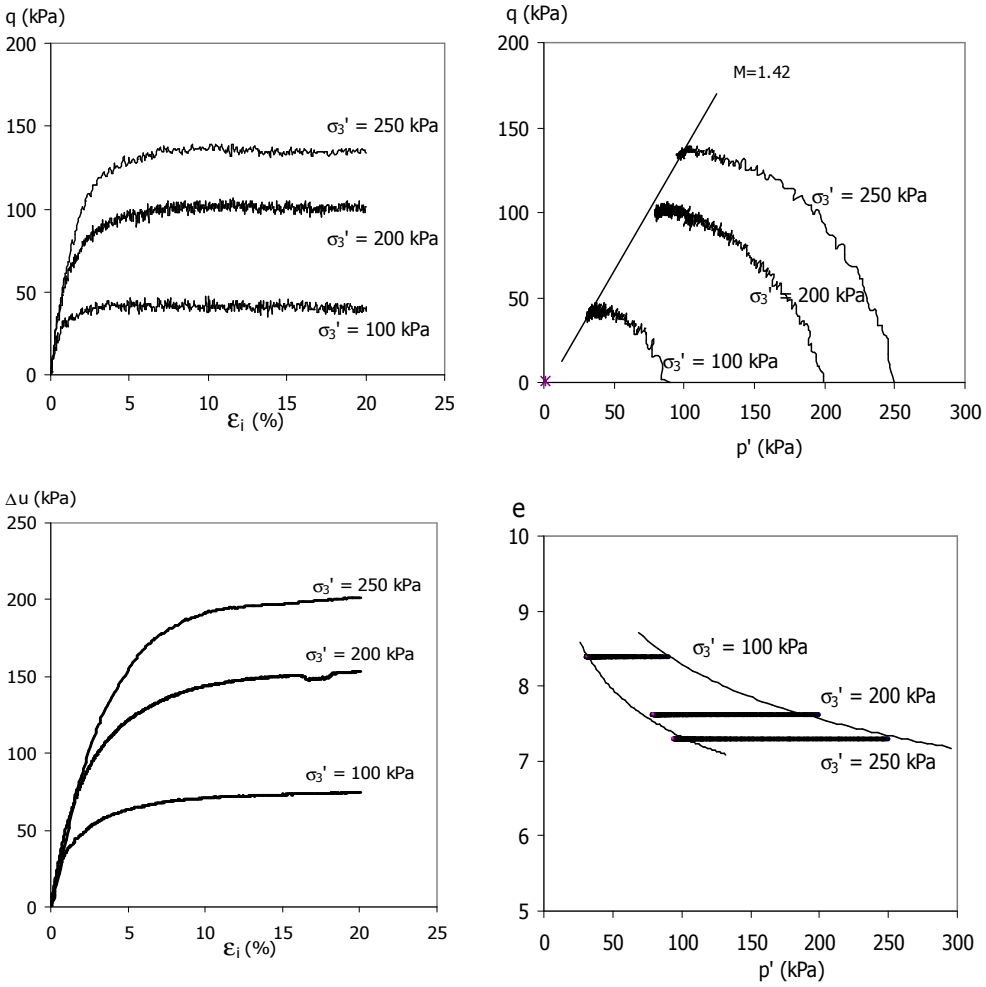

Figure 1. Consolidated undrained triaxial tests on undisturbed samples of Tampan-Riau peat, with 4 days of consolidation and 1 %/h strain rate

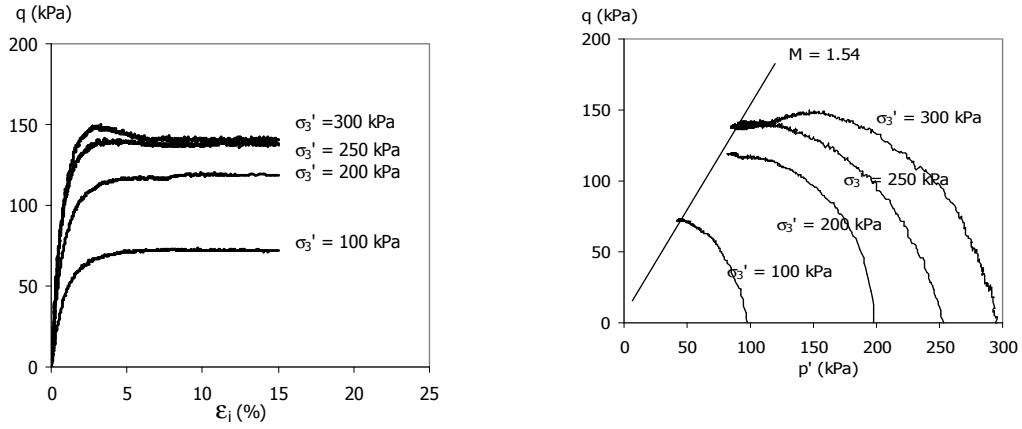

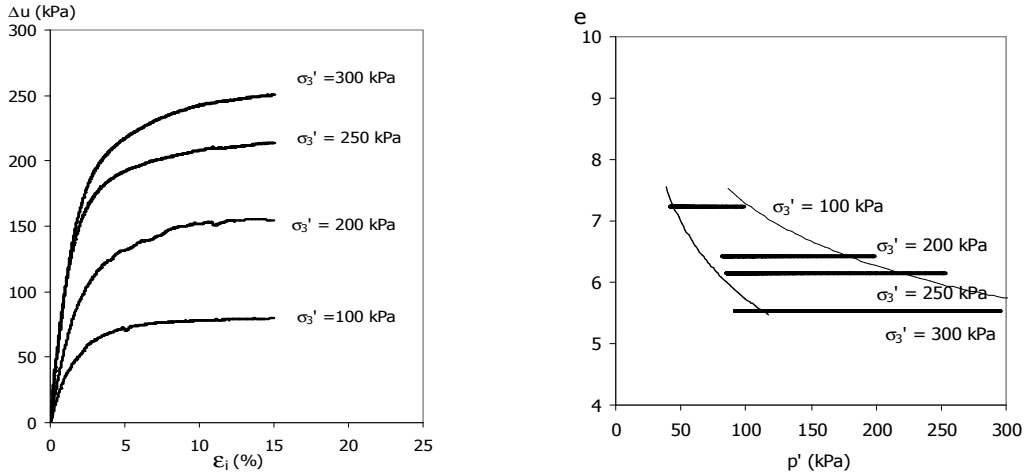

Figure 2. Consolidated undrained triaxial tests on undisturbed samples of Tampan-Riau peat, with 12 days of consolidation and 1 %/h strain rate

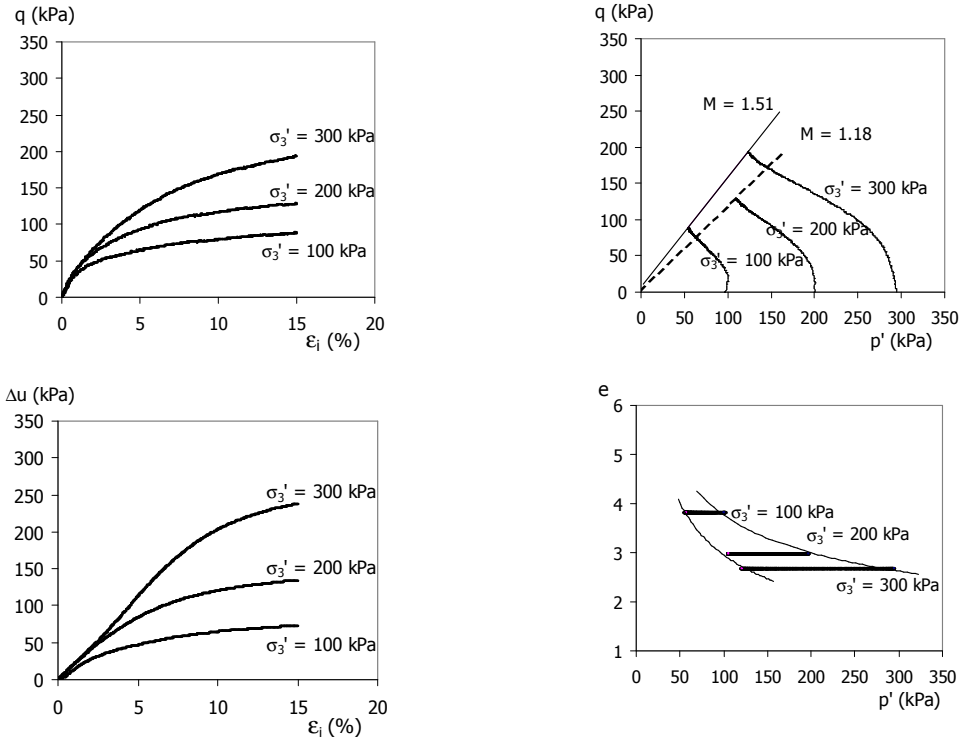

Figure 3. Consolidated undrained triaxial tests on remoulded samples, at 1 %/h strain rate

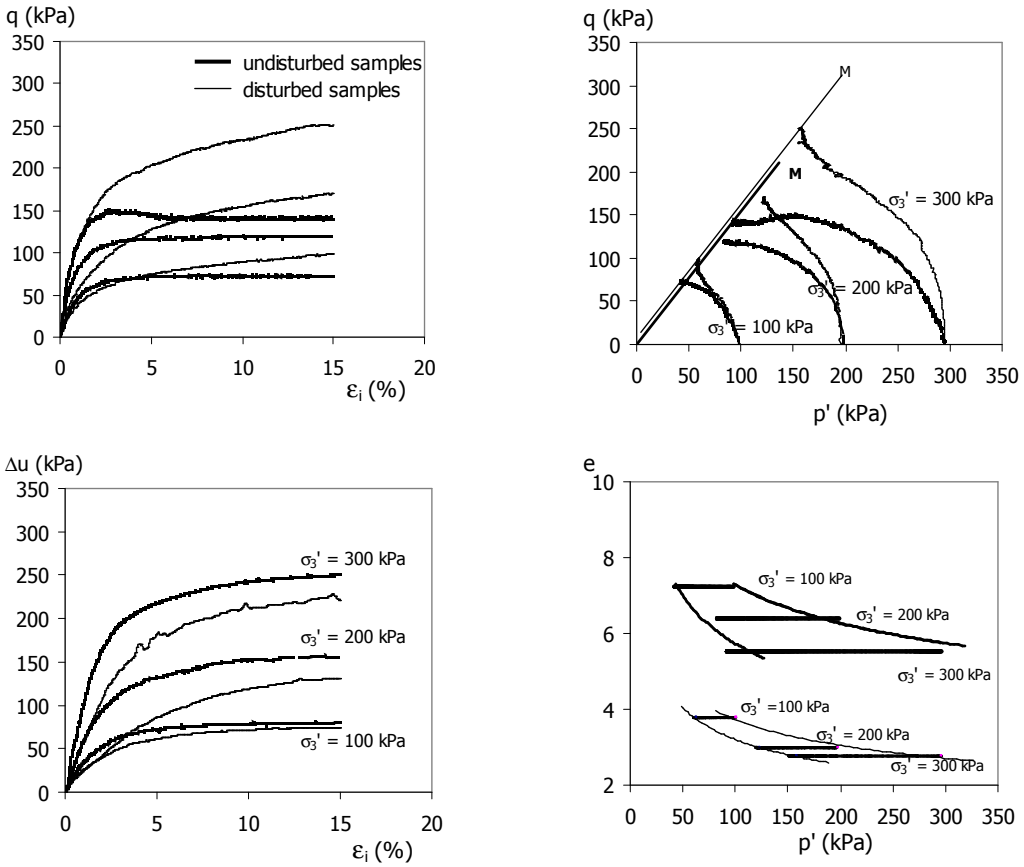

Figure 4. Comparison of triaxial tests results on undisturbed and remoulded samples of Tampan Riau peat

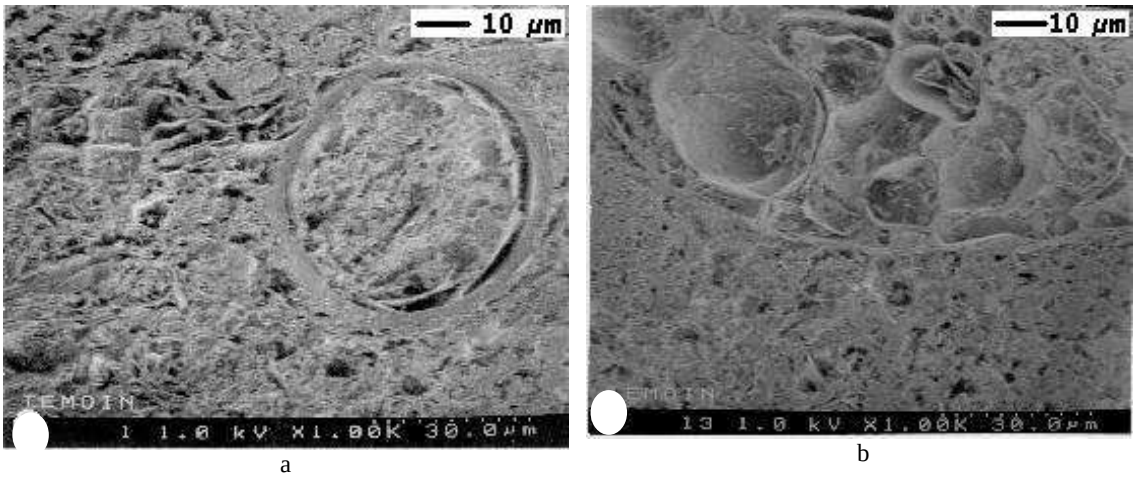

a b

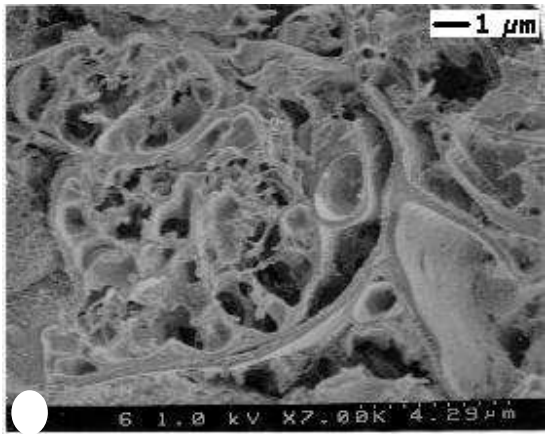

c

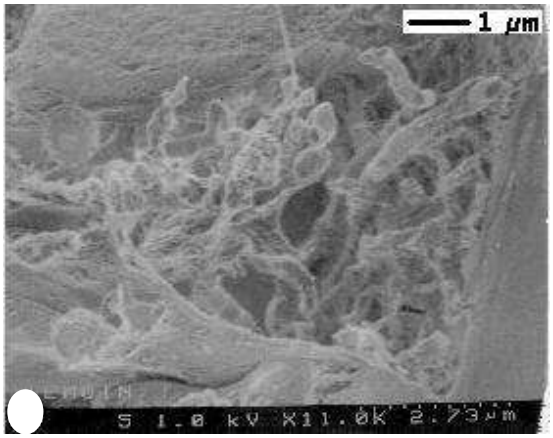

d

Figure 5. Cryo-SEM photos of undisturbed peat specimens in their initial state (w = 551 %, e = 9,3):
(a) homogenous amorphous zone; (b) preserved fibrous zone; (c) reticular organic structures in some cavities; (d) micro-organisms on the plant walls

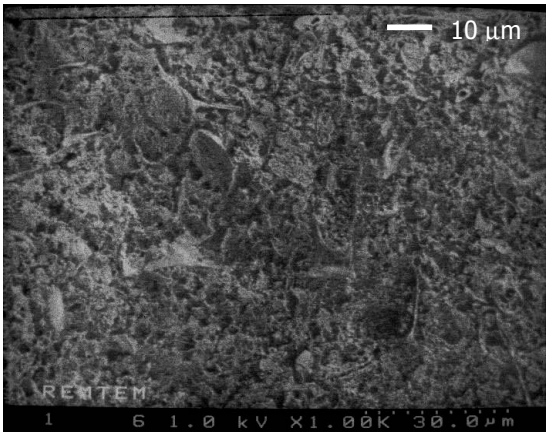

a

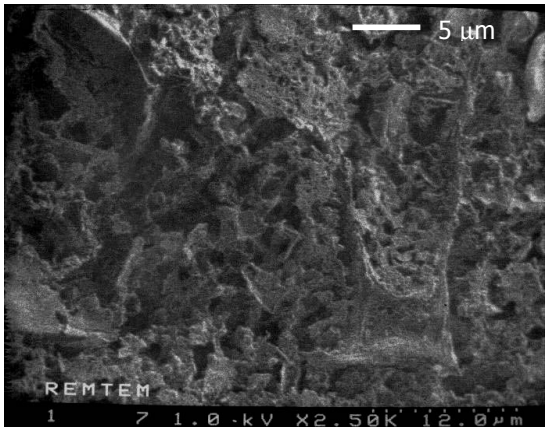

b

Figure 6. Cryo-SEM photos of remoulded peat specimens (fibres larger than 0.08 mm were removed):
(a) a more homogenous amorphous organic material; (b) detail of photo a

ISSN: 1411-1284

Comparison Analysis of Paddy Dryer Type Recirculatory Batch Original and Its Modification Through Implementation of CFD

Adi Surjosatyo

Dept.of Mechanical Engineering
Faculty of Engineering University of Indonesia
Kampus UI Depok 16424

Email: adisur@eng.ui.ac.id

Abstract

The Usage of Dryer at agriculture world become one of the very important component. This matter because of in agriculture there are "Grain Post-Harvest Processing" representing all important process after a period of Harvest. Where in this period a crop harvest abundance and a system " Grain Post-Harvest Processing" should have correct solution to avoid bad crop since depository of paddy still have abundant moisture content. This study has a purpose to analyze re-circulatory batch dryer original then compared to result of system modification of hot air ducting in the same dryer type to see which are more better, by seeing analysis pressure static distribution, temperature distribution and speed distribution at dryer room. Method that used by writer is application simulation of CFD. The result of analysis, is known that recirculatory batch dryer which have been modified better than recirculatory batch original of pressure static distribution = 73 %, speed distribution = 93.4 % and also temperature distribution = 72.87 %.

Keywords: paddy dryer, harvest, CFD, recirculatory

INTRODUCTION

Paddy drying process could be conducted at high and low temperature. Drying at high temperature has an advantage since this drying process faster than at low temperature, but, if too dry will lead cracking. A type of high drying process is a continuous type, namely, the grain flow through drying chamber continuously. This type uses two cylinders, and their wall has many holes, which has the function as dryer. These cylinders, namely, consists of inner and outer cylinder. The space between these cylinders work as paddy drying. The air is blown from inner cylinder through the outer cylinder passing the holes. It is therefore, air drying direction crosses with the paddy flow.

This study has used Re-circulating Batch Dryer as shown on Figure 1. This type has charastics to avoid gradient humidity inside dryer chamber through circulation of paddy during drying process.

The performance of paddy dryer depends on optimalization of drying process without reducing the quality of rice. The current design should have a better of air flow distribution according to reach a higher drying process. Inlet port position, especially inlet port angle, is one of the important factor reducing the pressure drops inside cylinders and effective air diffusion process.

The purpose of this study is firstly, modification of air inlet ducting of dryer chamber, from 90 degree through right side plenum to 45 degree through bottom side of plenum chamber. Secondly, characteristic

comparison static pressure distribution, velocity and air temperature.

CFD (Computational Fluid Dynamic) was implemented to simulate the air flow distribution such as static pressure, velocity and temperature. This simulation govern some important equation based on Mass Balance & Momentum equation.

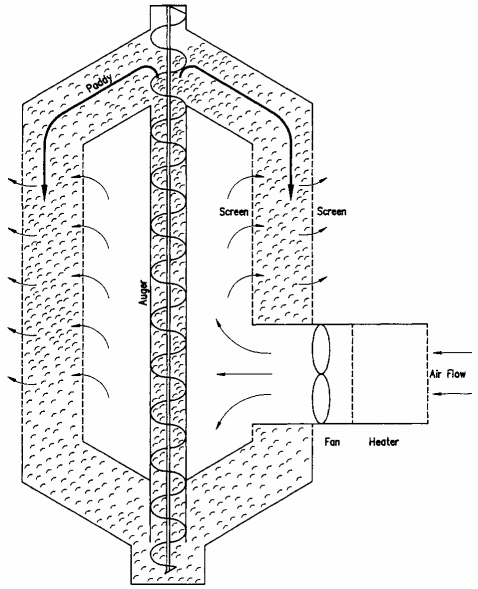

Figure 1. Drying process with Re-circulating Batch Dryer Method (http://www.fao.org)

RESEARCH METHOD

i. Governing Equation

a. Continuity Equation

ρ. A. v = m, where:

m = mass fluid flow (kg/s)

v = velocity of fluid (m/s)

A = flow area (m^2)

ρ = fluid density (kg/m^3)

b. Momentum Equation

a. Geometric Parameter

$$\rho\frac{Du}{Dt}=\frac{\partial(-p+\tau_{xx})}{\partial x}+\frac{\partial\tau_{yx}}{\partial y}+\frac{\partial\tau_{zx}}{\partial z}+SM_x$$

$$\rho\frac{Dv}{Dt}=\frac{\partial(-p+\tau_{yy})}{\partial y}+\frac{\partial\tau_{yx}}{\partial x}+\frac{\partial\tau_{zy}}{\partial z}+SM_y$$

$$\rho\frac{Du}{Dt}=\frac{\partial(-p+\tau_{zz})}{\partial z}+\frac{\partial\tau_{yz}}{\partial y}+\frac{\partial\tau_{xz}}{\partial x}+SM_z$$

c. Equation of Turbulent kinetic energy (k) and epsilon (ε)

$$\frac{\partial(\rho k)}{\partial t}+div(\rho_k U)=div\left[\frac{\mu_t}{\sigma_k}gradk\right]+2\mu_t.E_{ij}.E_{ij}-\rho\varepsilon$$

$$\frac{\partial(\rho\varepsilon)}{\partial t}+div(\rho_\varepsilon U)=div\left[\frac{\mu_t}{\sigma_\varepsilon}grad\varepsilon\right]+C_{1\varepsilon}\frac{\varepsilon}{k}2\mu_t.E_{ij}.E_{ij}-C_2\rho\frac{\varepsilon_2}{k}$$

d. Turbulence Intensity Equation

$$T_i=\frac{\sqrt{\frac{2}{3}k}}{U_{ref}}\text{ , where}$$

U_{ref} : Mean velocity at reference point

K : Turbulent kinetic energy

ii. Geometric Model

Model specification dryer as shown on Figure 2, in which the simulation input value similar with the actual condition, so that result value would be similar with real condition.

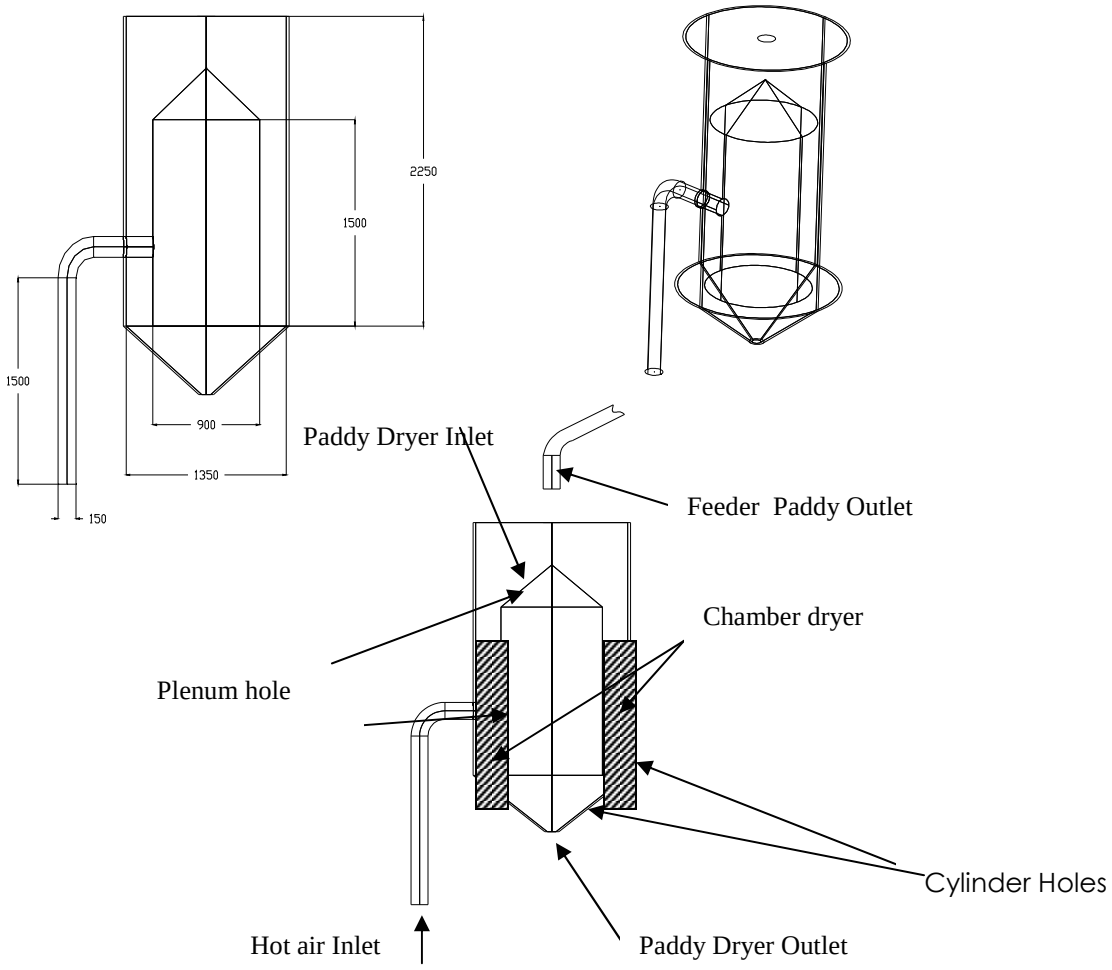

Figure 2. Recirculating Batch Dryer (Geometric Model-Original)

b. Geometric Parameter

- Flow of hot air : 8.5 m^3/min
- Temperature air Inlet : 70 ^oC
- Temperature Ambient : 27 ^oC

iii. CFD Simulation Process

This simulation consisted of two two model, namely: first, hot air flow with elbow ducting dryer original, second, hot air flow with elbow ducting dryer modification. Figure 3 & Figure 4 show both mesh geometry.

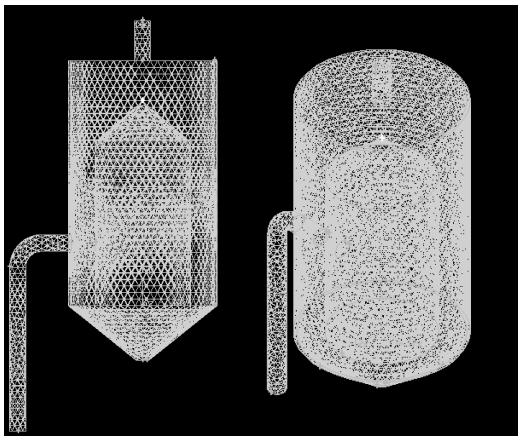

Figure 3. Original Model

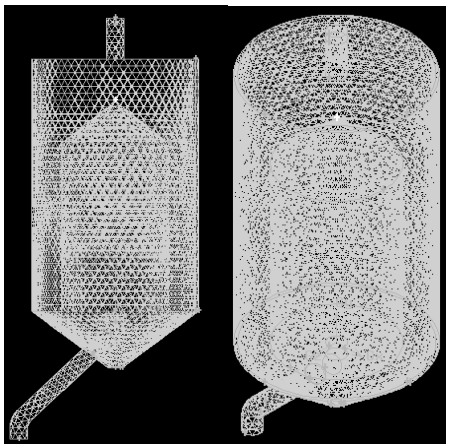

Figure 4.Modification Model

RESULT AND DISCUSSION

Figure 5 shows distribution zones at differrent height h_1 (0 mm), h_2 (750 mm) and h_3(1500 mm) respectively, 'samping' means posistion of measurement at distribution zone from side view, 'depan' means posistion of measurement at distribution zone from front view. It will be discussed comparison of pressure static, velocity and temperature distribution at h_3 respectively. The square box on the left and right of each plot graph shows dryer chamber, it can be indicated variation parameter during drying simulation.

On Figure 6 (a) and (b) shows a clear differrentiation of static distribution inside both cylinders, especially in the dryer chamber.Higher static pressure occurs in the original model. This means, air flow experiences higher resistance.As qonsequences, as indicated on Figure 7 (a), there is a low air velocity at original model, and after modication of air inlet velocity port, an higher velocity occurs. Smooth temperature disribution is showed on Figure 8 (b) since air flow velocity also well distributed.

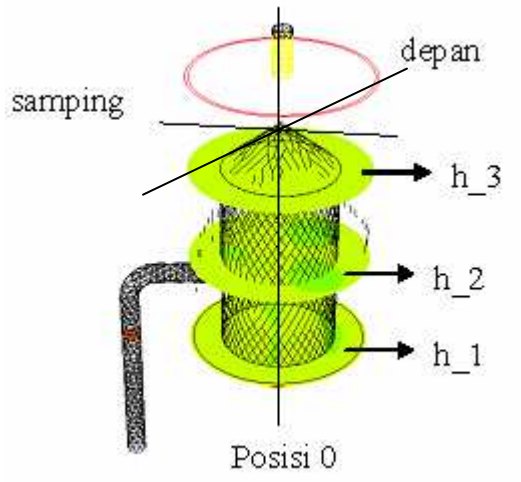

Figure 5. Zone distribution at differrent height

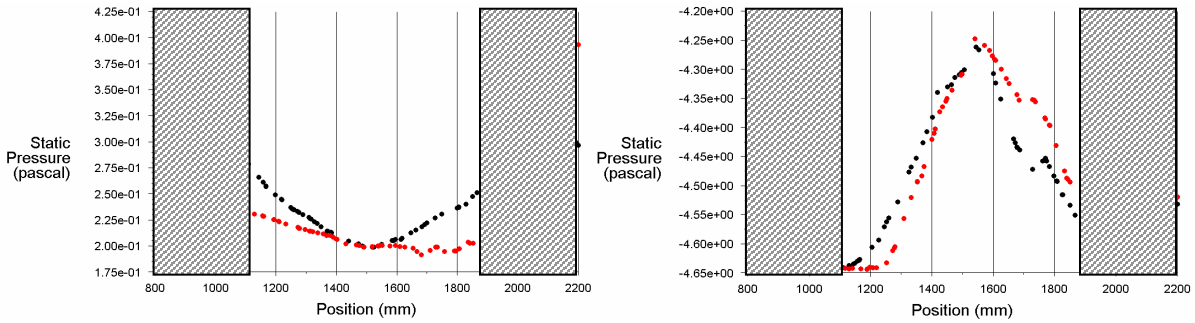

(a) Original (b) Modifikasi

Figure 6. Static Pressure Distribution at h_3

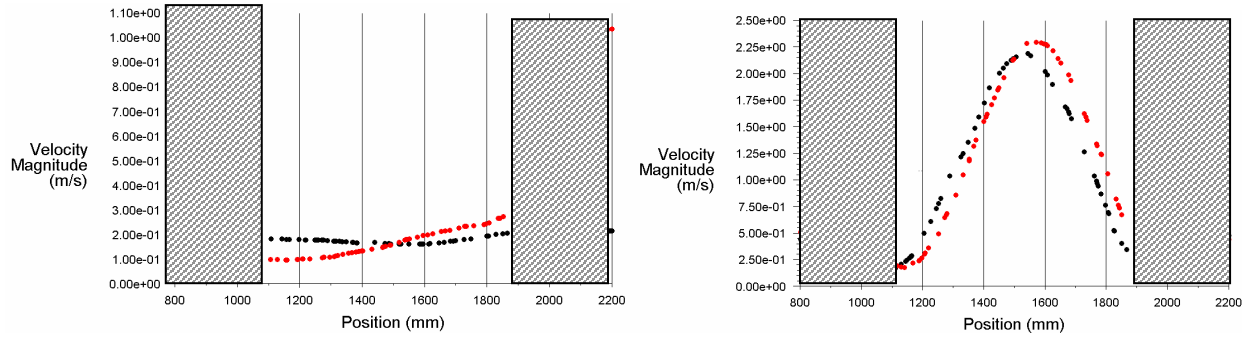

(a) Original (b) Modifikasi

Figure 7. Velocity Distribution at h_3

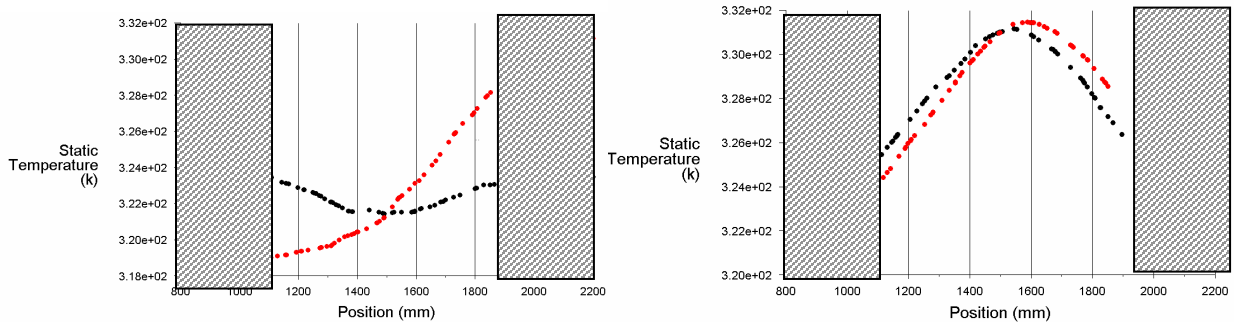

(a) Original (b) Modifikasi

Figure 8. Plot Graph Temperature Distribution at h_3

CONCLUSION

Simulation model using CFD-Computational Fluid Dynamic, which uses FLUENT 6.2, has been conducted. It shows modification model contributes better result, this has given better static pressure of 73%, velocity 93.4% and temperature 72.87%. Since modification by shifting inlet hot air flow to the bottom of dryer chamber, a better air diffusion could be reached.

REFFERENCES

[1] Gunasekaran, Sundaram ,"**OPTIMAL ENERGY MANAGEMENT IN GRAIN DRYING"**, Department of Agricultural Engineering University of Delaware Newark, Delaware, 1985.

[2] IPB**, "GRAIN POST-HARVEST PROCESSING TECHNOLOGY"**, M.Sc. Course IPB, Bogor, 1985.

[3] Kaban, Erol E., **"LAPORAN TUGAS PELATIHAN CFD - CCIT FTUI",** Februari 2005.

[4] *http://www.ex.ac.uk/~grtabor*, Fluent Software Training Fluent Inc., "**Combustion Modeling in FLUENT"**, 2005.

[5] *http://www.face.auc.dk/courses face8/applied_cfd*, November 2005

[6] *http://www.fao.org* , Oktober 2005.

[7] *http://www.iet.au.dk*. "**Applied Computational Fluid Dynamics 2003 "**, Institute of Energy Technology Aalborg University. November 2005.

[8] *http://www.simetric.co.uk*, Oktober 2005.

[9] *http://www.unu.edu* , Maret 2005.

ISSN: 1411-1284

MINIMIZE CERAMIC DEFECTS BASED ON SIX SIGMA TO DECREASE CUSTOMER COMPLAINT

(Case Study PT Muliakeramik Indahraya)

Insannul Kamil[1], Feri Afrinaldi[2], Yossy Risman[3]
sankamil@yahoo.com and yenssy_001@yahoo.com

Abstract

PT X is a ceramic produsen in Indonesian that have good image as Mulia Industrindo Group, and it's will impact to their explor and compete. Quality product is a customer require while higher competition and customer assential. But its'nt able to full by company, cause product defect that rises customer complain evenly 0,6% total production. The failure result of product is a problem that will impact to the customers satisfaction and the cost itself. Last 3 years,company had loss Rp. 3.656.916.270,- caused this problem.

The aim of this research is to decrease the defective or even to vanish it through the program of Six Sigma; identify the input characteristics, process, and output. Then, identify the critical to quality, calculate the Defect Per Million Opportunity and sigma capability and identify cause of defect. It is ended with suggestions to improve the process capability.

Based on research, it is found that the sigma capability process was just the rate 4,8 with 572,93 DPMO for FT 1 and 4,6 with 944,83 DPMO for FT 2. To improve the value of sigma capability, it suggests to design automatic inspection tools, include label Watermark at the box, prepare product Antiwatermark as alternative local customer chosen, accuracy inspection and packing product, machine calibration, and use inspection standart visual defect to test the crazing resisten problem. And then company suggests to distributor to save the product in dry place, full air, and don't be pile, sell the same bacth/lot product, inform about box code, and complete product sample and catalog for it's distributor or shop. For the customer, company have to determine the water proportion, design box code that easy to undertand, store in dry place, full air, and don't be pile, and suggest so that customer to follow the distributor suggestion.

Keyword : *Six Sigma, Defect Per Million Opportunity, Kapabilitas Sigma*

1. INTRODUCTION

1.1 Background

PT X is a producent of ceramic in Indonesian. Since 1998 company has producted 2 type of ceramics are fllor tile and wall tile with 100 Ha area and 7 factory. This company has good image as XY Groups that is be strongly their compete an deelop their bussiness. Product hae choosen by customer and delight in to another country. This is a special oppurtunity and so be a threat for company to produce quality product.

Quality product is standart of customer [Crosby dalam Besterfield, Dale H, 1994]. Cause of that, company has to rise product thar fullfilt customer specification order to existence and take probability. Customer complaint can be a measurement tools quality of product. And its object in this research.

Based on survey TCS Department PT X, we knew that customer complaint is high (312.059 m^2 dari 79.217.219 m^2). Its indicated product has passed OK from factory dont fullfilt the customer request yet. It will be bad impact for company, because will decrease the product imag and high cost to. Table 1 shown that in years 2005 and 2006 company had lost more than 1 billion rupiah. Thr cost is consist of verification cost are replacement cost, additional cost, survey cost, and incurrent cost

This case will be bad efcet to image company as a produsent ceramics and decrease the respect of customer.

Table1 Cost of Ceramic Defects in years 2004, 2005, and 2006

Tahun	*Cost of Poor Quality*				Total (Rp.)
	Replacement (Rp.)	*Additional Cost* (Rp.)	Biaya *Survey* (Rp.)	Biaya Lain (Rp.)	
2004	668,706,600	87,970,000	16,970,000	200,000	773,846,600
2005	1,109,553,580	80,122,350	16,869,194	200,000	1,206,745,124
2006	1,277,042,151	192,904,844	20,467,190	200,000	1,490,614,185

1.2 Purpose of Research

1. Minimize customer complaints.
2. Give a solution to improve the product quality based on Six Sigma.

1.3 Boundaries of Research

1. Research based on production years 2003-2006.
2. Only for floor type.
3. Only count cost of complaint.

2. THEORETICAL

Six Sigma is a set of practices originally developed by Motorola to systematically improve processes by eliminating defects.[1] A defect is defined as nonconformity of a product or service to its specifications.

While the particulars of the methodology were originally formulated by Bill Smith at Motorola in 1986[2], Six Sigma was heavily inspired by six preceding decades of quality improvement methodologies such as quality control, TQM, and Zero Defects. Like its predecessors, Six Sigma asserts the following:

1. Continuous efforts to reduce variation in process outputs is key to business success
2. Manufacturing and business processes can be measured, analyzed, improved and controlled
3. Succeeding at achieving sustained quality improvement requires commitment from the entire organization, particularly from top-level management

The term "Six Sigma" refers to the ability of highly capable processes to produce output within specification. In particular, processes that operate with six sigma quality produce at defect levels below 3.4 defects per (one) million opportunities (DPMO).

Six Sigma's implicit goal is to improve all processes to that level of quality or better.

3. RESEARCH METHOD

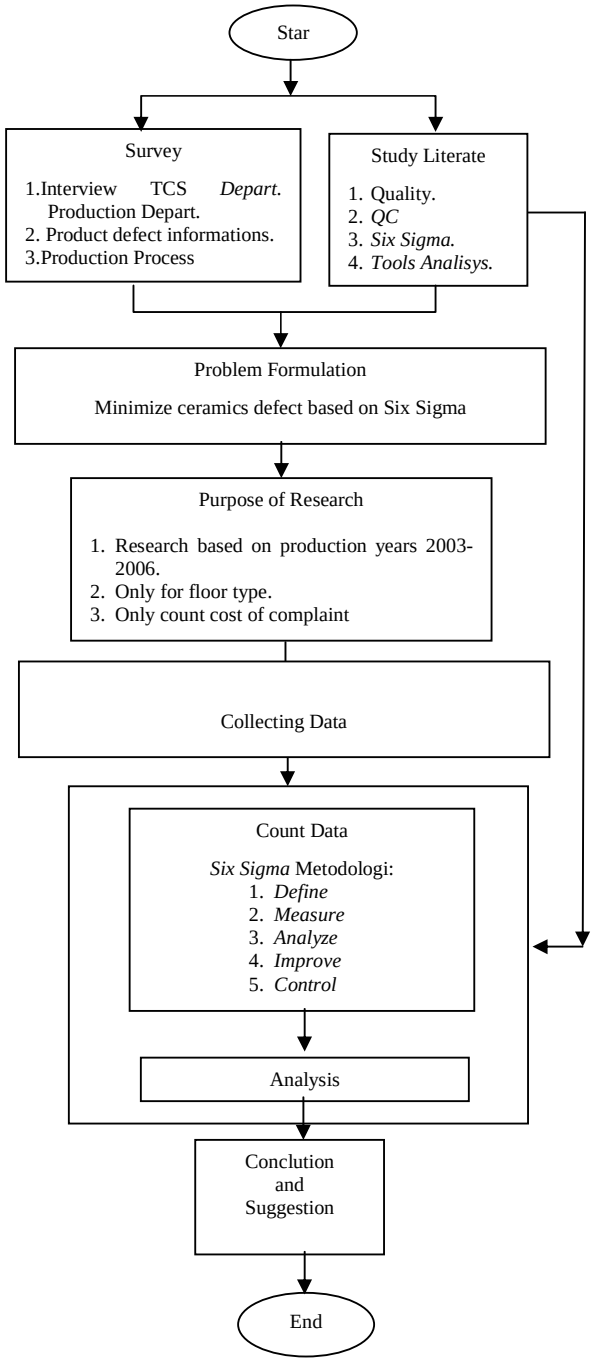

Picture 1 Research Method Scheme

4. COLLECTING DATA

Collecting data and ionformations need to solve the problem. The data are:

1. Object research.
2. Defects product informations.
3. Procedure handling the customer complaints.
4. Cost of complaints.
5. Production data years 2003-2006.
6. information about qualification quality product.

5. Pengolahan Data

5.1 Define

This step is identifiaction about the problem. The problem is ceramics defects that impact to complaint of customer. First to improve is identify the characteristic customer need. And conclude in Input Process Ouput Diagram (IPO). IPO Diagram shown in Picture 2.

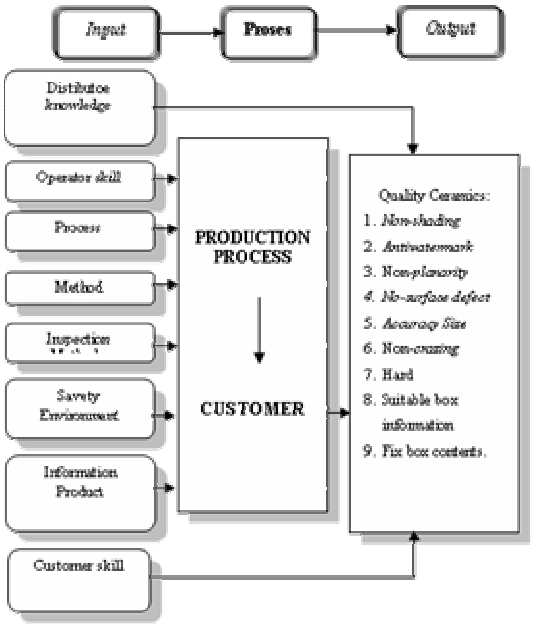

Picture 2 *Input* Process *Output* (IPO) Diagram

5.2 *Measure*

Measure is the second step of Six Sigma, that identify:

1 Flow process diagram.
2 Identify *Critical To Quality / CTQ*
3 Measure the capability process.

Picture 3 shown flow process diagram application ceramic.

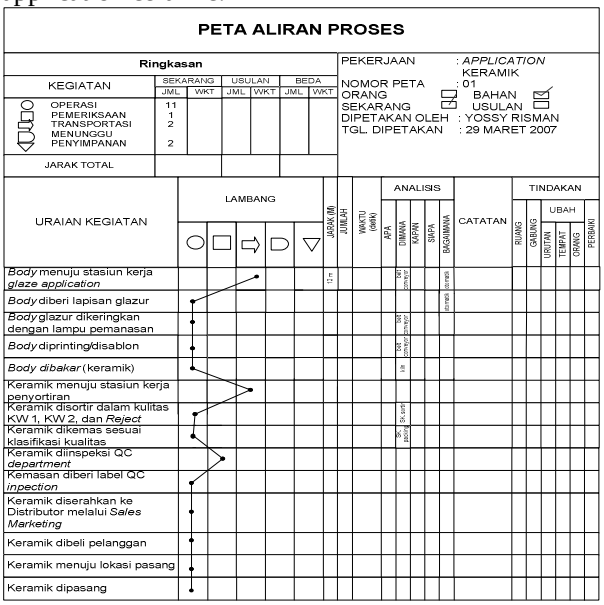

Picture 3 Flow Process Digram Application Ceramics

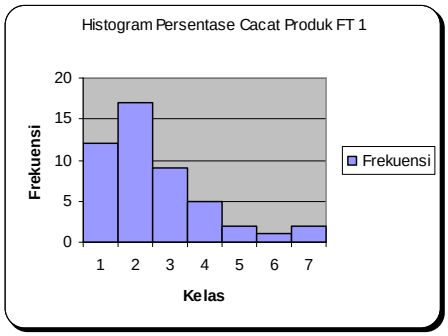

Picture 4 Histogram Frekuency Defect FT 1

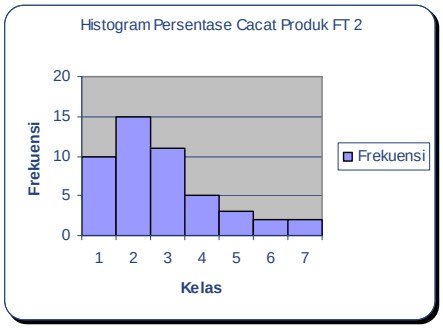

Picture 5 Histogram Frekuency Defect FT 2

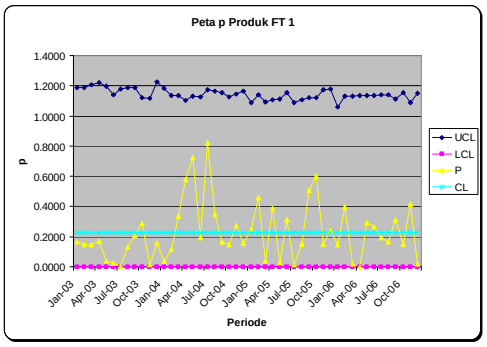

Picture 6 Control Chart Defect Proportion FT 1

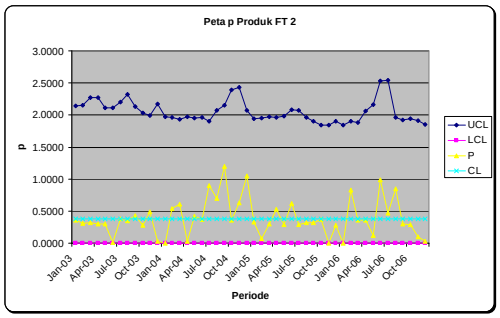

Picture 7 Control Chart Defect Proportion FT 2

Picture 8 *Output Calculator Sigma* FT 1

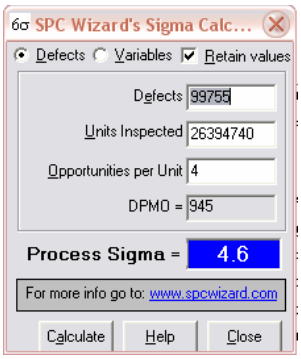

Picture 9 *Output Calculator Sigma* FT 2

5.3 Analyze

From analyse about cause and efect diagram can conclude the problem is caused by several factor are:

1. Man
   Man is a factor dominan that caused the problem. This factor is consist of 3 category are:
   a. Controler
   b. Operator
      There are several factor that implied operator are time inspection, speed of product, colour and product design type
   c. Skilled laborer
2. Machine
3. Material
4. Method
9. Information
10. Environment

Table 1 FMEA

Failure Mode and Analysis

System	: PT Muliakeramik Indahraya	*FMEA Number*	: 1
Sub System	: Departemen TCS	*Prepared By*	: Yossy Risman
Component	: Komplain Produk	*FMEA Date*	: 18-Apr-07
Core Team	: -	*Revision Date*	: -

No.	Component	Potential Failure Mode	Potential Effect of Failure	Sev	Potential Cause of Failure	Occ	Current Process Control	Det	RPN
1	Proses produksi	1. Variasi (cacat) produk melebihi batas	Operator sortiran bingung sehingga tidak teliti	5	1. Drop Gas 2. Operator pengontrol lengah 3. Mesin rusak	4	Persediaan gas lebih dikendalikan Kontrol supervisor diperketat Tidak ada	5	100
2	*Sorting /packaging*	1. Klasifikasi produk salah 2. Sortiran tidak terbaca sensor	Produk KW 2 dan *reject* masuk klasifikasi KW 1	8	1. Operator sortiran jenuh 2. Operator kurang teliti 3. Operator tidak konsentrasi	9	Tidak ada Tidak ada Tidak ada	9	648
3	Marketing	1. Informasi pada distributor tidak jelas dan tidak lengkap 2. Desain kemasan yang tidak menginformasikan detail produk	Komplain pelanggan terkait dengan kesalahan informasi produk dan kemasan	5	1. Marketing menjaga *image* produk 2. Distributor tidak mengerti 3. Distributor tidak memberi pengarahan pada pelanggan	4	Tidak ada Melengkapi informasi dokumen jual beli Tidak ada	9	180
4	Distributor	1. Produk pecah/retak 2. *Planarity* dan *calibre* 3. Distributor tidak memberi pengarahan pada pelanggan	Komplain pelanggan	7	1. Disimpan menumpuk 2. Suhu penyimpanan tinggi 3. Distributor tidak mengerti	6	Tidak ada Tidak ada Melengkapi informasi dokumen jual beli	4	168
5	Tukang	1. Produk pecah/retak 2. Keramik terlihat seolah olah berbeda ukuran	Komplain pelanggan	4	Tukang salah pasang, kurang pengalaman, tidak terampil	7	Jika ada komplain, tidak ada penggantian produk	5	140
6	Lingkungan Kerja	1. Klasifikasi produk salah 2. Variasi meningkat karena proses tidak terkendali	1. Operator tidak konsen kerja 2. Operator cepat lelah	7	1. Bising mesin 2. Suhu tinggi pengaruh proses pembakaran produk 3. Pekerjaan monoton dan memerlukan konsentrasi tinggi	6	Tidak ada Tidak ada Tidak ada	3	126
7	Metode kerja	1. Variasi meningkat 2. Klasifikasi produk salah	1. Operator sortiran kewalahan 2. Pelanggan tidak puas	4	1. Operator bekerja tidak konsisten 2. Operator bekerja tidak mengikuti prosedur	4	Tidak ada Tidak ada	7	112
8	Keahlian operator	Variasi meningkat	Proses tidak terkendali	3	Penempatan yang tidak tepat	4	Tidak ada	7	84

Table 2 Recapitulation CoPQ

CoPQ		*Justified*	*Unjustified*	*Commercial*	Total
Survei	2003		Rp 11,500,000		Rp 54,306,384
	2004		Rp 12,145,600		
	2005		Rp 14,876,900		
	2006		Rp 15,783,884		
Replacement	2003	Rp 468,753,800		Rp 111,814,800	Rp 3,248,607,470
	2004	Rp 606,118,780		Rp 216,535,600	
	2005	Rp 414,839,400		Rp 745,814,400	
	2006	Rp 540,063,772	Rp 99,047,903	Rp 45,619,015	
Additional Cost	2003	Rp 45,446,320			Rp 354,002,416
	2004	Rp 121,934,780		Rp 1,402,900	
	2005	Rp 113,703,600		Rp 55,823,950	
	2006	Rp 15,180,422		Rp 510,000	
Biaya Lain	2003	Rp 524,775	Rp 122,450	Rp 65,400	Rp 5,421,000
	2004	Rp 517,275	Rp 608,950	Rp 339,300	
	2005	Rp 691,950	Rp 156,450	Rp 607,400	
	2006	Rp 995,775	Rp 513,000	Rp 278,275	
Total					Rp 3,662,337,270

5.4 Improve

As a improve is a design the sensor that can inspect the ceramic automaticlly.

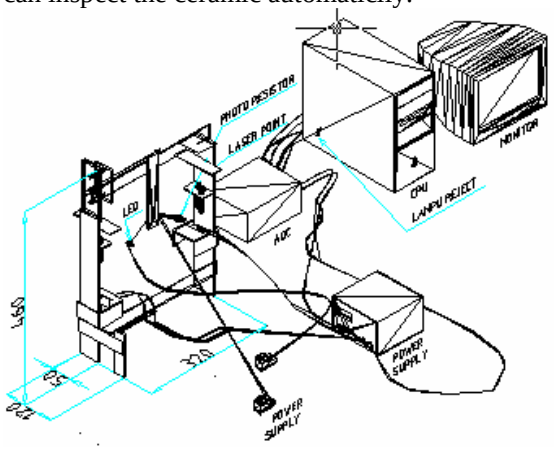

Picture 10 Automaic Sensor

5.5 *Control*

This step is only as recomendate to control thr process periodicly.

6. CONCLUSION

Conclude of the research are:

1. Kapability process PT X are 4,8 sigma for *Floor Tile* 1 with 572,93 DPMO and 4,6 sigma for *Floor Tile* 2 with 944,83 DPMO.

1) As the recomendation this research will improve the probelm with design the automatic tolls to inspect the ceramics defects.

7. SUGGESTION

1. Design tools complete with return mechanism, sensor ultrasonik, and camera.
2. Research continu with water proportion that save in using product anti-watermark.

8. REFERENSI

1. Augustine A. Stagliano, ***Six Sigma Advanced Tools Pocket Guide,*** Andi Yogyakarta, 2005.
2. Besterfield, Dale H, ***Quality Control***, fourth edition, Prentice-Hall inc, New Jersey.
3. Dwiningsih, Nurhayati, ***Desain Produk dan Manajemen Kualitas.***
4. Fitrizal, ***Minimasi Kegagalan Hasil Rontgen dengan Metode Six Sigma (Studi Kasus di Instalasi Radiologi Rumah Sakit Umum Pusat Dr. M. Djamil Padang),*** Jurusan Teknik Industri Fakultas Teknik Universitas Andalas, Padang, 2006.
5. Gasperz, Vincent, ***Pedoman Implementasi Program Six Sigma*: *Terintegrasi Dengan ISO 9001:2000, MBNQA, dan HACCP,*** PT Gramedia Pustaka Utama, Jakarta, 2002.
6. http://www.beranda.net, Manggala, D, ***Mengenal Six Sigma Secara Sederhana,*** 2005.
7. http://www.ebizzasia.com, Syahrizal, Aditya, ***Berharap dari Six Sigma,*** Information Technology Communications and e-Business Megazine, 2003.
8. http://www.pqm-iris.co-id, Irawan, Sonny, dkk***, Productivity & Quality Management Newsletter.*** 2003**.**
9. http://puslit.petra.ac-id/journals/management, Sugiharto, Sugiono, dkk***, Six Sigma: Perangkat Manajerial Perusahaan pada Era Ekonomi Baru (Sebuah Pendekatan Konseptual Terhadap Studi Literatur) .*** Jurusan Ekonomi Manajemen Fakultas Ekonomi Universitas Kristen Petra. 2004.
10. http://puslit.petra.ac-id/journals/industrial, Rahardjo, Jani, dkk***, Peningkatan Kualitas Melalui Implementasi Filosofi Six Sigma (Studi Kasus Sebuah Perusahaan Speaker).*** Jurusan Teknik Industri Fakultas Teknologi Industri Universitas Kristen Petra. 2003.
11. http://www.IEEEInt.net, Boukouvalas, dkk, ***Ceramic Tile Inspection for Colour and Structural Defects***, University of Surrey.
12. Peter S. Pande, dkk, ***The Six Sigma Way,*** Andi Yogyakarta, 1994.
13. Pyzdek, Thomas, ***The Six Sigma Project Planner,*** The McGraw-Hill Companies, 2003.
14. Pustaka Amani, ***Atlas Dunia untuk SD, SLTP & SMU***, Pustaka Amani, Jakarta, 1999.
15. Rosi Novrina, ***Analisis Pengendalian Mutu Komposisi Hotmix dengan Metode Statistical Process Control (SPC) pada PT Angkasa Teknik Raya***, Jurusan Teknik

Industri Fakultas Teknik Universitas Andalas, Padang, 2006.
16. Saltanera, ***Sistem Manajemen Mutu: Antara Kebutuhan dan Keharusan,*** Indonesia, 2007.
17. Setiadi, Dede, ***Pengertian ISO 9000: Sistem Standar Manajemen Mutu***, 2004.
18. Sutalaksana, I. Z., dkk, ***Teknik Tata Cara Kerja,*** **Edisi Pertama**, Jurusan Teknik Industri, Institut Teknologi Bandung, Bandung, 1979.
19. Telkom Indonesia, ***Buku Petunjuk-White Pages & Panduan Informasi Bisnis-Yellow Pages Padang April 2007-2008,*** Padang**,** Infomedia, 2007.
20. Ulrich, Karl T, ***Perancangan & Pengembangan Produk.*** Salemba Teknika. Jakarta. 2001.
21. Walpole, Ronald E dan Myers, Raymond H, ***Ilmu Peluang dan Statistik untuk Insinyur dan Ilmuwan,*** terjemahan RK Sembiring, ITB, Bandung, 1995.

ISSN: 1411-1284

Seismic Evaluation using Elastic Time History Analysis: Case Study Rumah Sakit Cahya Kawaluyan

Olga Pattipawaej*, Yosafat A. Pranata**, Edita S. Hastuti*

* Department of Civil Engineering, Maranatha Christian University, Jl. Suria Sumantri 65, Bandung 40164
Tel. +62-22-2012186 ext. 219, fax. +62-222017622 email : olga.pattipawaej@eng.maranatha.edu
** PhD Student, Parahyangan Catholic University, Jl. Ciumbuleuit 94, Bandung 40141, West Java, Indonesia
email : yosafat.ap@eng.maranatha.edu

Abstract– **In the last few years, several parts of Indonesia were shocked with the occurrence of earthquake. Building structures that were built in those areas should be planned to stand firm for the earthquake. One of the important buildings is a hospital building. To study the behavior of pasca-elastic building structure due to earthquake design, it must be studied the dynamic response of nonlinear time history analysis. This analysis is to determine the nonlinear effect of ground movement [6]. The aim of this paper is to evaluate the seismic behavior of building structure which is a hospital called Rumah Sakit Cahya Kawaluyan, Indonesia. The evaluation is covering the base shear, displacement, and drift structure using dynamic analysis of ground motion force based on time history. The analysis is numerically conducted using Software ETABS nonlinear. The ground motion force as an input data is used based on the acceleration earthquake record of El-Centro N-S 1940, Pacoima Dam 1971, Bucharest 1977, and Flores 1992. Those intensity are scaled for the earthquake region 4 of hard soil in Indonesia [6]. The results indicate that it can be concluded that the Flores earthquake showed the maximum of roof displacement and drift. At the medical support building due to Flores Earthquake is 13800000 N, the roof displacement is 0.007 m, and the drift is 0.0036. On the other hand, at the medical service building due to Flores Earthquake is 9732000 N, the roof displacement is 0.129 m, and the drift is 0.00438.**

Keywords– Elastic Time History Analysis, Rumah Sakit Cahya Kawaluyan, Base Shear, Displacement, Drift.

I. INTRODUCTION

In the last few years, the occurrence of earthquake shocked in several parts of Indonesia. Therefore, the structures that were built in those areas should be designed according to the earthquake's regulation. One of the important building structures that is used in this paper is a hospital building.

It is assumed that earthquake/ground motion force is a lateral force in a building structure. In principle, the earthquake vibration, which reached the building structure, is changed as predominant period, velocity, and acceleration. To study the behavior of pasca-elastic building structure due to earthquake design, the dynamic response of nonlinear time history analysis is analysed. This analysis is to determine the nonlinear effect of ground movement [6]. Particularly in Indonesia, the response analysis of time history is ussually conducted in the design of high rise buildings. This analysis is also used to verify the precise partition of shear force along the building elevation.

The aim of this paper is to assess the seismic behavior of building structure which is a hospital. The hospital is so-called Rumah Sakit Cahya Kawaluyan, Indonesia. The Rumah Sakit Cahya Kawaluyan Building has two parts separated with 2.5 cm of dilatation, i.e., the seven story building for medical service and the five story building for medical support (see Figure 1 and 2).

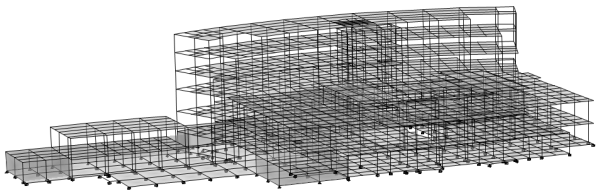

Figure 1. Three-Dimension of Rumah Sakit Cahya Kawaluyan

The evaluation will include the base shear force, displacement, and drift structure using dynamic analysis of ground motion force based on time history. Numerically, the analysis is implemented using Software ETABS nonlinear [2].

The ground motion force as an input data is used based on the acceleration earthquake record of El-Centro N-S 1940, Pacoima Dam 1971, Bucharest 1977, and Flores 1992. These intensities are scaled for the earthquake region 4 of hard soil in Indonesia [6].

Loading combination that is used in design based on Indonesian Code SNI 03-2847 [5] are:
(1). 1.4DL

(2). 1.2DL+1.6LL
(3). 1.2DL+0.5LL±E
(4). 0.9DL±E.

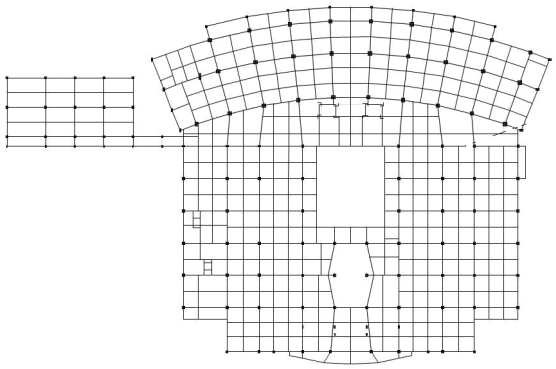

Figure 2. Plan view of Rumah Sakit Cahya Kawaluyan

II. BASIC THEORY

The time history analysis is the full dynamic equilibrium equation and is solved for each time step on the acceleration-time curve. The history of the deformation resulting from previous time step calculation is considered in computing the response for the current time step. The time-history analysis is in-fact a piece wise solution of the entire force histogram [1].

The input variables of the ground motion are the ground acceleration, damping ratio and circular frequency, and the final unknown is displacement (and its derivatives) by using the following formula:

$$\ddot{u} + 2\xi\omega\dot{u} + \omega^2 u = -\ddot{u}_g \quad (1)$$

The dynamic response of the irregular building structure to influence due to the earthquake design, can be conducted based on three-dimensional of analysis dynamic in the form of response analysis of linear dynamic and nonlinear time history with an accelerogram of the earthquake as an input data of ground displacement. The dynamic response in each time step is calculated using direct integration method as follows:

$$K\,u(t) + C\,\dot{u}(t) + M\,\ddot{u}(t) = r(t) \quad (2)$$

$$r(t) = \sum_i f_i(t) p_i \quad (3)$$

where K is the stiffness, C is damping, M is mass. u, $\dot{u}$, $\ddot{u}$ is the displacement, velocity and acceleration, respectively. r(t) is the ground motion force with respect to time.

The earthquake force is a function of time, so that the building structure's response depends on time. An effect of the earthquake design, the behavior structure will be inelastic.

The calculation of dynamic response of the irregular building structure due to earthquake design can be done using three dimension of dynamic analysis that is the analysis response of linear dynamic and non-linear time history of the earthquake's accelerogram.

In ETABS software, the acceleration of the earthquake's record at each time time is due to displacement, velocity, and accelaration that is measured from ground movement.

According to the Indonesian Earthquake Code SNI 1726-2002 method [6], at least four time histories should be used, i.e., the magnitude, fault distance and source mechanism should be scaled to consistent with Maximum Considered Earthquake. If actual records not available then use simulated records.

Input data for time history analysis are mass and stiffness distribution, the acceleration-time record, the scaling factors, directional factors, and analysis time step. While the output data are displacements, stress resultants and stresses are each time step, and the envelop values of response.

Scalling results are important to recognize that a global scaling factor is computed on the basis of base shear only. Local member actions may differ significantly between the static analysis results, the response spectrum and the time history analysis results. All of the results need to be scaled uniformly using the same scaling factor.

The dynamic analysis will be more "accurate" for irregular and unsymmetrical structures. The accelerogram record that used for analysis are showed in Figure 3, Figure 4, Figure 5, and Figure 6.

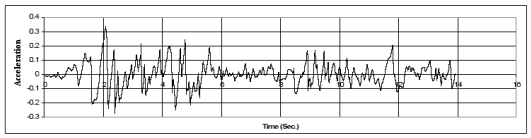

Figure 3. El Centro 1940 earthquake record.

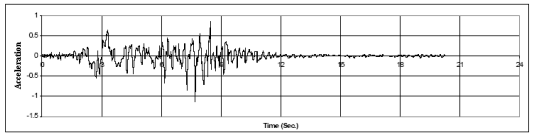

Figure 4. Pacoima Dam 1971 earthquake record.

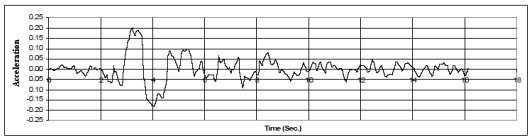

Figure 5. Bucharest 1977 earthquake record.

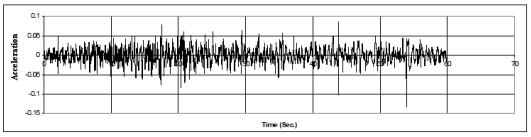

Figure 6. Flores 1992 earthquake record.

The velocity record that obtained using SeismoSignal software [4], that used for analysis are showed in Figure 7, Figure 8, Figure 9, and Figure 10.

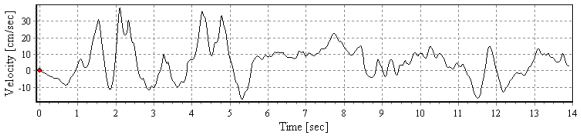

Figure 7. El Centro 1940 velocity.

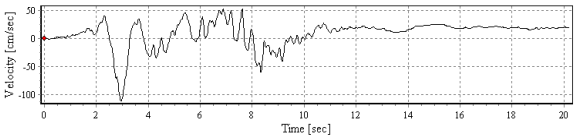

Figure 8. Pacoima Dam 1971 velocity.

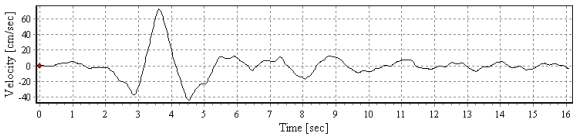

Figure 9. Bucharest 1977 velocity.

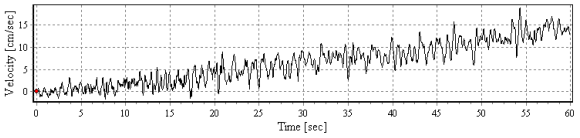

Figure 10. Flores 1992 velocity.

Analysis of earthquake design is using four earthquake records which are intensity-scaled to maximum peak ground amplitude (A_o) of spectrum respons curve [6] at T = 0. An example of the calculation for intensity-scale of El Centro 1970 record (0.3417g) to zone 4 Indonesian Seismic Zone (0.24g), is $\frac{0.24}{0.3417}.1 = 0.7024$ g.

The peak ground acceleration and the intensity scale results for four earthquake records can be seen in Table 1.

Table 1. Intensity scale results.

Ground Acceleration	Acceleration Ground Peak Record (g)	Earthquake Region 4	
		Acceleration Ground Peak (g)	Earthquake Design Scale (g)
El Centro	0.3417	0.24	0.7024
Bucharest	0.2015	0.24	1.1911
Pacoima Dam	1.1469	0.24	0.2093
Flores	0.1300	0.24	1.8462

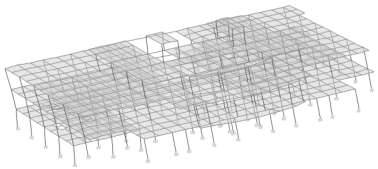

(a). Mode-1

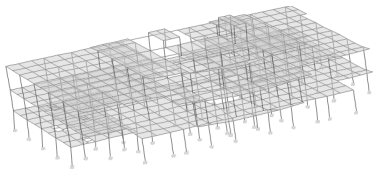

(b). Mode-2

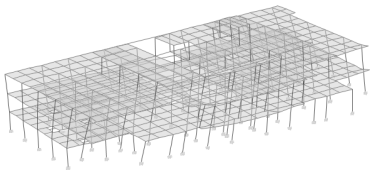

(c). Mode-3

Figure 11. Medical Support Building.

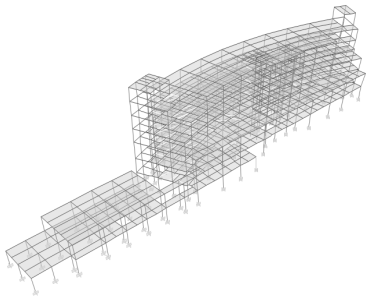

(a). Mode-1

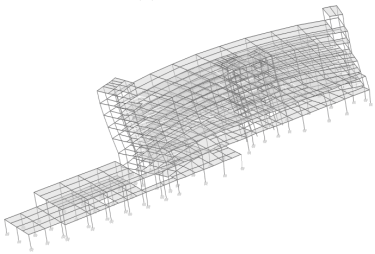

(b). Mode-2

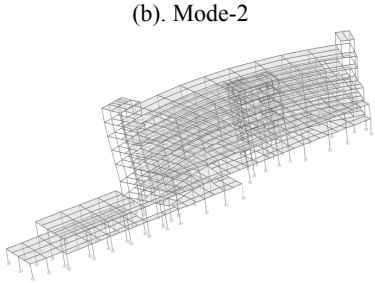

(c). Mode-3

Figure 12. Medical Service Building.

Both of modal participacing mass ratios for mode-1, mode-2 and mode-3, for medical support building and medical service building are presented in Figure 11, Figure 12, Table 2 and Table 3.

Table 2. Modal participating mass ratio
Medical Support Building

Mode	Period	UX	UY	RZ
1	0.652618	75.0237	0.0222	0.3664
2	0.644723	0.0239	75.9607	0.8267
3	0.570664	0.5966	0.0107	73.1879

Table 3. Modal participating mass ratio

Medical Support Building

Mode	Period	UX	UY	RZ
1	0.848706	6.1796	41.1252	27.9897
2	0.75351	52.2721	5.9445	0.8524
3	0.670223	0.5037	13.3138	16.5598

III. EXPERIMENTAL RESULTS

The analysis result of the time history using ETABS showed that the maximum base shear is the earthquake of Flores. The results are demonstrated in Figure 13, Figure 14, Figure 15 and Figure 16.

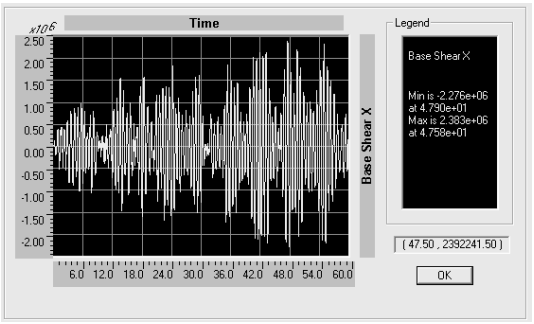

Figure 13. Base Shear x-direction of Medical Support Building of Flores earthquake.

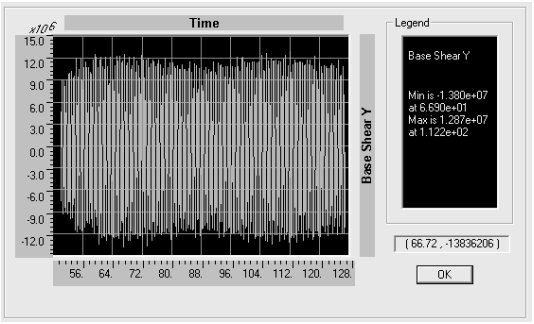

Figure 14. Base Shear y-direction of Medical Support Building of Flores earthquake.

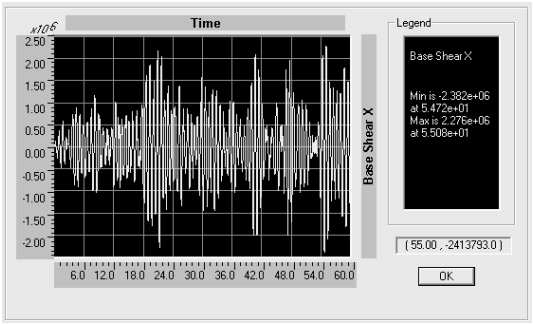

Figure 15. Base Shear x-direction of Medical Service Building of Flores earthquake.

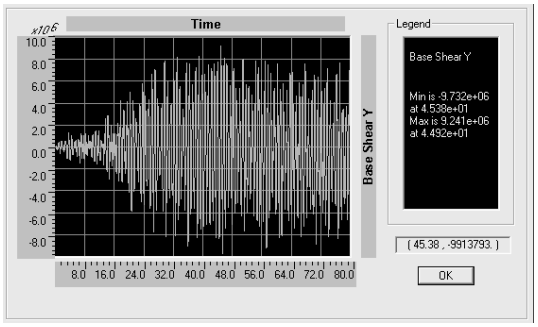

Figure 16. Base Shear y-direction of Medical Service Building of Flores earthquake.

Figure 17 and Figure 18 present the displacement result. Furthermore, Figure 19 and Figure 20 show the drift result.

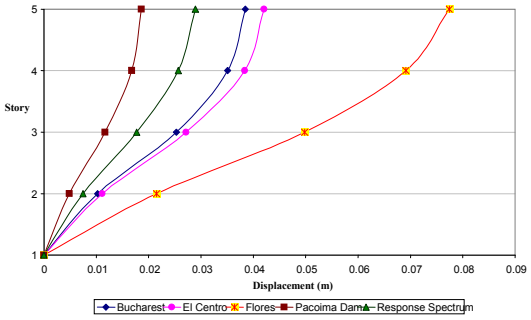

Figure 17. Displacement of Medical Support Building.

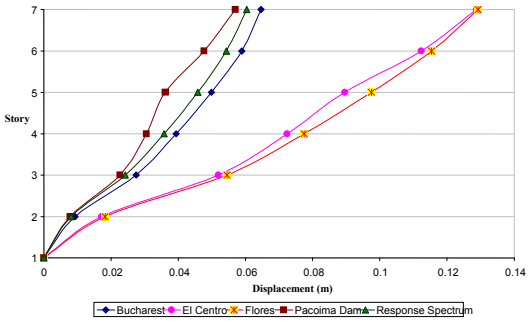

Figure 18. Displacement of Medical Service Building.

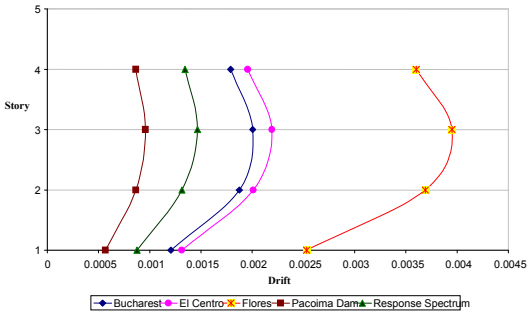

Figure 19. Drift of Medical Support Building.

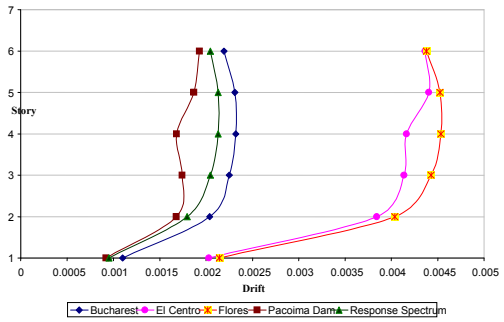

Figure 20. Drift of Medical Service Building.

The results show that the maximum base shear force at the medical support building due to Bucharest earthquake is 5918000 N, El Centro is 6619000 N, Flores is 13800000 N, and Pacoima Dam 2783000 N. The roof displacement is 0.035 m for Bucharest earthquake, El Centro is 0.042 m, Flores is 0.007 m, and 0.019 m for Pacoima Dam. The drift is 0.00179 for Bucharest, 0.00196 for El Centro, 0.0036 for Flores, and 0.00087 for Pacoima Dam.

On the other hand, the result of the maximum maximum base shear force at the medical service building due to Bucharest earthquake is 5607000 N, El Centro is 9729000 N, Flores is 9732000 N, and Pacoima Dam 4383000 N. The roof displacement is 0.065 m for Bucharest earthquake, El Centro is 0.128 m, Flores is 0.129 m, and 0.057 m for Pacoima Dam. The drift is 0.00219 for Bucharest, 0.00436 for El Centro, 0.00438 for Flores, and 0.00193 for Pacoima Dam. It can be concluded that the Flore earthquake showed the maximum of roof displacement and drift.

IV. CONCLUSIONS

The dynamic analysis result for the maximum base shear force showed that the earthquake of Flores is the biggest base shear compared to the other earthquake. The same results showed for the analyse spectrum dynamic response at earthquake region 4 for hard land.

Based on the result of dynamic analysis, the displacements due to Flores earthquake have biggest value. At the record acceleration of earthquake, the earthquake of Flores have velocity maximum that the smallest is 19,42679401 cm/det at 54,36 second so that the earthquake is long enough and generate the continu friction. However the displacement of structure due to earthquake of Flores was not extremely reached the goals according to SNI 1726-2002.

In general, the analysis result indicate that the drift due to the earthquake of Flores has also the biggest value, but the drift of structure due to earthquake of Flores was not extremely reached the goals according to SNI 1726-2002. In conclusion, these results indicate that the building is strong and stiff enough to all four of earthquake motion.

REFERENCES

[1] N. Anwar, “Seismic Analysis and Design of Buildings”, Workshop Introduction and Application of Pushover Analysis for Seismic Design/Evaluation of Buildings, University of Atma Jaya, Yogyakarta, 8 November 2007.

[2] E.L.Wilson, “Three-Dimensional Static and Dynamic Analysis of Structures”, Computer and Structures, Inc., 2002.

[3] PT. Waskita Karya, “Laporan Perencanaan Struktur Proyek Rumah Sakit Cahya Kawaluyan, Bandung”, PT Waskita Karya, 2005.

[4] Seismosoft, “"SeismoSignal - A computer program for signal processing of strong-motion data" [online]. Available from URL: http://www.seismosoft.com.”, Seismosoft, 2007.

[5] Standar Nasional Indonesia, “Tata Cara Perhitungan Struktur Beton untuk Bangunan Gedung SNI 03-2847-2002”, Standar Nasional Indonesia, 2002.

[6] Standar Nasional Indonesia, “Standar Perencanaan Ketahanan Gempa untuk Struktur Bangunan Gedung SNI 1726-2002”, Standar Nasional Indonesia, 2002.

[7] Y.A.Pranata, “Pushover Analysis for Regular and Irregular Reinforced Concrete Buildings”, Master Thesis, Graduate Program, Parahyangan Catholic University, Bandung, Indonesia, 2005.